SEAWATER ALTERATION OF EARLY PRECAMBRIAN (ARCHEAN) VOLCANIC ROCK AND EXPLORATION CRITERIA FOR STRATIFORM GOLD DEPOSITS, PORCUPINE CAMP, ABITIBI GREENSTONE BELT, NORTHEASTERN ONTARIO

By

© JOHN ANDREW FYON, B.Sc. (Geological Engineering, Queen's University)

A Thesis

Submitted to the School of Graduate Studies

in Partial Fulfilment of the Requirements

for the Degree

Master of Science

McMaster University

March, 1980

SEAWATER ALTERATION OF EARLY PRECAMBRIAN (ARCHEAN) VOLCANIC ROCK AND EXPLORATION CRITERIA FOR STRATIFORM GOLD DEPOSITS, PORCUPINE CAMP, ABITIBI GREENSTONE BELT, NORTHEASTERN ONTARIO

MASTER OF SCIENCE (1980)
(Geology)

McMASTER UNIVERSITY
Hamilton, Ontario

Title: Seawater Alteration of Early Precambrian (Archean) Volcanic Rock and Exploration Criteria for Stratiform Gold Deposits, Porcupine Camp, Abitibi Greenstone Belt, Northeastern Ontario

Author: John Andrew Fyon, B.Sc. (Geological Engineering, Queen's University)

Supervisor: Dr. James H. Crocket

Number of Pages: xviii , 238

THE FIRST BRICK

Who is that gink having lunch in the diner?
A consulting geologist, - he's not a miner.
For a fat enough fee he'll report on your ground
He can see through the rock where the gold may be found.
It will take him a month all his data to sort
and here is the way he will write his report:
"Re your instructions: - My Dear Mr. James:-
I proceeded up north to examine your claims.
You can reach them by auto, by air or by rail,
If you had a canoe and some wind you could sail.
You have plenty of water, and wood is at hand,
And a good place for buildings, as I understand
The rocks are quite ancient, or so it appears.
The ones that I noticed had been there for years.
The schistosity planes are on parallel lines,
A condition that's common to all the big mines.
The contacts observed are all metamorphosed,
I could see this in places where they are exposed.
Veins of importance so far I've not seen,
But I did find some crystals of black tourmaline.
Tourmaline, as you know, denotes a great heat,
So now that I've found them the picture's complete.
And now, in conclusion, My Dear Mr. James,
I'd advise you at once to develop these claims.
They are under the muskeg and high on the hills,
This should be proven by two diamond drills".
He's out for his fee, so he pours it on thick.
(But he wasn't there when we poured the first brick.)

- Lloyd Otto (circa 1948)

ABSTRACT

Regionally distributed, low temperature (<250°C), synvolcanic interaction between seawater and Early Precambrian (Archean) tholeiitic and komatiitic volcanic rocks in the Timmins area is characterized by relict palagonitization textures, elevated abundances of K_2O, Rb, Li, Ba, B, H_2O and CO_2 in the altered flows, and localized, intensely altered chlorite and carbonate-rich zones which occur throughout the tholeiitic and komatiitic volcanic stratigraphy as discordant and stratabound zones. These localized alteration zones formed at the seawater/seafloor interface and in a subseafloor volcanic environment. Only the alteration zones which developed in the seafloor environment are associated with local accumulations of felsic volcanic rock and exhalative, auriferous, cherty dolomites. Subsequent to the low temperature, seawater alteration of the flows, the volcanic pile was metamorphosed to greenschist facies.

Gold is leached from the volcanic rock during the most intense stages of the carbonate alteration. There is no significant difference between the gold content of komatiitic and tholeiitic flows.

Altered magnesium tholeiitic basalts which are spatially associated with auriferous, cherty dolomite-type mineralization are enriched in Li (> 30 ppm), B (> 30 ppm), Sb (> 0.35 ppm), Au (> 5 ppb), and As (> 70 ppm) and are depleted in Cu (< 70 ppm), with respect to altered basalts not associated with such gold mineralization. Ore-related, altered komatiitic flows can be screened only using Au (>5 ppb) and As (>70 ppm).

ACKNOWLEDGEMENTS

The author wishes to thank Dr. Bill Karvinen, whose efforts were instrumental in initiating this study, and who provided helpful discussion during the early part of this investigation. Financing for two summers of fieldwork and many trace element analyses, sponsored by the Mineral Deposits Section of the Ontario Geological Survey, is gratefully acknowledged. Access to active mining areas and to mine maps was graciously provided by Pamour Mines Ltd., Schumacher Division.

I express my appreciation to Dr. J.H. Crocket who supervised this research and offered much advice throughout the program.

This research was supported in part by a N.S.E.R.C. grant to Dr. J.H. Crocket.

TABLE OF CONTENTS

LIST OF FIGURES

LIST OF TABLES

LIST OF PLATES

LIST OF MAPS

CHAPTER 1

INTRODUCTION

The Timmins-Porcupine gold camp is located 600 km (400 miles) north of Toronto in the Abitibi greenstone belt (Figure 1). Since the first discovery in 1908, approximately 1.7×10^9 grams (60 million ounces) of gold have been produced from twenty-three properties located in Whitney, Tisdale, Deloro and Ogden townships (Figure 2). Only the former McIntyre, Dome, Pamour, Aunor and Delnite mines are currently in production, although salvage operations have been extracting additional surface ore from the Buffalo Ankerite and Hollinger mines. Of this total gold production approximately 40%, 25%, and 20% came from the Hollinger, McIntyre and Dome, respectively.

Descriptions of the gold ore bodies are given by Buffam (1948a,b), Jones (1948), Furse (1948), Carter (1948), Longley and Lazier (1948), Hawley and Hart (1948), Holmes (1948), Bell (1948), Backman (1948), Price and Byers (1948), and Ferguson et al. (1968). Apparent in these descriptions

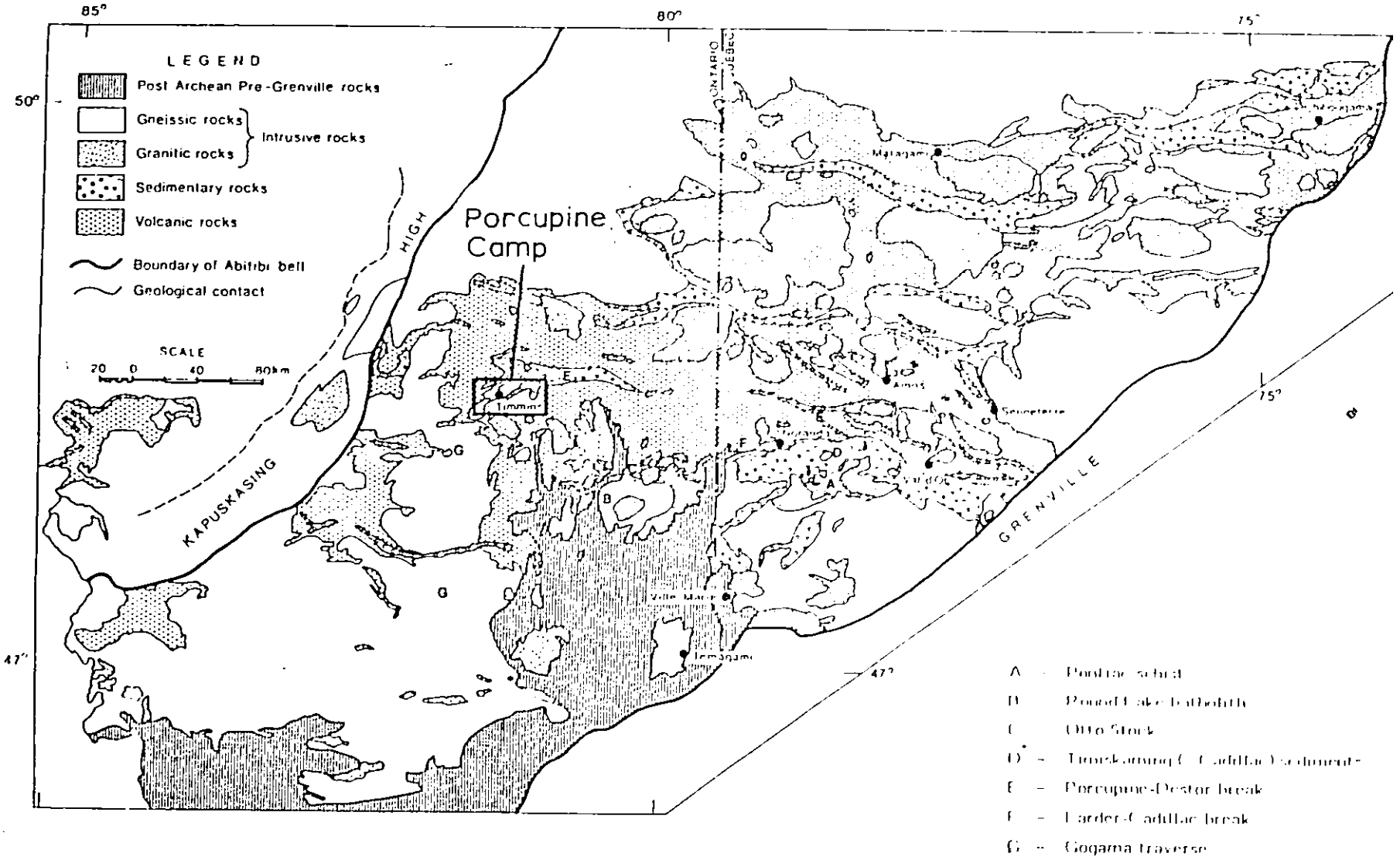

FIGURE 1: LOCATION OF THE TIMMINS-PORCUPINE GOLD CAMP WITHIN THE ABITIBI GREENSTONE BELT, NORTHEASTERN ONTARIO.

from Jolly, 1978.

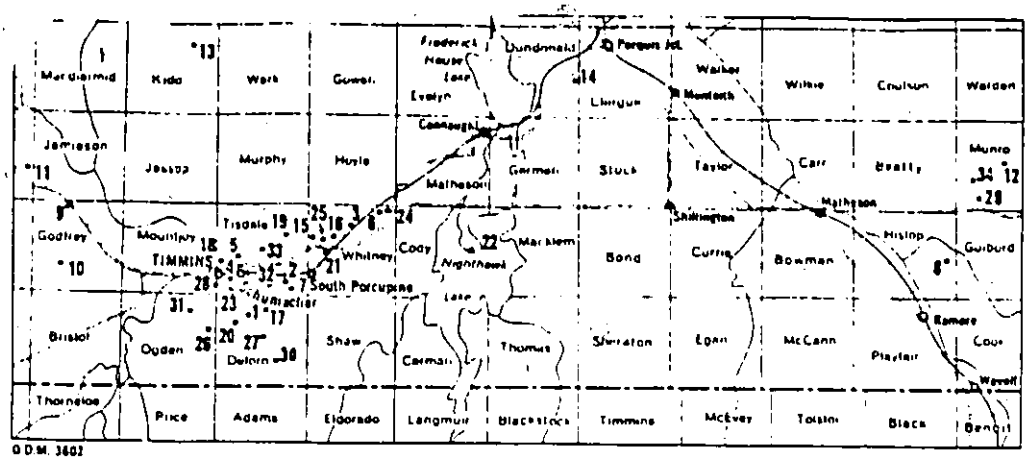

O.D.M. 3602

MINES IN THE PORCUPINE AREA

	Name of Mine	Started Production	Ceased Production	Total Value of Production (end of 1965)
	Gold Mines in Production			
1.	Aunor Gold Mines	1980		62,173,234
2.	Dome Mines Limited	1910		264,264,345
3.	Hallnor Mines Limited	1938		48,225,189
4.	Hollinger Consolidated GML	1910		553,910,754
5.	McIntyre Porcupine Mines	1912		305,902,365
6.	Pamour Porcupine Gold Mines	1936		60,905,568
7.	Preston ML (formerly Preston East Dome)	1938		54,427,248
8.	Ross Mine (Hollinger Consolidated GML)	1936		20,519,169
	Base Metal Mines: Producers, former producers, or under development			
9.	Canadian Jamieson	1966		
10.	Genex Mines	1966		
11.	Kam-Kotia Porcupine Mines Ltd	[illegible]		22,658,192
5.	McIntyre Porcupine	1965		6,449,618
12.	Munro Copper	1966		
13.	Texas Gulf Sulphur Company[1]	1965		650,074
14.	Noranda Mines Ltd (Aleso Nickel)	1912	1944	518,046
	Gold Mines — Past Producers			
15.	Banner Porcupine Mines Limited (formerly Canusa)	1927	1933	14,840
16.	Broulan Reef Mines Limited (formerly Broulan Porcupine, Porcupine Reef, Bonetal, Bonwhit)	1938	1965	11,255,877
17.	Buffalo Ankerite Gold Mines Limited (includes Marbuan)	1926	1956	33,483,898
18.	Consolidated Gillies Lake Mines Limited (formerly Gillies Lake Porcupine, Porcupine United, Rochester)	1929	1937	462,482
19.	Davidson Tisdale Mines Limited (formerly Davidson Consolidated Porcupine Davidson Mines)	1918	1920	53,914
20.	Delnite Mines Limited	1937	1964	13,052,567
21.	Gold City Porcupine Mines Limited (formerly Porcupine Lake)	1933	1934	50,100
22.	Hollconic Mines Limited (formerly Nightcaps, Goldhawk)	1947	1947	1,862
23.	Hollinger Consolidated Gold Mines Limited (formerly Mace, Vipond, Anglo-Huronian, Northcrown, Porcupine Crown)	1911	1941	12,721,178
24.	Hoyle Mining Company Limited (formerly Hoyle Gold Mines)	1941	1949	2,689,438
25.	High-Pam Porcupine Mines Limited	1948	1965	4,129,947
26.	Kenilworth Mines Limited (formerly Naybob, Hayden)	1932	1964	1,933,336
27.	McLaren-Porcupine (J. M. McLaren)	1933	1937	6,819
28.	Moneta Porcupine Mines Limited	1936	1943	5,589,356
29.	Munro-Croesus Mines Limited	1915	1948	326,894
30.	Nakhodas Mining Companies Limited (formerly Laymar, includes production from lease on Fuller claim, Tisdale township)	1940	1944	1,106,084
31.	New Hope Porcupine Mines Limited (formerly DeSantis)	1926	1942	1,366,707
32.	Porcupine Paymaster Limited (formerly Paymaster Consolidated, Consolidated West Dome Lake, Dome Lake West Dome Lake)	1922	1966	41,607,895
33.	Westfield Minerals Limited (formerly Carium, Contarum, Newray Rea Mine of Mines Leasing and Development Company)	1911	1961	37,396,410
	Miscellaneous			637,715
	Asbestos Mines			
34.	Canadian Johns-Manville Company Limited (Munro Mine)	1950	1964	57,204,074
35.	Canadian Johns-Manville Company Limited (Reeves Mine)			

[1] Under development, production expected in 1966.

Total Production of all mines in the Porcupine area to the end of 1965:

Gold	1,580,245,191
Base Metals	30,295,930
Asbestos	57,204,074
	1,667,745,195

FIGURE 2: Distribution and production value of gold and base metal mines from the Timmins area (from Brown,1967).

is the strict adherence to the structural dogma of the day. From a reinterpretation of these descriptions, based on personal examination of some of the ores, personal communication from Karvinen (1977, 1978) and recent independent studies (Roberts et al., 1978; Roberts and Spiteri, 1979; Fryer et al., 1979), it is proposed that most of the gold has come from the following deposit types:

1. Exhalative, stratiform, chert-carbonate sediments, consisting of chert, dolomite, pyrite, tourmaline (Hollinger, McIntyre, Dome, Pamour (?), Hallnor (?), Coniaurum, Paymaster Porcupine, Buffalo Ankerite, Aunor, Delnite, Preston);

2. Pyritized flows - large zones of disseminated, auriferous pyrite in carbonatized rock (Hollinger);

3. Discordant, hydrothermal pipes consisting of stockwork quartz-pyrite veins cutting carbonatized, pyritized wallrock (McIntyre);

4. Discordant breccia pipes cemented by auriferous pyrite, but lacking stockwork veining (McIntyre);

5. Stratabound, sedimentary pyrite-carbonaceous zones (Hollinger, Moneta, McIntyre);

6. Quartz-sulfide veinlets localized in felsic, quartz-feldspar-sericite schists (Paymaster Porcupine, Preston, Hollinger, Dome);

7. Turbidite-fluvial sedimentary hosted detrital (?) gold (Pamour, Hoyle, Broulan Reef, Dome);

8. Structurally controlled quartz veins (entire camp).

Such a classification not only reveals the myriad of gold deposit types, but also emphasizes the importance of non-tectonic controls on synvolcanic ore deposition. Because these deposit types are not differentiated in the older literature, it is impossible to estimate the relative importance of each type in terms of grade and tonnage. Fryer et al. (1979) indicate that about 20% of the Dome mine production has come from type 1, exhalative, chert-carbonate sediments. From personal examination of the Buffalo Ankerite, Delnite and Aunor workings it is contended that better than 80% of the ore from these mines was of chert-carbonate, exhalative type.

The spatial association of the carbonate-rich rock, quartz-feldspar "porphyries" and gold deposits in the Porcupine camp was recognized by Burrows (1924), and has been reiterated by Ferguson et al. (1968), Pyke (1975) and Karvinen (1976, 1978a). This relationship is illustrated in

Figure 3.

That many gold deposits and carbonate-rich rock in the Porcupine camp are spatially associated, implies a genetic relationship links the two. The absence of gold deposits in stratigraphically and chemically equivalent volcanic rock lacking carbonate alteration further emphasizes this genetic link. However, the presence of carbonatized rock not associated with gold mineralization indicates that carbonate alteration is only one of a set of geological criteria which collectively define the optimum environment for gold deposition. Hence a better understanding of the gold metallogeny will be gained through acquiring a better understanding of the volcanic environment in which the gold deposits occur and the processes which caused the carbonate alteration. As a consequence, viable gold exploration criteria can then be proposed.

Embodied in this thesis are the field data acquired by the author during the 1977, 1978 and part of the 1979 field seasons, the laboratory, analytical data and an interpretation of these data in terms of geological and lithogeochemical guides to gold mineralization in the Timmins-Porcupine camp.

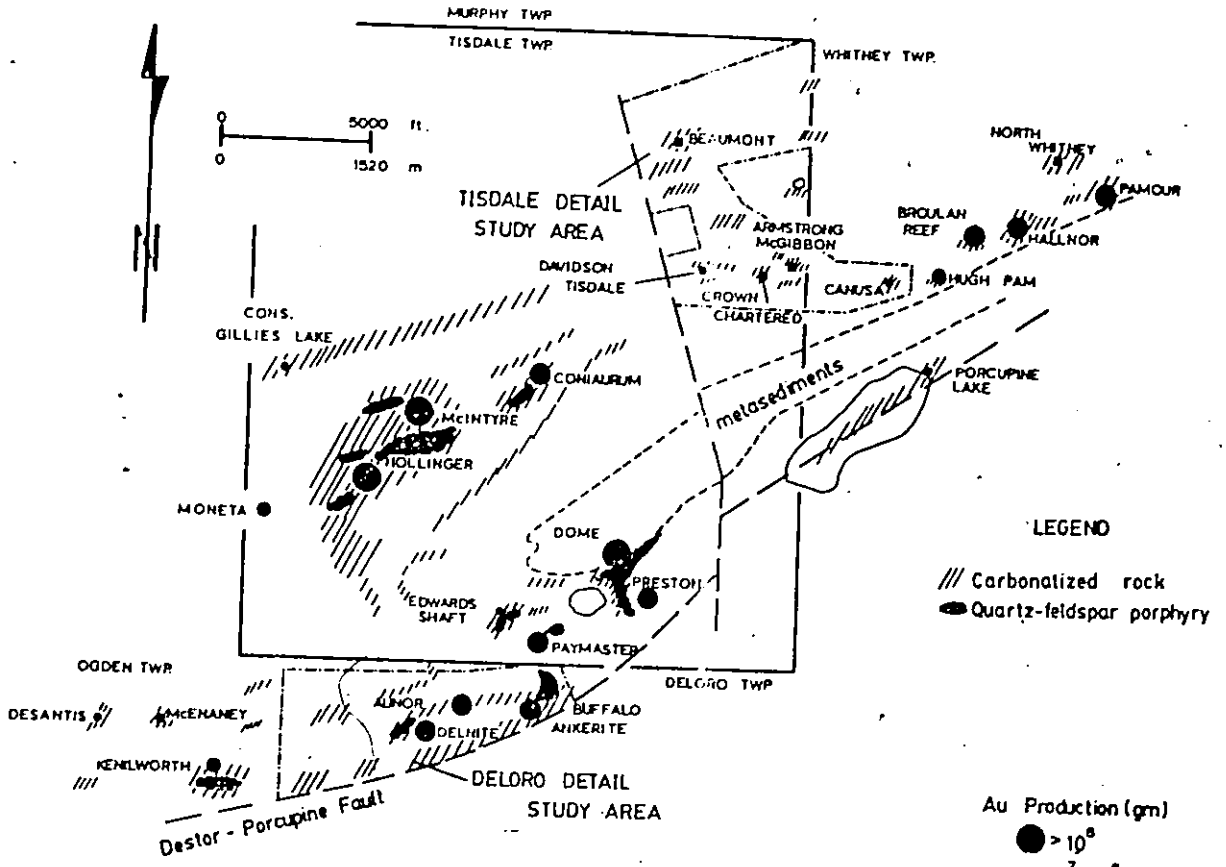

Figure 3

DISTRIBUTION OF PORPHYRIES, GOLD DEPOSITS AND CARBONATIZED VOLCANIC ROCK IN THE TIMMINS AREA

after Karvinen, 1978; Pyke, 1975; Ferguson 1958 ab

CHAPTER 2

OBJECTIVES AND THESIS

This study is concerned with only one gold deposit type consisting of syngenetic, stratiform, chert-dolomite interflow sediments. It is contended that by application of fundamentals, such as detailed field mapping, and petrography combined with theoretical concepts (geothermal and metasomatic systematics) and applied lithogeochemistry, a coherent gold metallogeny can be deduced and effective gold exploration criteria can be offered.

My thesis is threefold. Firstly, within the Upper Supergroup, the carbonate alteration which occurs as strata-bound and discordant zones throughout the Lower and Middle Metavolcanic Group stratigraphy, was synvolcanic and developed in two distinct volcanic environments as a result of rock/seawater, hydrothermal interaction.

Secondly, the formation of auriferous, exhalative, dolomitic sediment was intimately related to the geological evolution of only one of the two volcanic environments.

Thirdly, it is possible to effectively discriminate between the carbonate alteration zones of the mineralized and unmineralized volcanic environments using selected trace element screens and field relations.

CHAPTER 3

METHODOLOGY

3.1 FIELD APPROACH

As a follow-up to the preliminary field work by Karvinen (1976, 1978a), a detailed mapping and lithogeochemical sampling program within Whitney, Tisdale, Deloro and Ogden townships (Figure 2) was instituted in 1977 by the Mineral Deposits Section of the Ontario Geological Survey in conjunction with McMaster University.

From older maps (Ferguson et al., 1968; Pyke, 1974) two control areas, one hosting mineable gold deposits and the other only gold prospects, were selected for detailed study and comparison. Both areas are characterized by relatively simple structure, by the presence of carbonate-rich rocks and by stratigraphic and geochemical equivalence of their lithologies. The Buffalo Ankerite, Aunor and Delnite mines, each of which has produced about 2.8×10^7 g (1×10^6 ounces), lie within the Deloro township or south study area (Figure 3). Only prospects (Beaumont, Davidson-

Tisdale, Armstrong-McGibbon, Crown Chartered) occur within the Tisdale or north study area (Figure 3). The south study area represents a mineralized control area, whereas the north study area represents an unmineralized control area.

Stratigraphic equivalence of the study areas is confirmed by the same relative, stratigraphic juxtaposition of major rock types. A komatiitic sequence at the base is stratigraphically overlain by magnesium and iron tholeiitic basalts and calc-alkalic pyroclastics. Regional mapping by Pyke (1978b) and Jensen (1978b) has demonstrated the viability of this approach to Archean, volcanic, stratigraphic subdivision.

Because of this refined approach to Archean volcanic, stratigraphic analysis using more recent rock nomenclature (e.g. komatiitic, magnesium and iron tholeiitic basalts), older geological maps of the area (Ferguson et al., 1968; Carlson, 1967) were found to be unsatisfactory for detailed, lithogeochemical, stratigraphic correlation. Consequently both study areas were remapped by the author. Detailed mapping was carried out on grids established by pace or chain and compass (1 inch to 100 feet, 1 cm to 12 m; 1 inch to 25 feet, 1 cm to 3 m) or by using airphoto control (1 inch to 528 feet, 1 cm to 62 m). Where possible, surface geology was supplemented with composite underground data compiled by the

author. Reconnaissance mapping (1 inch to 1320 feet, 1 cm to 156 m) was carried out in parts of Whitney, Tisdale, Deloro and Ogden townships to confirm and supplement the regional distribution of carbonate-rich rock, as mapped originally by Karvinen (1976) and to acquire a regional data base.

Only after the detailed volcanic stratigraphy had been established was it possible to define the relationships between the carbonate alteration and the volcanic rock. During the course of the detailed mapping, many more zones of carbonate alteration were located which had not been previously recognized (e.g. c.f. maps by Ferguson et al., 1968; Karvinen, 1978a).

It is within this detailed volcanic, stratigraphic framework that observations have been gathered and conclusions relevant to the gold metallogeny deduced.

3.2 ANALYSIS OF GOLD

Gold abundances have been determined using radiochemical (RNAA) and epithermal instrumental (EINAA) neutron activation analysis. The stable nuclide ^{197}Au, when subjected to neutron bombardment, undergoes the reaction $^{197}Au(n,\gamma)^{198}Au$. This radionuclide has a half-life of 2.696 days and emits a gamma-ray of 412 KeV during decay to the stable nuclide ^{198}Hg. A

sample's gold content is determined by measurement and comparison of the induced sample activity with that of a simultaneously irradiated standard. Counting of the 412 KeV photo-peak was carried out using an Ortec, Li drifted Ge detector having an active volume of 30 cm^3. This detector has a resolution of 2.0 KeV at 662 KeV (^{137}Cs) and a peak to background ratio of 15 to 1.

The heterogeneous distribution of gold in geological materials poses a severe constraint on analytical precision and hence the selection of a sample of adequate size to ensure a specified degree of precision is critical. It has been demonstrated mathematically (Clifton et al., 1969) that a sample weight of 1 g was found to be adequate to ensure a relative analytical error of 50% at the 95% confidence level, at the 1 to 4 ppb abundance range. Precision improves greatly at higher gold abundances (> 5 ppb). All samples were irradiated in the McMaster pool-type, nuclear reactor. The sample package was continuously rotated during the irradiation. A horizontal flux variation of 0.6% per centimeter was calculated in one experiment using iron wire flux monitors wrapped around vials carrying chemical standards.

3.2.1 Radiochemical Neutron Activation Analysis (RNAA)

For all RNAA experiments, the irradiation package consisted of: ten, 1 gram rock samples; one, 1 gram rock standard; and two chemical standards. Rock standards used were W-1 and a house standard, JK-153. The house standard is a tholeiitic basalt collected from the Kakagi Lake area by Kwong (1975). The chemical standards were prepared by doping #42 Whatman, ashless, filter paper with a standard, gold-chloride solution, which was then dried and loaded into a sample container. Heat sealed, industrial grade, polystyrene vials were used as sample containers for all RNAA irradiations. The sample package, sealed in a polystyrene wrap, was irradiated in a "RIFLS", high flux position in the McMaster pool type nuclear reactor with a neutron flux of 1.5×10^{13} neutrons/cm^2/sec for 1 MW hour. The surface gamma activity of the irradiated package at time of acquisition ranged between 1.0 to 100.0 MR/hour. A carrier based, wet chemical procedure was followed (Appendix 1) to separate activated gold from the activated residual rock material. Sample counts were normalized to a common time to correct for the decay of ^{198}Au and a direct comparison with the chemical standard yields the sample's gold content. Time required for the wet chemistry was approximately twelve hours and for

counting thirteen samples, up to twenty-six hours.

3.2.2 Epithermal Instrumental Neutron Activation Analysis (EINAA)

EINAA has three distinct advantages over the RNAA. First, the researcher is exposed to less radiation. Second, the procedure minimizes the possibility of cross-sample contamination, as all wet-chemistry is eliminated. Finally, the use of a cadmium shield suppresses the thermal neutron (energy E <0.4 ev) flux bombarding the sample, and enhances the activation of elements like gold which have large capture resonance peaks with respect to other major elements. The major disadvantages are that sub-ppb gold abundances cannot be determined and only one chemical standard can be used because of time constraints.

The irradiation package consisted of: six, 1 gram rock samples; one, 1 gram rock standard; and one chemical standard, all loaded into fused quartz vials and sealed with a polybond glue-polystyrene cap. The chemical standard was a rock powder doped with a concentrated gold-chloride solution such that the ratio of gold in standard solution to gold in standard rock powder was about 50 to 1. To minimize matrix absorption effects (Croudace, 1979), the rock samples and chemical standards of a given INAA experiment were of similar

bulk composition and mineralogy.

The package was irradiated for 24 MWH in a cadmium shielded, high flux facility, and a six day cooling period elapsed prior to sample counting. Following the cooling period, the irradiated samples were transferred from their fused glass vials into 4 dram, glass, counting vials. This step is required because up to 6 ppb gold was detected in a blank, fused quartz vial which was capped by polybond glue and a polystyrene seal. In addition, the larger diameter, 1 dram counting vial increases the sample surface area which is exposed to the detector, effectively improving the counting geometry.

For EINAA experiments the whole rock sample may be regarded as a mixture of two components - gold atoms and all other rock forming atoms. In an irradiated sample, a background gamma energy spectrum is generated by the decay of the rock forming atoms. For an ultramafic rock, this background will be dominated initially by decay of radionuclides having half lives shorter than ^{24}Na and ^{42}K (e.g. 24 hours) and after decay of these nuclides, by ^{51}Cr, ^{59}Fe, and ^{57}Co. Clearly the rock background will decay at a rate different from that of ^{198}Au, which in turn will cause the ^{198}Au 412 KeV gamma peak to background (P/b) ratio to change with time (Figure 4). As a consequence the standard count rate per unit

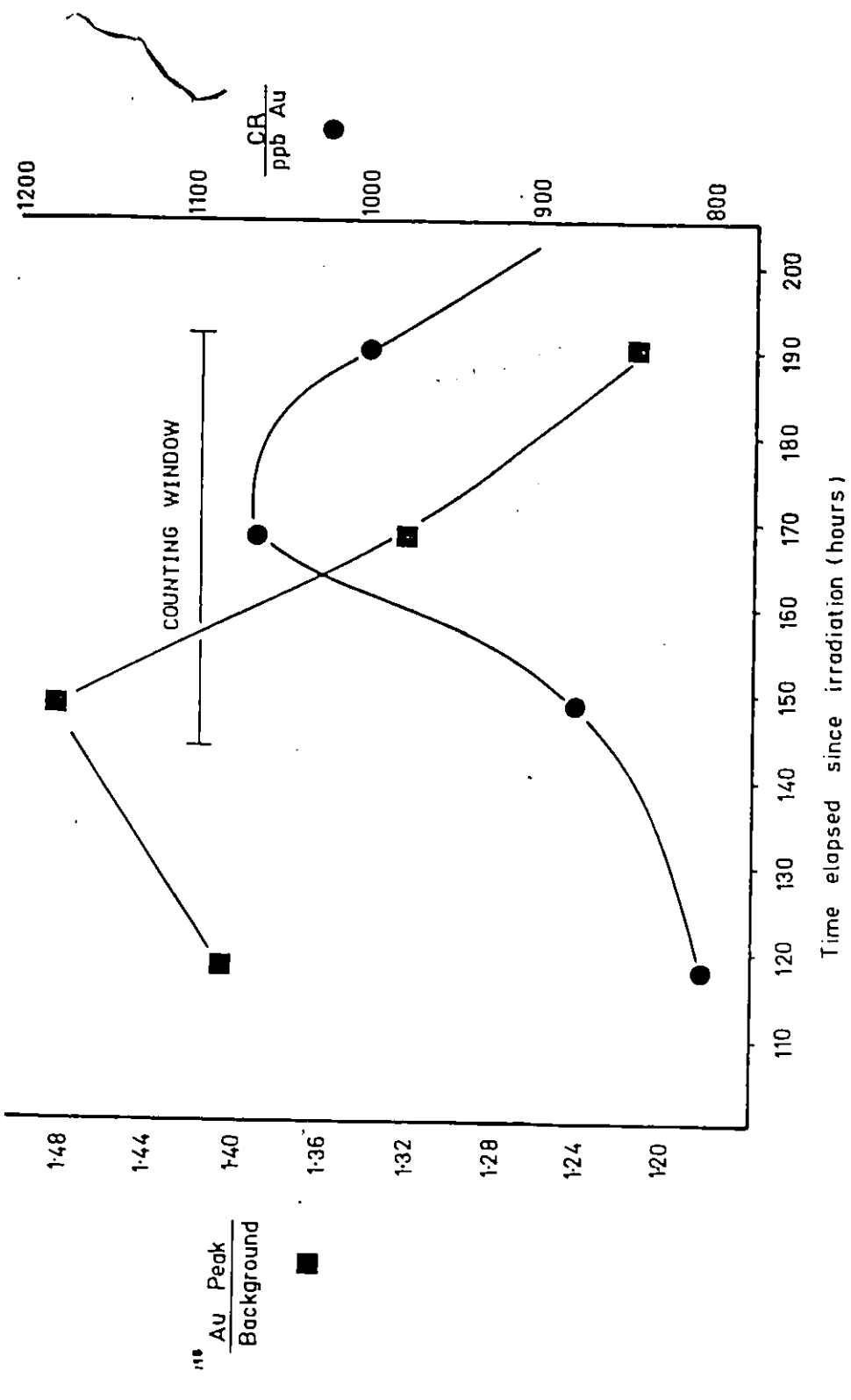

FIGURE 4: Variation of Au^{198} gamma photo peak to background ratio and count rate (CR) per unit mass of Au (ppb Au) as a function of time elapsed since irradiation for an EINAA experiment. Optimum counting time is 6 to 8 days after irradiation.

mass of gold, corrected for radioactive decay of gold (CR/ppb Au, Figure 4) will also vary with time. To compensate for this effect, the chemical standard was counted every 10 to 12 hours until all rock samples had been counted. All data were corrected for radioactive decay of gold and a calibration plot of corrected, standard counts/ppb gold against clock time elpased was constructed (Figure 5). To determine the gold content of a rock sample, the time at which that rock sample was counted is noted (B, Figure 5) and the corresponding corrected standard count rate per unit weight of gold is read from the plot (C, Figure 5). A direct comparison of this standard count rate with that measured for the rock sample yields the gold abundance of the rock sample.

To optimize counting statistics, all samples were counted between the sixth and eighth day following the irradiation.

3.2.3 Comparison of EINAA and RNAA Data

A rigorous comparison of the EINAA and RNAA data is impossible due to the small number of duplicate analyses. In general, the agreement between the two analytical methods is good, although the EINAA values are systematically higher

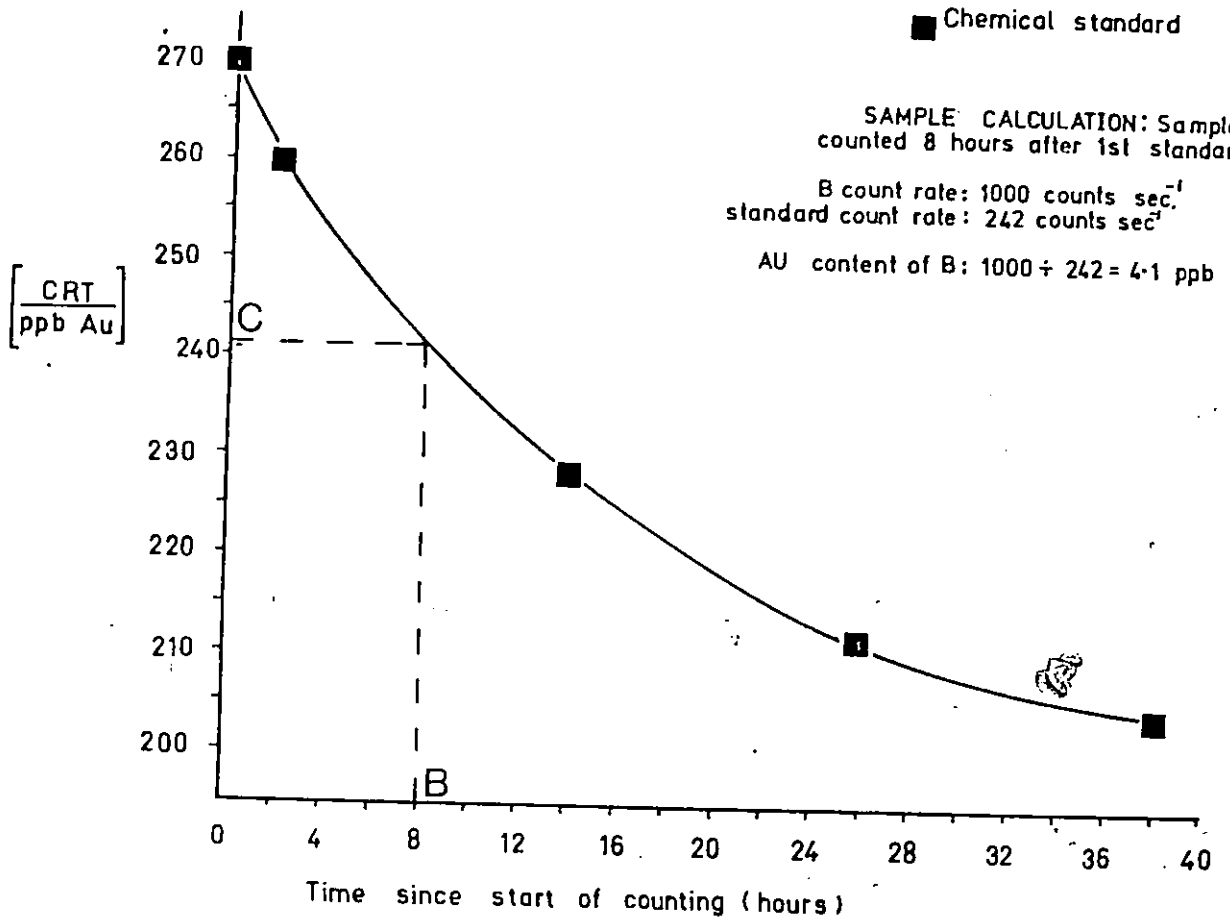

FIGURE 5: Variation of the standard count rate (CRT) per unit mass of Au (ppb Au) as a function of time elapsed since the start of counting. The gold concentration of sample B is determined by comparing the count rate of sample B, counted at time B with the standard count rate C. All data is corrected for radioactive decay of gold .

than those done by RNAA (Table 1).

3.2.4 Accuracy

The standard results (Table 1) lie within the ranges reported by Fritze and Robertson (1969) and Kwong (1975). Fritze and Robertson (1969) conclude that gold is heterogeneously distributed in W-1, possibly reflecting the presence of sulfide, gold-carrier. The one high gold value for W-1 (9.4; Table 1) is consistent with that conclusion.

3.3 XRF ANALYSIS OF MAJOR ELEMENTS

Rock samples were crushed to -200 mesh using a ceramic lined pulverizer and shatterbox. Fusion pellets, prepared by a method described by Norrish et al. (1969), were analysed on a model PW 1450, Philips, automatic, sequential spectrometer at McMaster University. Each sample set of three was run with a drift monitor sample to permit correction of machine variation. Rock standards used were GSP-1, NIM-D, NIM-G, NIM-N, NIM-L, NIM-S, BCR-1, 1a and a house standard WH-22. Two hundred and fifty-seven samples were analysed. A computer listing is included in the map pocket.

TABLE 1
Comparison of R.N.A.A. and I.N.A.A Data

Sample No.	Au p.p.b. I.N.A.A	R.N.A.A
B-34	3.1	0.8
A-6	28.9	28.2
B-24	1.2	0.9
DR-93	94.6	94.4,93.9
TR-402	3.0,2.6	1.8,2.0

Duplicate Analyses

	I.N.A.A	R.N.A.A.
W-1		3.8,4.4,4.4,9.4
JK-153		0.7,0.8,1.0
DR-93		94.4,93.9
TR-512		1.4,4.4
TR-402	3.0,2.6	1.8,2.0

Reported values for rock standards; W-1....3.9-6.2 (Fritze et al, 1969)

....4.1-4.6 (Kwong and Crocket,1978)

JK-153..0.9 (Kwong,1975)

3.3.1 Analytical Precision and Accuracy

Precision has been estimated by plotting duplicate analyses on a binary plot (Figure 6). Ideally, all data would plot along the dashed line having a slope of +1 (Figure 6). In practice there is some dispersion about this line and an envelope is drawn to enclose all duplicate data points. This envelope provides a measure of the maximum precision limits for the analytical method. It is assumed that precision is linear over a range of oxide concentrations, although Thompson and Howarth (1976) argue that this assumption is valid only when oxide concentrations are at least two orders of magnitude greater than the detection limit. However, the calculated precision for the major element analyses, except that for Na_2O, MnO, and MgO, is excellent (Table 2) and therefore the graphical technique is deemed suitable for these data. Detection limits estimated for the major oxide data are listed in Table 2. These detection limits were established by examination of precision data for an oxide over a range of concentrations. The abundance level at which the precision exceeded 50% was deemed the detection limit.

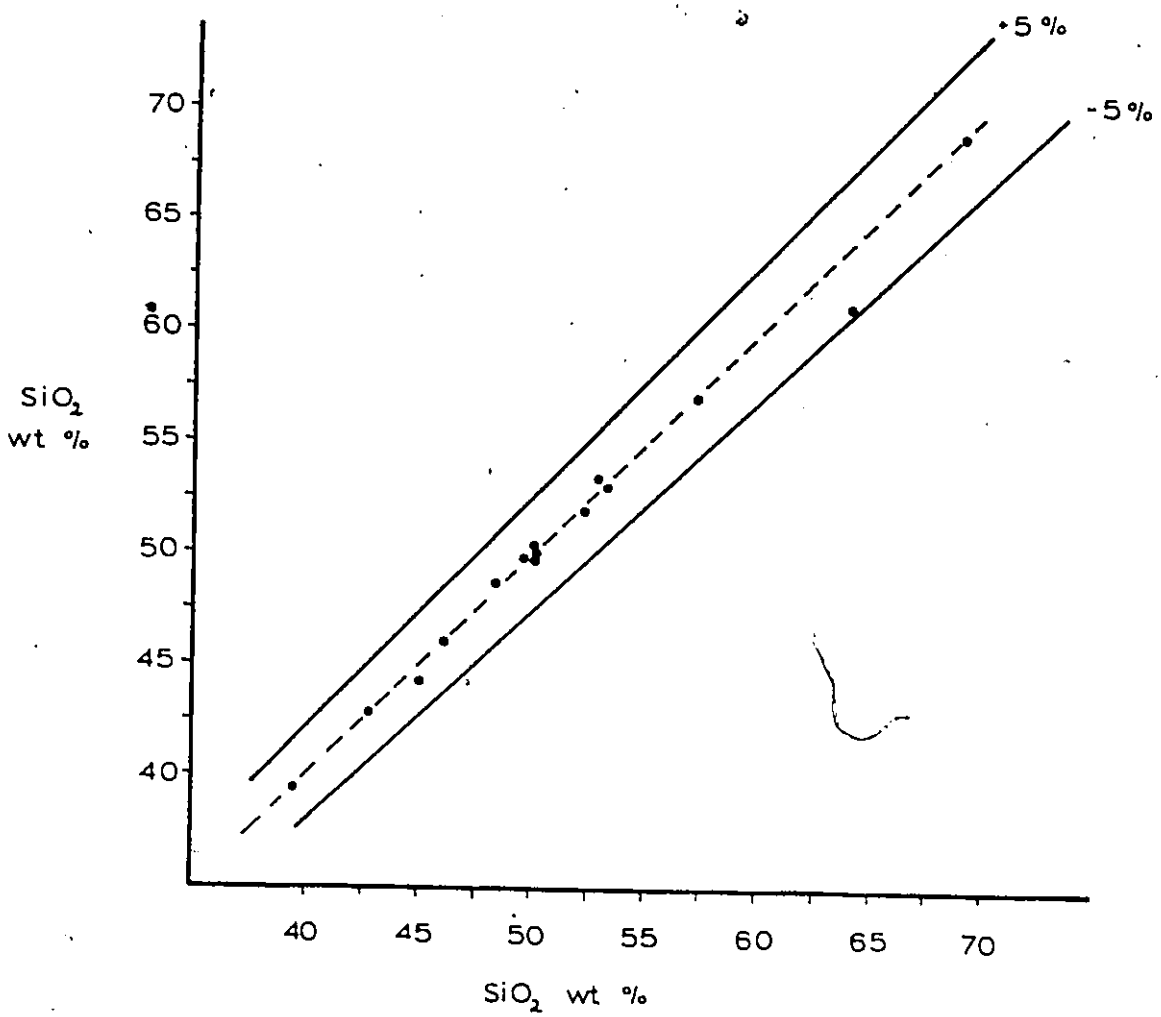

FIGURE 6: SiO_2 PRECISION ESTIMATED FROM A BINARY PLOT OF DUPLICATE DATA.

TABLE 2

Major and Trace Element Precision Estimates

Oxide/Element	Detection Limit	Precision	Analytical Method
SiO_2	0.1 wt.%	± 5 %	X.R.F. glass pellet
Al_2O_3		± 4 %	
Fe_2O_3		± 4 %	
MgO		± 17%	
CaO		± 4 %	
Na_2O	2.0 wt.%	±90%, < 2 wt.%	
K_2O	0.1 wt.%	± 6 %	
TiO_2	0.01 wt.%	± 4 %	
MnO	0.05 wt.%	± 23 %	
P_2O_5	0.04 wt.%	± 11 %	
Ni	10.0 p.p.m.	±10 %	X.R.F. powder pellet
S	50.0	± 24 %	
Rb	5.0	± 33%	
Sr	10.0	± 20%	
Y	50.0(?)	± 100%	
Zr	20.0	± 44%	
Nb	?	?	
Cr	10.0	± 15%	
Co		± 15%	
Cu		± 20%	
Pb	?	?	
Zn	10.0	± 15%	
As	70.0	± 5%	

Analyses carried out at McMaster University

3.4 DETERMINATION OF TRACE ELEMENTS

Trace elements were determined by XRF at McMaster University and by various techniques at the laboratories of the Ontario Geological Survey. A computer listing is included in the map pocket.

The McMaster University data (Cr, Ni, Co, S, Rb, Sr, Y, Zr, Nb, Pb, Cu, Zn, As) was determined by XRF analysis using a powder pellet preparation method described by Marchand (1973). Analytical precision and detection limit estimates are included in Table 2. The poor precision of Y, Zr, Nb, Rb and As (<70 ppm) is attributed to abundance levels of these elements near or below the XRF detection limit.

Listed in Table 2b are the precision estimates and the detection limits for the trace element analyses carried out at the Ontario Geoscience Laboratory.

3.5 ROCK CLASSIFICATION

Rock classification has been established using textural characteristics of volcanic rocks (Pyke et al., 1973; Pyke, 1978a; Arndt et al., 1977; Arndt et al., 1979; Jensen, 1978a) and the Jensen Cation Plot (Figure 7). The term, komatiite, although presently under review (Arndt et al., 1979), is used

TABLE 2b

Precision And Detection Limits For The Trace Element Analyses Carried Out At The Ontario Geoscience Laboratories.

Element	Precision	Detection Limit (ppm)	Analytical Method
Pb	± 10 %	10	Atomic Absorption
As		1	
Bi		0.1	
Li		5	
Ba		5	
Co		5	
Cr		5	
Cu		5	
Ni		5	
Sb		0.1	
Sr		1	Spectroscopic
B		5	
Ag		1	
S		0.01	Leco
CO_2		0.01	

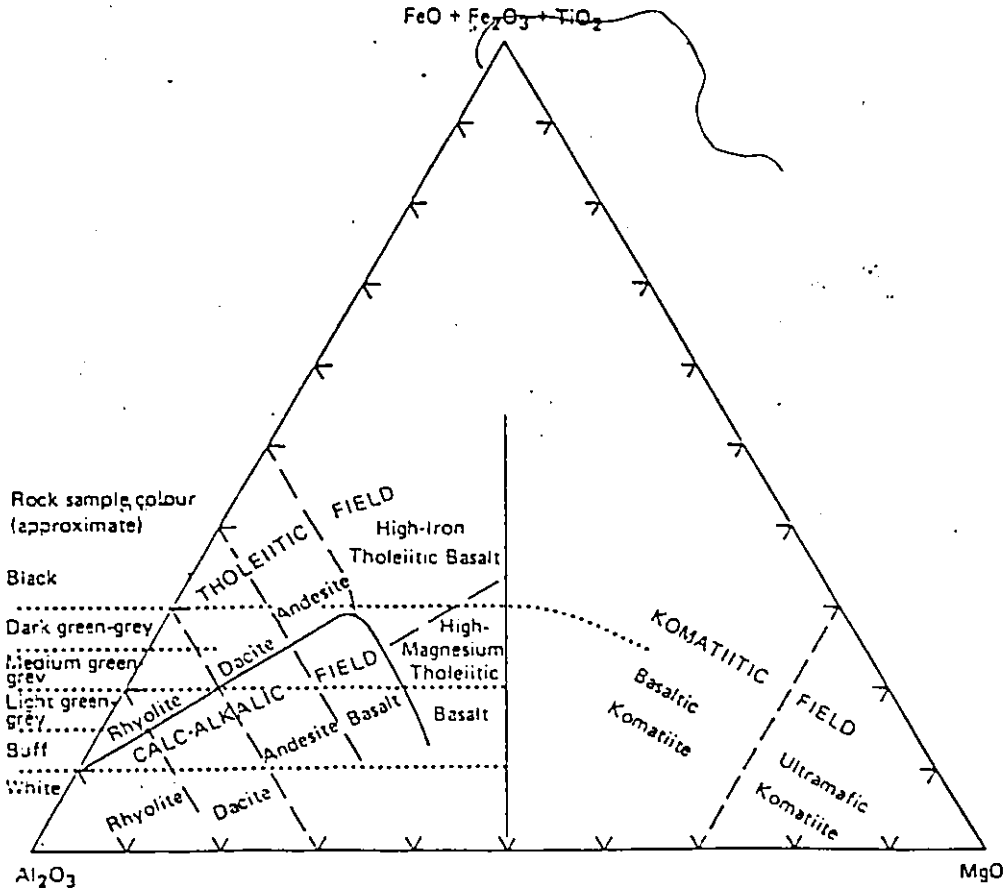

FIGURE 7 :Jensen cation plot using the cation percentages of Al_2O_3, Fe_2O_3+FeO+TiO_2, and MgO. From Jensen(1976).

here to describe a suite of volcanic rocks having distinctive field and chemical characteristics (Pyke et al., 1973; Arndt et al., 1977; Arndt et al., 1979, Nesbitt et al., 1979).

Altered flows have been identified using petrographic criteria (Dimroth and Lichtblau, 1979; Gélinas et al., 1977) or by their excessive volatile content (Pineau et al., 1976; LOI >0.4 wt %). In the study areas, no fresh volcanic rock was identified; hence purely lithogeochemical classification screens must be applied with caution until the magnitude of the chemical variations attributed to the alteration is evaluated. Field classification criteria, utilizing volcanic textures, are particularly useful in this regard because the volcanic rock suites have distinctive textural characteristics which generally are preserved regardless of the degree of rock alteration.

3.6 SIGNIFICANCE OF THE CHEMICAL DATA

Many studies of Archean volcanic rock weigh heavily on interpretations of geochemical data (Baragar, 1968; Jolly, 1975; Jensen, 1976; Goodwin, 1977; Gélinas et al., 1977). However, it is now apparent that Phanerozoic and Archean, submarine, volcanic rocks have undergone some degree of

seawater alteration which has modified the original bulk rock geochemistry (Hart, 1969; Hart and Nalwalk, 1970; Dimroth and Lichtblau, 1979; Garlick and Dymond, 1970; Humphris and Thompson, 1978a,b; Keays and Scott, 1976; Muehlenbachs and Clayton, 1972; Spooner et al., 1974; Spooner and Bray, 1977; Thompson and Melson, 1970; Tómasson and Kristmannsdottir, 1972). Alteration that is virtually undetectable optically can drastically change the alkali content of a rock (Hart, 1969). Furthermore, altered rocks having as little as 0.4 wt % H_2O show marked changes in oxidation state of iron and shifts to heavier $^{18}O/^{16}O$ whole rock isotopic ratios (Pineau et al., 1976). Interpretation of Archean rock geochemical data is more complex as these rocks have locally undergone polyphase metamorphism/deformation histories (Dimroth and Lichtblau, 1979). From studies in the Rouyn-Noranda area, where the prehnite-pumpellyite metamorphic rank is one of the lowest reported for an Archean terrain, Dimroth and Lichtblau (1979) conclude that there is no fresh Archean pillow lava and that chemical analyses of these rocks give at best only an approximate estimate of the original magmatic chemistry. Needless to say, not all elements are equally mobile at a given degree of alteration. Humphris and Thompson (1978a,b) indicate that at relatively low degrees of hydration (2 to 6 wt %), Ni and Cr appear to be immobile, whereas MgO

is notably enriched in Phanerozoic pillow lavas. Baragar et al. (1979) argue that the pillow core of an Early Precambrian submarine lava from the Yellowknife Supergroup has undergone little net chemical change during seawater palagonization and subsequent regional metamorphism. Jolly (1975) contends that certain elements, notably Cr, Ni, Mg, are sufficiently immobile that their distributions in metamorphosed Archean pillow lavas still reflect original magmatic trends.

For this research, rock geochemical data has been used to supplement the detailed lithostratigraphic volcanic subdivisions, established using textural criteria , and to describe the geochemical characteristics of hydrothermal alteration zones relative to those of the least altered rocks.

3.7 SIGNIFICANCE OF THE STRATIGRAPHIC THICKNESSES

Indicated on the stratigraphic sections (Figures 11, 12) are the apparent stratigraphic thicknesses of the volcanic sequences in the two study areas. Pyke (1978b) estimates the thickness of the Upper Supergroup to be approximately 12,000 m (39,000 feet). A brief review of the problems associated with the estimation of stratigraphic thicknesses in the Abitibi belt is given by Jolly (1978). Based on the widely

varying composition of pumpellyite, the absence of typical high-pressure, basaltic replacements such as aragonite, lawsonite, glaucophane (Winkler, 1976) and the comparison of the low-pressure, very low grade, Abitibi, metamorphic assemblages with those developed in Phanerozoic rocks, Jolly (1978) concludes that the thickness of the Abitibi lava pile at the time of prehnite-pumpellyite metamorphism was less than 12 km. The greenschist facies assemblage in mafic rocks (albite, actinolite/tremolite, epidote, chlorite and stilpnomelane) in the Abitibi belt is broadly associated with intrusives rather than depth of burial (Jolly, 1978). As the metamorphic characteristics do not reflect burial to depths in excess of 12 km, Jolly (1978) concludes that the apparent thicknesses reflect structural thickening or topographic irregularities produced during and after volcanism. Hence, although the stratigraphic thicknesses reported in this study are reasonable, it must be realized that these stratigraphic sections represent only a minor part of the entire volcano-sedimentary sequence preserved in the Timmins area. Because of incomplete exposure, structural thickening would be impossible to recognize and therefore, the reported stratigraphic thicknesses must be regarded as being apparent.

CHAPTER 4

GENERAL GEOLOGY

Early Precambrian (Archean) metavolcanic and metasedimentary rocks, subdivided into a Lower and Upper Supergroup (Pyke, 1978b) underlie the map area (Figure 8). Listed in Table 3 is a comparison of the stratigraphic subdivisions of Dunbar (1948), Ferguson et al. (1968), Pyke (1975), Pyke (1978b), and Pyke et al. (1978).

Two cycles of volcanism, locally separated by the Destor-Porcupine fault, were recognized by Dunbar (1948), who deduced that the Lower Supergroup was older than the Upper Supergroup. Pyke (1975) confirmed the older age of the Lower Supergroup by correlating komatiitic flows on both sides of the Destor-Porcupine fault. Nunes et al. (1978), using U-Pb zircon age determinations, dated the tops of the Lower and Upper Supergroups at 2725 ($^{+10}_{-2}$) and 2710 (±6) million years, respectively.

The Lower Supergroup consists predominantly of calc-alkalic basaltic to felsic volcanic flows and pyroclastics

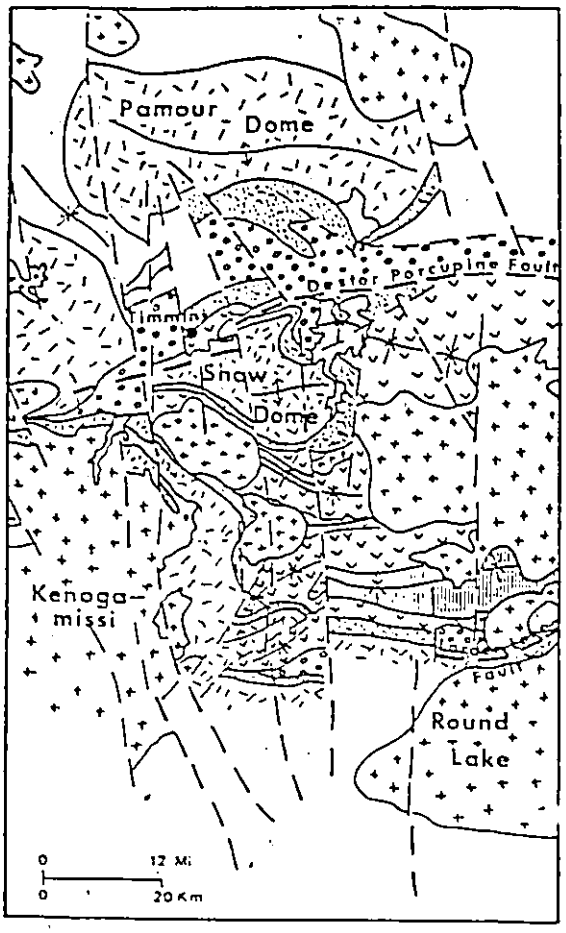

LEGEND
EARLY PRECAMBRIAN

PORCUPINE SUPERGROUP
UPPER SUPERGROUP
Upper Metavolcanic Group (calc alkalic)
Middle Metavolcanic Group (iron tholeiitic)
Lower Metavolcanic Group (komatiitic+mg tholeiitic)
LOWER SUPERGROUP
Unsubdivided

Figure 8 Regional stratigraphy of the Timmins area.

from Pyke, 1978b

TABLE 3

Volcanic and Sedimentary Stratigraphic Subdivision, Timmins Area

Dunbar (1948)	Ferguson et al (1968)	Pyke (1975)	Pyke et al. (1978)	Pyke (1978b)
Timiskaming	Timiskaming	Porcupine Group Upper Formation	Porcupine Group Upper Formation	Porcupine Supergroup Upper Group
	Keewatin	Lower Formation	Lower Formation	Lower Group
Hoyle				
	Tisdale Group	Tisdale Group Krist Formation	Tisdale Group Upper Metavolcanic Formation	Upper Supergroup Upper Metavolcanic Group
Tisdale Group	Gold Center Subgroup Vipond Subgroup Central Subgroup Northern Subgroup	Schumacher Formation	Middle Metavolcanic Formation	Middle Metavolcanic Group
		Goose Lake Formation	Lower Metavolcanic Formation	Lower Metavolcanic Group
Deloro Group	Deloro Group	Deloro Group Boomerang Formation	Deloro Group Upper Metavolcanic Formation	Lower Supergroup Upper Metavolcanic Group
		Redstone Formation	Middle Metavolcanic Formation	Middle Metavolcanic Group
		Donut Formation	Lower Metavolcanic Formation	Lower Metavolcanic Group

Note: Lower portion of the Porcupine Supergroup is time equivalent with the top of the Lower Supergroup and with the entirety of the Upper Supergroup.

which overlie a basal sequence of komatiitic flows. Chert-magnetite ironstones are interlayered with the mafic to intermediate calc-alkalic volcanic rocks, whereas chert sulfide ironstones occur near, or at, the transition into the Upper Supergroup (Pyke, 1978b). Dunitic intrusions occur throughout the Lower Supergroup. Within the Upper Supergroup, komatiitic ultramafic to mafic and magnesium tholeiitic basaltic flows occupy the basal section. This magnesium rich sequence is overlain by iron tholeiitic basalts which, in turn, are capped by calc-alkalic, felsic volcanic rocks. Ironstones having magnetic or conductive, electromagnetic signatures are notably lacking from the Upper Supergroup (Pyke, 1978b). Interlayering of komatiitic and calc-alkalic felsic volcanic rock along the contact zone between the Lower and Upper Supergroups is common (Pyke et al., 1978). The lower part of the Porcupine Supergroup (Lorsong, 1975), consisting predominantly of interlayered greywacke, siltstone and lesser conglomerate, is time equivalent to the upper portion of the Lower Supergroup and to the entirety of the Upper Supergroup (Pyke et al., 1978). The two detail study areas cover stratigraphically equivalent parts of the Lower Metavolcanic Group in the Upper Supergroup (Figure 9).

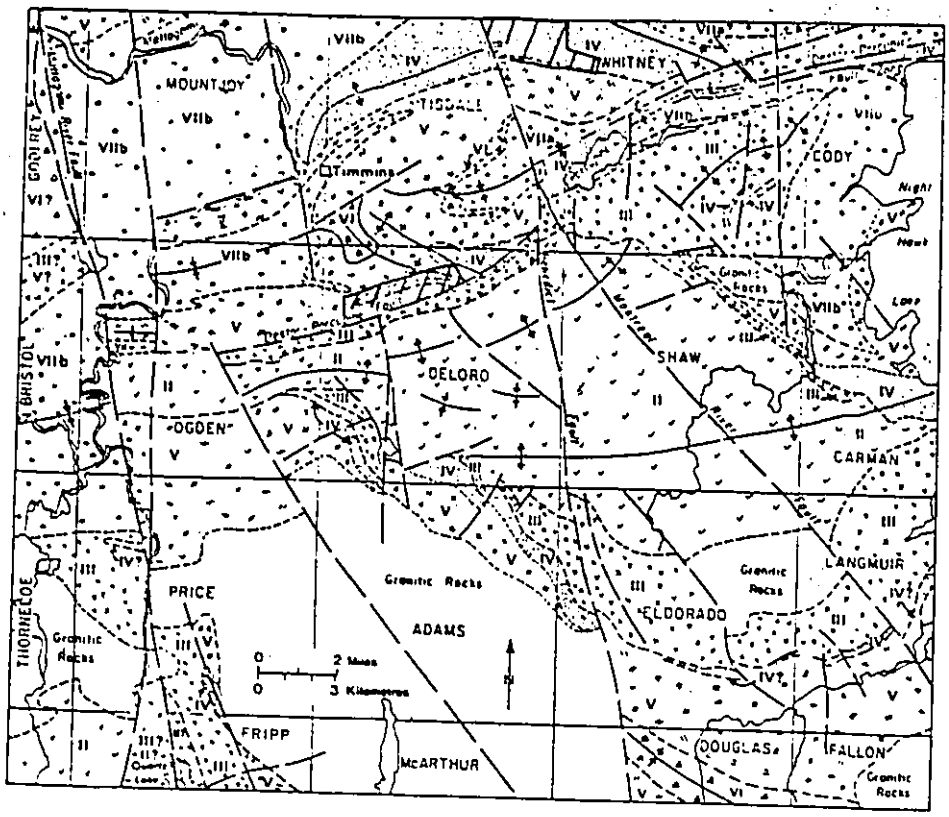

LEGEND

VII Porcupine Supergroup
a) Upper Formations
b) Lower Formations

Upper Supergroup
VI Upper Metavolcanic Group
V Middle Metavolcanic Group
IV Lower Metavolcanic Group

Lower Supergroup
III Upper Metavolcanic Group
II Middle Metavolcanic Group
I Lower Metavolcanic Group

SYMBOLS
Geological boundary
Fault
Anticlinal axis
Synclinal axis
Study areas

FIGURE 9 : Location of detailed study areas within regional stratigraphic setting. (from Pyke, 1975)

4.1 STRUCTURAL GEOLOGY OF THE UPPER SUPERGROUP

The structural interpretation of the Upper Supergroup has been subject to debate. Pyke (1975) concluded that an early period of isoclinal folding of the ultramafic and mafic volcanics (Lower and Middle Metavolcanic Groups) about a north-south axis predated the deposition of the Upper Metavolcanic Group (felsic pyroclastics) and the upper part of the Porcupine Supergroup. Later folding of the metavolcanics and metasediments, about an east-west axis produced the Porcupine Syncline (Figure 10) and was related to the development of the Destor-Porcupine fault (Pyke, 1975). Davies (1977) also favours two periods of folding, and relates the formation of the Porcupine Syncline to the second phase; however, Davies' (1977) interpretation differs in detail (Figure 10) from that of Pyke (1975). Criticism of Davies' (1977) interpretation has been levied by Karvinen (1978b). Roberts and Spiteri (1979) contend that the Porcupine Syncline is a complex series of structures which were initiated early during the development of the volcanic-sedimentary basin, and later modified by tectonic deformation.

The major fold structures within the Deloro study area are the Kayorum Syncline, and an unnamed, east-west trending, anticlinal structure located between the Destor-

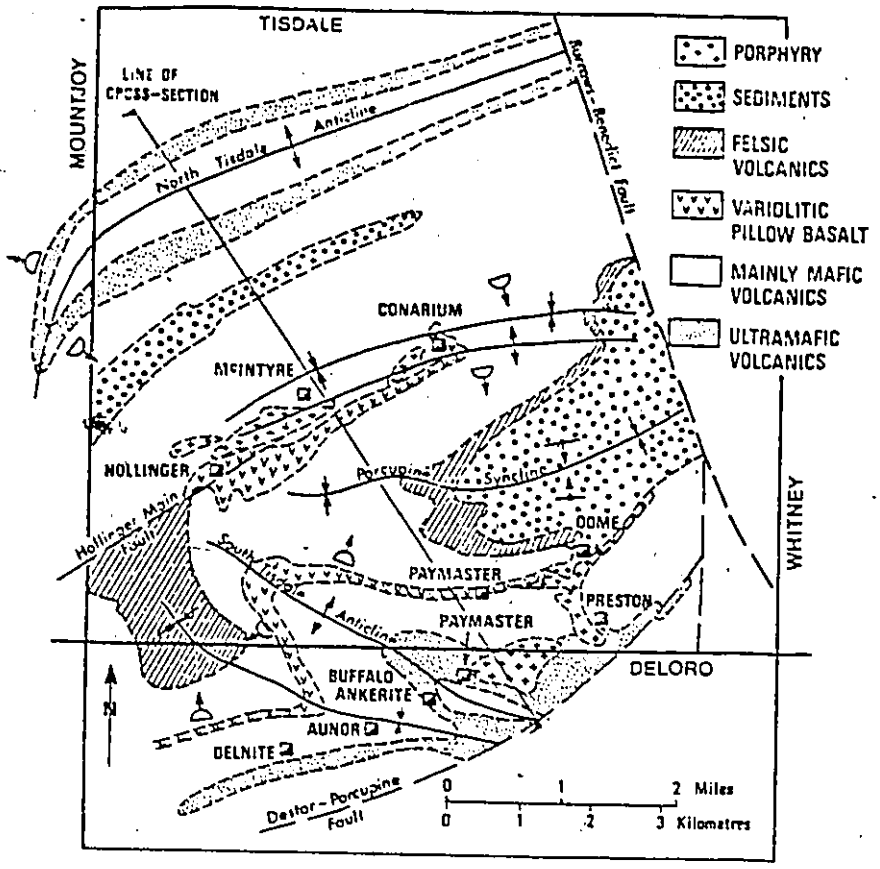

(from Pyke,1975)

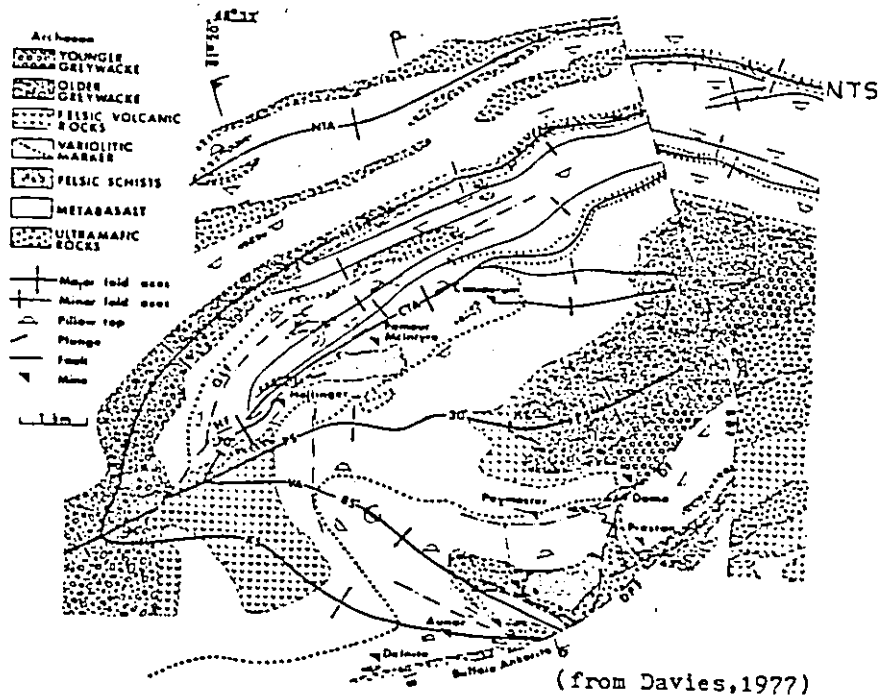

(from Davies,1977)

FIGURE 10 : Structure of the Timmins area(NTA North Tisdale Anticline;NTS North Tisdale Syncline;CTA Central Tisdale Anticline;PS Porcupine Syncline;VA Vipond Anticline;KS Kayorum Syncline;GLF Gilles Lake Fault;HF Hollinger Fault;DF Dome Fault;DPF Destor-Porcupine Fault;BBF Burrows-Benedict Fault).

Porcupine fault zone and the Delnite mine (Map 1).

Within the north study area, east of the Burrows-Benedict fault (Map 2), there are no field data to support the existence of the North Tisdale Syncline, postulated by Ferguson et al. (1968) and Davies (1977). This section is a south facing, homoclinal sequence.

Two sets of major faults cut and displace both the Upper and Porcupine Supergroup rocks. These late tectonic features trend northeast-southwest (Hollinger, Gilles Lake, Dome faults, Figure 10) or northwest-southeast (Burrows-Benedict, Montreal River faults, Figure 10). The Destor-Porcupine fault is of regional extent (Burrows, 1924; Ferguson et al., 1968) and is interpreted as part of a major fracture zone in the early Precambrian crust along which komatiitic volcanism and sedimentation were prominent (Pyke et al., 1978). Middleton (1976), citing gravity data, argues that west of Night Hawk Lake the Destor-Porcupine fault is not a major crustal feature and may not even exist. Detail field mapping during the course of this research (Map 1) reveals that the fault zone in Deloro township is marked by a topographical depression, bounded on the north by intensely deformed south facing, komatiitic and magnesium tholeiitic flows and on the south by north facing, andesitic tuffs (?). Thus a major structural discontinuity is present.

4.2 STUDY AREA GEOLOGY

4.2.1 Tisdale Township Study Area

The volcanic stratigraphy of this area is subdivided into three domains, in each of which one rock type predominates (Map 2; Figure 11). The stratigraphically lowest domain is dominated by ultramafic and mafic komatiitic flows, interbedded with lesser amount of magnesium (Mg), tholeiitic basalt and rare iron (Fe) tholeiitic basalt. The ultramafic komatiitic flows are polygonally jointed (Plate 1-1), although two spinifex bearing flows (Plate 1-2) crop out on the Beaumont property (Map 3). Interbedded with these ultramafic lavas are pillowed, locally vesicular, basaltic lavas which are Mg tholeiitic in composition. However, the spatial association of these basaltic lavas with ultramafic komatiitic flows and the local development of intrapillow, polygonal joints (Plate 2-1) confirms the komatiitic affinity of these basaltic flows (Pyke, 1979; personal communication). Microvariolitic, basaltic flows are exposed northwest of the Beaumont shaft (Map 3).

In this lowest domain, carbonatized, volcanic flows are exposed intermittently across northern Tisdale township (Map 2). On the Beaumont property (Map 3), both komatiitic and Mg-tholeiitic volcanic rocks have been altered. This

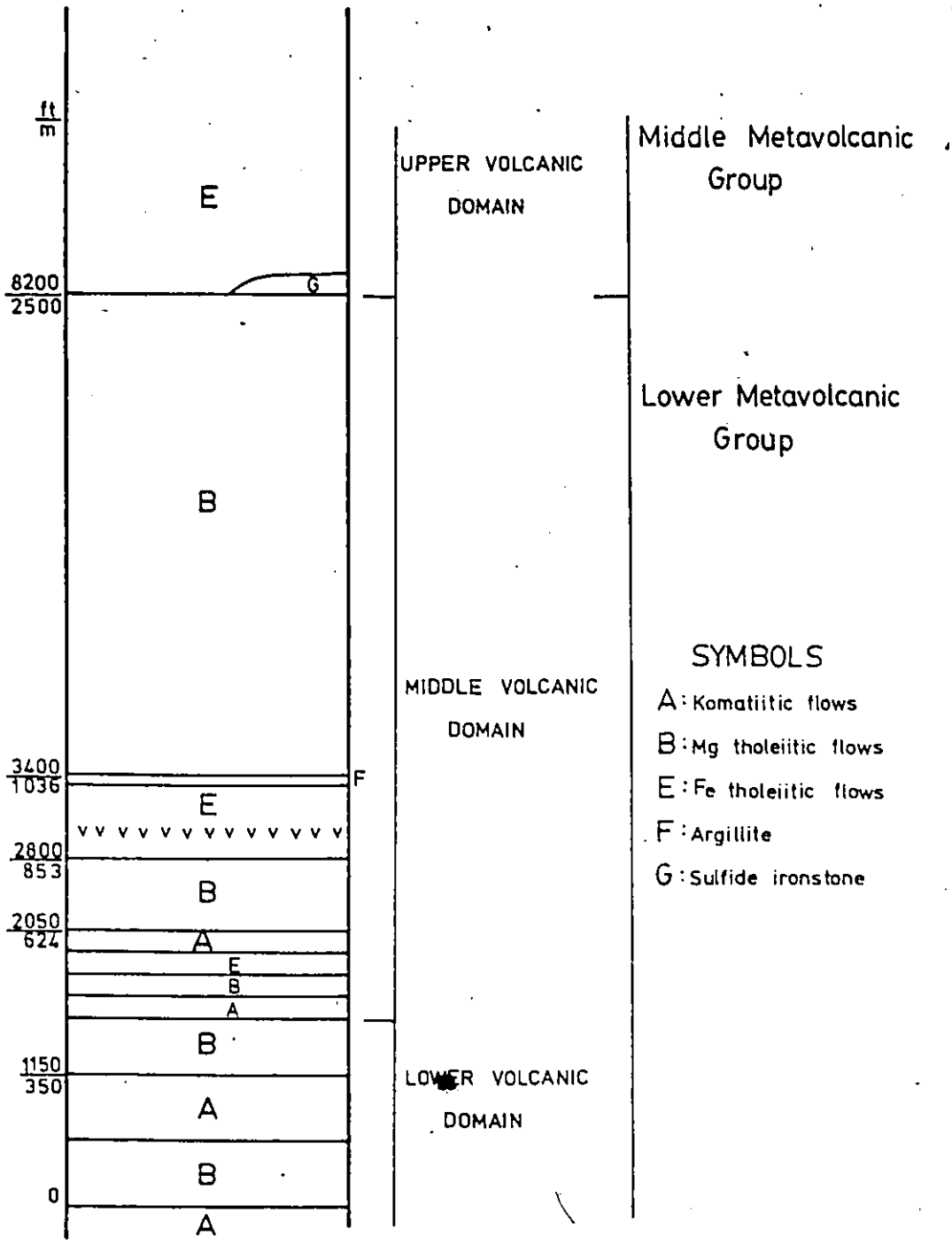

FIGURE 11: Simplified stratigraphic section through the Tisdale township study area. Group subdivision from Pyke (1978b).

PLATE 1-1. Polygonal jointing developed in carbonatized ultramafic, komatiitic flow exposed on the Buffalo Ankerite property (map 7)

PLATE 1-2. Olivine spinifex developed in a carbonatized ultramafic, komatiitic flow exposed on the Beaumont property (sample TR-241, map 3)

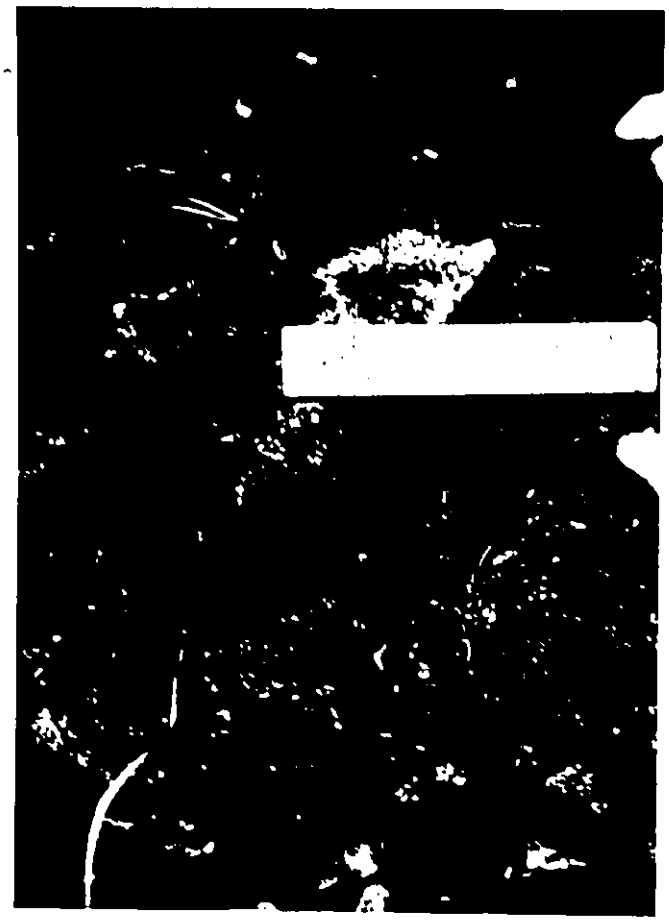

PLATE 2-1. Intrapillow, polygonal jointing developed in a mafic komatiitic flow exposed on the Beaumont property, north of sample B-2 (map 3). Locality revealed to the author by D. Pyke (Geologist, Precambrian Division, Ontario Geological Survey)

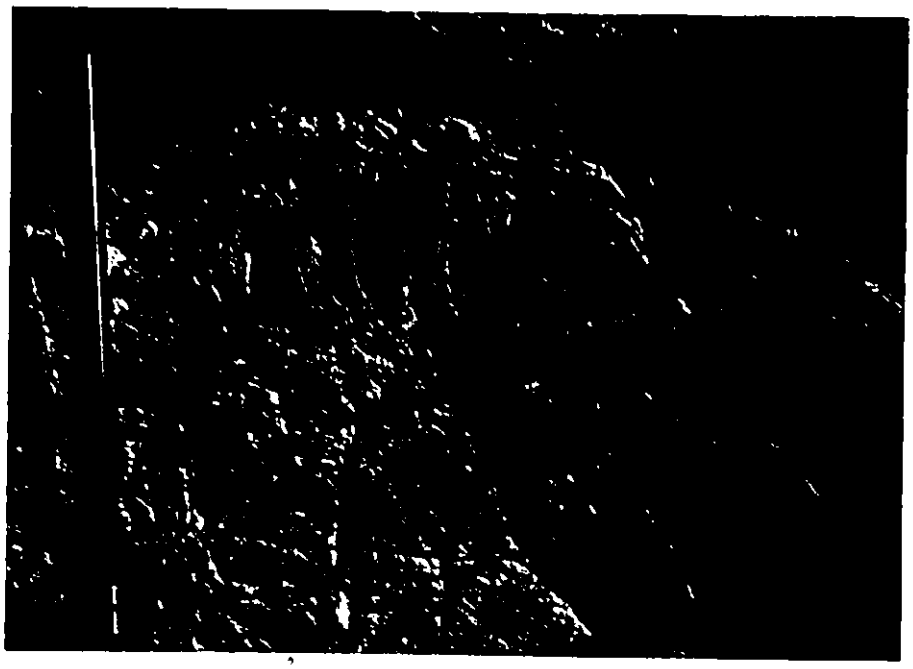

discordant alteration cross cuts a komatiitic-Mg tholeiitic flow contact where a massive, Mg-tholeiitic basalt lies in contact with the underlying komatiitic flows. No production was achieved from this property (Ferguson et al., 1968).

Within the middle volcanic domain, pillowed and "massive" Mg tholeiitic flows predominate, although Fe tholeiitic basalt, locally variolitic, occurs infrequently. Many of the Mg tholeiitic basalts are massive (proximal flow facies; Dimroth and Rocheleau, 1979). The thickest (60 m, 200 ft) Mg tholeiitic basalt flow, exposed on the east edge of the Kinch property (Map 4), consists of a massive base and core and a relatively thin pillowed top. Mg tholeiitic basalt pillows, which are bun shaped and average less than 1 m in length, generally have concentric cooling joints (Plate 3-1) and thicker selvages. Re-entrant pillows, although not common, are present locally (Plate 3-2). Lateral transitions from massive to pillowed facies have been observed on the Davidson Tisdale and Kinch properties (Maps 5, 6, 4). Massive lava tongues or branches, enclosed by pillowed facies are exposed above a prominent flow top breccia on the Davidson Tisdale property (Map 5). Flow top breccias consist of pillow breccia (Plate 4-1), hyaloclastite granules (Plate 4-2) or mixtures of both.

PLATE 3-1. Concentric cooling joints in a pillowed, magnesium tholeiitic flow exposed on the Kinch property (map 2)

PLATE 3-2. Re-entrant pillow containing an intrapillow, silica filled void, developed in a pillowed, magnesium tholeiitic basalt flow exposed on the Davidson-Tisdale property (map 5)

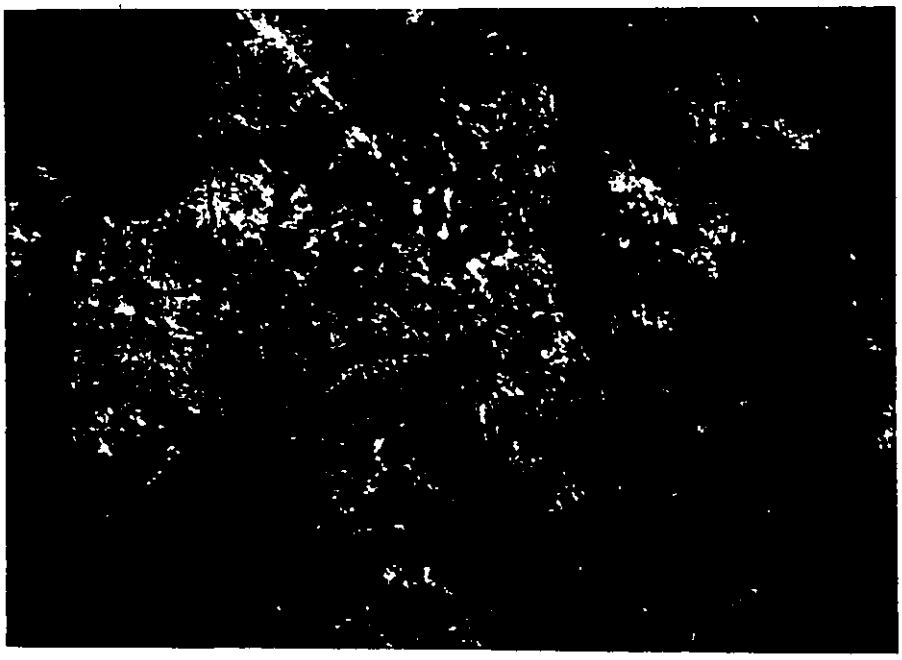

PLATE 4-1. Flow top breccia consisting of vesicular pillow fragments, which caps a magnesium tholeiitic basalt flow, exposed south of the Canusa property (map 2)

PLATE 4-2. Flow top breccia consisting of hyaloclastite granules which caps a magnesium tholeiitic basalt flow exposed on the Kinch property (map 4)

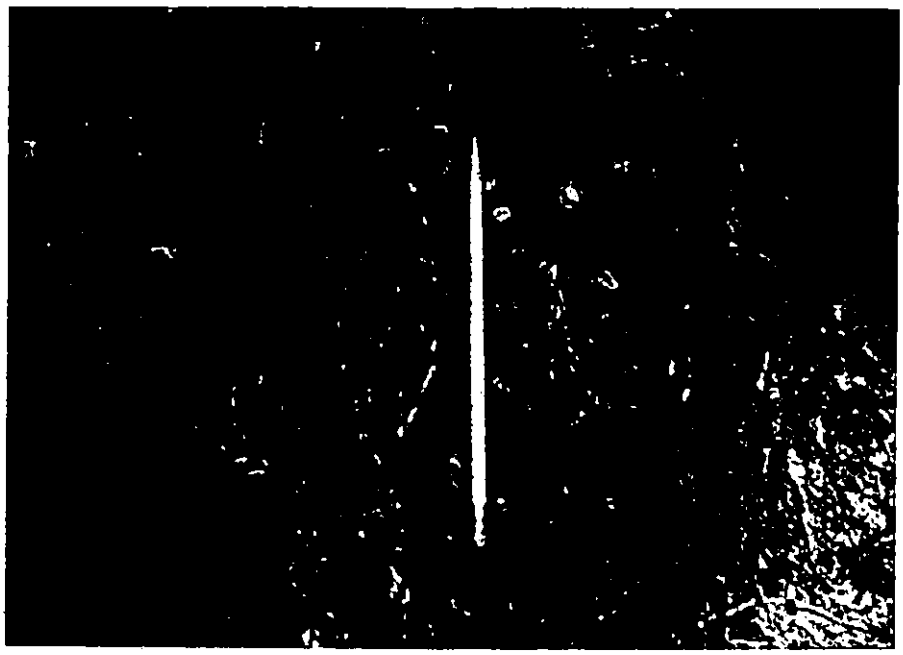

Fe tholeiitic flows in this middle domain occur on the Kinch property as pillowed, variolitic units and as a massive, regionally extensive flow unit which lies between the Kinch and Dobell properties (Maps 4, 2). This massive flow was interpreted as a porphyritic latite containing over 10% mafic minerals (Ferguson et al., 1968; Davies, 1977); however, texturally and chemically this flow is an Fe tholeiitic basalt (Map 5).

The only interflow sediment exposed in this middle volcanic domain is a thin (<6 m, <20 ft), finely laminated argillite (Plate 5-1) which overlies the regionally extensive, massive, Fe tholeiitic flow north of the Dobell property (Map 2). The presence of this argillite attests to a local volcanic hiatus following the termination of a volumetrically small pulse of Fe tholeiitic magma, prior to the ensuing Mg tholeiitic volcanism.

Many zones of carbonate alteration occur within this middle domain (e.g. Kinch, Dobell, Davidson Tisdale, Armstrong McGibbon, Crown Chartered properties, Map 2). Only the Davidson Tisdale mine realized any production (2400 oz; Ferguson et al., 1968. Much of the alteration is localized at flow contacts (e.g. Kinch property, Map 4) or as discordant zones (e.g. Kinch, Davidson Tisdale, Crown Chartered properties; Maps 4, 5, 6) cutting massive or

PLATE 5-1. Finely laminated "argillite" which lies upon the massive, iron tholeiitic flow, exposed north of the Dobell property (map 2)

pillowed flows. Clearly, within the Lower Metavolcanic Group, carbonate alteration occurs throughout the volcanic stratigraphy as both stratabound and discordant zones.

The upper volcanic domain consists primarily of Fe tholeiitic basalts, many of which are variolitic (formerly Vipond Supergroup; Ferguson et al., 1968). The contact between the middle and upper volcanic domains corresponds to the contact between the Lower and Middle Metavolcanic Groups, defined by Pyke (1975, 1978b). To the east, in Whitney township (Map 2), a thin sulfide ironstone lies along this contact attesting to a local volcanic hiatus following the arrest of the Mg tholeiitic volcanism and before the onset of Fe tholeiitic volcanism. These Fe tholeiitic basalts define the limit of the study area and they were not examined in detail.

No felsic volcanic rocks (e.g. quartz-feldspar porphyry or sericite schist) are known to exist in this section of the camp.

4.2.2 Deloro Township Study Area

This volcanic succession (Map 1) is stratigraphically equivalent to that of the North Tisdale section, in that both study areas encompass komatiitic and Mg tholeiitic

flows of the Lower Metavolcanic Group. Mg tholeiitic basalts define a middle volcanic domain which is overlain by an Fe tholeiitic basalt rich upper domain and underlain by a komatiitic rich, lower volcanic domain (Figure 12). In detail (Figure 13), the lower domain consists of interbedded komatiitic and Mg tholeiitic flows, local accumulations of chemical and volcaniclastic sediments and felsic volcanic rocks (qiartz-feldspar porphyry). Hence, a significant difference between the Deloro and Tisdale study areas is the presence of felsic volcanic rocks and chemical and volcaniclastic sediments in the former area.

Within the middle, Mg tholeiitic basaltic domain exposed on the Buffalo Ankerite property (Map 7), is a massive, siliceous limestone which lies conformably within a fissile tuff or volcaniclastic argillite unit. The lack of volcanic textures, its lithological association and its major and trace element geochemistry (Table 4) confirm the chemical, sedimentary nature of this limestone.

On the Buffalo Ankerite property (Map 7) a chemical and volcaniclastic sedimentary sequence overlies komatiitic flows of the lower volcanic domain (Figure 13). The oldest sedimentary member is a highly siliceous rock averaging 1 m (3 ft) in thickness which, based on the following observations, is interpreted as an exhalative chert:

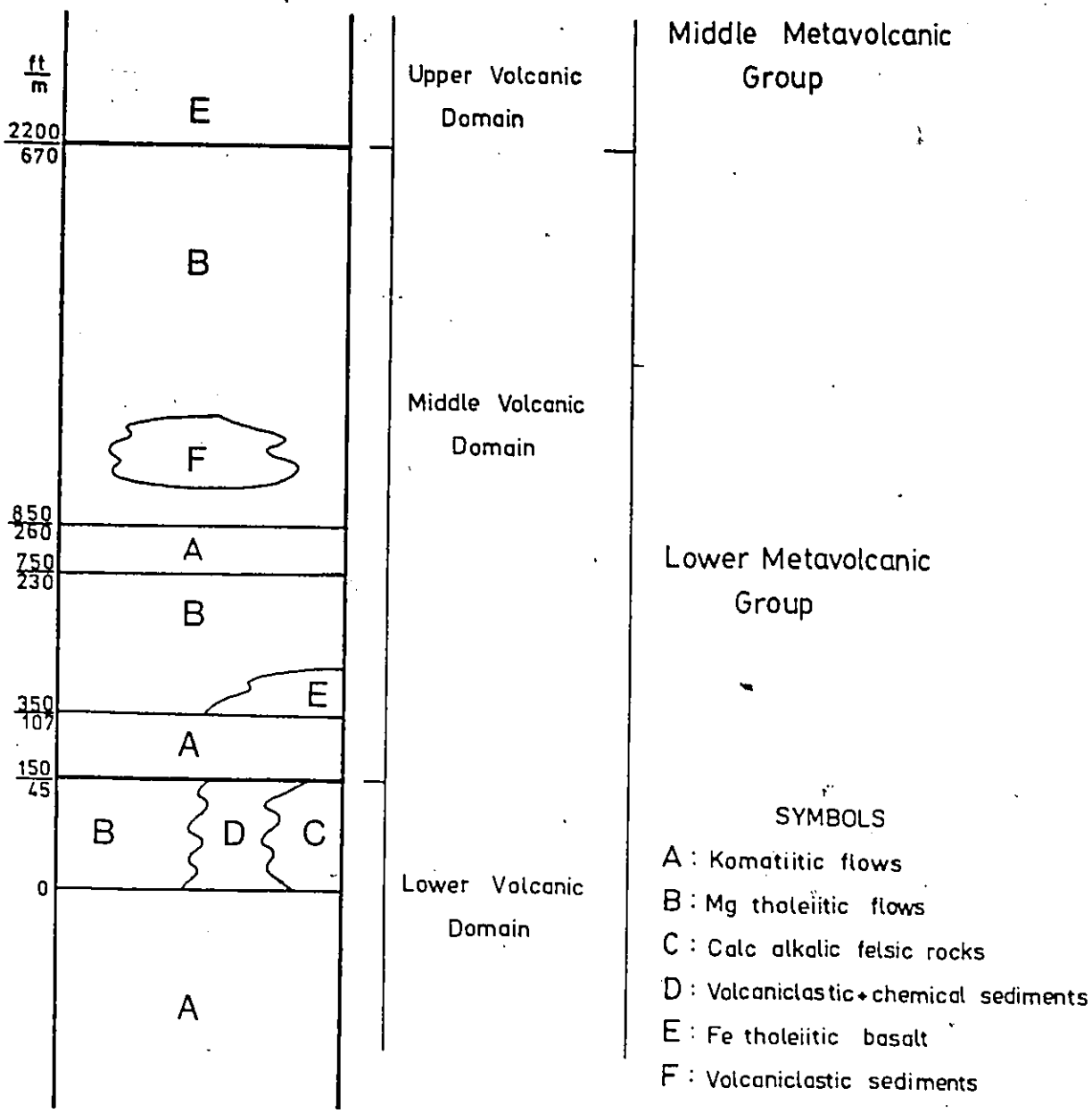

FIGURE 12: Simplified stratigraphic section through the Deloro township study area. Group subdivisions from Pyke(1978b)

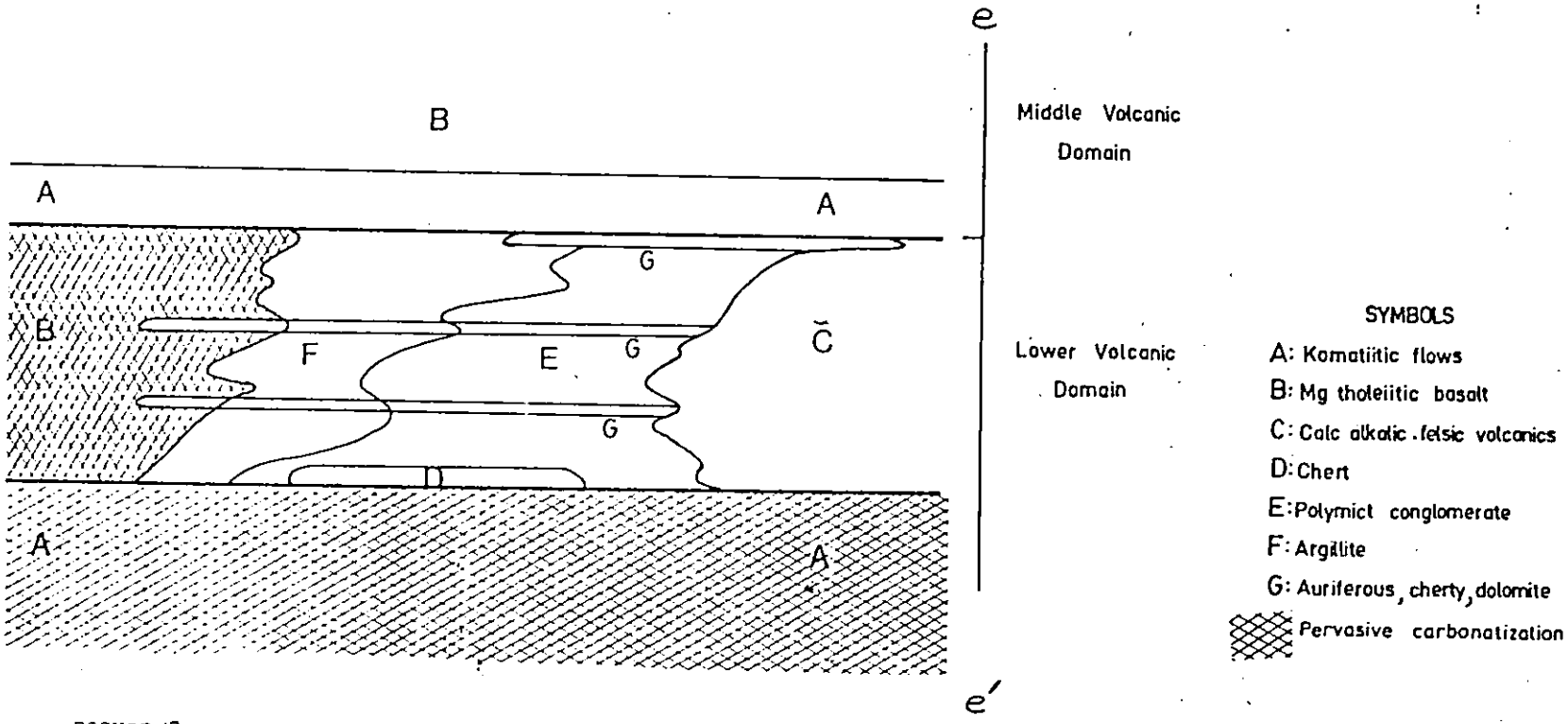

FIGURE 13 : Schematic cross-section e-é through the Buffalo Ankerite south ore zone.

TABLE 4

Chemical Composition Of Sedimentary, Siliceous Limestone on the Buffalo Ankerite Property

Sample No:	DR-102	DR-110	DR-115	DR-123	Lab affiliation + units
SiO_2		24.78	10.67		McMaster University
Al_2O_3		4.81	1.54		
Fe_2O_3		4.75	4.78		
MgO		7.84	12.55		
CaO		25.10	27.61		
Na_2O		nd	nd (<2·0)		weight percent
K_2O		0.41	0.18		
TiO_2		0.24	0.07		
MnO		0.04	0.10		
P_2O_5		0.09	0.21		
L.O.I.		31.92	42.30		
Ni		55.	32.		McMaster University
S		57.	203.		
Rb		22.	5.		
Sr		118.	122.		p.p.m.
Zr		41.	47.		
Cr		33.	12.		
Co		15.	9.		
Cu		21.	7.		
Zn		41.	66.		
As		nd	nd (<70·)		
As	6.	6.	nd	nd (<1·0)	Ontario Geoscience Laboratory
Ba	90.	50.	70.	50.	
Bi	nd	nd	nd	nd (<0·1)	
Co	12.	15.	9.	nd (<5·)	
Cr	19.	10.	15.	10.	p.p.m.
Cu	6.	10.	nd (<5·)	5.	
Li	9.	7.	4.	4.	
Ni	15.	13.	15.	8.	
Pb	16.	22.	23.	21.	
Sb	0.3	0.2	0.1	0.2	
Zn	54.	42.	63.	62.	
CO_2	34.4	37.3	42.7	33.2 wt %	
S	nd	nd	nd	nd wt % (<0·01)	

nd ≡ not detected

1. The unit conformably overlies the basal ultramafic komatiitic flows;

2. There is a regular lamination, defined by colour variation, on a centimeter scale, the attitudes of which are parallel to local bedding attitudes (Plate 6-1);

3. Locally the rock contains intraformational breccia (Plate 6-2);

4. Quartz stockwork feeder veins, which are orthogonal to the local bedding attitudes, cross-cut the komatiitic footwall rocks and terminate at the base of the siliceous unit.

Conformably overlying this chert is a polymictic, matrix supported conglomerate containing clasts of carbonatized mafic and ultramafic lava, chert, quartz-feldspar porphyry (Plate 7-1) and flow banded rhyolite (Plate 7-2). The clasts are angular to subrounded in cross-section. Nowhere have "fresh" clasts of mafic or ultramafic volcanic rock been observed. The conglomerate unit is thickest where exposed in the pit area (Map 7) and thins to the east and west where intercalations of finely laminated, volcaniclastic argillites and Mg tholeiitic basalts appear. The

PLATE 6-1. Colour lamination parallel to the hanging-wall contact developed in a siliceous chert exposed south of the open pit on the Buffalo Ankerite property (map 7). Hangingwall is a polymict, matrix supported volcaniclastic conglomerate

PLATE 6-2. Intraformational breccia present in the chert exposed south of the Buffalo Ankerite open pit (map 7). Same locality as Plate 6-1

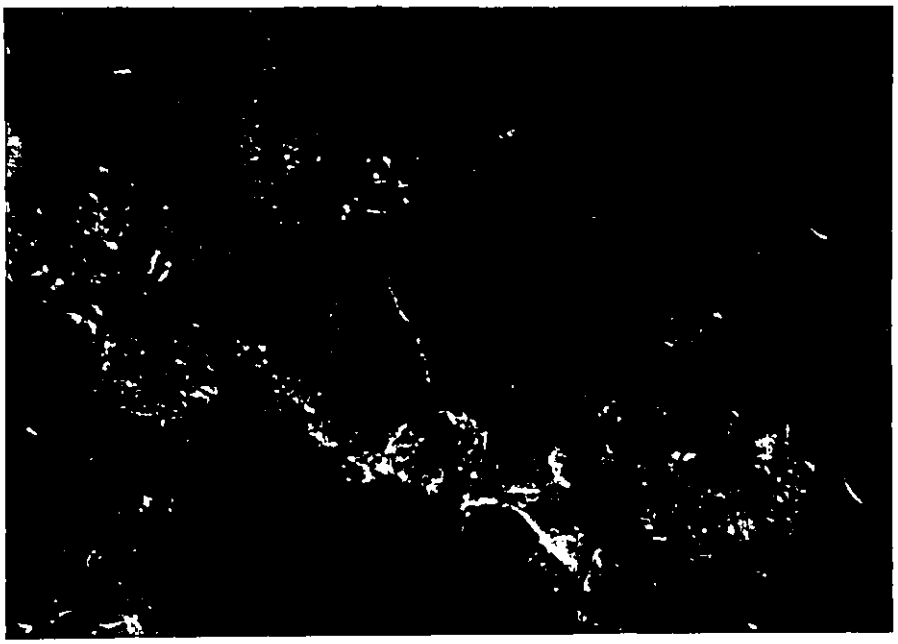

PLATE 7-1. Matrix supported, volcaniclastic conglomerate consisting of angular quartz-feldspar porphyry fragments (white) and carbonatized, ultramafic, komatiitic flow fragments, exposed in the Buffalo Ankerite open pit (map 7)

PLATE 7-2. Flow banded rhyolite fragment hosted in the matrix supported, volcaniclastic conglomerate exposed in the Buffalo Ankerite open pit (map 7)

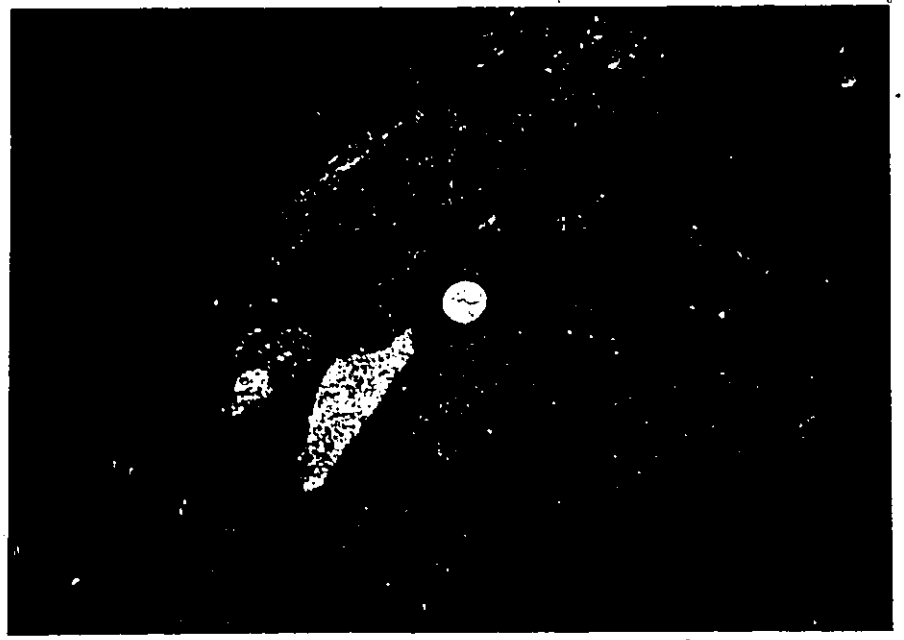

chemical composition of this volcaniclastic conglomerate/ argillite unit (Table 5) confirms its derivation from a predominantly komatiitic source area. Note also the high CO_2 content of the samples. The transitional change from clastic sediments to effusive, Mg tholeiitic lavas confirms their time equivalence. Uncarbonatized ultramafic and mafic komatiitic flows, forming the base of the middle volcanic domain (Figure 13), conformably overlie the sedimentary package and time equivalent Mg tholeiitic basalts of the lower volcanic domain. Down dip, the stratigraphic section containing the carbonate-rich, clastic sediments, is occupied by the stratabound, Buffalo Ankerite quartz-feldspar-sericite schist (Q.F.P.). This Q.F.P. lies conformably between the komatiitic flows of the lower domain and those which define the base of the middle volcanic domain (Figure 13). The fragments of Q.F.P. and flow banded rhyolite found in the volcaniclastic conglomerate must have been derived by denudation of this large Q.F.P. body.

Stratiform, exhalative, auriferous, cherty dolomites (Fryer and Hutchinson, 1976; Fryer et al., 1979) lie within the clastic sedimentary sequence and within the lateral, time equivalent, tholeiitic and komatiitic flows of the lower volcanic domain (Figure 13).

TABLE 5

Chemical Composition Of Polymict, Matrix Supported Conglomerate And Argillite Unit Exposed In The Buffalo Ankerite Mine Pit Area.

Rock Type	Cong.	Cong.	Arg.	Arg.	Cong.	
Sample Number	DR-144	DR-145	DR-146	DR-148	DR-149	
SiO_2	30.13					wt %
Al_2O_3	6.16					
Fe_2O_3	9.67					
MgO	17.81					
CaO	10.71					
Na_2O	<2.0					
K_2O	0.2					
TiO_2	0.41					
MnO	0.12					
P_2O_5	0.05					
CO_2	24.2	26.00	22.30	24.70	28.50	
S	0.11	0.01	0.05	0.01	0.02	
LOI	24.75					
Au	49.2			0.5	24.60	ppb
As	99.	13.	4.	2.	240.	ppm
Ba	30.	30.	20.	20.	100.	
Bi	0.1	0.1	0.1	0.1	0.2	
Co	77.	68.	61.	68.	76.	
Cu	25.	30.	104.	44.	57.	
Li	28.	18.	11.	23.	14.	
Ni	990.	1070.	620.	1120.	980.	
Pb	10.	11.	11.	10.	11.	
Sb	1.3	0.3	0.2	0.2	2.6	
Zn	42.	58.	58.	32.	40.	
Cr	1870.	2090.	1490.	1470.	1690.	

Cong: Conglomerate
Arg : Argillite

The sedimentary package exposed on the Buffalo Ankerite property is significant as it represents material which was deposited during a local tholeiitic/komatiitic volcanic hiatus. Felsic volcanic rocks (Q.F.P.) also accumulated locally during this hiatus. The absence from the conglomerate of relatively fresh mafic or ultramafic material derived from the overlying middle domain volcanics has two alternate implications regarding the timing of the carbonatization process. Firstly, it is conceivable that the alteration was very late (post-middle volcanic) and that the distribution of the alteration was governed primarily by porosity factors such that only the comglomerate, related argillites and associated mafic and ultramafic volcanic rocks of the lower domain were affected. Alternatively, the carbonatization process was essentially synvolcanic and was focused in one stratigraphic block within the lower volcanic domain spatially related to the Q.F.P. The CO_2 rich nature of the clastic sediments reflects their derivation from a pre-existing carbonatized source area, or alternatively the clastic detritus was itself carbonatized on the seafloor during the accumulation of the sedimentary unit.

The intimate association of chemical sediments, manifest as chert and auriferous, cherty dolomites, within,

and stratigraphically, juxtaposed against pervasively, carbonatized volcanics of the lower volcanic domain confirms the genetic link between the carbonate alteration, the felsic volcanics and the chemical sediments. The spatial restriction of the auriferous sediments and the carbonate alteration to the top of the lower volcanic domain in the mine area strongly suggests that the hydrothermal alteration took place prior to the commencement of the komatiitic and Mg tholeiitic volcanism of the middle volanic domain. That is, the carbonate alteration was synvolcanic/synsedimentary in the lower volcanic domain.

Carbonatized tholeiitic and komatiitic volcanic rocks occur throughout the stratigraphy in this study area (Map 1). On the Buffalo Ankerite property (Map 7) the komatiitic flows at the base of the lower volcanic domain (Figure 13) are extensively carbonatized, whereas the komatiitic flows at the base of the middle domain are generally carbonate free. Carbonatized Mg tholeiitic basalts are exposed south of Skynner Lake, on the Delnite, Aunor and Buffalo Ankerite properties, on the McBine Porcupine ground and south of McDonald Lake (Map 1). The altered rocks lie at various stratigraphic elevations and collectively do not define two

discrete, regionally continuous stratabound altered zones as proposed by Karvinen (1976, 1978).

4.3 NATURE OF THE GOLD ORE IN THE DELORO TOWNSHIP STUDY AREA

Detail geological studies (Roberts and Spiteri, 1979; Karvinen, 1976, 1978; Fyon and Karvinen, 1978; Fyon and Crocket, 1979), petrographic and geochemical studies (Fryer and Hutchinson, 1976; Fryer et al., 1979; Kerrich and Fryer, 1979) reveal that some ore material in the Hollinger, McIntyre, Dome, Aunor, Delnite, and Buffalo Ankerite mines consisted of exhalative, stratiform, auriferous, cherty dolomite (Plate 8-1). These sediments consist of millimeter scale lamination defined by chert (Fryer et al., 1979), dolomite and tourmaline, although the phase proportions are quite variable. The most striking feature of these interflow sediments is the presence of transverse, gash of "ladder" quartz veins (Plate 8-1), which rarely cut into the adjacent host rock. Underground examination of the Aunor workings and surface inspection of the Buffalo Ankerite open pits, reveals that the cherty, dolomite, interflow sediments range in thickness from several centimeters to in excess of

PLATE 8-1. Stratiform, auriferous, cherty-dolomite, 0.3 meters in thickness, exposed on the 1000 level, Aunor Mine in the Deloro township study area. Transverse tensional, "ladder", quartz veins cross cut cherty dolomite, but terminate at the sediment/ host rock contact. Note abundant, disseminated pyrite (yellow) in wallrock and in cherty dolomite

20 cm

3 meters (Plates 9-1, 9-2). These auriferous sediments are hosted in finely laminated tuffs and volcaniclastic sediments (Plate 9-1), or lie conformably along flow contacts (Plate 10-1). Gold is reported to be included in pyrite grains and in a native state often at the edge of the quartz "ladder" veins (Fryer et al., 1979). At the Paymaster mine, Longley and Lazier (1948) reported that the silica to carbonate ratio and gold tenor of the interflow ore increased with increasing proximity to the Paymaster Q.F.P., although quartz "ladder" veins were developed in these carbonate rich sediments, regardless of proximity to the Q.F.P. The interflow sediments of the Aunor and Buffalo Ankerite mines are carbonate rich in distal areas, and become silica and tourmaline rich with increasing proximity to the Buffalo Ankerite Q.F.P.

Within the Deloro township study area, all the auriferous, cherty dolomites occur within a thin (60 m, 200 ft) stratigraphic section, which is continuous from the Delnite to the Buffalo Ankerite mines (Figure 14). This stratigraphy lies at the top of the lower volcanic domain (Figure 12) and consists of pillowed, Mg tholeiitic basalt, volcaniclastic sediment and the Delnite and Buffalo Ankerite Q.F.P.'s.

PLATE 9-1. Thin cherty dolomites hosted in a volcaniclastic argillite exposed in the Buffalo Ankerite west pit (map 7)

PLATE 9-2. Thick (2 meter) cherty dolomite overlying the volcaniclastic conglomerate exposed at the east end of the east pit on the Buffalo Ankerite property. Hammer handle lies parallel to the contact between the cherty dolomite (left) and the polymict, komatiitic conglomerate (right).

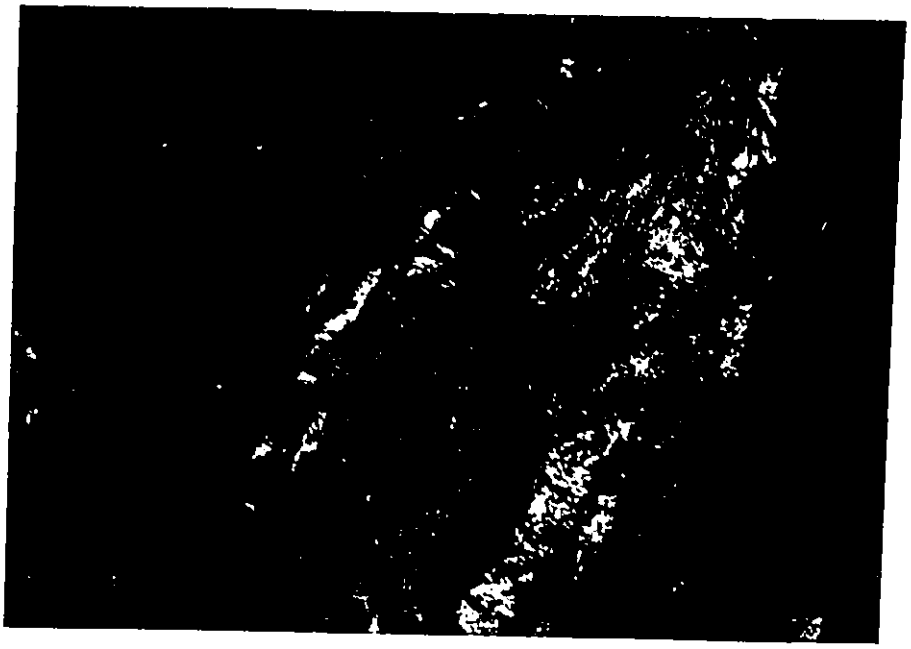

PLATE 10-1. Auriferous, cherty dolomite (0.05 meters), cut by quartz "ladder" veins, which lies conformably above a flow top breccia, exposed on the 1000 level of the Aunor Mine. Note that the hyaloclastite granules sit in a dark coloured dolomitic matrix

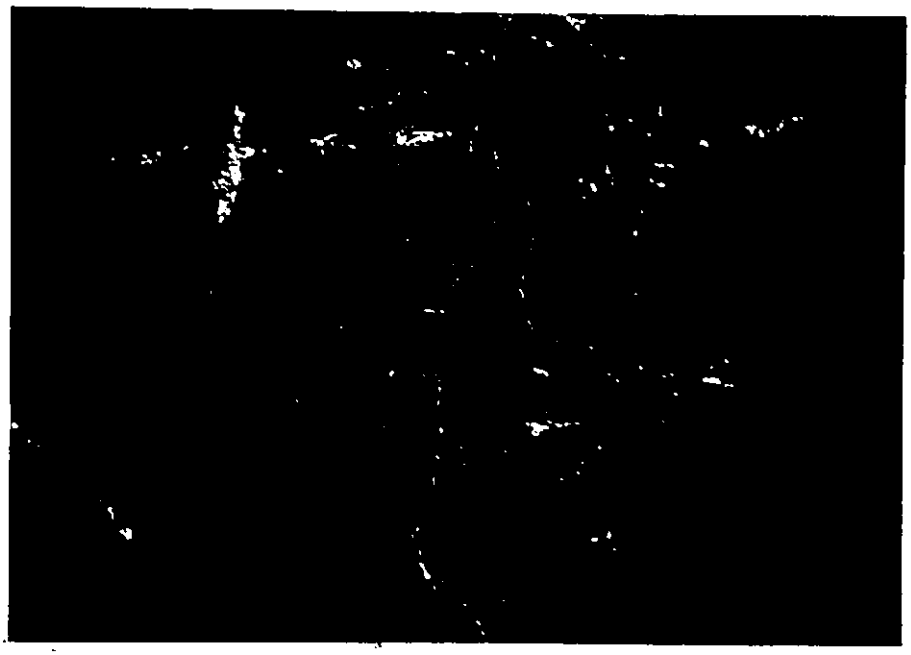

10 cm

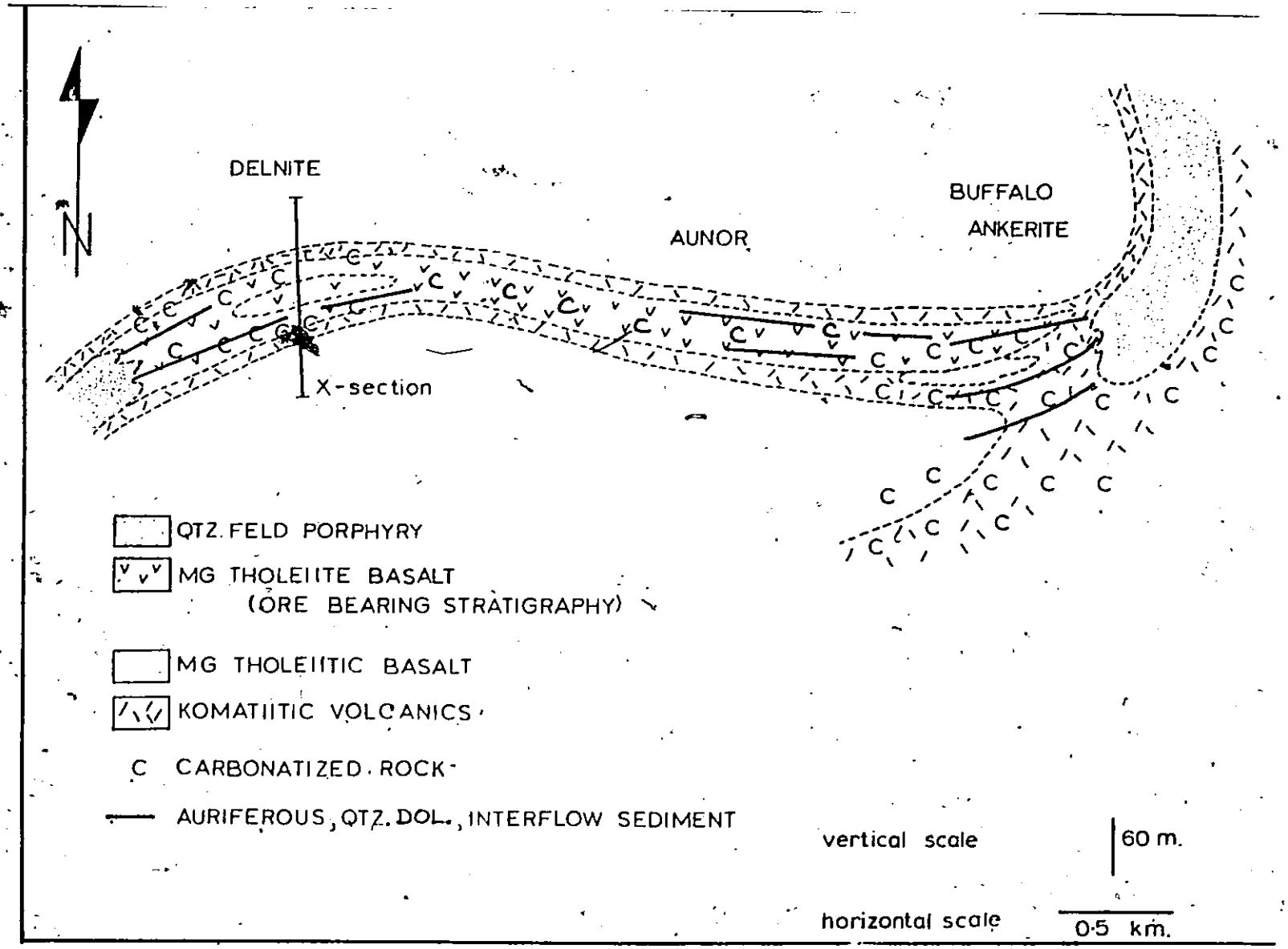

FIGURE 14 : Generalized, underground, geological plan of the 1000 level which illustrates the regional stratigraphic control of the exhalative dolomites, the stratabound, felsic volcanics (Q.F.P.) and carbonatized rock. (Geology after Taylor, 1948, and Kinkel, 1948)

CHAPTER 5

PETROGRAPHY

5.1 KOMATIITIC VOLCANIC ROCK

Ultramafic and mafic komatiitic flows occupy the lower 600 m (2000 ft) of the Upper Supergroup stratigraphy. A general chemical evolution from ultramafic to mafic komatiite occurs with increasing stratigraphic distance from the base of the Upper Supergroup.

5.1.1 Ultramafic Flows

Polygonal jointing (Plate 1-1), spinifex textures (Plate 1-2) and the red-brown colour of the weathered surface serve as the most useful field identification criteria. By far, the most common flow texture is polygonal jointing. Spinifex texture is rare, but is developed in carbonatized, peridotitic flows on the Beaumont property and at the Pamour mine (Figure 2). Poor exposure hinders accurate estimation of flow length; however, flow units can be traced for tens

of kilometers (Pyke, 1978b). Flowtops are indicated by hyaloclastites, by decreasing size of polygonal joints or by spinifex orientation and grain size when present. Pillowed, ultramafic, komatiitic flows, although not common in the study areas, are exposed on the Kinch property (Map 4).

All primary mineralogy has been altered to secondary hydrous or quartz-carbonate rich assemblages (Figure 15). Least hydrous flows consist of alpha-serpentine or lizardite (Wicks et al., 1977) mesh textures after olivine. Hour-glass and uniform-mesh textures are most common (Plate II-1). Rarely magnesium chlorite pseudomorphs the olivine grains, but only in more hydrated samples (loss of ignition [L.O.I.] >8.0 wt %). Carbonate grains are found in the least hydrous samples (TR-408, L.O.I. = 6.2 wt %), but the proportion of carbonate does not exceed 0.5 % by mode until the volatile content of the rock exceeds 9 wt % (B-16). Tremolite occurs in veinlets and as disseminated grains in the freshest flows (TR-408; 6.2 wt % L.O.I.), but the veinlets have diffuse boundaries with the serpentine (lizardite) -tremolite matrix. With increasing degree of alteration, carbonate grains appear in veinlets, associated with tremolite and talc. The carbonate grains, although anhedral in shape, generally have intergranular angles of 120°, suggesting there has been annealing since their precipitation. On a

FIGURE 15. Variation of the alteration mineral assemblages in ultramafic komatiitic flows from the Timmins area as a function of alteration intensity, expressed as a loss on ignition.
Abbreviations are as follows:
ch (Mg-rich chlorite), S (serpentine), tr (tremolite), tc (talc), D (dolomite), C (calcite), M (magnesite), Q-Ab (quartz and albite), O (opaques)

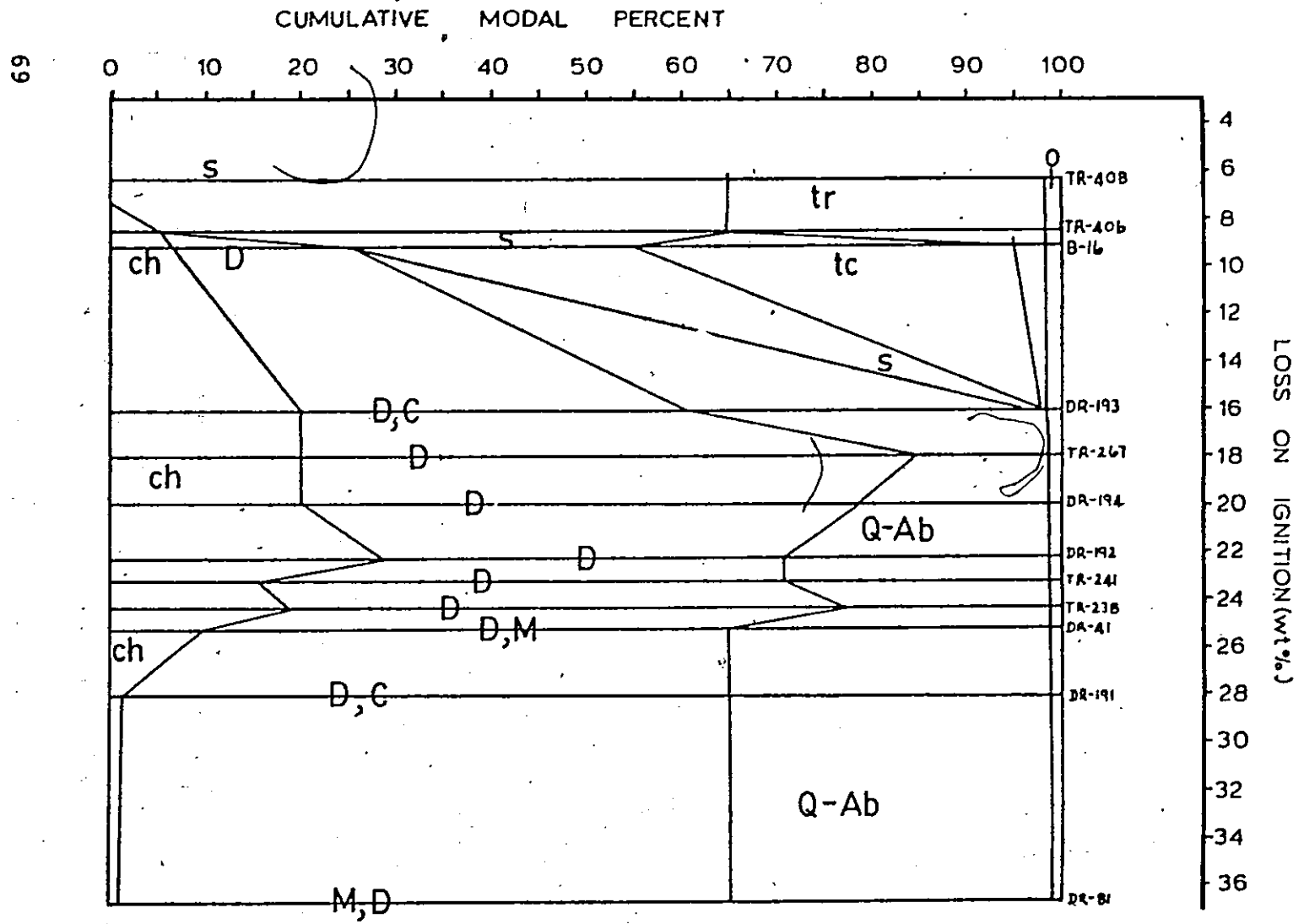
CUMULATIVE MODAL PERCENT
0
10
20
30
40
50
60
70
80
90
100
LOSS ON IGNITION (wt%)
4
6
8
10
12
14
16
18
20
22
24
26
28
30
32
34
36
TR-408
TR-406
B-16
DR-193
TR-267
DR-194
DR-192
TR-241
TR-238
DR-41
DR-191
DR-81
s
tr
ch
D
tc
D,C
Q-Ab
M,D

PLATE 11-1. Typical, serpentinized olivine, hour-glass mesh texture developed in an ultramafic, komatiitic flow.

0·5 cm

centimeter scale, assemblages within veins include carbonate, carbonate-tremolite, carbonate-tremolite-talc, and talc. The talc occurs at the veinlet termination (Plate 5-3), whereas the carbonate assemblages occur in the wider parts of the veinlet (Plate 5-4). This microscopic alteration assemblage sequence of hydrosilicate, hydrosilicate plus carbonate to carbonate is identical to the megascopic alteration assemblage sequence developed on a flow scale in response to increasing degree of alteration (as measured by increasing volatile content). Quartz, associated with abundant chlorite does not appear as a matrix phase until virtually all serpentine has been destroyed (DR-193; L.O.I. = 16.0 wt %). The chlorite, quartz, dolomitic-carbonate assemblage characterizes the altered ultramafic komatiites over a wide range of volatile content (16 to 26 wt % L.O.I.); however, chlorite is present only in trace amounts in the most intensely carbonatized rocks (DR-191; L.O.I. >28 wt %). Traces of green mica, assumed to be fuchsite, are present in the pervasively carbonatized samples.

Magnetite and chromite occur in most komatiitic flows regardless of degree of alteration; however, chromite is always mantled or replaced by a magnetite rim. Magnetite also occurs as disseminated, bladed crystals or in veinlets cutting serpentinized olivine. Both magnetite and chromite

PLATE 12-1. Talc in the terminal parts of a talc-tremolite-carbonate veinlet which cuts a serpentinized, ultramafic, komatiitic flow

PLATE 12-2. Carbonate-tremolite in the wider part of the talc-tremolite-carbonate veinlet which cuts a serpentinized, ultramafic, komatiitic flow

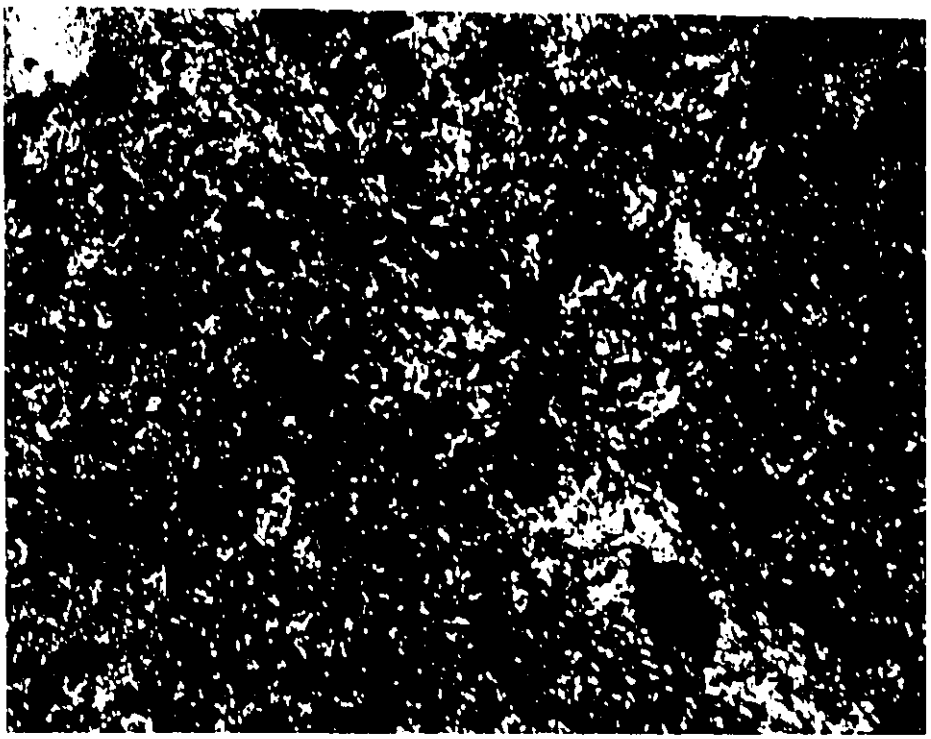

2mm

1mm

are partially replaced by carbonates (Plate 3-1).

A detailed examination of the sulfide mineralogy, as a function of degree of alteration, was not carried out. However, Eckstrand (1975) describes the following sulfide alteration assemblages in a serpentinized and carbonatized ultramafic sill:

1. magnetite + pentlandite + awaruite (partly serpentinized);
2. magnetite + awaruite ± heazlewoodite;
3. magnetite + heazlewoodite;
4. magnetite ± pentlandite ± heazlewoodite;

(2, 3, 4: completely serpentinized)

5. magnetite + pentlandite ± heazlewoodite ± millerite (talc-carbonate).

These silicate buffered, sulfide-oxide assemblages are characteristic of virtually all described, altered ultramafic bodies (Eckstrand, 1975).

5.1.2 Mafic Flows

Mafic komatiitic flows are distinguished from tholeiitic basalts on the basis of colour, volcanic textures (intra-pillow polygonal jointing), their distinctive tremolite rich metamorphic assemblage (Plate 3-2) and their spatial association with ultramafic komatiitic flows. Magnesium content of

PLATE 13-1. Partial replacement of magnetite by dolomite in a carbonatized, ultramafic, komatiitic flow.

PLATE 13-2. Tremolite-rich mafic komatiitic flow.

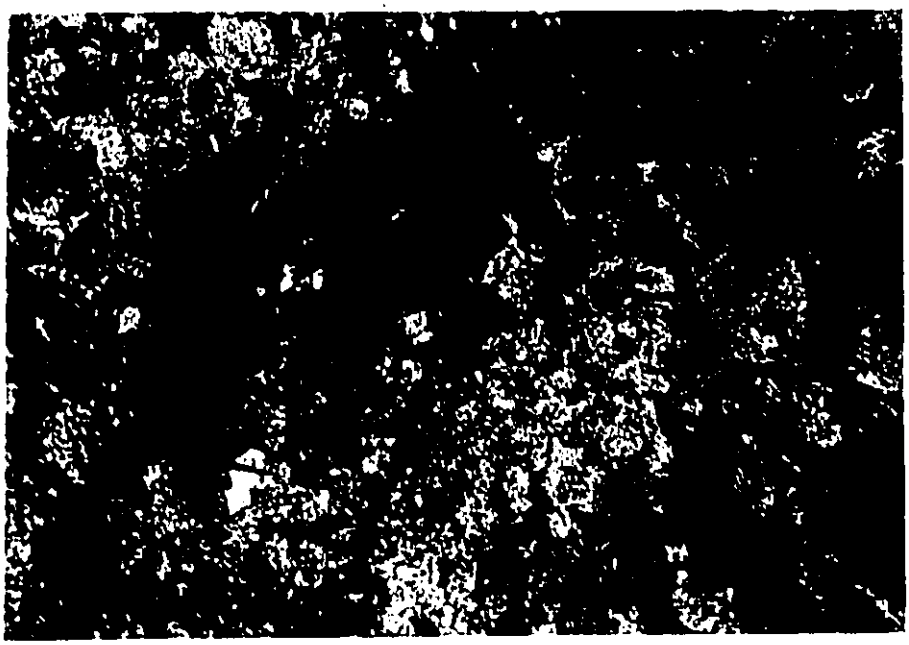

0·5 cm

1 cm

the least hydrous samples, although modified somewhat by alteration, serves as the best chemical screen. The mafic flows occur as pillowed and massive varieties, capped by pillow breccia and hyaloclastite. Flows are light grey to dark green in colour on fresh surface and range up to 30 m (100 ft) in thickness. Pillows are vesicular, occasionally polygonally jointed (Plate 2-1) and often contain radial and concentric cooling joints (Plate 4-1).

The primary igneous mineralogy of the mafic, komatiitic flows has been altered to tremolite, non-ferroan zoisite, quartz and albite. In the more magnesium, "pyroxenitic" flows, tremolite is the most abundant phase. No serpentinized olivine has been observed. Tremolitized pyroxene spinifex (Plate 4-2) has been identified on the Beaumont property (Map 3) in the Tisdale township study area. No detailed petrographic examination of the carbonatized mafic komatiitic flows has been undertaken for this research.

Exposed at the North Whitney mine, in Whitney township (Figure 16) are pillowed ultramafic and mafic komatiitic flows which have been carbonatized. Locally within interpillow voids in the mafic komatiites, rusty weathering, dolomitic-carbonate (Plate 5-1) or siliceous material (Plate 5-2) occurs. Similar pore space fillings have been interpreted as products of seawater weathering of submarine

PLATE 14-1. Concentric and radial cooling joints developed in a pillowed, mafic, komatiitic flow exposed at the same locality as Plate 2-1.

PLATE 14-2. Tremolitized, pyroxene spinifex in a mafic komatiitic flow exposed on the Beaumont property (sample B-21, map 3).

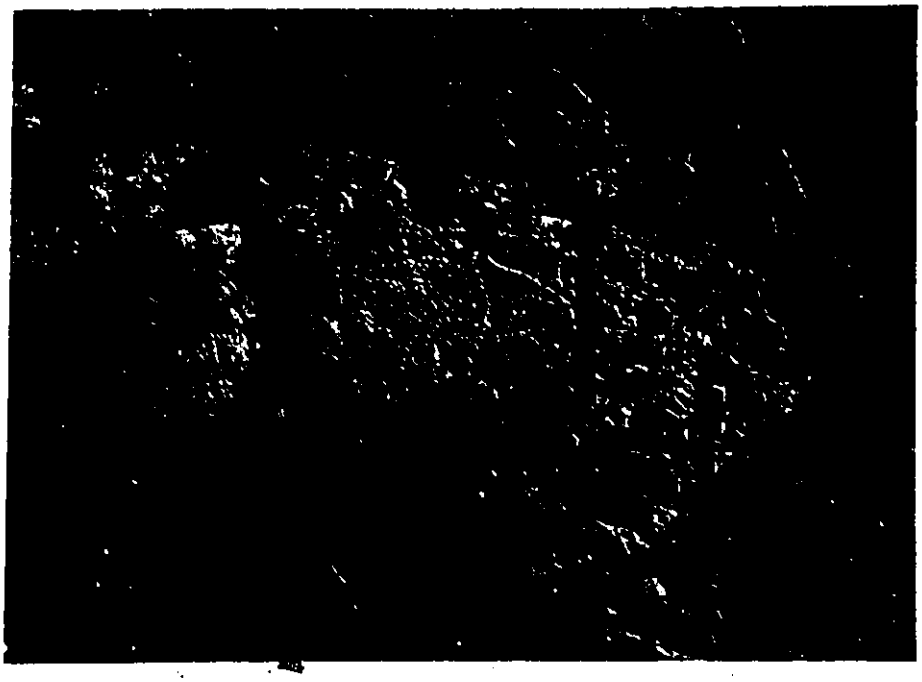

1 cm

NORTH WHITNEY MINE
Whitney Twp.

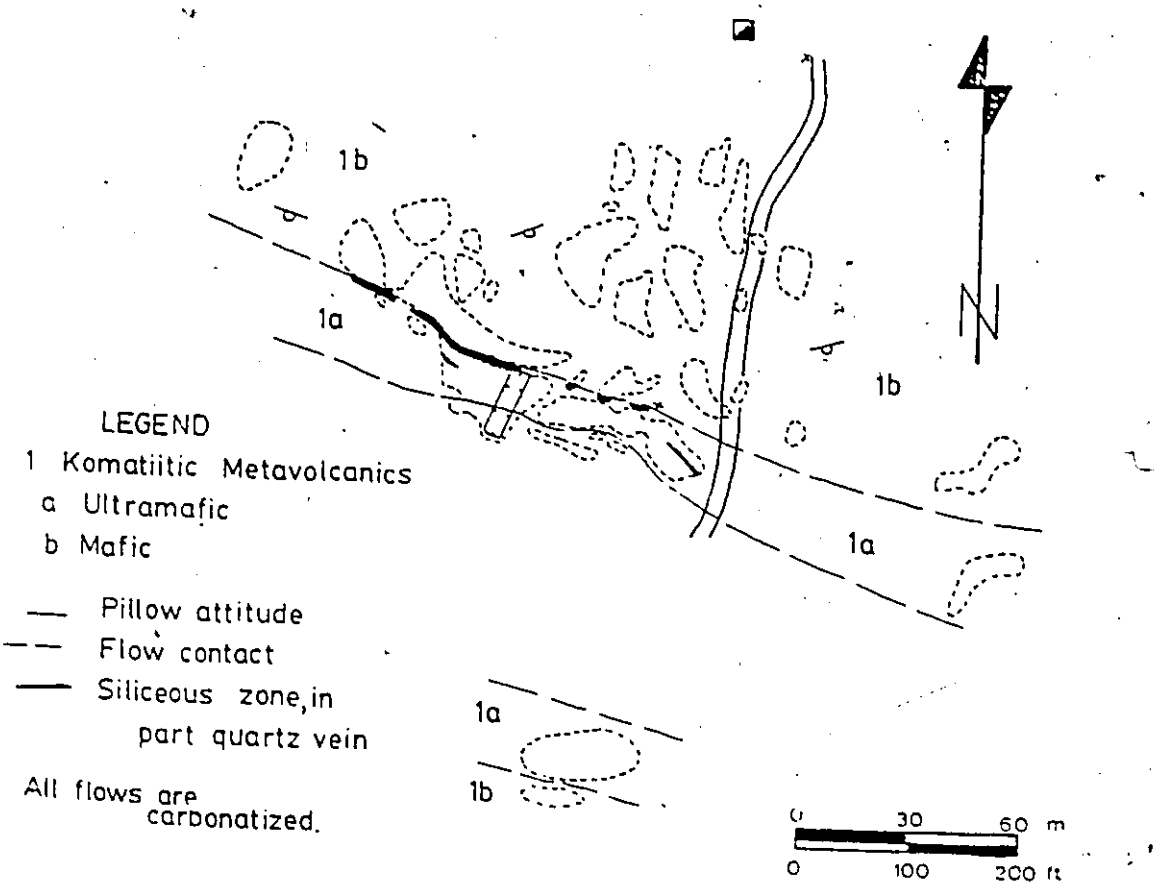

Geology by J A Fyon 1979
modified after Ferguson (1958)

FIGURE 16 : Surface geology of the North Whitney Mine property, Whitney Township.

PLATE 15-1. Interpillow void filled by a rusty weathering dolomitic carbonate exposed on the North Whitney Mine, in Whitney township (fig 3)

PLATE 15-2. Laminated, cherty material filling interpillow voids in a sequence of mafic komatiitic flows exposed north of sample B-2 on the Beaumont property (map 3). Locality revealed to the author by D. Pyke (Geologist, Precambrian Section, Ontario Geological Survey)

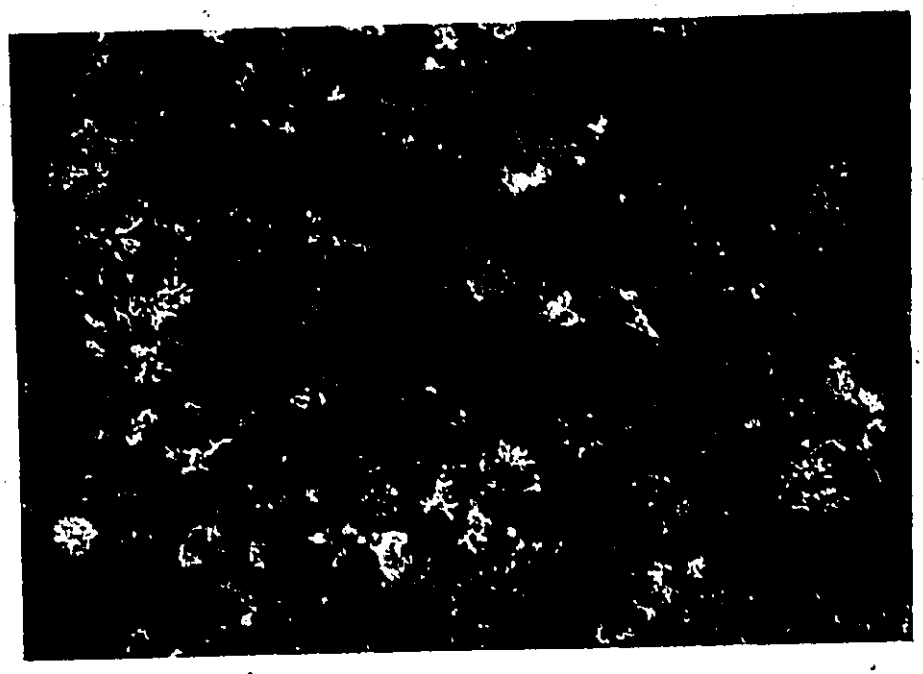

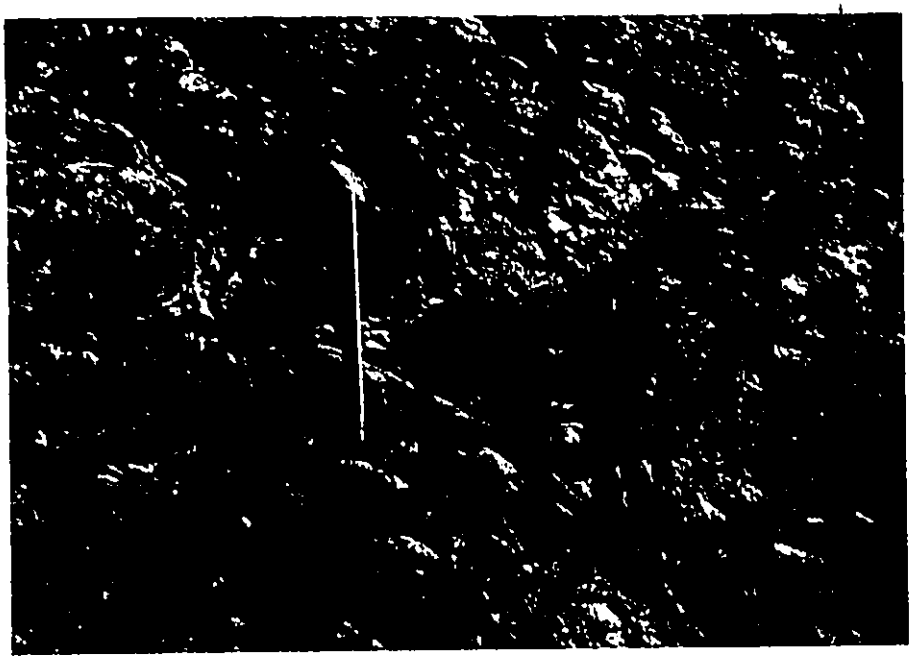

basalts (Dimroth and Rocheleau, 1979).

It is noteworthy that the most alumina-rich "mafic" komatiites north of the Beaumont shaft (Map 3; B-2, B-3) lie within the magnesium tholeiitic basalt field of the Jensen Cation Plot. This plot is best interpreted in terms of differentiation trends and overlap into adjacent, arbitrarily defined chemical fields is probable. In such a situation, the chemical group affiliation of a flow is identified by the inherent volcanic textures, such as spinifex or polygonal jointing.

5.2 MAGNESIUM THOLEIITIC BASALT

Magnesium rich tholeiitic basalt occurs within the Lower Metavolcanic Group of the Upper Supergroup (Pyke, 1978b). Pillowed, vesicular flows are most abundant, and range up to 60 m (200 ft) in thickness. Pillow breccias and/or hyaloclastites cap these pillowed flows. Pillow lava is light grey to light green in folour on fresh surface and weathers grey. Pillows range in size from 0.3 m to 1 m (1 to 3 ft) and both radial and concentric cooling joints are found in the pillow interiors. Selvages are generally dark in colour and average 0.75 cm in thickness.

In thin section these pillowed flows consist of very fine grained tremolite, non-ferroan zoisite, quartz, albite, and magnesium chlorite. It is the presence of the non-ferroan zoisite and abundant quartz-albite that distinguishes these tholeiitic basalts from the mafic komatiites. Vesicles are filled with calcite, quartz and chlorite (Plate 16-1a,b). Commonly, thicker (greater than 50 m), massive, laterally extensive flows crop out. Better than 80% of such a flow, in cross-section, consists of fine to medium grained (1 to 4 mm), ophitic plagioclase (now albitized) set in a chloritic, ground mass. This medium grained phase grades vertically into a thin, aphanitic, vesicular, occasionally pillowed zone and is capped by pillow breccia and hyaloclastite. The pillows are poorly formed and often are absent. Lateral facies variations of these massive flow domains into pillowed domains have been observed on the Davidson Tisdale property (Map 5) and are inferred elsewhere. Rarely, megapillows or lava tubes have been observed surrounded by normal, bun-shaped pillows (Map 5).

Like the komatiitic lavas, all Mg tholeiitic basalts have been hydrated and locally carbonatized. At least three periods of rock alteration can be discerned. The earliest is interpreted to be an initial palagonization of hyaloclastite granules. The palagonite rim and sideromelane

PLATE 16-1 Vesicles in a magnesium tholeiitic basalt which are filled by calcite, quartz and chlorite.

a. chlorite, zoisite in vesicle; wall lined by quartz

b. chlorite and carbonate resorb relict quartz wall lining in vesicle (x-nicols)

1 mm

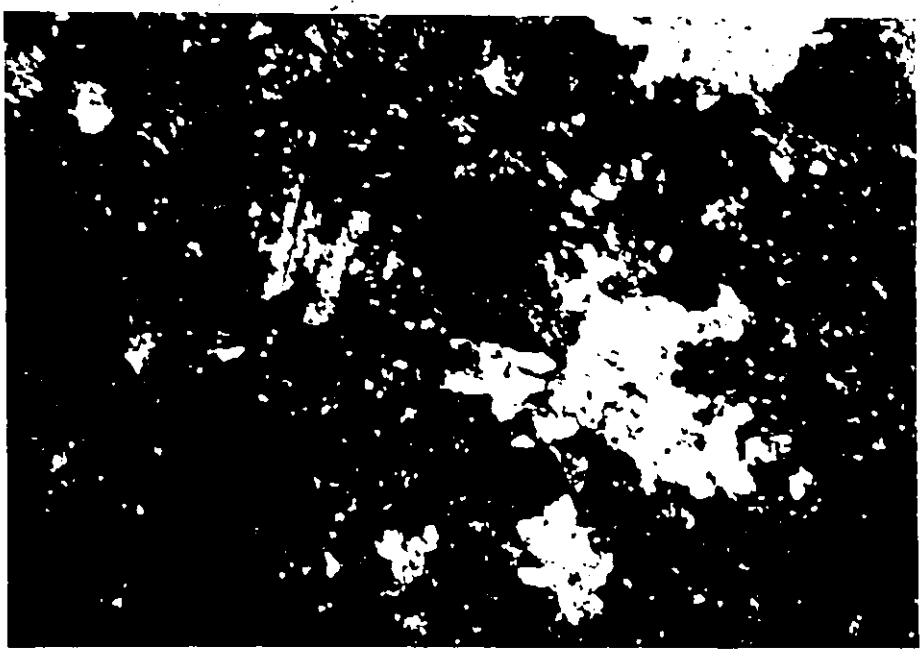

core have since been replaced by chlorite and silica respectively (Plate 17-1), although the pre-existing fabrics are retained. A detailed description of palagonitized, Archean hyaloclastites which have been later chloritized and silicified is given by Dimroth and Lichtblau (1979). In addition to the palagonitized hyaloclastite granules, flows are cut by veinlets now consisting of chlorite (in the basalts) or talc-tremolite (in the ultramafic komatiites). All plagioclase grains have been altered to albite, locally "limpid-like" (Gelinas et al., 1977), and the opaque mineral assemblage consists of pyrite-chalcopyrite-sphalerite-magnetite, typical of modern, seawater-metamorphosed, submarine basalts (MacLean, 1977). In addition, this basaltic rock alteration is characterized by variable, but generally increased alkali and water contents (Table 6), typical of spilitic rocks (Hyndman, 1972, p.99).

The second type of alteration consists of the localized development of chlorite and carbonate-rich discordant and stratabound zones. Within such an alteration zone, a chloritic envelope encloses a dolomitic core. A detailed description of this alteration type is given in section 6.2.

In response to the third alteration or metamorphic event, the silicate mineralogy of the palagonitized basalts was transformed to an assemblage consisting of chlorite-

PLATE 17-1. Relict palagonitized, hyaloclastite granule. Sideromelane core (S) has been replaced by quartz and the palagonite rim (P) has been chloritized. Note the oxide (O) concentrations between the sideromelane core and the palagonite rim and at the outer edge of the palagonite rim.


O
P
S
1 cm

TABLE 6

Mineralogical and Chemical Data Which Imply That Some Mg Tholeiitic Basalts in the Timmins Area were Spilitized.

Chemical Data

Average Spilite(Hyndman,1972)	Oceanic Tholeiite(Hyndman,1972)	Timmins Data (wt%)
CaO = 7.1 (0.07-16.54)	10.9	4.0-20.0
Na_2O = 4.4 (0.31-6.95)	2.7 } wt %	nd-3.57
K_2O = 1.0 (0.0-4.55)	0.26	0.03-3.3
(wt. %)		H_2O=3-5 wt %

Mineralogical Data

Presence of 1) Limpid albite

2) Albitized plagioclase

3) Pyrite-sphalerite-chalcopyrite-magnetite assemblage

tremolite-zoisite-quartz-albite-calcite, typical of greenschist facies. Texturally it is difficult to establish whether this assemblage represents mineralogical equilibrium attained during burial or contact metamorphism, or whether the assemblage is a product of high temperature (>350°C), seawater-hydrothermal alteration of the type described by Aumento et al. (1970) and Muehlenbachs and Clayton (1972b). This problem is addressed in Chapter 8.

It is not possible to precisely describe the chemical changes induced by the "spilitization" process as no fresh volcanic rock has been identified. However, all "spilitic", Mg tholeiitic basalts have major element compositions which are statistically similar with respect to variance and define tight clusters on variation diagrams (see section 7.4.1). It is probable that with the exception of volatiles and alkalies, the major element geochemistry of the "spilites" approximates that of the fresh, parent rock.

Most samples, regardless of degree of alteration, contain chalcopyrite, pyrite, and sphalerite. Magnetite is present only in spilitic rocks (<4 wt. % L.O.I.) and is degraded to leucoxene with increasing degree of alteration. Sphalerite occurs almost entirely as a resorption mantle, replacing pyrite and chalcopyrite grains. No hematite has been observed in any sample, regardless of degree of

carbonate alteration.

5.3 IRON THOLEIITIC BASALTS

Because these basalts occur in greatest abundance outside the detail map areas, little time was spent examining these rocks. Excellent descriptions of the field and petrochemical characteristics of this rock type are given by Jensen (1978a) and Pearce and Birkett (1974). In the Porcupine camp, variolitic massive and pillowed flows exist. These variolitic, Fe tholeiitic basalts, formerly called the Vipond series (Ferguson et al., 1968) are regionally extensive and form an excellent marker unit.

5.4 CALC-ALKALIC FELSIC VOLCANIC ROCKS

Several stratabound, porphyritic bodies of quartz-albite-sericite schist occur within the Upper Supergroup. These enigmatic rocks are of great importance in the Porcupine camp because they are spatially associated with most of the gold deposits and a disseminated copper deposit (McIntyre). Chemically these rocks range in composition from calc-alkalic dacite to rhyodacite; however, nowhere in

the literature have either igneous or volcanic textures been described. Polyphase deformation and very low grade metamorphism has transformed these rocks into quartz-albite porphyritic sericite schists. Graton and McKinstry (1933) and Hurst (1936), argue that the felsic porphyries have undergone the same multiple deformation as their enclosing volcanic rocks and therefore the porphyries were pre-"Timiskaming" in age. Evans (1944), Moore (1954), Holmes (1944), Griffis (1962) and Griffis (1978) contend that the porphyries have cross-cutting relationships with the local stratigraphy. Davies (1977) and Davies and Luhta (1978) cite petrochemical, geological and petrographic data and argue that these schists are metasomatized extrusive felsic volcanic rocks. Pyke and Middleton (1971) cite the disseminated copper deposit at the McIntyre mine as being an intrusion hosted, porphyry copper type.

The nature of these porphyritic, quartz-feldspar-sericite (Q.F.P.) schists in the south study area was studied as comprehensively as possible. No underground exposures of the felsic schists are now available in either the Delnite or Buffalo Ankerite mines; hence a composite level plan was compiled from all available underground geological plans of the Aunor, Buffalo Ankerite and Delnite mines. Major lithological contacts were projected to surface (over

30 to 60 m vertical distance), which facilitated a comparison between mine and present rock classification terminology. The following features are of importance regarding the stratigraphic relationships of the Delnite and Buffalo Ankerite Q.F.P.'s:

1. The felsic schists bear planar and linear tectonic fabrics, equivalent in terms of fabric attitude, to those developed in the surrounding mafic volcanic material (Graton and McKinstry, 1933; Hurst, 1936).

2. Both Q.F.P.'s have a long axis averaging 1200 m (4000 ft), an intermediate axis averaging 300 m (1000 ft), and a thickness ranging up to 120 m (400 ft).

3. The Q.F.P.'s lie along the same stratigraphic horizon (Figure 14) and occupy this stratigraphic level over a dip length in excess of 900 m (3000 ft).

4. Along its periphery, the Buffalo Ankerite Q.F.P. interdigitates with a polymict conglomerate (Figure 13) and locally both Q.F.P.'s are interbedded with magnesium tholeiitic basalt flows.

5. The Q.F.P.'s and stratigraphically equivalent rocks rest conformably upon a basal komatiitic platform (lower domain) (Figure 12).

6. Nowhere do the Delnite or Buffalo Ankerite Q.F.P.'s cross-cut major lithological contacts.

7. All recorded carbonate alteration in the mine workings occurs within the komatiitic tholeiitic volcanics adjacent to, and stratigraphically below, the felsic schists.

8. The only plausible source of the Q.F.P. and flow banded rhyolite fragments enclosed in the polymict conglomerate, exposed in the Buffalo Ankerite pit, is the Buffalo Ankerite Q.F.P. body which lies down dip from the conglomerate.

Collectively these data indicate that the Buffalo Ankerite Q.F.P. is a stratabound body which was exposed on the seafloor during an erosional event. Such a body is most likely of extrusive, felsic volcanic origin, although the presence of hypabyssal intrusive equivalents within such an extrusive sequence cannot be denied. By inference, the Delnite stratabound Q.F.P. is also interpreted as a felsic

volcanic pile. The complex nature of these Archean Q.F.P.'s is revealed by Hopwood (1976, 1977) and Vernon and Flood (1977).

CHAPTER 6

CARBONATE ALTERATION

Coexisting with the "spilitic" rocks are zones of intense, localized hydration and carbonatization. Field and petrographic data acquired during the course of this research reveal that the localized chlorite and carbonate rich alteration assemblages are spatially and genetically related; however, for convenience, this alteration assemblage dyad is referred to as carbonatized rock. Within the Upper Supergroup (Pyke, 1978b) carbonatization has affected komatiitic, Mg and Fe tholeiitic rock. Because of their initial bulk composition, mafic and ultramafic rocks have been intensely carbonatized.

The importance of this distinctive alteration and its spatial association with the gold deposits was recognized by Burrows (1924), and Ferguson et al. (1968) and has been reiterated by Pyke (1975) and Karvinen (1976, 1978a). In the Porcupine camp, this carbonatization has been interpreted as localized, late, epigenetic, wall rock alteration related

to the gold-quartz vein formation (Burrows, 1924; Ferguson et al., 1968), as a synvolcanic, seafloor, hydrothermal alteration product (Karvinen, 1978a; Fyon et al., 1978, 1979) and, as a late, structurally controlled, tectonic feature (Whitehead et al., 1979). Thompson (1943) interpreted carbonatized rock in the Kirkland Lake camp as late shear or fault zones.

6.1 ALTERATION ASSEMBLAGES

Listed in Table 7, according to initial rock type, are the alteration assemblages which collectively constitute an alteration zone. Phase identification was accomplished using XRD and transmitted and reflected light microscopy. Depicted also is the direction of increasing alteration intensity, expressed as increasing loss on ignition.

Throughout the text the alteration zones are referenced by their field names (pervasive carbonate, calcite carbonate, disseminated carbonate, hydrous) which identify the alteration mineralogy according to rock type.

In any given alteration zone, not all alteration assemblages need be present, but in all cases, the relative juxtaposition of the assemblages present remains constant.

TABLE 7

Alteration Assemblages as a Function of Rock Type and Degree of Alteration

Rock Type		Alteration Assemblage	L.O.I. Range	Field Name
Ultramafic Komatiite		Serpentine, tremolite, chromite, magnetite, sulfides	?-7 wt %	Serpentinite
	Carbonate Alteration	Serpentine, tremolite, chlorite, chromite, magnetite, sulfides	7-8.5 wt %	Serpentinite
	Carbonate Alteration	Serpentine, talc, chlorite, tremolite, dolomite, chromite, magnetite, sulfides	8.5-12 wt %	Disseminated Carbonate
	Carbonate Alteration	Dolomite, quartz, chlorite, chromite, magnetite, sulfides, trace magnesite and calcite	12-40 wt %	Pervasive Carbonate
	Carbonate Alteration	Dolomite, quartz, chromite, magnetite, sulfides, trace magnesite and calcite	12-40 wt %	Pervasive Carbonate
Magnesium Tholeiitic Basalt		Tremolite, non-ferroan zoisite, quartz-albite, chlorite, magnetite, pyrite, sphalerite, chalcopyrite	?-4 wt %	Spilite
	Carbonate Alteration	Tremolite, chlorite, quartz-albite, non-ferroan zoisite, leucoxene, trace dolomite, pyrite, sphalerite, chalcopyrite	4-8 wt %	Chloritic
	Carbonate Alteration	Chlorite, dolomite, quartz-albite, trace sericite, leucoxene, pyrite, sphalerite, chalcopyrite	8-12 wt %	Disseminated Carbonate
	Carbonate Alteration	Dolomite, quartz-albite, trace chlorite, sericite, leucoxene, pyrite, sphalerite, chalcopyrite (Calcite predominate in some assemblages)	12-18 wt %	Pervasive Carbonate

Boundaries between alteration assemblages are gradational over several meters in some cases, although the transition from the hydrous to pervasive carbonate assemblage generally occurs over a horizontal scale of less than one meter. Within an alteration zone, better than 80% of the rock consists of hydrous and pervasive carbonate assemblages; the disseminated carbonate zone is relatively minor, but persistent.

6.2 FIELD CHARACTERISTICS OF THF ALTERATION

The relationships to be discussed are general in nature and apply equally well to komatiitic and Mg tholeiitic basaltic flows. However, because exposure is best in areas underlain by tholeiitic flows, the alteration of these rocks is described at length and inferences are extrapolated to komatiitic flows.

Based on geometrical shape and detail stratigraphic relationships, the alteration zones are subdivided into discordant and stratabound types. In stratabound alteration zones the alteration assemblage boundaries trend parallel to the flow contacts. Alteration intensity is greatest in the flow top or hyaloclastite and decreases symmetrically

into the overlying and underlying flow domains (Figure 17). In some cases, hydrated, flow top breccia fragments sit in a rusty weathering, carbonate matrix (Plate 18-1). This type of alteration is interpreted to have developed by rock/water interaction in response to lateral flow of hydrothermal solutions through the permeable flow top breccia.

Discordant alteration zones are characterized by alteration assemblage boundaries which trend transverse to the attitudes of the flow stratigraphy (Figure 18). These zones are pipe or funnel shaped and range up to 90 m (300 ft) in apparent cross-sectional thickness. The core of a discordant alteration zone consists of pervasive carbonate, which grades outward through a thin zone of disseminated carbonate into the hydrous or chloritic zone about the periphery. The largest such alteration zone in the north study area is found on the Dobell Porcupine property (Map 2) where in excess of 150 m (500 ft) of vertical stratigraphy is altered. Other discordant alteration zones are exposed on the Beaumont, Davidson Tisdale, Armstrong McGibbon, and Crown Chartered properties in the north study area (Map 2) and at the Buffalo Ankerite mine and Skynner Lake area in the south study area (Map 1).

All the discordant alteration zones exposed in the north study area are spatially associated with, and crosscut,

STRATABOUND ALTERATION ZONE GEOMETRY AND DEDUCED VOLCANIC ENVIRONMENT

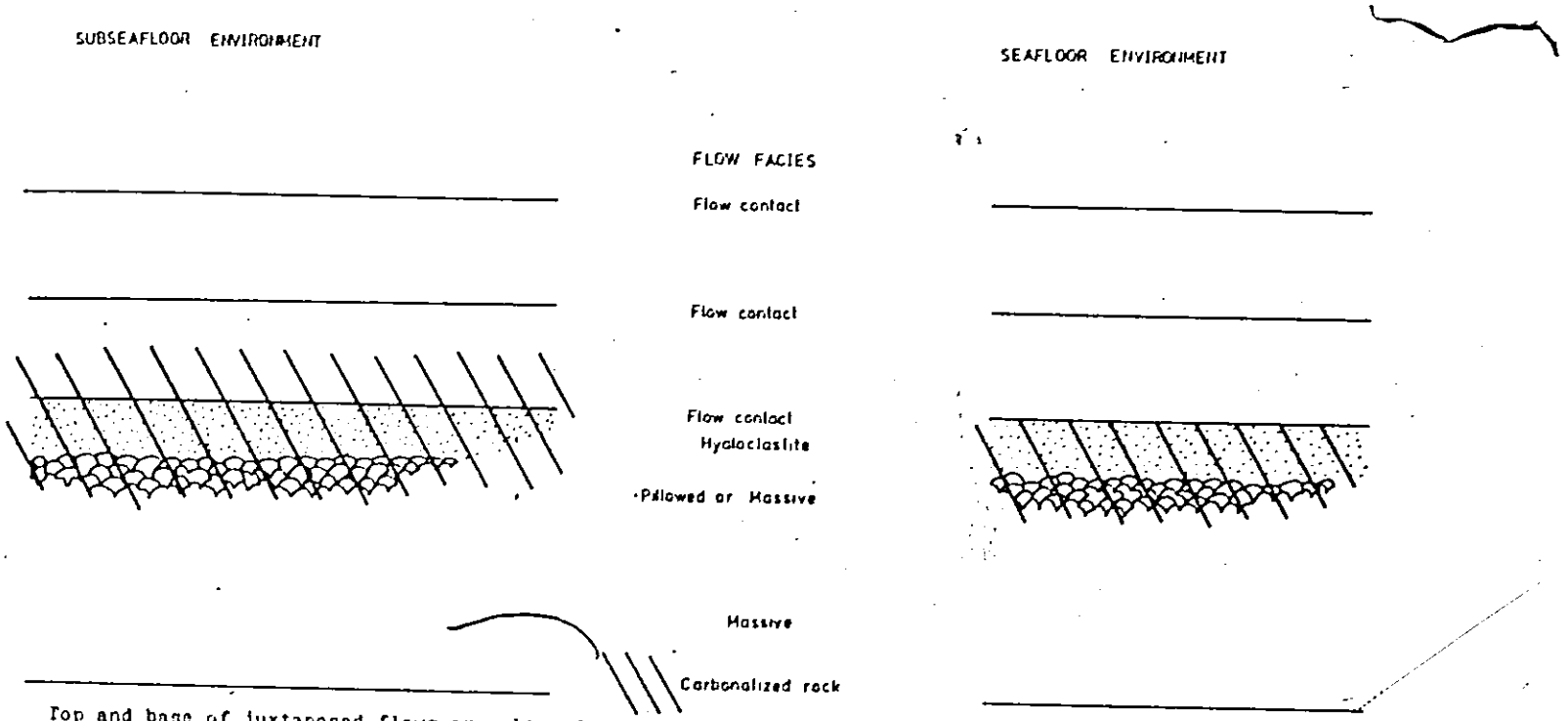

FIGURE 17 : Schematic representation of stratabound carbonate alteration geometry characteristic of a subseafloor and seafloor environment.

PLATE 18-1. Chloritized flow top breccia fragments which sit in a dolomitic matrix. Sample collected from the Middle Metavolcanic Group (Fe tholeiitic basalt), 1 km north of the Edwards shaft, in Tisdale township.

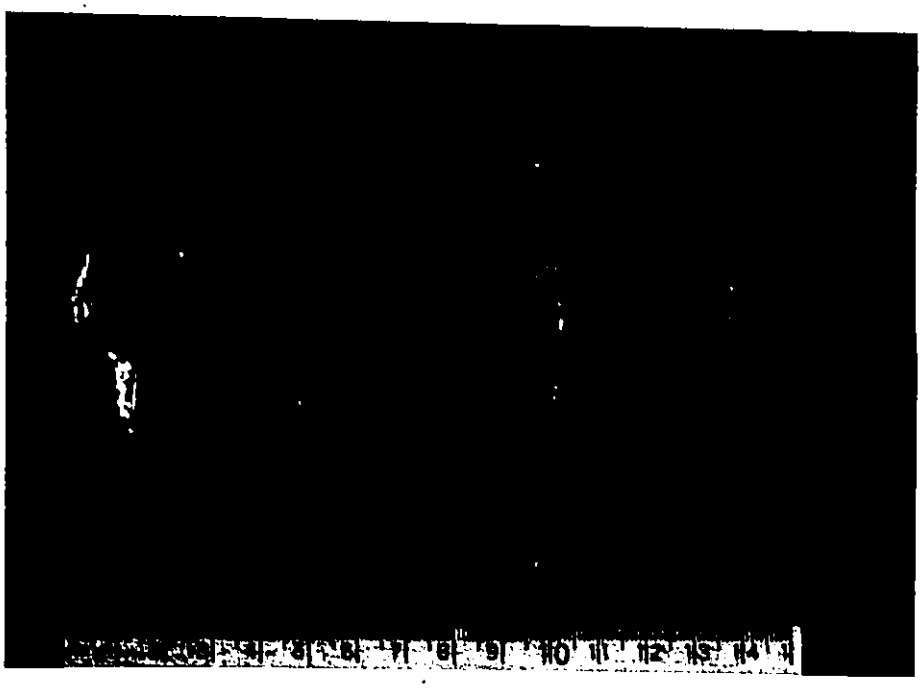

DISCORDANT ALTERATION ZONE GEOMETRY AND DEDUCED VOLCANIC ENVIRONMENT

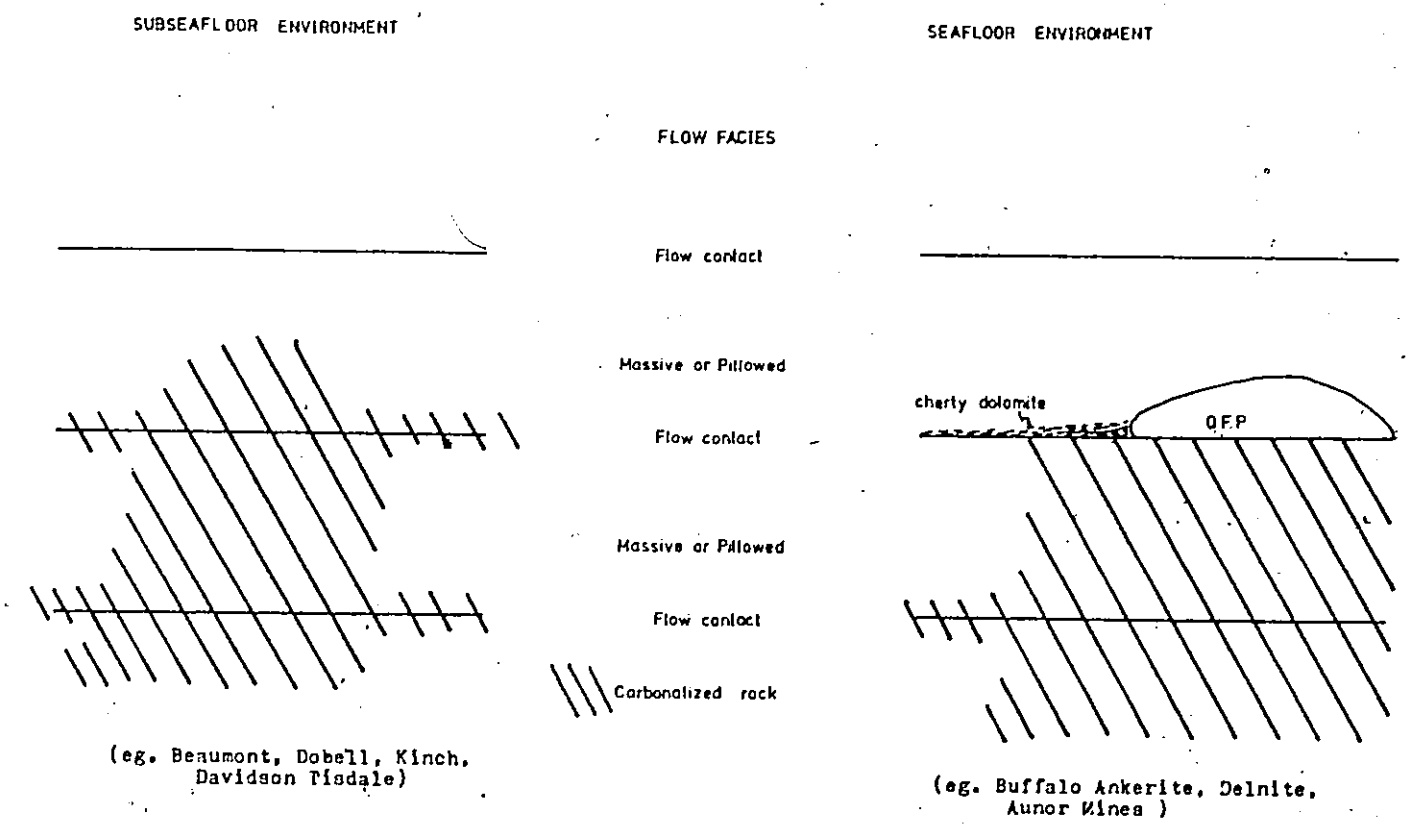

FIGURE 18: Schematic representation of discordant alteration zone morphologies which are characteristic of subseafloor and seafloor environments. Subseafloor environment characterized by discordant alteration zones which terminate gradationally in a flow. Carbonatized rock which devel oped at the seafloor are overlain by carbonate free flows, implying the overlying flows were emplaced after the carbonatization process had terminated. Extrusive, felsic volcanic rocks and exhalative, auriferous, cherty dolomites are restricted to the seafloor environment.

thick (greater than 60 m, 200 ft) massive flows (e.g. Beaumont, Kinch, Dobell Porcupine, Davidson Tisdale, Armstrong McGibbon and Crown Chartered). A similar relationship has not been observed in the south study area, although exposure is poor. In the vertical dimension, discordant alteration zones may terminate abruptly against the overlying carbonate-free volcanic flows (e.g. Buffalo Ankerite property, Figure 13), suggesting the alteration took place prior to the deposition of the overlying fresh flows or may terminate gradationally within a flow (e.g. Davidson Tisdale, Map 5; Beaumont, Map 3). Locally, extending laterally from a discordant alteration zone are stratabound "fingers" of carbonatized rock, usually along flow contacts (Figure 18). Exposed on the eastern edge of the Kinch Property (Map 4), a quartz vein, 0.3 m (1 ft) in width, crops out intermittently within such a stratabound carbonate zone.

The most complete exposure of discordant alteration exists at the Davidson Tisdale property (Map 5). In detail, a massive Mg tholeiitic basalt (Davidson Tisdale flow or D-T flow), has been extensively altered to hydrous and carbonate rich assemblages. The morphology of the alteration zone is one which resembles a funnel, with the alteration root cutting down into the stratigraphically lower pillowed flows. Zones of calcite rich rock locally separate the pervasive

carbonate (dolomitic) alteration zone from the overlying and underlying "spilitic", pillowed flows. Patches of chloritic rock exist within the carbonate zone and indicate that the carbonatization process was only locally pervasive. A thin disseminated carbonate zone separates the pervasive carbonate from the chloritic alteration zones. The pervasive carbonate alteration extends vertically up through the overlying pillowed flow, but has altered only part of the flow top breccia.

Discordant alteration zones are interpreted as major hydrothermal solution conduits, from which solutions were fed along other, adjacent, permeable aquifers. Nowhere has the root of a discordant alteration pipe been exposed.

In addition to these large scale carbonate alteration zones, megascopic quartz-dolomite veins, averaging 2 cm in width (Plate 19-1) are exposed on the McBine Porcupine property (Map 1) cross-cutting a weakly chloritized, Mg tholeiitic basalt. The veins which are isoclinally folded are also interpreted as hydrothermal solution conduits.

PLATE 19-1. Dolomite-quartz veins, averaging 2 cm in width cut a chloritized, magnesium tholeiitic basalt exposed on the McBine Porcupine property (map 1)

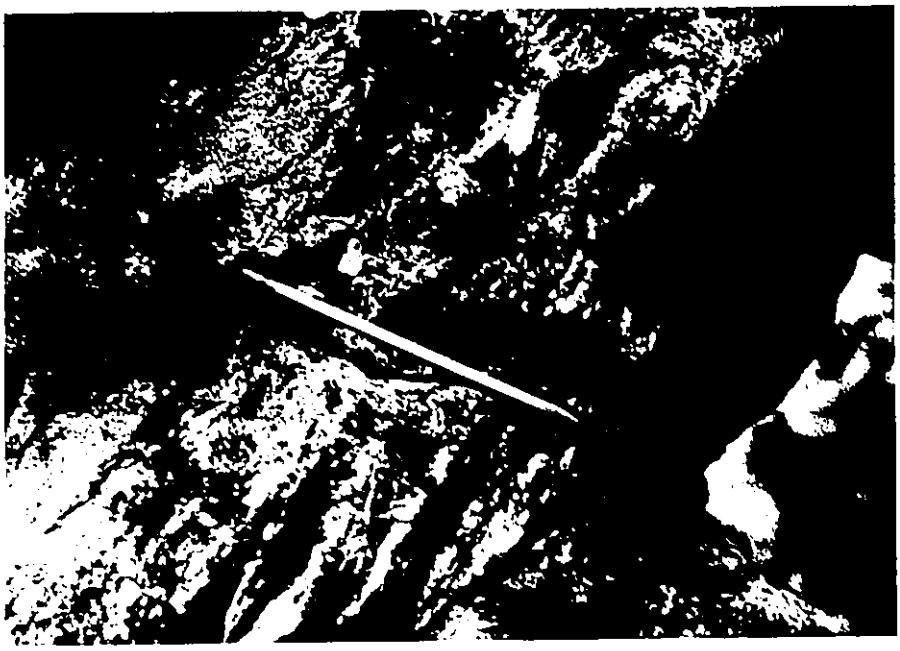

6-3 DETAIL ALTERATION PETROGRAPHY OF MAGNESIUM THOLEIITIC BASALTS

Prior to discussing the alteration petrography, indication of some data limitations is warranted. All modal abundances have been estimated visually. Point counting on very fine grained mineral aggregates (0.01 mm) is a tedious and often fruitless task. Secondly, because of the intimately intergrown nature of the matrix phases (primarily chlorite, quartz and albite) errors in the estimated modal abundance of these minerals are likely. Because the distinction between matrix quartz and albite could not be made consistently, these two phases are collectively referred to as quartz-albite. Some silicate phases, notably zoisite and tremolite, most likely were formed during the metamorphic requilibration of the palagonized and carbonatized rocks (see section 8, and hence their distribution reflects the pre-metamorphic bulk rock chemistry. Finally, textures considered most useful by petrographers to establish mineral paragenesis (e.g. resorption) are notoriously difficult to interpret in metamorphic rocks which have undergone polyphase deformation. Nevertheless, a systematic relationship is found between degree of rock alteration and mineralogy, and hence, these limitations do not appear to severely

constrain the usefulness of the petrographic observations.

Indicated on Map 5 is the location of altered samples which were collected from the Davidson Tisdale flow. Thin and polished section examination of these samples reveals that progressive alteration, measured quantitatively by increasing volatile content, is associated with corresponding mineralogical changes (Figure 19). For the alteration suite, the proportion of total volatiles ranges from 3.5 to 17.5 wt %. All samples, regardless of degree of alteration, contain leucoxene, quartz-albite and magnesium rich chlorite. From the following petrographic observations, important implications regarding the nature of the volatile alteration process are deduced:

1. No fresh igneous mineralogy exists in any sample.

2. The essential alteration minerals are tremolite, magnesium, chlorite, quartz-albite, non-ferroan zoisite, and dolomitic carbonate, while sericite, leucoxene, chalcopyrite, sphalerite and pyrite occur in accessory amounts.

3. Tremolite and non-ferroan zoisite are restricted to the "spilitic" rocks and disappear completely commensurate with the appearance of a dolomitic phase (Figure 20, 4 to 8 wt % volatiles).

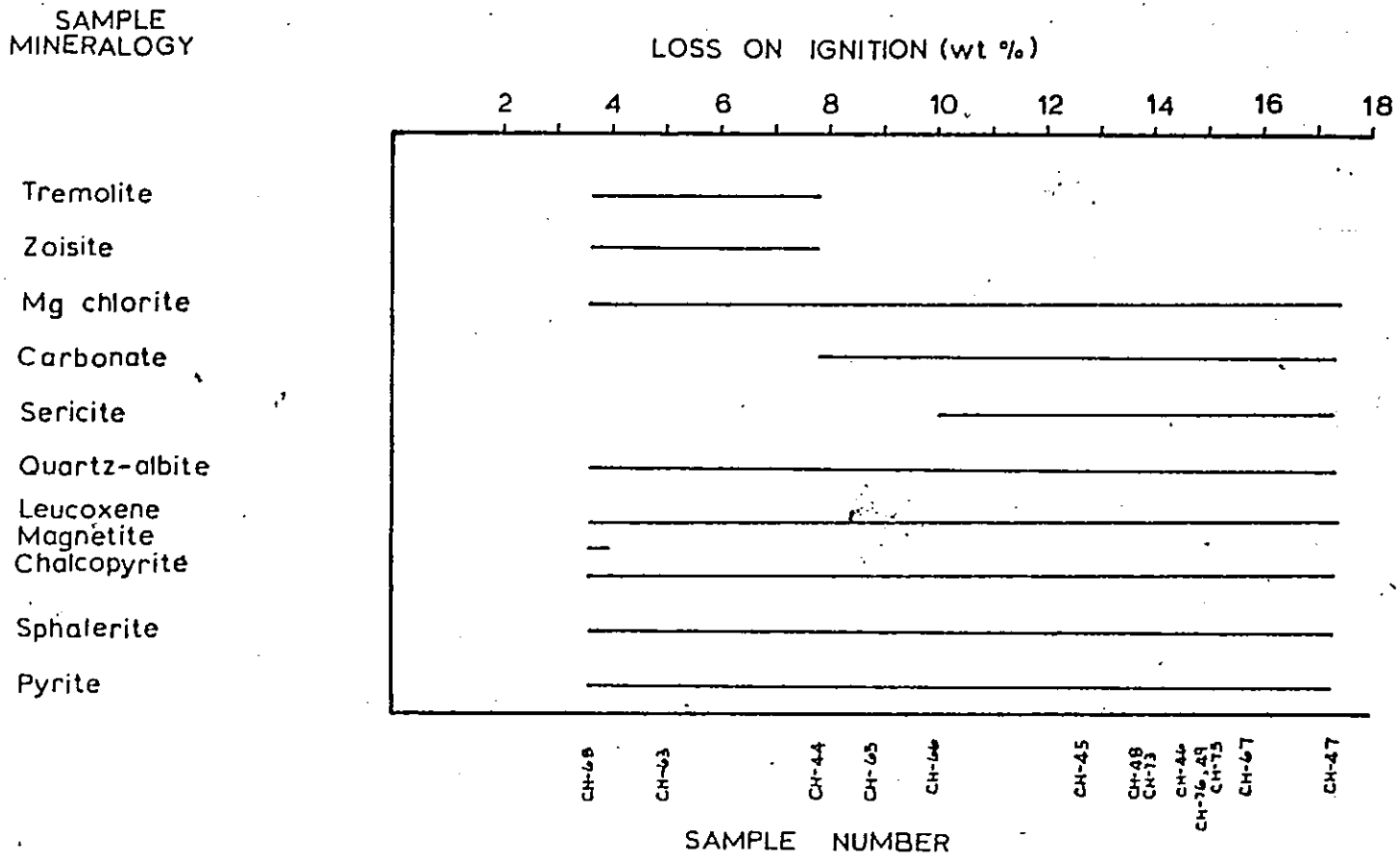

FIGURE 19 : Variation of magnesium tholeiitic basalt mineralogy as a function of degree of rock alteration, expressed as loss on ignition. All samples were collected from the D-F flow on the Davidson Tisdale property in the Tisdale study area.

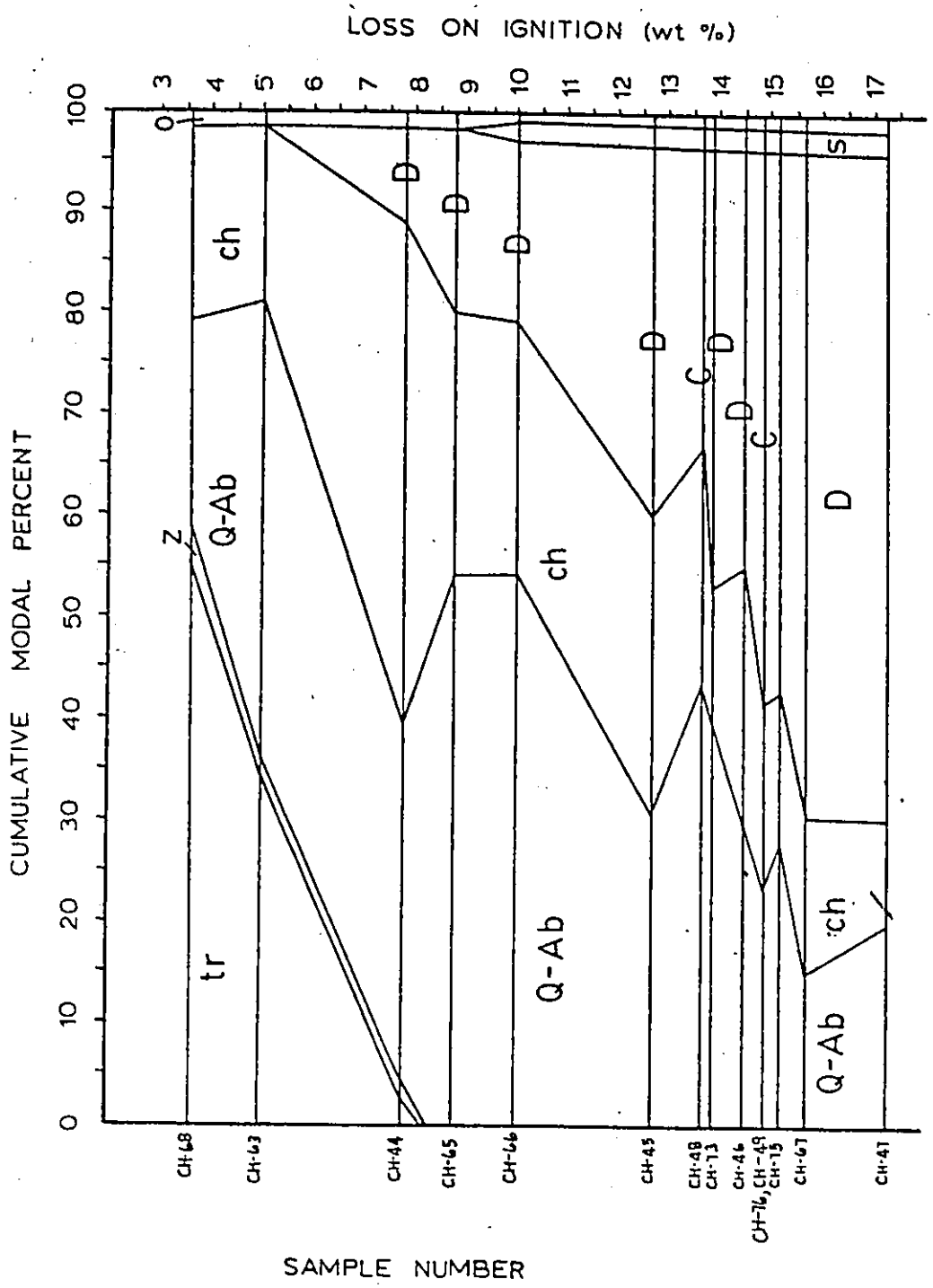

FIGURE 20 : Variation of mineral assemblages in magnesium tholeiitic basalt as a function of degree of rock alteration, expressed as loss on ignition. All samples were collected from the D-F flow, on the Davidson Tisdale property, in the Tisdale study area. Abbreviations are: tr(tremolite), z(zoisite), Q-Ab(quartz ±albite), ch(mg rich chlorite), D(dolomite), C(calcite), s(sericite), o(opaques).

4. Magnesium chlorite and quartz-albite attain maximum modal abundance within the 8 to 10 wt % volatile range and both degrease in abundance with increasing or decreasing volatile content from that maximum (Figures 20, 21).

5. A significant amount of dolomite does not appear until a volatile threshold of 5 wt % is exceeded (Figures 20, 21). Abundance of dolomitic carbonate increases rapidly at volatile contents exceeding 10 to 12 wt %, corresponding to 25 modal % dolomite (Figure 21).

6. Sericite appears as an accessory phase when the dolomite/chlorite modal abundance ratio exceeds 1 (10 to 12 wt % volatiles) and only after the disappearance of tremolite and non-ferroan zoisite.

Texturally, incipient hydration is manifest by:

1. Magnesium chlorite filling vesicles which are often lined by quartz (Plate 6-1);

2. Magnesium chlorite occurring as a very fine grained (0.01 mm), ubiquitous matrix phase related to and pervading from quartz-chlorite veinlets.

With increasing degree of alteration, dolomitic carbonate appears as uniformly distributed, disseminated grains

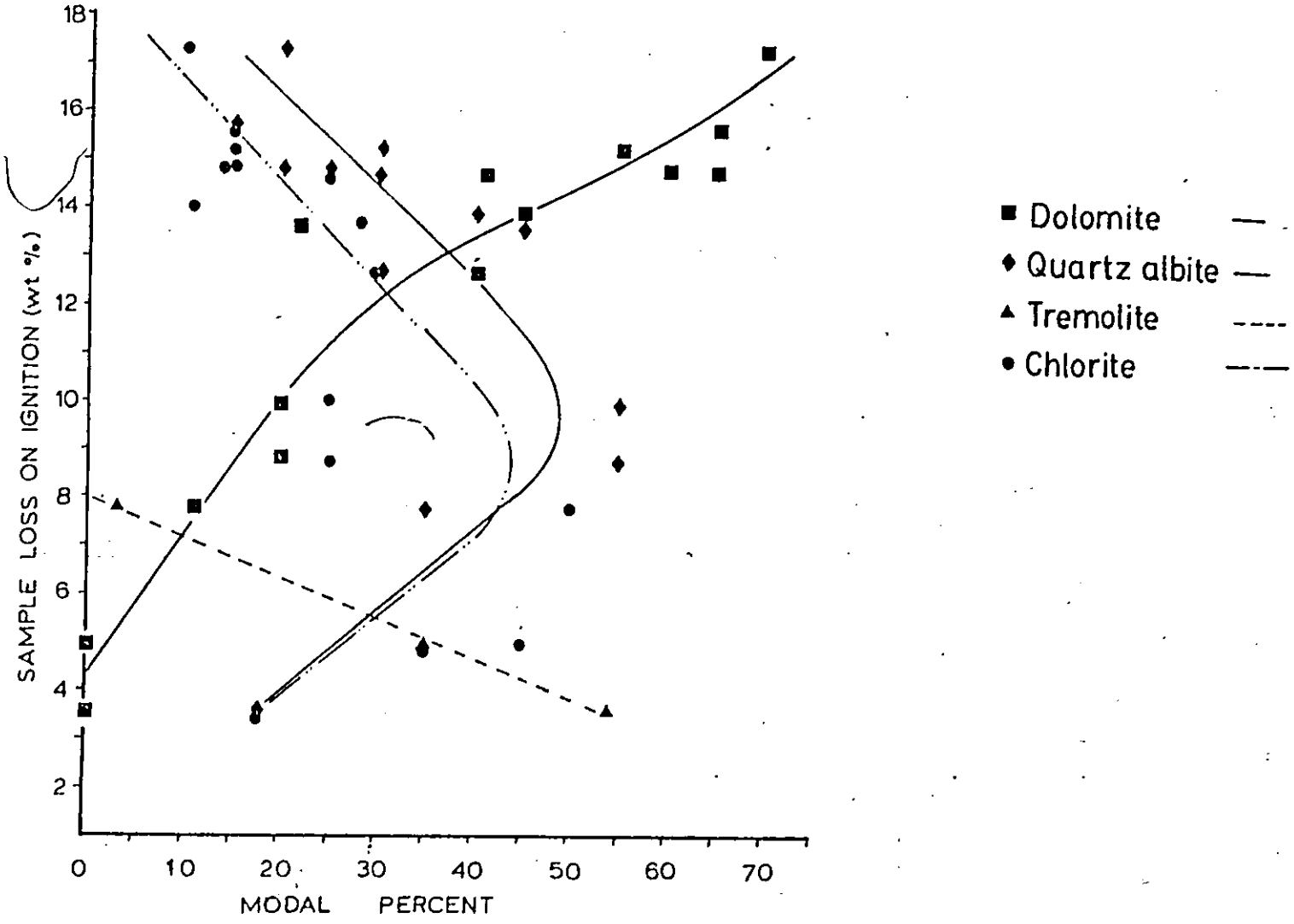

FIGURE 21: Modal percent variation of dolomite, quartz-albite, tremolite and chlorite as a function of degree of rock alteration, expressed as loss on ignition. All samples collected from the D-F flow on the Davidson Tisdale property in the Tisdale study area.

(0.1 to 0.2 mm), locally associated with quartz-chlorite-carbonate veinlets, and as vesicle fillings. Sericite also occurs in these veinlets and as a matrix phase (Plate 20-1,2). There is generally a transitional boundary between veinlet hosted chlorite and matrix chlorite. All chlorites, whether matrix or veinlet hosted, carbonate related or not, are optically identical. More intense carbonate alteration is marked by the disappearance of chlorite in veinlet form. This disappearance of veinlet chlorite also marks the degree of alteration at which microvolcanic textures (vesicles) are no longer recognizable (sample CH-73). Within the most intensely altered samples dolomitic carbonate is disseminated throughout the matrix or occurs in discrete quartz-carbonate veinlets (Plate 20-2). When quartz-carbonate veinlets are relatively abundant (1 to 2 veinlets/cm), the intervening matrix material is extensively carbonatized (greater than 60% by mode dolomitic carbonate) and the veinlet boundaries lose their integrity.

In summary, the major hydration/carbonatization alteration is characterized by vesicle and veinlet filling and matrix pervasion by magnesium chlorite and quartz (4 to 8 wt % L.O.I.). The appearance of matrix and veinlet dolomite is accompanied by a sympathetic decrease in the abundance of veinlet magnesium chlorite. In this transitional or

PLATE 20-1. Sericite (S) present in the dolomite-quartz matrix of a carbonatized Mg tholeiitic basalt. Relict chlorite patches (dark areas) persist.

PLATE 20-2. Sericite (S) present in a dolomitic vein which cuts a chloritized Mg tholeiitic basalt.

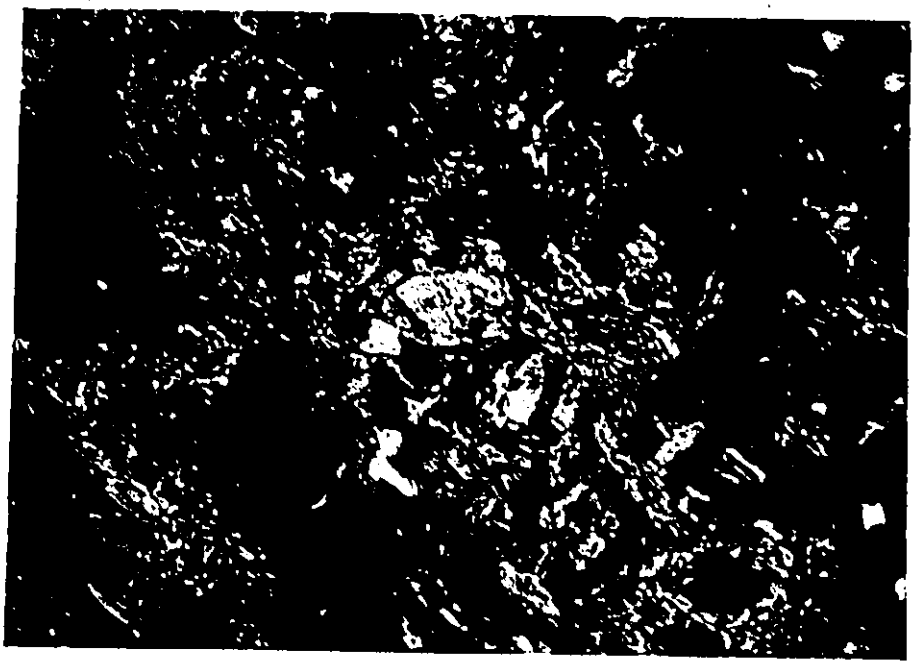

1mm

2mm

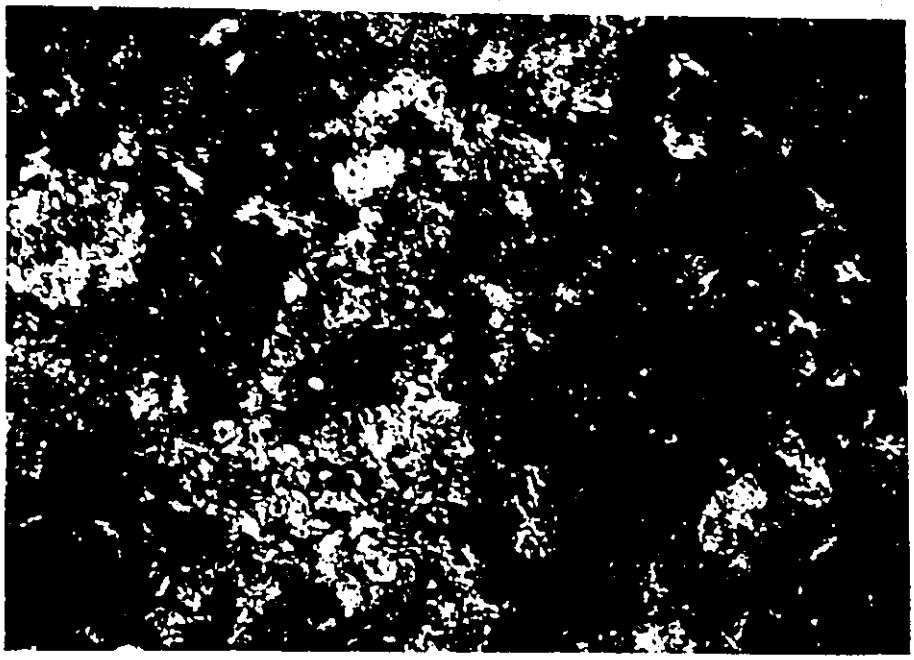

disseminated-carbonate alteration assemblage (8 to 12 wt % L.O.I.), veinlet and matrix sericite appear only after matrix tremolite and non-ferroan zoisite have disappeared. During the most intense alteration (12 to 18 wt % L.O.I.), veinlet chlorite is absent and dolomite develops at the expense of matrix chlorite and quartz-albite.

CHAPTER 7

GEOCHEMISTRY

7.1 SPECIFIC GRAVITY OF ALTERED MAGNESIUM THOLEIITIC BASALT

To calculate the chemical gains or losses per unit volume of an altered sample as a function of alteration intensity (section 7.2), the composition-volume relationship derived by Gresens (1967) is used such that the analyses of different rock samples are standardized to equivalent mass units. In order to carry out these calculations, the relative specific gravity of the rock sample with respect to that of the freshest sample is required.

Three methods were attempted to obtain precise specific gravity data; pycnometer, Berman torsion balance using rock powder (-100 mesh), and Berman balance using rock chips (0 to 130 mesh). The wetting agent used in all cases was toluene. Results are listed in Table 8 with precision estimates. In all cases, data reproducibility

TABLE 8

Specific Gravity of D-T Flow Samples

Sample Number	Berman Balance Rock Chip Value	Mean	Standard Deviation	Precision
CH-44	2.71			
CH-45	2.82			
CH-46	2.78			
	2.79	2.78	0.007	0.3 %
CH-47	2.85			
	2.86	2.85	0.007	0.3 %
CH-67	2.84			
CH-68	2.78			
	3.06			
	2.89			
	2.88	2.90	0.12	4.0 %

Sample Number	Berman Balance Rock Powder Value	Mean	Standard Deviation	Precision	Pycnometer Rock Powder Value	Mean	Standard Deviation	Precision
CH-22	2.15							
	2.07	2.11	0.06	1.9 %	2.89			
CH-23	2.36							
	2.54							
	2.23							
	2.41							
	2.22	2.35	0.13	8.1 %	3.00			
					3.07	3.04	0.05	1.6 %
CH-24	2.25				2.94			
	2.30	2.28	0.04	1.3 %				
CH-25	2.24				3.12			
	2.16	2.20	0.06	1.8 %				
CH-26	2.18				2.82			
	2.31							
	2.11							
	2.28	2.22	0.09	5.0 %				
CH-27	2.17				2.73			
	2.17				2.95	2.84	0.16	5.5 %
	2.26							
	2.25	2.21	0.05	2.3 %				
CH-28	2.19				2.83			
	2.20				2.98	2.91	0.11	3.6 %
	2.17	2.19	0.02	0.9 %				
CH-29	2.14				2.57			
	1.95							
	2.15							
	2.15	2.10	0.10	7.1 %				
CH-30	2.07				2.75			
	2.07				2.78	2.77	0.02	0.8 %
	1.89							
	1.82	1.96	0.13	7.1 %				
CH-32	2.24							
	2.11							
	2.37							
	2.36							
	2.25	2.27	0.11	7.0 %				

is excellent. Data variation is attributed to: loss of sample from sample mesh basket of Berman torsion balance; lag time between room and toluene temperature equilibration; difficulty in cleaning the pycnometer; volume changes induced in the pycnometer during handling; rapid toluene evaporation from the pycnometer during weighing.

These data are plotted (Figure 22) against total volatile content of the corresponding sample. Determinations acquired using the Berman balance and rock powder are systematically lower than those obtained by the other two methods. This systematic difference is attributed to a design error of the sample basket and counter weight system which was reconstructed by the author.

With increasing degree of alteration, the chloritic and pervasive carbonate zones are marked by decreasing and increasing specific gravity trends, respectively. It is in the intermediate, disseminated carbonate zone that the specific gravity reaches a minimum, reflecting the changing physico-chemical conditions of the alteration reactions. The specific gravities of the most altered samples (CH-27, 47, 67) are similar to those of the least altered samples (CH-24, 23, 25, 26).

Plotted in Figure 23 is the relative specific gravity of each altered sample with respect to the freshest or

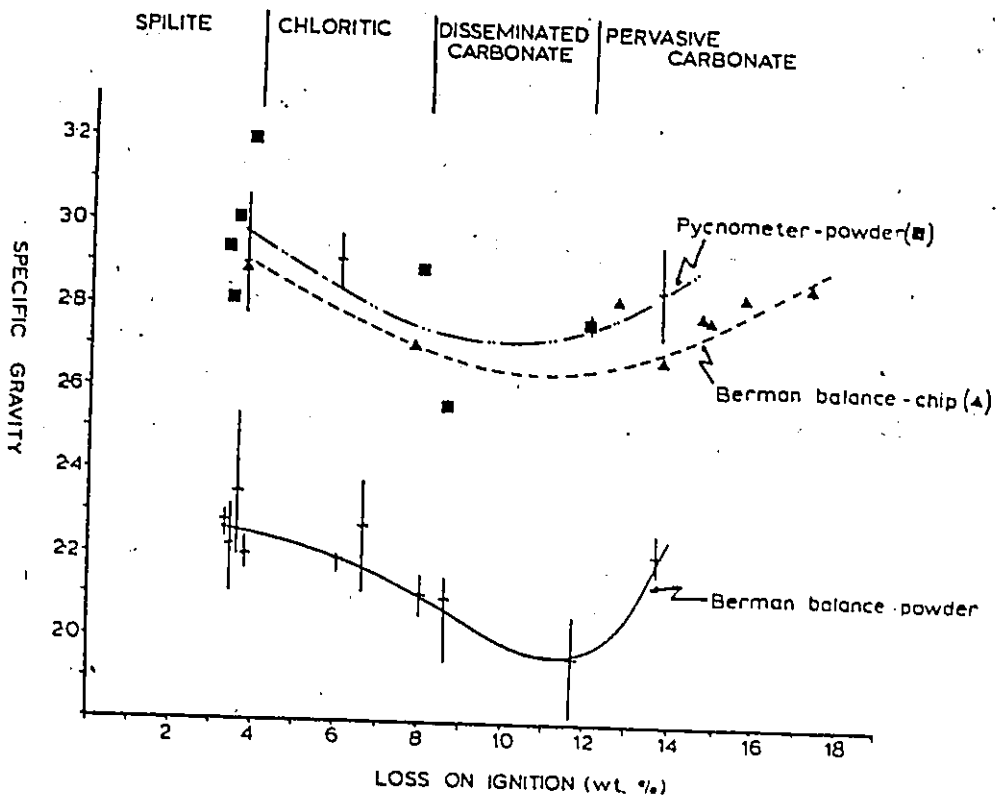

FIGURE 22. Specific gravity variation of altered Mg tholeiitic basalt as a function of degree of rock alteration, expressed as loss on ignition. All samples were collected from the D-T flow. Vertical dars represent the range of data for a given sample.

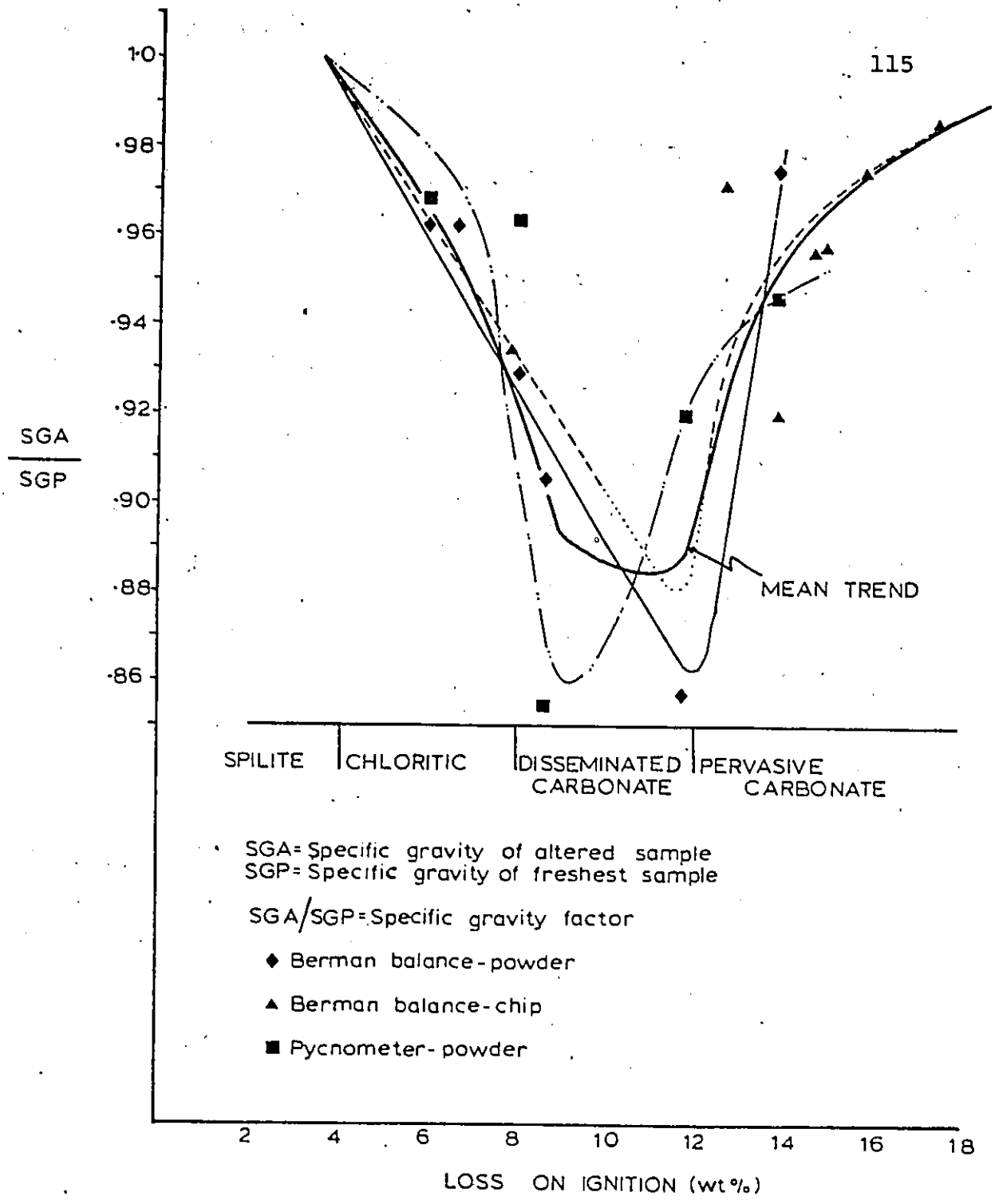

FIGURE 23: Relative specific gravities of altered D-T flow (Mg tholeiitic basalt) samples with respect to the least altered samples, as a function of increasing degree of rock alteration, expressed as loss on ignition.

parent sample for each analytical method. An average trend line is indicated.

7.2 CHEMICAL VARIATIONS RELATED TO CARBONATIZATION

There are many methods of manipulating chemical data (Chayes, 1964; Gresens, 1967; Babcock, 1973; Pearce, 1968; Beswick and Soucie, 1978). This section deals with absolute chemical changes of Mg tholeiitic basalt which took place during the alteration. On a scale defined by the limits of the alteration zone, metasomatic alteration assemblages represent partial equilibration states between two end members - in this case between Mg tholeiitic basalt and a CO_2 rich aqueous phase. As such the study of the metasomatic assemblages provides general information about the reactions which took place in that environment. The revelation of those reaction systematics is not only fundamental to the understanding of the alteration mechanism and the ambient physical-chemical conditions, but also describes the types, proportions and direction of cationic diffusions related to the alteration process. These are the parameters required to understand the genetic processes leading to metallic accumulation and ultimately, to ore deposit formation.

Because the most obvious characteristic of the metasomatic reactions is the introduction of H_2O and CO_2, total volatiles is used as a crude measure of alteration intensity, with intensity increasing sympathetically with increasing volatile content. Chemical data used have not been recalculated to anhydrous proportions for two reasons. First, this recalculation eliminates one of the metasomatic parameters, namely volatiles. Second, by using a simple proportional recalculation to anhydrous, it is implied that the alteration did nothing more than dilute the non-volatile chemical elements. This procedure might obscure real chemical variations related to the alteration process. For simplicity, concentrations are expressed in weight percent (major oxides), parts per million, ppm (Ni, Cr, Co, Cu, Zn, Rb, B, Sr, As, Li, Ba, Sb) and parts per billion, ppb (Au).

The composition-volume relationship applicable to metasomatism derived by Gresens (1967) has been applied to the altered samples of the D-T flow to calculate the absolute gains and losses of major and some trace elements.

Simply the composition-volume relationship derived by Gresens (1967) is:

$$\Delta X_n = a \frac{K_v \chi_n^B \rho^B}{\rho^\alpha} - \chi_n^\alpha$$

where: ΔX_n = chemical transfer of component n between phases A and B

K_v = ratio between initial and final volume of rock

$\rho^{\alpha B}$ = density of parent rock, product rock, respectively

χ_n^α = weight fraction of component n in rock A

χ_n^B = weight fraction of component n in rock B

a = mass of parent sample

When working with oxide weight percents it is convenient to designate "a" as 100 g so that ΔX_n becomes grams per 100 g or weight percent. However, for trace elements, "a" is set equal to 1 ppm (or ppb) and the resultant ΔX_n then becomes the absolute amount by which that element is enriched or depleted in the altered product rock with respect to the parent.

To apply the Gresens (1967) equation, the following data must be known or inferred:

1. the chemical composition of the parent and product rocks;

2. the specific gravity of the parent and product rocks;

3. either the volume change of the rock mass or the magnitude of chemical transfer of any chemical component.

The first two parameters have been measured. Because it is the magnitude of chemical change which is being sought, some discussion of the volume relationships is warranted. Textural evidence supporting a constant volume alteration are the uniform scalar dimensions of vesicles, pillows, and flow thicknesses regardless of the degree of rock alteration. Hence, it is assumed that the alteration process did not significantly change the volume of the rock.

To summarize, the following assumptions have been made to facilitate calculation of the absolute chemical variations as a function of degree of alteration using samples from the D-T flow:

1. Alteration was isovolumetric.

2. Spilitic rocks (least altered) best approximate the parent rock compositions.

3. The chemical components either were homogeneously

distributed throughout the parent rock on a hand sample scale, or were introduced with the aqueous solutions which altered the rock.

4. The average relative specific gravity factor (Figure 23) at a given volatile content can be used in Gresen's (1967) equation.

7.2.1 Major Oxide Variations

Listed in Table 9 are the compositions of the samples used for the calculations. The composition of the parent rock was determined by averaging the compositions of the samples containing less than 4 wt % volatiles (CH-23, 24, 25, 26). Two groups of trace element data are listed - one obtained from the laboratories of the Ontario Geological Survey, the other from the McMaster University facilities.

Figures 24 to 27 show the absolute, major oxide variations as a function of alteration intensity, and Table 10 summarizes the percentage changes with respect to the parent sample. Because of poor XRF precision (Table 2), Na_2O has not been included.

The absolute variation trends are grouped into four types. Group 1 (Figure 24) oxides (SiO_2, MgO, TiO_2), in general, are lost from the rock with increasing degree of

TABLE 9

Chemical Analyses Of The D-T Flow Samples

Sample Number	CH-22	CH-23	CH-24	CH-25	CH-26	CH-27	CH-28	CH-29	CH-30	CH-32	CH-44
SiO_2	48.45	49.11	50.73	50.06	50.35	45.42	50.17	51.19	46.58	48.99	47.91
Al_2O_3	13.76	13.85	13.86	13.79	13.67	11.57	12.79	12.54	12.41	13.70	13.32
Fe_2O_3	11.16	11.68	11.79	11.36	11.72	9.43	12.47	9.83	10.33	11.66	11.85
MgO	6.98	7.98	7.94	8.33	7.57	7.17	9.51	7.83	7.95	8.06	6.67
CaO	9.40	10.81	10.28	10.22	12.25	9.06	8.09	7.77	9.23	9.89	8.64
Na_2O	DL	DL	DL	DL	DL	DL	DL	DL	DL	DL	2.60
K_2O	0.06	0.06	0.07	0.07	0.06	1.09	0.04	0.06	0.07	0.05	0.10
TiO_2	0.80	0.76	0.75	0.80	0.73	0.66	0.64	0.69	0.72	0.81	0.77
MnO	0.18	0.22	0.21	0.24	0.19	0.19	0.23	0.15	0.17	0.18	0.25
P_2O_5	0.08	0.06	0.06	0.07	0.07	0.07	0.06	0.07	0.09	0.06	0.07
LOI	8.0	3.7	3.3	3.7	3.4	13.8	6.0	8.6	11.7	6.6	7.82
CO_2	4.03x					11.90x	1.66x	4.87x	6.09x	2.53x	4.94x

x denotes Ontario Geoscience Laboratory analysis

DL denotes value at or below detection limit

TABLE 9 continued

Sample Number	CH-22	CH-23	CH-24	CH-25	CH-26	CH-27	CH-28	CH-29	CH-30	CH-32	CH-44
As	1x	1x	1x			1x	1x	1x	1x	1x	DL
Au	4.2	3.3	4.3	3.6	3.6	3.2	2.7	3.2	3.4	2.7	2.3
B	5x	5x	5x			15.x	6x	5x	5x	5x	5x
Ba	40x	40x	290x	780x	60x	690x	30x	50x	140x	40x	80x
Co	46x	47x	47x			40x	50x	41x	42x	47x	59
Cr	158x					111x	113x	121x	128x	137x	113
Cu	139x					120x	113x	111x	107x	133x	116
Li	14x	12x	12x	12x	10x	18x	16x	22x	28x	18x	5x
Ni	66x					51x	53x	54x	58x	65x	88
Sb	0.3x	0.5x	0.3x			0.1x	0.8x	0.2x	0.1x	0.5x	0.2x
Sr	150x	200x	150x			100x	200x	80x	80x	100x	100x
Zn	83x					68x	98x	75x	80x	84x	113

x denotes Ontario Geoscience Laboratory analysis

DL denotes value at or below detection limit

TABLE 9 continued

Sample Number	CH-45	CH-46	CH-47	CH-67	CH-68	CH-76
SiO_2	44.69	44.09	38.70	42.42	48.64	44.41
Al_2O_3	12.48	12.35	12.67	12.18	13.97	12.18
Fe_2O_3	11.12	11.34	10.64	10.07	12.51	9.59
MgO	8.15	7.23	5.82	5.97	8.66	7.35
CaO	7.87	7.15	12.22	10.88	8.81	9.22
Na_2O	DL	DL	DL	DL	DL	DL
K_2O	2.08	1.40	1.57	1.80	1.56	1.65
TiO_2	0.73	0.77	0.55	0.59	0.73	0.59
MnO	0.10	0.15	0.17	0.14	0.21	0.16
P_2O_5	0.08	0.08	0.10	0.10	0.10	0.06
LOI	12.70	14.70	17.30	15.70	3.60	14.80
CO_2	10.75x	10.50x	16.10x	14.50x	x	12.00x

Sample Number	CH-45	CH-46	CH-47	CH-67	CH-68	CH-76
As	DL	DL	DL	DL	1	DL
Au	1.0		0.2		1.9	1.2
B	20x	10x	20x	5		15x
Ba	565x	320x	260x	360x	660x	190x
Co	52	57	39	40		45
Cr	83	43	104	97		127
Cu	130	174	11	125		30
Li	19	14x	16x	16x	8x	22x
Ni	59	52	75	68		71
Sb	0.1x	0.1x	0.1x	DLx	0.3x	0.3x
Sr	80x	80x	80x	150x		80x
Zn	91	73	85	80		63

x denotes Ontario Geoscience Laboratory analysis

DL denotes value at or below detection limit

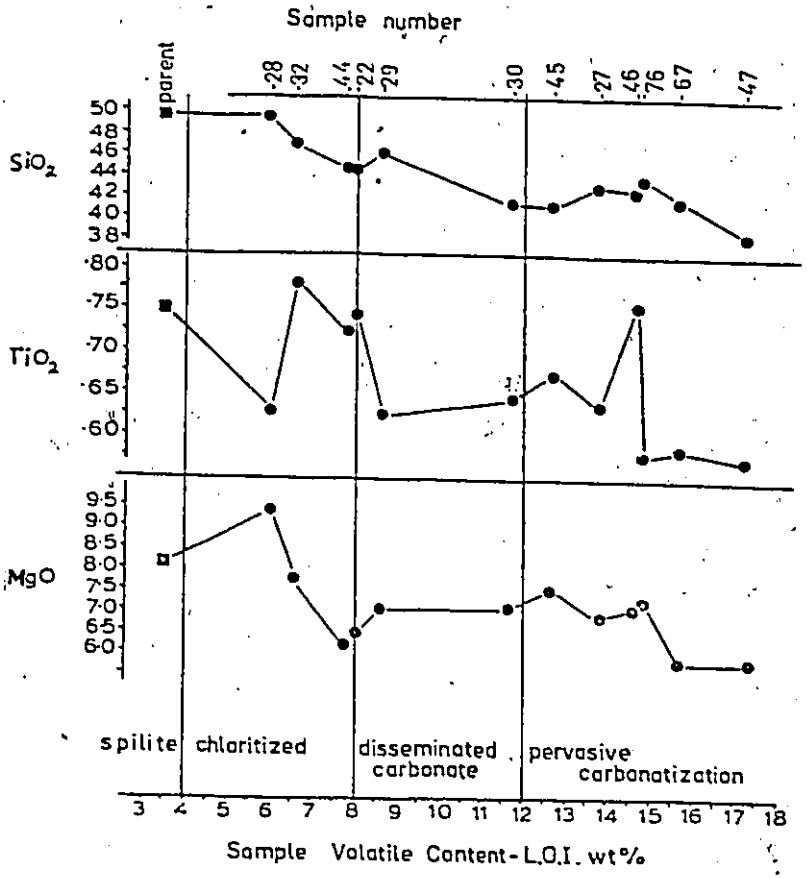

FIGURE 24: Variation of Group 1 oxides (SiO_2, TiO_2, MgO) as a function of degree of rock alteration, expressed as loss on ignition. All sample numbers bear prefix CH-, and were collected from the D-T flow (Mg tholeiitic basalt). Parent composition is average of least altered samples (CH-23,24,25,26). Oxides expressed as weight percent.

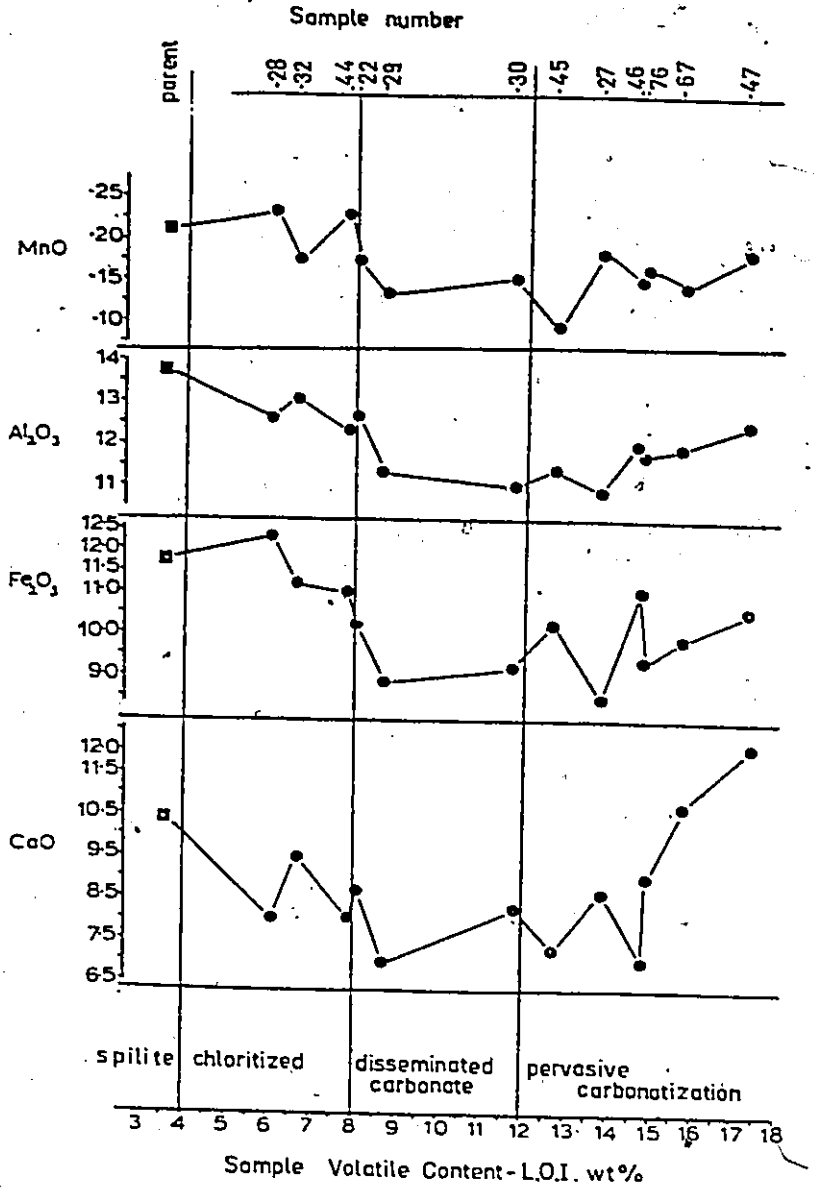

FIGURE 25: Variation of Group 2 oxides (MnO, Al_2O_3, Fe_2O_3, CaO) as a function of degree of rock alteration, expressed as loss on ignition. See figure for sample description. Oxides expressed as weight percent.

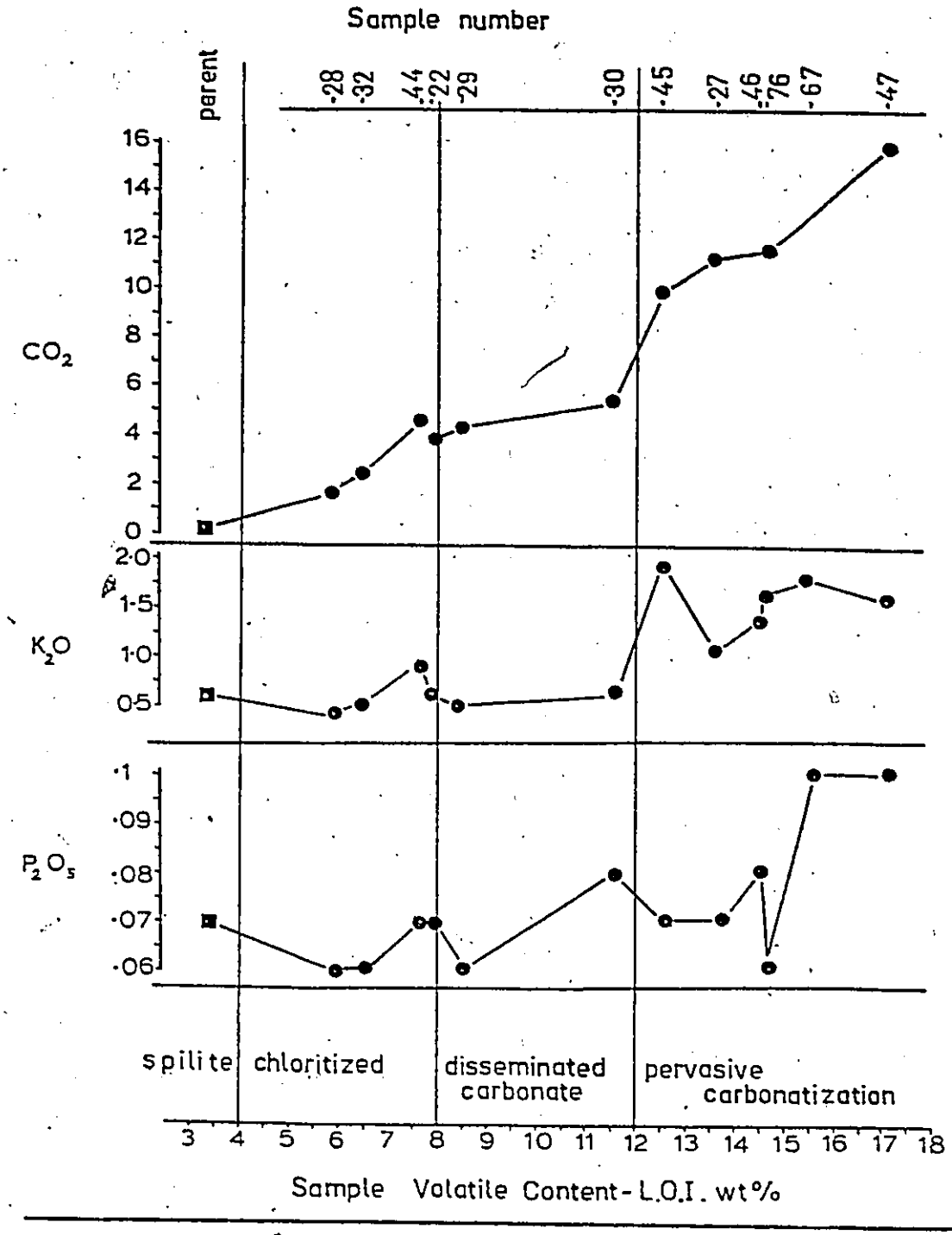

FIGURE 26: Variation of Group 3 oxides (CO_2, K_2O, P_2O_5) as a function of degree of rock alteration, expressed as loss on ignition. See figure for sample description. Oxides expressed as weight percent.

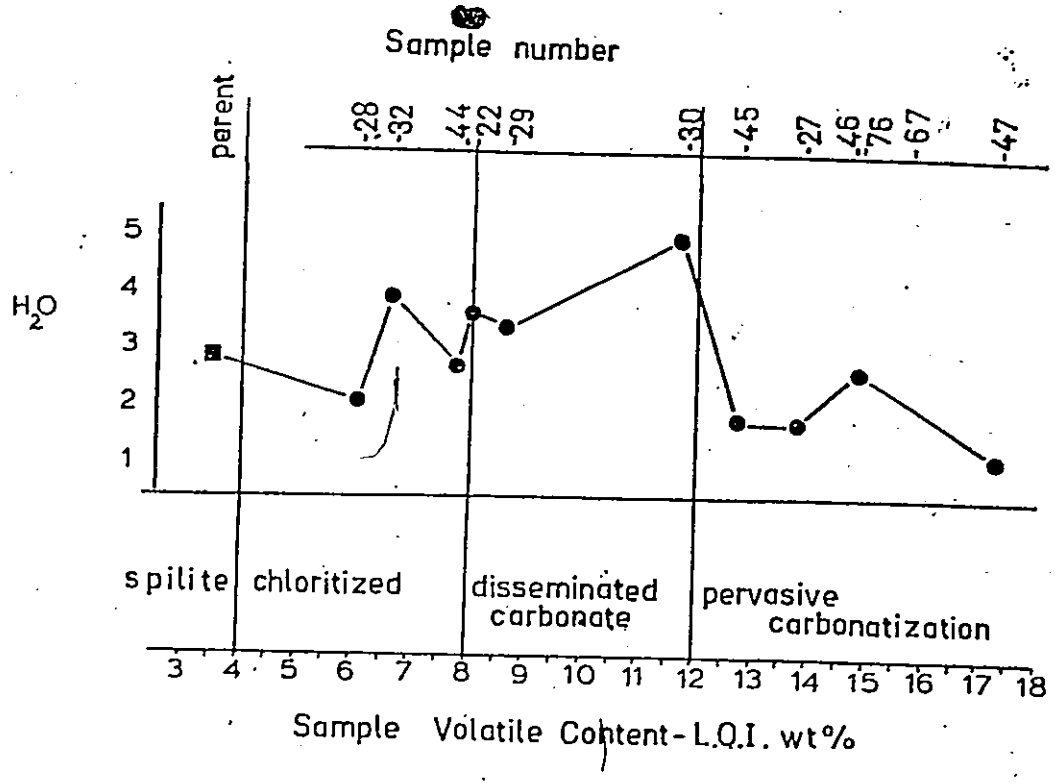

FIGURE 27 : Variation of H_2O (Group 4) as a function of degree of rock alteration, expressed as loss on ignition. See figure for sample description. (H_2O = L.O.I. - CO_2). H_2O in weight percent.

TABLE 10

Absolute Gains or Losses of Major Oxides Per Unit Volume As a Function of Degree of Alteration for Samples from The D-T Flow

Oxide	Percentage Change in Most Altered Sample of a Particular Alteration Assamblage With Respect To Least Altered Sample.		
	Chloritic (CH-22)	Disseminated Carbonate (CH-30)	Pervasive Carbonate (CH-47)
SiO_2	-10	-17	-23
Al_2O_3	-8	-20	-9
Fe_2O_3	-13	-22	-11
MgO	-21	-13	-29
CaO	-17	-22	+16
K_2O	0	0	+2483
TiO_2	-1	-15	-28
MnO	-19	-29	-19
P_2O_5	0	+14	+43
CO_2	+1225	+1836	+5593
H_2O	+26	+73	-59
Au	+38	+8	-93
Ni	-6	-20	-12
Cr	-3	-24	-24
Co	-9	-20	-43
Cu	-4	-28	-88
Zn	-23	-30	-26
B	0	0	+295
Li	+12	+117	+38
As	+5	0	+45
Ba	-26	+150	+415
Sb	-24	-76	-76
Rb	-86		+220
Sr	-21	+27	-55

Note: - denotes loss with respect to least altered sample
+ denotes gain with respect to least altered sample

alteration. MgO and TiO_2 are slightly enriched in the chloritic zone, possibly due to their incorporation (with iron) in chlorite, a feature noted by Carswell et al. (1978) and Humphris et al. (1978a). Group 2 (Figure 25) oxides (Al_2O_3, Fe_2O_3, CaO, MnO) are depleted from the chloritic zone, drop to minimum abundances in the transitional, disseminated carbonate zone and increase in the pervasive carbonate zone. Only CaO is more abundant in the most intensely altered sample (CH-47) than in the parent sample. Of the Group 3 (Figure 26) oxides (K_2O, P_2O_5, CO_2), K_2O and P_2O_5 are enriched only in the carbonatized samples. CO_2 increases with increasing alteration intensity; however, there is an inflexion point (11 to 12 wt % L.O.I.) above which the rate of CO_2 addition increases. This inflexion point, occurring at the transition from the disseminated to the pervasive alteration zone, is marked by corresponding mineralogical and textural changes (see section 6.3), notably the absence of veinlet-hosted chlorite. K_2O distribution matches that of sericite. Carbonate bearing apatite, $Ca_5(PO_4, CO_3, OH)_3(F,OH)$, is a possible host for phosphorous in the carbonate rich rocks (Deer et al., 1974, p.509).

H_2O, the only major element in Group 4 (Figure 27) is most abundant in the disseminated carbonate assemblage, and decreases with increasing or decreasing degree of

alteration from that zone. Note that the H_2O distribution is similar to that of chlorite modal abundance (Figure 21).

All major oxide variation trends involve abundance changes which exceed the precision of the analytical method, and therefore, the trends are real.

7.2.2 Trace Element Variations

The treatment of trace element data is more complex, because the data were generated at both McMaster University and the Ontario Geological Survey. The two sets of analytical data are systematically different, because of the different analytical techniques; however, to minimize error, the data sets were treated individually. Elemental percentage changes with respect to the spilitic parent, as a function of increasing degree of rock alteration are illustrated in Figures 28 to 30, and are summarized in Table 10. Of the elements plotted (Au, Ni, Cr, Co, Cu, Zn, B, Li, As, Ba, Sb, Rb, Sr), Au, Co, Cu, Sb and Sr have Group 1 type depletion trends (Figure 28), and all show a trend perturbation at the chlorite/disseminated carbonate alteration assemblage boundary (CH-44, 22, 29). Ni, Cr, and Zn have Group 2 (Figure 29) type trends, although it is only in the two most intensely carbonatized samples (CH-67,

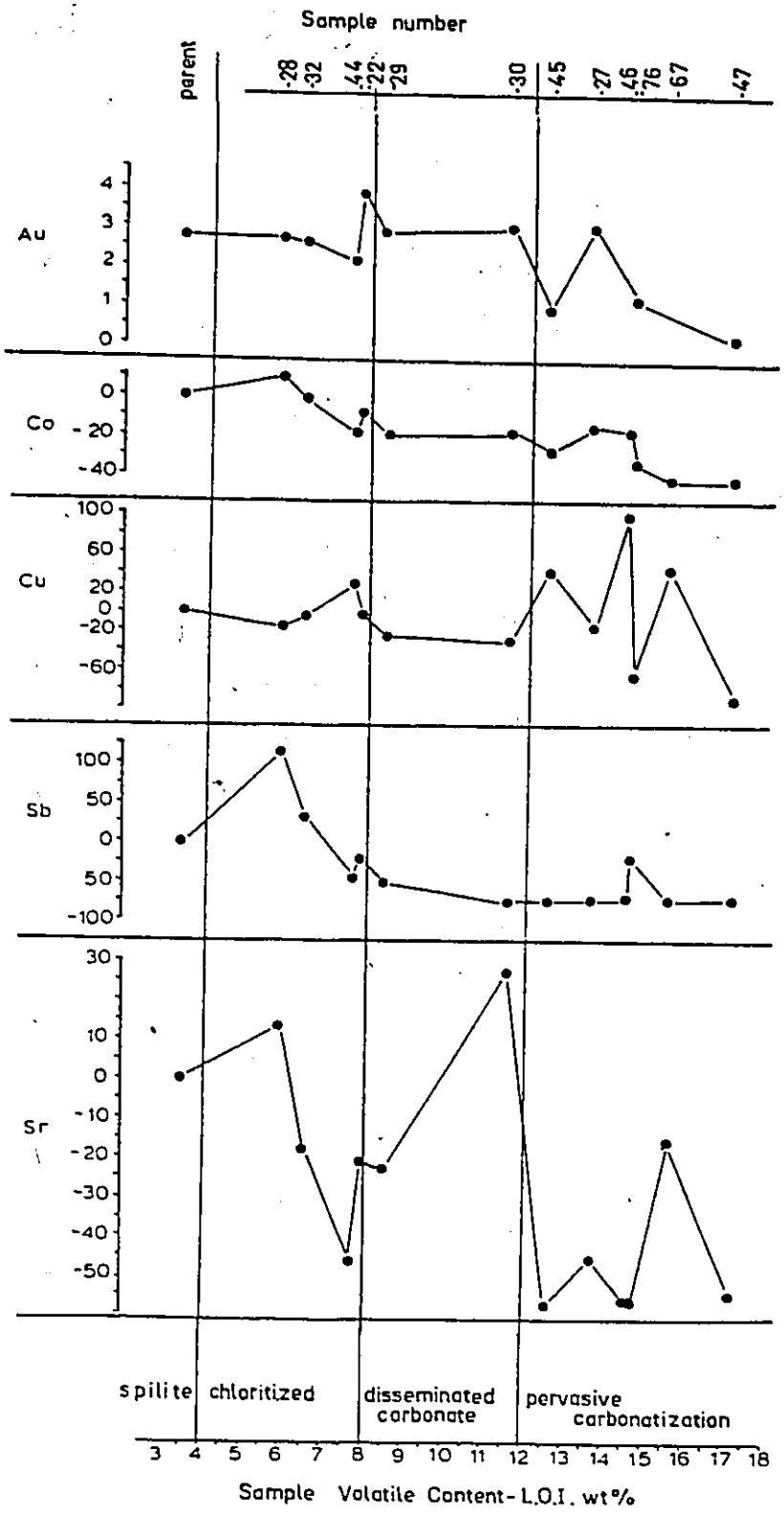

FIGURE 28 : Variation of Group 1 elements (Au, Co, Cu, Sb, Sr) in the D-T Flow as a function of alteration intensity expressed as loss on ignition. Element variation expressed as percent change with respect to the least altered or spilitic sample. Au expressed as parts per billion (ppb).

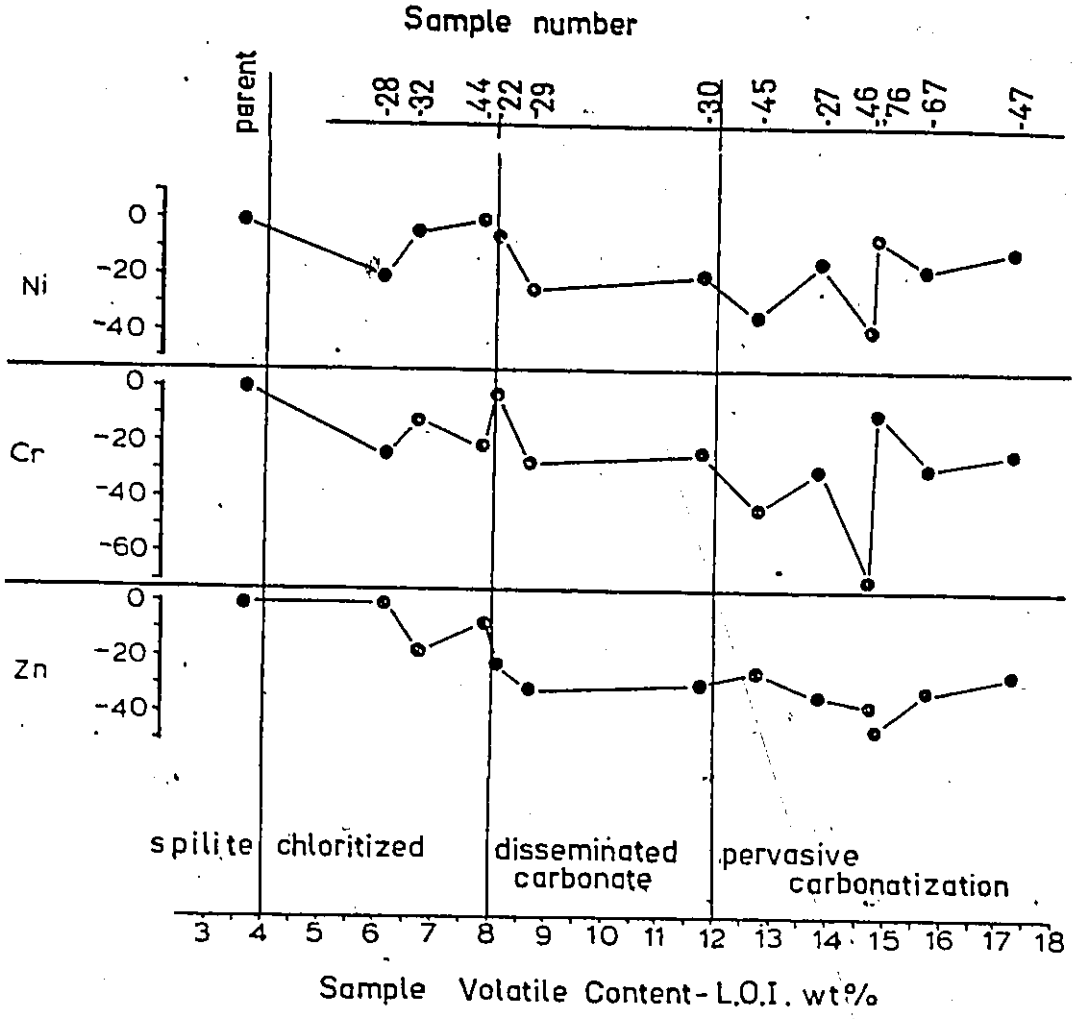

FIGURE 29 :Variation of Group 2 elements (Ni,Cr,Zn) in the D-T Flow as a function of alteration intensity,expressed as loss on ignition. Element variation expressed as percent change with respect to the least altered or spilitic samples.

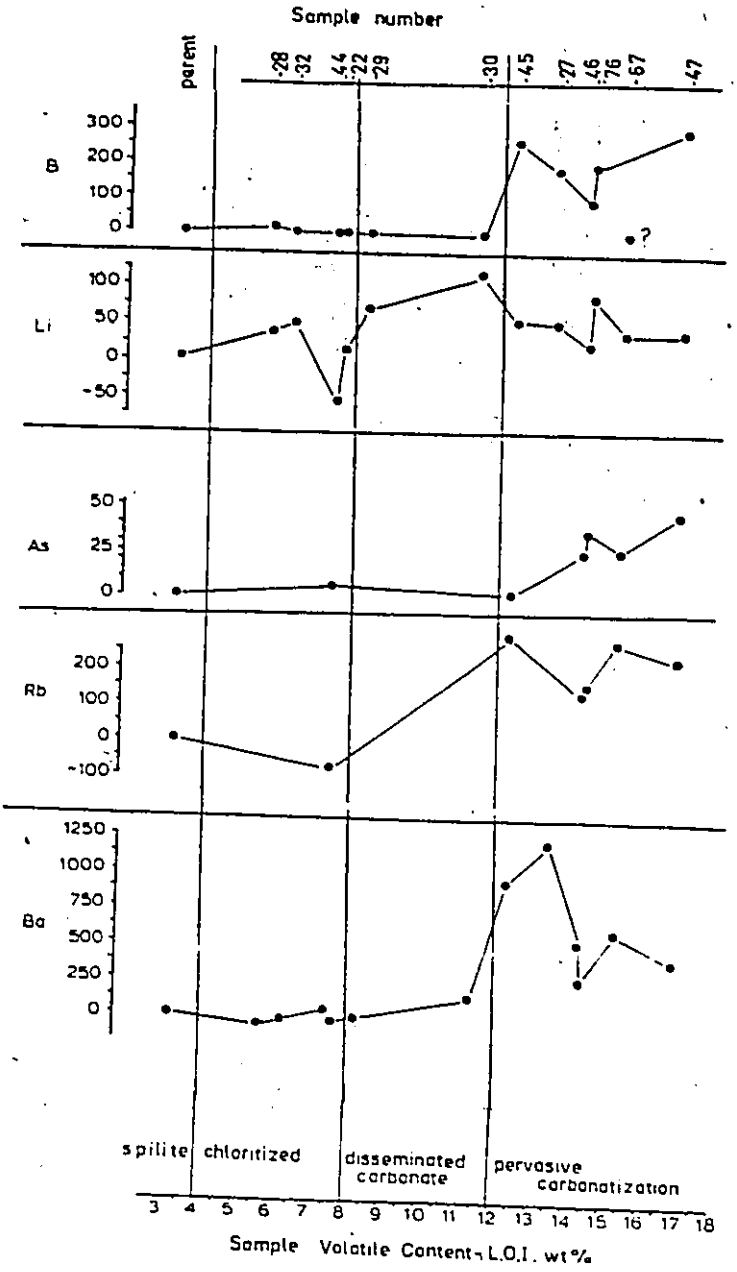

FIGURE 30: Variation of Group 3 elements (B,Li,As,Rb,Ba) in the D-T Flow as a function of alteration intensity expressed as loss on ignition. Element variation expressed as percentage change with respect to the least altered or spilitic samples.

47) that there is a slight enrichment of these elements. Ni and Cr patterns are very similar and each is enriched in the chloritic zone. B, Rb, Li, Ba and As trends are similar to K_2O (Group 3), each becoming enriched in the more intensely carbonatized samples (Figure 30).

7.3 DISCUSSION

The efficiency with which gold is leached during the most intense stages of carbonatization is significant in view of the observed spatial association between gold deposits and carbonatized rock. Relative to lesser altered rocks of the D-T flow, the most intensely carbonatized sample (CH-47) contains 93% less gold.

Silica, liberated initially during the destruction of ferromagnesium silicates, is leached from a volcanic rock during carbonate alteration. The silica is probably mobilized as amorphous silica (Holland, 1967) by the hydrothermal solutions and may precipitate elsewhere in gold-quartz veins or as cherty, carbonate-rich, seafloor sediments.

Although there is a net loss of iron in the most intensely carbonatized sample (CH-47) with respect to the spilitic parent (Figure 24), there is a trend towards

increasing iron content in the three most carbonate rich samples (CH-76, 67, 47) relative to the disseminated carbonate bearing samples (CH-29, 30). This increasing iron trend is accompanied by a corresponding increase in calcium and decrease of magnesium and may be attributed to a change from a dolomitic to an ankeritic carbonate with increasing degree of carbonate alteration.

There are a number of similarities between these major and trace element distributions and those reported for altered, modern, oceanic, basaltic rocks. The sympathetic increase of Li, B, K_2O, Rb, and Ba with increasing degree of alteration is a seafloor alteration phenomenom described by Thompson and Melson (1970), and Hart (1969). Original secondary alteration clays, now transformed to chlorite and sericite, most likely hosted these elements (Schwarcz et al., 1969). Data from Thompson and Melson (1970) indicate that at higher temperatures (200 to 300°C) boron is preferentially retained in the liquid phase of a basalt-seawater system. The enrichment of B, Li, K_2O in the altered rocks is consistent with the low temperature seawater/rock alteration model elaborated in Chapter 8 . Major element variations in the chloritized or hydrous assemblages, specifically the loss of SiO_2, CaO and the increase of MgO are similar to those described by Humphris

and Thompson (1978a). Some differences exist at higher volatile contents because of the predominance of carbonate phases.

The results of this study clearly demonstrate that Al_2O_3 and TiO_2 are not immobile during carbonate alteration. A similar conclusion was reached by Gibson and Watkinson (1979) for silicified rocks. The variation of the Al_2O_3/TiO_2 ratio as a function of alteration intensity is indicated in Figure 31. It has been suggested that this ratio is a reliable indicator of rock type (Kerrich and Fryer, 1979); however, it is evident that significant variations in the ratio are induced by the carbonate alteration. Descriptions of rock metasomatism using computational models based on the assumption of constant alumina or titania (c.f. Beswick and Soucie, 1978; Davies et al., 1979; Humphris and Thompson, 1978a; Beswick and Nichol, 1979) must be regarded with some caution. In fact, calculation of the volume factor in the Gresen (1967) composition-volume expression, assuming constant TiO_2 or Al_2O_3, reveals the altered volcanic rock underwent a volume expansion of 180 and 120%, respectively - a consequence having no field or petrographic support!

In conclusion, the major and trace element geochemical data are consistent with a lower temperature (<250°C) carbonate alteration developed in response to a rock/seawater

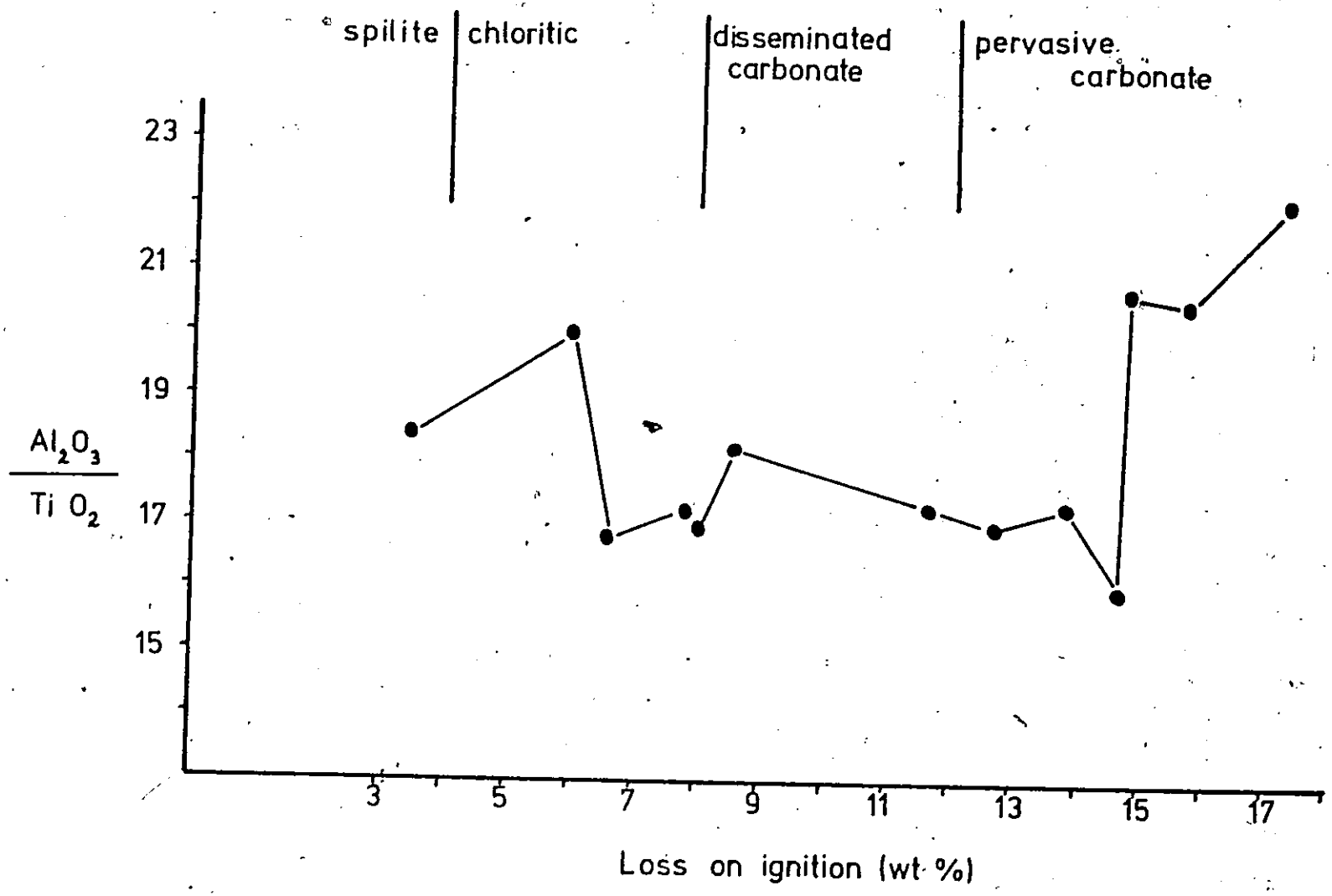

FIGURE 31 : Variation of Al_2O_3 TiO_2 ratio as a function of degree of rock alteration, expressed as loss on ignition. Samples were collected from the D-T flow (mg tholeiitic basalt). Absolute abundances of Al_2O_3 and TiO_2 used for calculation.

interaction.

7.4 EFFECTIVENESS OF CHEMICAL ROCK CLASSIFICATIONS USING ALTERED ROCK SAMPLES

Fundamental to the understanding of the volcanic and gold metallogenic evolution in the study areas is a knowledge of primary (pre-alteration) lithology. To supplement the field classification based on textural criteria, rocks were also classified by chemical composition using the Jensen Cation Plot (Jensen, 1976). To determine whether this chemical plot correctly classifies altered rocks, a comparison was made between rocks representing a wide range of degree of alteration. Initially control samples were collected from altered zones within the D-T flow (Map 5). There are no cumulate zones at the base of the flow suggesting that the chemical differences between samples are attributed to the alteration process.

7.4.1 Jensen Cation Plot

Illustrated on Figure 32 is an enlarged portion of the Mg tholeiitic basalt field of the Jensen Cation Plot, showing the groups of samples representative of spilitic,

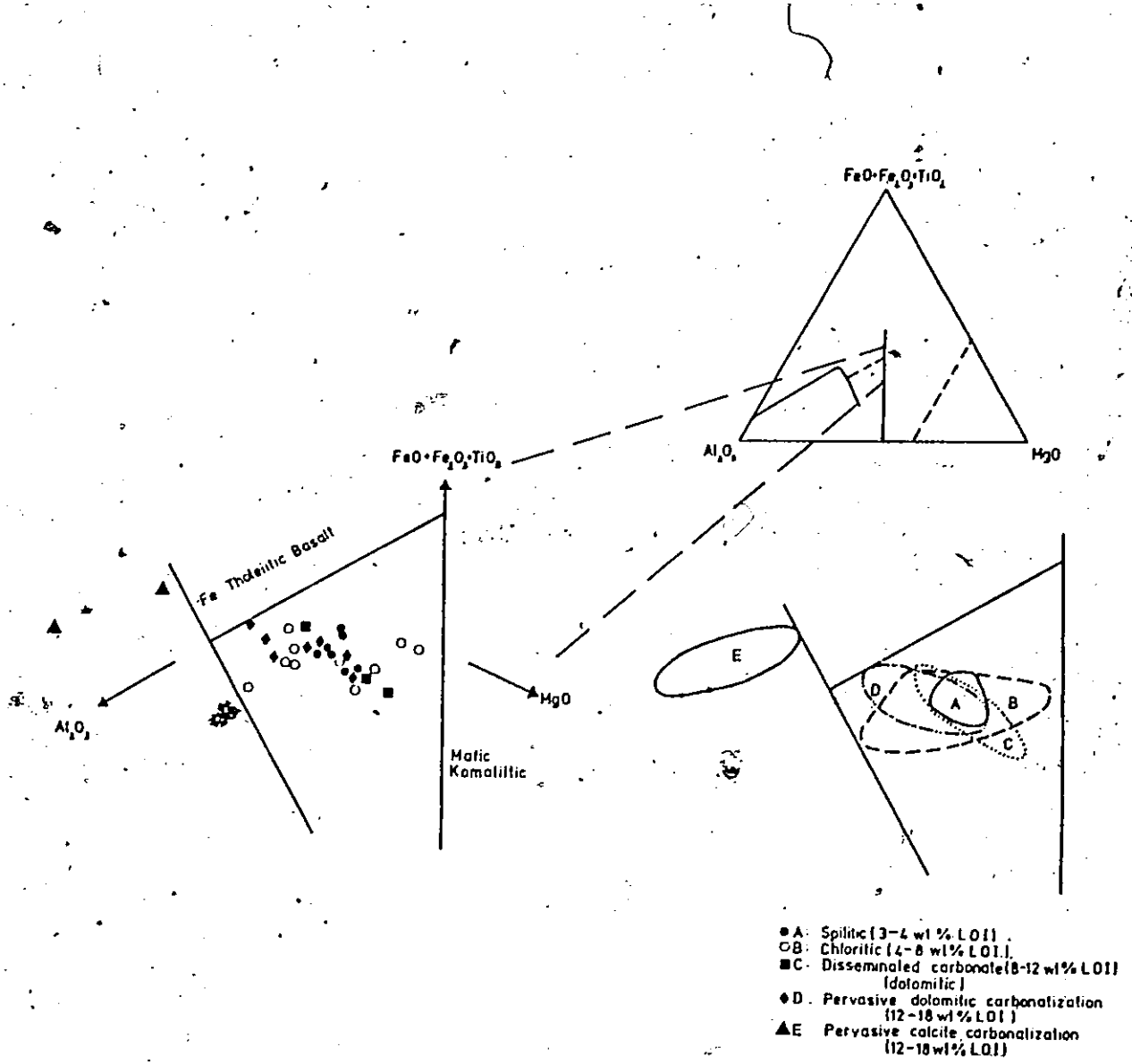

FIGURE 32. Expanded, magnesium tholeiitic basalt field of the Jensen Cation Plot on which have been plotted the altered volcanic rock samples collected from the D-F Flow. The alteration assemblage fields are outlined in the diagram on the right.

chloritic and carbonate-rich assemblages.

Compared with the field for spilitic rocks, data scatter increases with increasing volatile content. The relatively small number of data per group, particularly for the pervasive calcite and disseminated carbonate groups, prohibits a rigorous quantification of the relative geochemical trends as a function of volatile content. However, for pervasively dolomitized rock, there is a relative increase in Al_2O_3 and a decrease in MgO and (TiO_2 + FeO + Fe_2O_3) with increasing sample volatile content. This trend is consistent with the major element trends discussed in section 7.2.1.

To further quantify the differences between the groups a statistical test (ANOVA) was applied to determine if the variance between groups was greater than that which could be attributed to sampling. It is assumed that the parent population of the altered rocks is represented by the spilitic rock samples. A simplified description of the statistical procedure is presented in Appendix 2. The computed statistics, listed in Table 12, all exceed the critical value of $_{0.05}X^2$ [6], which implies the variance-covariances of the alteration assemblages (chloritic, pervasive carbonate) exceeds that variance which may be attributed to sampling. The number of data for the calcite

TABLE II

ANOVA* For Two Groups Of Data To Test The Equality Of Variance-Covariance Matrices Multivariate Equivalent Of The F-Test. Data From The D-T Flow, Using Al+Mg+Fe+Ti Cation Proportions

Jensen Cation Plot

Group 1 (n1)	Group 2 (n2)	M Statistic	C^{-1} Transform	X^2 Statistic	$X^2_{0.05}$ [6] Critical
Spilitic (5)	Chloritic (8)	23.6070	0.7679	18.1263	12.59
Spilitic (5)	Pervasive Dolomitic Carbonate (7)	39.8068	0.7279	29.0258	12.59
Using Oxide Weight Proportions Al_2O_3-MgO-CaO					
Spilitic (5)	Chloritic (8)	34.6376	0.7679	26.5967	12.59
Spilitic (5)	Pervasive Dolomitic Carbonate (7)	24.3536	0.7292	17.7578	12.59
Chloritic (8)	Pervasive Dolomitic Carbonate (7)	6.7404	0.7292	4.9149	12.59

rich and the disseminated carbonate alteration assemblage groups are too few to permit such a statistical evaluation.

It is apparent (Figures 32, 7) that a sample, originally of Mg tholeiitic basalt composition, may be classified as calc-alkalic, Mg tholeiitic or possibly even komatiitic, depending on the degree of sample alteration. With continued magmatic evolution, the fresh Mg tholeiitic basalts plot closer to the Fe/Mg tholeiitic basalt boundary on the Jensen Cation Plot (Figure 7). The classification of these altered rocks becomes more severe, for they could plot not only within the calc-alkalic, Mg tholeiitic and komatiitic fields, but also in the Fe tholeiitic field.

7.4.2 Al_2O_3-MgO-CaO Plot

A similar evaluation of the Al_2O_3-MgO-CaO plot reveals that group data variation is also increased with increased volatile content with respect to the fresh field (Figure 33). In addition, for pervasively carbonatized samples, there is a relative increase of CaO and a slight decrease in MgO with increasing volatile content.

The statistical data (Table 11) indicate that the volatile rich assemblages differ in variance-covariance from that of the fresh samples at the 5% significance level.

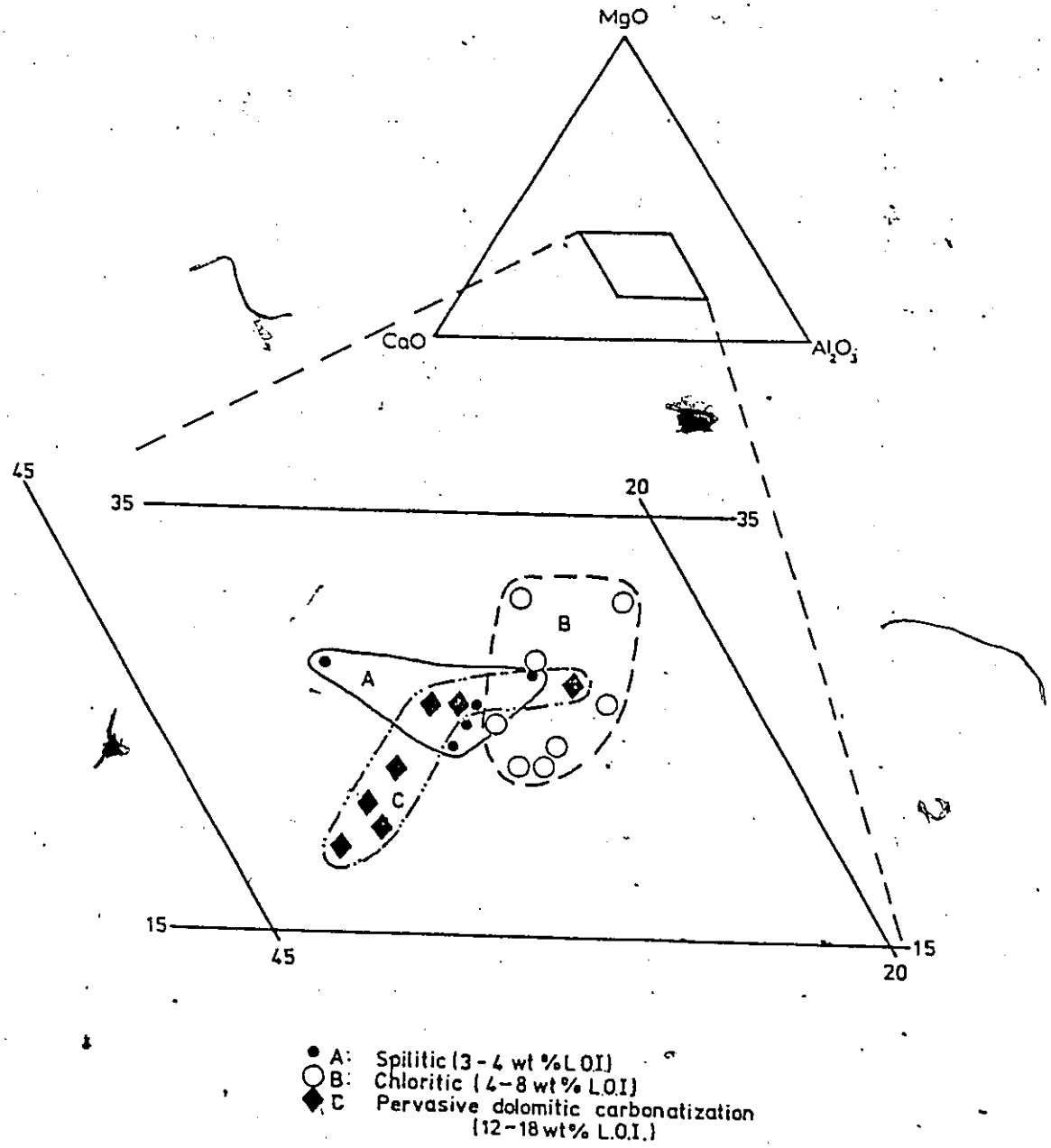

FIGURE 33 : Enlarged portion of the Al_2O_3-MgO-CaO plot on which have been plotted the compositions of altered samples collected from the D-T Flow.

As noted in Appendix 2, the minimum number of data required for this statistical test is approximately 20. Because the D-T flow variance equivalence test was carried out with less than 20 samples per group the conclusions reached have been verified using a larger data group. Approximately 100 samples, altered to various degrees based on L.O.I. content, were selected from the regional data file and have been tested for variance equivalence with respect to the fresh population. Only data for the MgO-Al_2O_3-CaO plot has been re-evaluated using the regional data base (Table 12).

When working with regional data, an additional element of variance is introduced by magmatic evolution of the source region(s) from which the basalts were derived. This additional element of geochemical variance does not seriously constrain the general application of the ANOVA test if the spilitic and intensely altered samples are equally representative of both lateral and vertical extents of the study areas. Spilitic and intensely altered samples were selected from the regional data file to satisfy this criterion.

Using the regional data, it is confirmed that the hydrated and carbonatized rock samples have different variance-covariances relative to the spilitic population;

TABLE 12

ANOVA For Two Groups Of Data To Test For Equality Of Variance-Covariance Matrices. Data From Regional Sample File, Using Oxide Weight Proportions Al_2O_3-MgO-CaO

Group 1 (n1)	Group 2 (n2)	M Statistic	C^{-1} Transform	X^2 Statistic	$X^2_{0.05}$ [6] Critical
Spilitic (19)	Chloritic (46)	43.1525	0.9639	41.5942	12.57
Spilitic (19)	Pervasive Dolomitic Carbonate (64)	45.5773	0.9742	44.4017	12.57
Chloritic (46)	Pervasive Dolomitic Carbonate (64)	7.2162	0.9742	7.0300	12.57

however, the hydrated and pervasively dolomitized groups are themselves drawn from populations having equal variances at the 5% significance level (Table 12).

7.4.3 Discussion

Hydration and carbonatization processes induce variable changes on the original composition of a Mg tholeiitic basalt. On the Jensen Cation Plot (Jensen, 1976) volatile rich Mg tholeiitic basalts might plot in the calc-alkalic, Mg or Fe tholeiitic or possibly the komatiitic fields (Figure 7), depending on the degree of sample alteration and the degree to which the fresh chemical composition is iron enriched. Iron or magnesium enriched Mg tholeiitic basalts plot close to either the Fe tholeiitic or the komatiitic fields, respectively. Altered samples of these compositions are the most likely to be incorrectly classified, by virtue of the increase data scatter, and could plot in the adjacent chemical field. Similar classification problems are encountered using the MgO-Al_2O_3-CaO plot. Therefore, chemical classifications of the altered rocks containing greater than 4 wt % volatiles, must be interpreted with caution, particularly when field criteria (e.g. volcanic textures, local lithological association) do not accompany a sample description.

7.5 SUMMARY

The carbonate alteration is assumed to be a constant volume reaction. Specific gravity of the rock decreases with increasing degree of hydration and increases with progressive carbonatization. Intensely carbonatized, Mg tholeiitic basalt has approximately the same specific gravity as the spilitic parent.

Major oxide and trace element distributions in altered rock are characterized by four distinct trends. Group 1 elements (SiO_2, MgO, TiO_2, Au, Co, Cu, Sb, Sr) are generally depleted with increasing degree of alteration, although a slight enrichment of MgO and TiO_2 occurs during initial hydration. Group 2 elements (Al_2O_3, Fe_2O_3, CaO, MnO, Ni, Cr, Zn) are depleted during hydration, but enriched during carbonatization. Only CaO is enriched, in excess of that amount in the parent, in the most intensely carbonatized rock. Group 3 elements (K_2O, P_2O_5, CO_2, B, Li, As, Rb, Ba) are enriched in an altered rock with increasing degree of carbonate alteration. Only H_2O, which constitutes Group 4, attains maximum abundance in the disseminated carbonate zone and decreases in abundance with increasing or decreasing degree of alteration with respect to the disseminated carbonate zone. For altered rocks containing

in excess of 4 wt % total volatiles, no element examined during this study can be considered immobile. As a consequence, chemical classification diagrams can yield incorrect rock classifications.

The noted enrichment of Li, B, K_2O, H_2O, Rb in the altered flows is similar to the geochemistry of modern, submarine, basalts which have interacted with seawater at low temperatures (<250°C).

CHAPTER 8

TIMING OF THE CARBONATE ALTERATION EVENT

It is imperative to establish whether the alteration assemblages represent a mineralogical equilibration at greenschist metamorphic facies attained during burial or whether these assemblages represent a high temperature (>300°C) seawater/rock alteration product analogous to modern, sea-floor greenstones (c.f. Andrews, 1977; Muehlenbachs and Clayton, 1972b, for summary). There are several textural criteria which help constrain the relative age of the localized, intense chlorite/carbonate alteration event. Quartz-chlorite-carbonate veins in these rocks generally are not oriented parallel to either the F_1 or F_2 foliation planes, corresponding to the original north-south and subsequent northeast-southwest fold axes. Many of the microscopic and megascopic veins are isoclinally folded. The vein quartz has a strained, undulose extinction and has been polygonized. Similarly, vein and matrix carbonate has been annealled as indicated by the 120° intergranular angles. Sericite, present in the pervasive

quartz-carbonate assemblages, often is aligned parallel to both F_1 and F_2 planes. On an outcrop scale, both spilitic and carbonatized rock bear the same linear and planar tectonic fabrics. Specifically, on the Beaumont (Map 3) and Davidson Tisdale (Map 5) properties, spilitic and carbonatized rocks have north-northeast trending lineation fabrics, consistent with those imprinted during the initial north-south deformation of the Porcupine camp. Additional salient field data are the presence of carbonatized rock clasts within the turbiditic, matrix supported komatiitic conglomerates of the Porcupine Supergroup exposed at the Pamour (Plate 21-1) and Buffalo Ankerite mines (Plate 7-1, Map 12) and on the Thomas Ogden property (Figure 34, Plate 21-2), and the presence of carbonate rich, komatiitic, turbiditic argillite interbedded with carbonate free mafic and felsic argillites exposed at Wawaitin Falls (Figure 35).

Clearly the microscopic textures indicate that the localized chlorite-carbonate alteration assemblages have undergone a superimposed, tectonic re-equilibration. Furthermore, the megascopic field data indicate that not only were the rocks carbonatized prior to the earliest north-south period of rock deformation, but the sedimentalogical evidence demonstrates conclusively that a carbonatized, volcanic rock terrain was present as a source area from which

PLATE 21-1. Rounded, carbonatized, ultramafic, komatiitic flow clasts in a matrix supported, komatiitic, turbiditic conglomerate, exposed at the Pamour Mine (fig 3).

PLATE 21-2. Carbonatized, ultramafic, komatiitic flow clasts in a matrix supported, komatiitic, turbiditic conglomerate exposed on the Thomas Ogden property, Ogden township Figure 34).

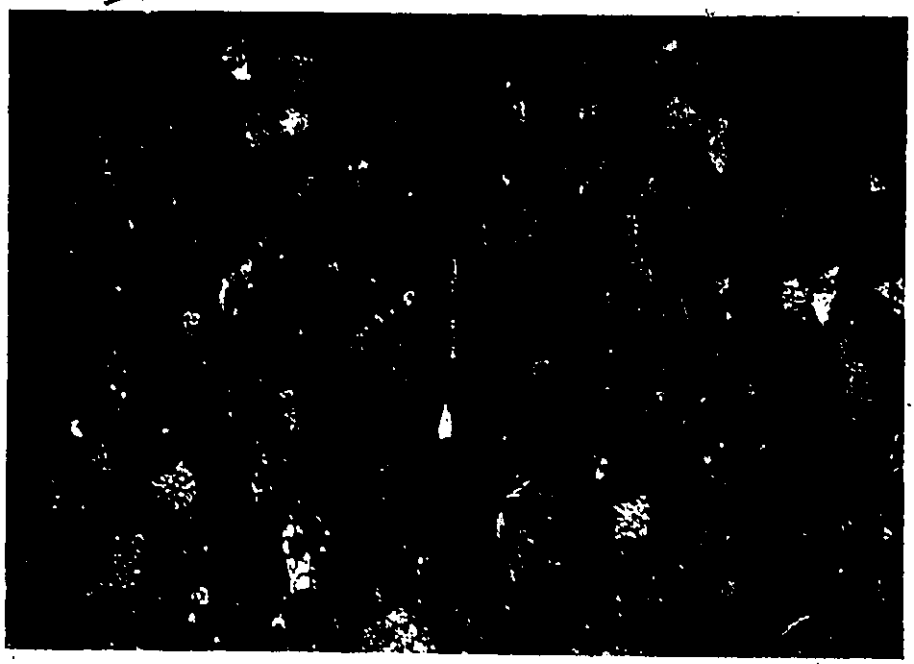

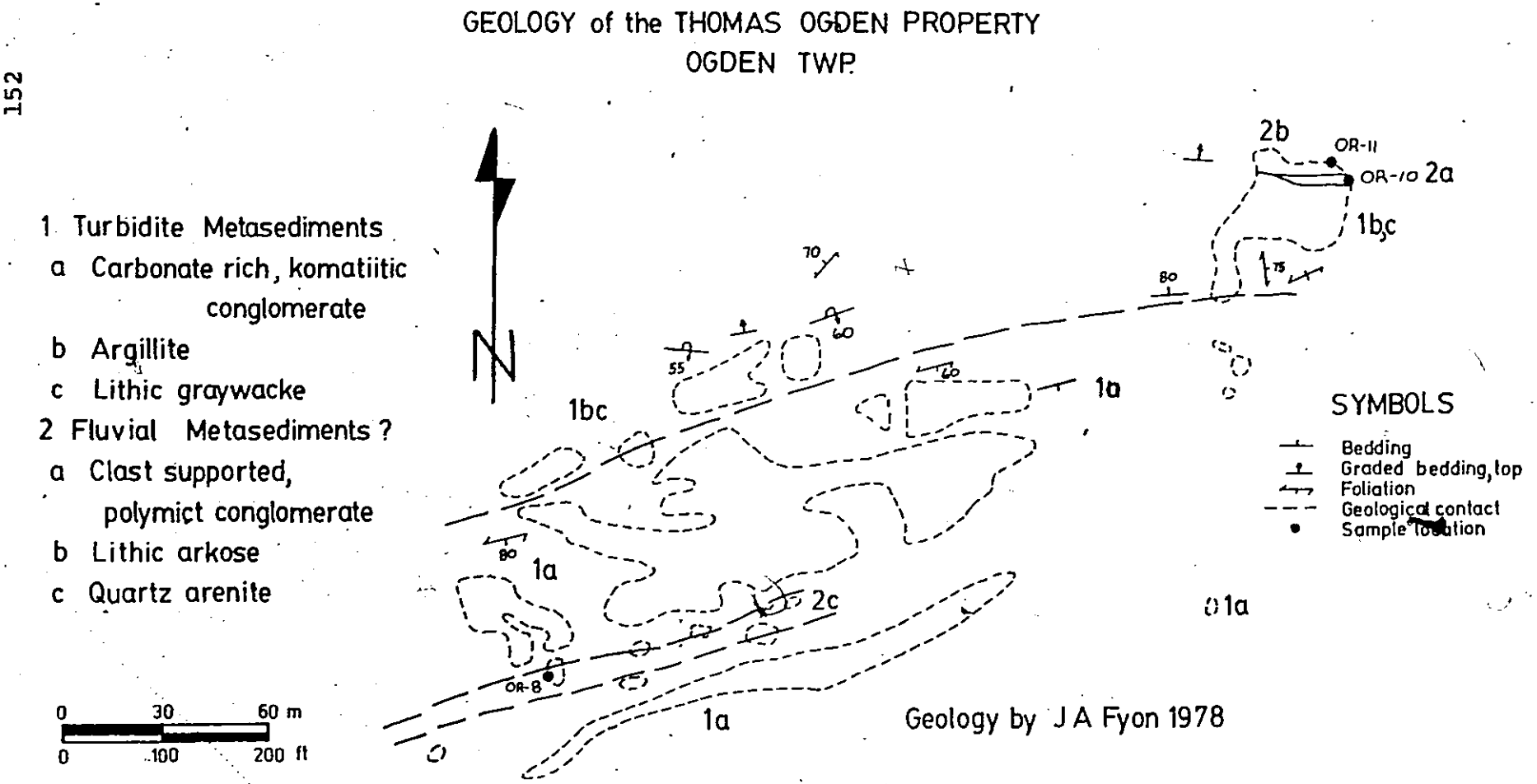

FIGURE 34 : Surface geology of the Thomas Ogden property, in Ogden Township.

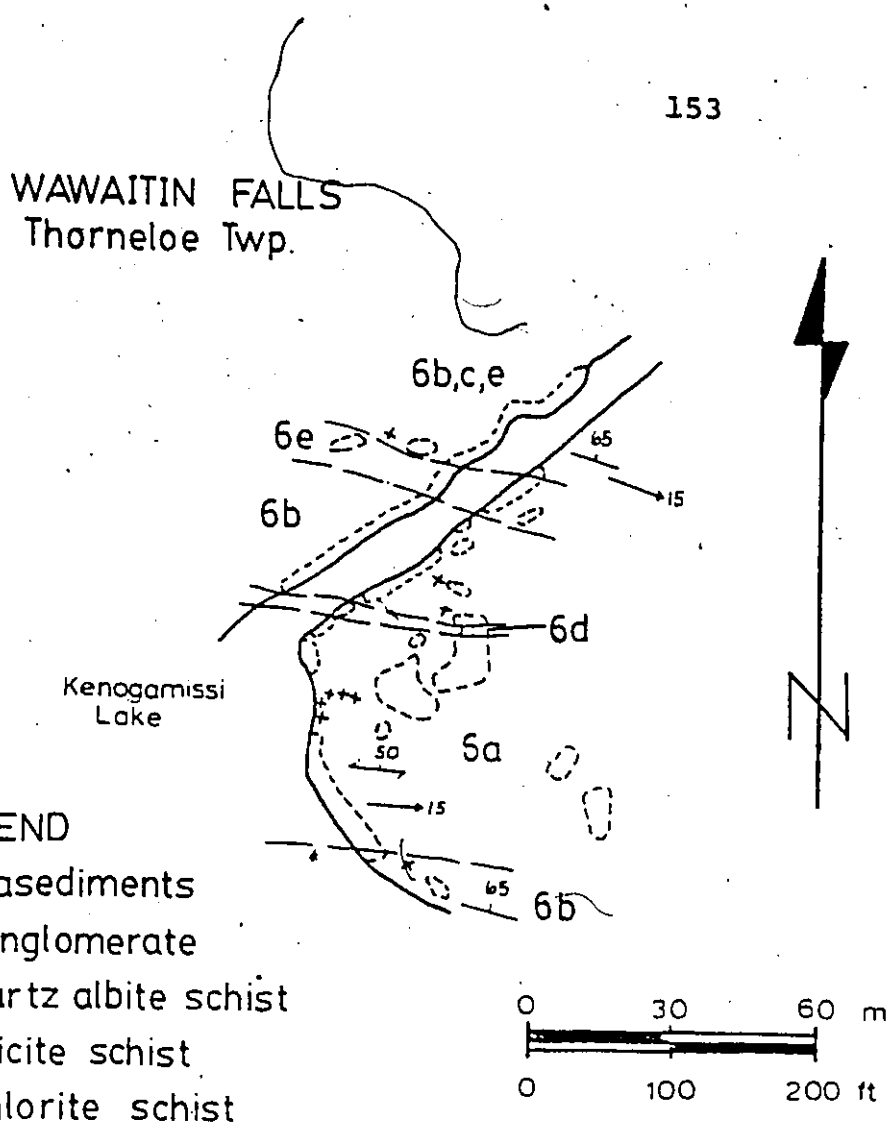

LEGEND

6 Turbidite Metasediments

- a Polymict conglomerate
- b Chlorite quartz albite schist
- c Quartz sericite schist
- d Feldspar chlorite schist
- e Carbonate chlorite fuchsite schist

Geology by J.A. Fyon 1979.

FIGURE 35 : Surface geology along the aqueduct at Wawaitin Falls, Thorneloe Township.

the Porcupine Supergroup turbidites were derived. Pyke et al. (1978) demonstrated that the Porcupine Supergroup is time equivalent with the entirety of the Upper Supergroup, and hence, the carbonatization process was contemporaneous with the volcanic evolution of the Upper Supergroup.

Having established that some of the carbonate alteration was synvolcanic, what can be deduced about the timing of the event which produced the regionally extensive chlorite-quartz-albite-zoisite-tremolite or spilitic assemblages in the Mg tholeiitic basalts? This age relationship is revealed by examination of certain geochemical characteristics of the carbonatized and the spilitized volcanics (Table 13). No mafic volcanic rock analysed contains less than 3.3 wt % total volatiles, compared with the 0.4 wt % or less H_2O found in fresh, modern submarine basalts (Pineau et al., 1976). Furthermore, these "spilitic" rocks have a higher ferric/ferrous ratio (0.35, Fryer et al., 1979) and are enriched in oxygen-18 ($\delta^{18}O$ whole rock = +9 to +14.3°/$_{oo}$, Kerrich and Fryer, 1979). Both the carbonatized tholeiitic and komatiitic volcanic rocks are enriched in Ba, Li, K_2O, B, H_2O, CO_2 with respect to fresh, modern, submarine basalts (Table 13). These geochemical data are consistent with those of modern, submarine basalts which have undergone a low temperature (<250°C) seawater alteration of the type described by

TABLE 13

Comparison of Certain Geochemical Characterisics of Fresh and Seawater Weathered, Modern, Submarine Basalts With Those of Altered Flows Form The Timmins Area

	Modern Submarine Basalts		Timmins Data	
Element	Fresh	Seawater Weathered	Ore Associated	No Ore Association
B ppm	2-8(1)	5-130(1,2)	$\bar{X}$=521 <5-3000 n=26	$\bar{X}$=10.7 <5-40 n=83
Li ppm	3-8(1)	3-60 (1,2)	$\bar{X}$=42 17-58 n=52	$\bar{X}$=17.5 <5-56 n=160
K_2O wt %	.06-.18 (3)	.07-.56 (3)	$\bar{X}$=1.13 .20-3.0 n=19	$\bar{X}$=.68 .03-3.2 n=97
Ba ppm	<5 (1)	<5-20 (1)	$\bar{X}$=87 20-200 n=52	$\bar{X}$=130 20-690 n=160
Sr ppm	90-190 (1)	100-260 (1)	$\bar{X}$=80 n=15	$\bar{X}$=96 45-200 n=93
H_2O wt %	<0.3 (4)	.4-7.0 (1,4)	>3.3	
Fe^{3+}/Fe^{2+}	.3 (4)	.4-1.1 (4)		$\bar{X}$=.35 (6) .32-.41 n=3
δO^{18} ‰ whole rock	5.5-6.5 (7)	5.5-18 (7)		9 to 14 (5) n=11

1: Humphris and Thompson (1978b)
2: Thompson and Melson (1970)
3: Hart (1969)
4: Hart and Nalwalk (1970)
5: Kerrich and Fryer (1979)
6: Fryer et.al. (1979)
7: Muehlenbachs (1977)

Muehlenbachs and Clayton (1972), Hart (1969), Thompson and Melson (1970), and Hart and Nalwalk (1970). This low temperature, seawater/rock interaction transforms the basalt into zeolites, clays, palagonite and lesser amounts of carbonate (Dimroth and Lichtblau, 1979; Andrews, 1977), and produces distinctive palagonization textures (c.f. Dimroth and Lichtblau, 1979; Baragar et al., 1977; Scarfe and Smith, 1977). Similar relict textures are preserved in some hyaloclastites in the Timmins area (Plate 7-3). Nowhere in Archean mafic volcanic rocks do primary, low temperature zeolite, clay phases exist; however, their former presence is confirmed by the preservation of their mineral forms and textures which have been pseudomorphed by chlorite, and silica (Dimroth and Lichtblau, 1979). Clearly, these early alteration phases were transformed to tremolite-zoisite stable assemblages during metamorphism to greenschist facies, related either to burial or subsequent contact metamorphic effects (Jolly, 1978).

The time relationships between alteration types are summarized in Figure 36. All alteration reactions were most likely contemporaneous, at least locally within the evolving volcanic center, although palagonitization of the hyaloclastite granules was most likely the first manifestation of rock/hydrothermal solution interaction (Dimroth and Lichtblau, 1979).

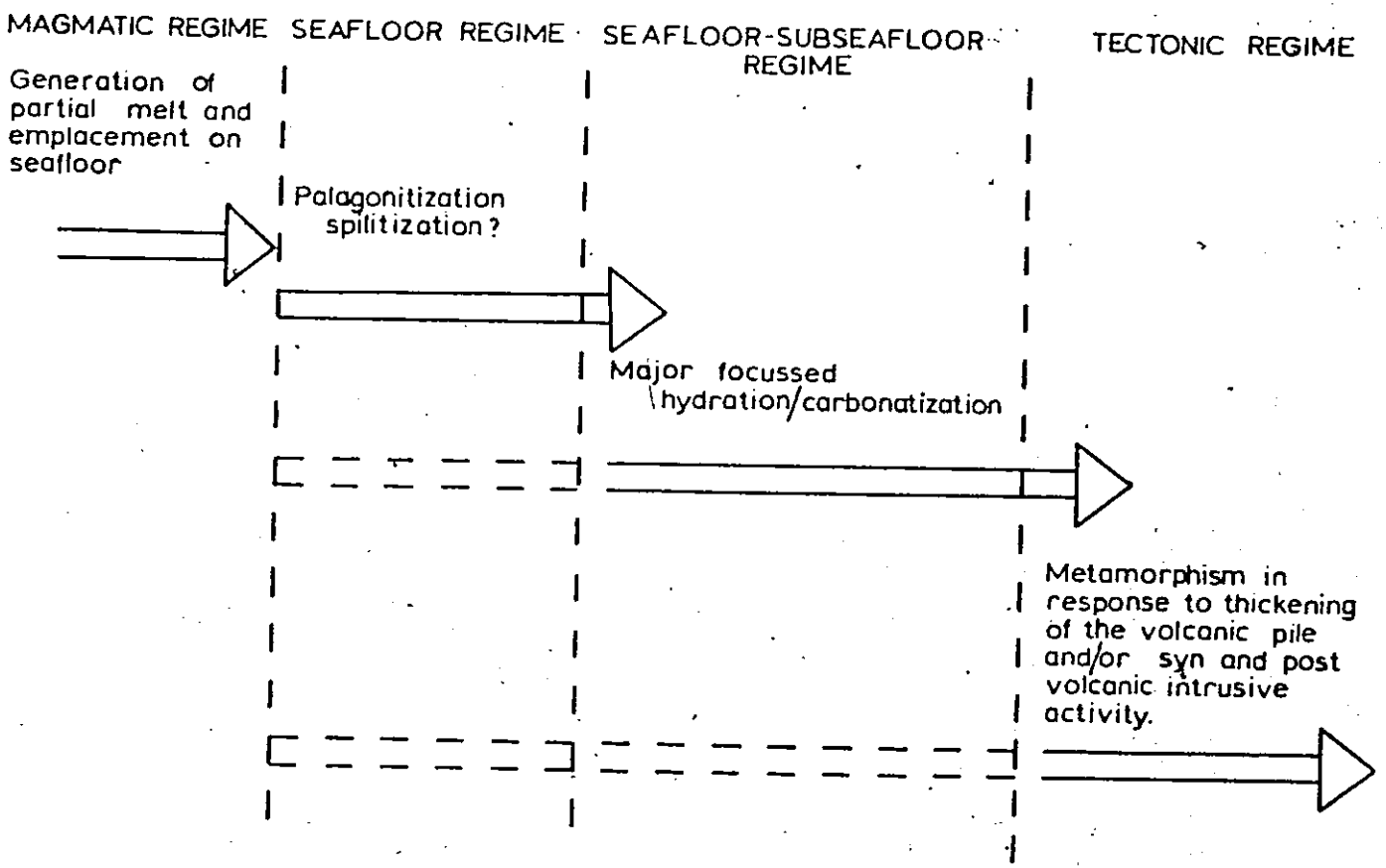

FIGURE 36: Schematic representation of the sequentially superimposed alteration events which affected the tholeiitic and komatiitic flows in the Timmins area. Space-time restriction of an alteration event is indicated by a solid tail on the arrow. Dashed tails on the arrows indicate probable contemporaneity of events.

8.1 CARBONATE ALTERATION ENVIRONMENTS

The carbonate alteration zones developed in two different volcanic environments. Hydrothermal solution flow through permeable aquifers within the volcanic pile, beneath the seafloor is typified by stratabound alteration zones, localized along flow contacts, which have symmetrically disposed alteration assemblages developed in the top and base of juxtaposed flows (Figure 17); and by discordant alteration zones which terminate gradually within a flow unit, rather than abruptly at a flow contact (Figure 18). This subseafloor alteration environment is characterized by the absence of chemogenetic, interflow sediments and felsic volcanic rocks or porphyries. Within the Tisdale township study area, most, if not all of the alteration zones developed in this subseafloor environment.

Conversely, the chloritic and carbonate-rich, alteration assemblages within stratabound and discordant alteration zones which developed at, or immediately beneath, the seawater ocean-floor interface, are restricted to one flow or flow unit. Overlying flows in contact with the pervasively carbonatized flows are carbonate free (Figures 17, 18). Carbonate alteration zones which developed at, or proximal to, this marine, hydrospheric environment are

spatially associated with Q.F.P. bodies and exhalative, auriferous, cherty dolomites. The ore zones of the Buffalo Ankerite, Aunor and Delnite mines formed in this environment.

8.2 SUMMARY

Localized zones of intense hydration and carbonatization exist throughout the volcanic stratigraphy as discordant and stratabound alteration zones within which a chlorite-rich subzone encloses a carbonate-rich core. Carbonatized tholeiitic and komatiitic rocks were exposed to mechanical erosion and detritus accumulated as clastic sediments throughout the volcanic evolution of the Upper Supergroup, which demonstrates conclusively that the carbonatization was synvolcanic. The elevated abundances of Ba, Li, B, K_2O, H_2O, CO_2 and oxygen-18 whole rock, isotopic compositions of the altered volcanic rocks and the presence of relict palagonization textures are analogous to similar characteristics of low temperature (<250°C), seawater altered, modern, submarine basalts. Carbonatized volcanic rocks in the Timmins area which developed well beneath the seawater/ocean floor interface are not associated with either Q.F.P. bodies or exhalative, auriferous, cherty dolomites. Conversely carbonate alteration

zones which developed at, or very near, the seawater/ocean floor interface are spatially associated with Q.F.P. bodies and exhalative, auriferous, cherty dolomite sediments.

The interpretation of the geochemical and textural data of these altered, Archean flows in terms of a low temperature (<250°C) seawater/rock interaction model, based on the similarity of these data with those of modern, seawater altered basalts in turn implies that the composition of the Archean seawater was not drastically dissimilar from that of modern seawater, a contention supported by Muehlenbachs and Clayton (1976), Schidlowski et al. (1975) and Dimroth and Lichtblau (1979). However, there are strong arguments favouring the hypothesis that the isotopic composition (Veizer and Hoefs, 1976; Perry et al., 1978; Perry, 1967; Weber, 1965), and/or the temperature (Perry et al., 1978; Knauth and Epstein, 1976), and the solute flux (Fryer et al., 1979b) of the oceans have varied significantly with time. A notable exception is the abundance of carbonate in the altered, Archean rock, a feature having no modern analogue. This abundant carbonate implies that the partial pressure of CO_2 in the Archean atmosphere might have been greater than it is presently, consistent with some aspects of Cloud's (1973) model of atmospheric and hydrospheric evolution. This

view is not shared by Dimroth and Lichtblau (1979), who maintain that the similarity of Archean and Cenozoic seafloor alteration products excludes large changes of seawater chemistry since Archean time.

CHAPTER 9

SYNGENETIC ORE FORMATION AND VOLCANIC ENVIRONMENT

Fryer and Hutchinson (1976), Fryer et al. (1979) and Kerrich and Fryer (1979) appeal to a two stage model involving initial, syngenetic precipitation of gold, dolomitic carbonate, chert and minor amounts of base metals on the seafloor from hydrothermal fluids, which later is gold enriched by circulation of metamorphogenic fluids, derived by dehydration of the volcanic pile at the greenschist-amphibolite metamorphic transition. The source of the large volumes of fluids required initially to hydrate the fresh, pristine, submarine basalts was not discussed. Karvinen (1978a) favours an initial syngenetic gold enrichment in dolomitic chemical precipitates related to exhalative activity and wallrock alteration during periods of felsic volcanism. Later deformation locally enriched the syngenetic gold into discordant veins of tectonic origin. Roberts and Spiteri (1979), based on detailed mapping in the Dome mine, also contend that the cherty dolomites represent chemical sediments. The conclusions

of these studies are consistent with the observations presented in this thesis. However, formation of the auriferous, cherty dolomites in a marine environment implies that seawater, undoubtedly chemically modified during its interaction with the volcanic rock, was the major aqueous component in the hydrothermal system.

Although these independent studies have clearly documented the sedimentary nature of the auriferous, cherty dolomites, little insight has been gained into the volcanic environment in which these sediments formed. That the nature of the volcanic environment dictates the likelihood of auriferous, cherty dolomite precipitation is demonstrated by the regional stratigraphic restriction of these exhalative deposit types to the lower portions of the Upper Supergroup, within 10 km (6 mi) of the Destor-Porcupine fault (Pyke, 1978b). On a mine scale, all major deposits having exhalative, auriferous, cherty dolomite ore (Hollinger, McIntyre, Coniaurum, Dome, Aunor, Delnite, Buffalo Ankerite) are spatially associated with carbonatized flows and Q.F.P. bodies. From the detailed study of the Buffalo Ankerite property, it is apparent that the cherty dolomites accumulated near the top of the lower volcanic domain (Figures 11, 12, 13) in a volcanic environment characterized by episodic, tholeiitic and komatiitic volcanism. During one such hiatus, calc-

alkalic, felsic volcanics (Q.F.P.) and volcaniclastic and chemical sediments accumulated in a submarine environment. Pervasive hydration and carbonatization of the seafloor beneath, and adjacent to, the felsic volcanic dome was facilitated by the lengthy rock/seawater exposure. Due to increasing alteration intensity, soluable material was extracted from the altered rock by the circulating, seawater, hydrothermal brines. Because of the orientation of the physico-chemical gradients, the geothermal solutions locally discharged through vent areas onto the seafloor, where the dissolved species precipitated. The auriferous, cherty dolomite, interflow sediments represent this precipitation product. Depending on the number of discharge vents, the rate of solution discharge and the density (salinity) of the hydrothermal fluid, chemical sedimentation could have been areally widespread, but would have been continuous until the geothermal system was effectively sealed by a major pulse of effusive komatiitic or tholeiitic volcanism (in this case, the komatiitic flows which define the base of the middle volcanic domain). The continuous, background chemical sedimentation would have been effectively diluted in areas of vigorous clastic sedimentation or volcanism and hence only thin cherty dolomites, if any, accumulated (Plate 4-3). In the Aunor mine ore zone, which is time equivalent with those of the

Delnite and Buffalo Ankerite mines, thicker (0.5 m), cherty dolomites accumulated along flow contacts by virtue of the longer periodic breaks in the Mg tholeiitic volcanism (Plate 4-2), which enabled thicker accumulation of the chemical precipitates.

In summary, the auriferous, cherty, dolomites accumulated in a submarine volcanic environment characterized by isolated felsic volcanism, and numerous hiatuses in mafic and ultramafic volcanism. Such pauses facilitated pervasive, seafloor alteration by CO_2 charged, heated, seawater brines, solution mass transport to the ocean floor/seawater interface and areally widespread chemical precipitation.

A fundamental parameter of this volcanic environment is the length of time that the ocean crust is exposed to seawater, either by direct seafloor exposure or by seawater percolation through permeable zones in the crust. The felsic volcanic rocks (Q.F.P.) define one such optimal environment, whereby virtue of the more numerous and lengthy volcanic hiatuses which characterize this stage of Archean volcanic evolution, seawater/rock interaction is most intense and widespread. Thicker chemical precipitates accumulated only during lengthy volcanic/clastic sedimentary hiatuses.

CHAPTER 10

GEOCHEMICAL AIDS FOR GOLD EXPLORATION

10.1 SEARCH FOR THE ILLUSIVE SOURCE ROCK

Recent genetic models of gold metallogenesis favour a source bed concept (Viljoen et al., 1970; Pyke, 1975; Keays, 1979) whereby komatiitic rocks are thought to be significantly enriched in gold with respect to other rock types. This gold enrichment has been documented in sulfide rich ultramafic rock from western Australia (Keays, 1979). Listed in Table 14 are gold abundances of ultramafic and mafic komatiitic and magnesium tholeiitic basalt flows collected from the study areas. All samples have been altered to various degrees, but none are spatially associated with economic gold mineralization. It is apparent that the mean gold content of the komatiitic rocks is less than that of the Mg tholeiitic basalts. To establish if these means are statistically different, the two-tailed t test was applied. The validity of this test requires that the samples are selected at random, that the gold distributions are Gaussian,

TABLE 14

Gold Analyses Of Komatiitic And Magnesium Tholeiitic Flows Which Are Not Spatially Associated With Economic Gold Deposits

Sample Number	Rock Type	Volatile Content L.O.I	CO_2	Au (ppb)	
B-2	MK	6.	0.9	1.0	
B-14	MK	24.0	19.6	1.0	
B-18	MK	5.2	1.0	2.3	
TR-406	UK	8.5	4.5	1.3	
TR-408	UK	6.7	2.5	0.5	
TR-411	UK	26.5	23.0	1.8	n=13
DR-41	UK	25.5	23.0	2.6	
DR-72	UK		7.4	4.5	$\bar{X}$=1.8
DR-79	UK	13.1	10.2	1.5	
DR-95	UK	26.4	25.5	3.0	σ =1.2
DR-99	UK	7.8	3.5	0.6	
DR-100	UK		20.3	0.7	
DR-76	MK	24.0	21.8	3.2	
B-7	MTB	4.0	0.8	1.8	
B-24		5.0	1.0	1.2	
B-25		16.9	14.6	2.7	
B-33		7.5	3.5	1.6	
B-34		15.8	12.0	3.1	
B-39		3.6	0.3	2.4	
CH-22			4.0	4.2	
CH-23			0.5	3.3	
CH-24			0.2	4.3	
CH-25			0.3	3.6	
CH-26			0.2	3.6	
CH-27			11.9	3.2	
CH-28			1.7	2.7	
CH-29			4.9	3.2	
CH-30			6.1	3.4	n=34
CH-32			2.5	2.7	
CH-44		7.8	4.9	2.3	$\bar{X}$=2.6
CH-45		12.7	10.7	1.0	
CH-47		17.3	16.1	0.2	σ =1.2
CH-49		14.8	10.7	2.1	
CH-68		3.6	0.3	1.9	
CH-70		13.6	10.6	1.9	
CH-71		7.2	1.8	4.2	
CH-74		10.0	3.6	1.2	
CH-76		14.8	12.0	1.2	
TR-402		9.5	5.5	2.0	
TR-512		12.6	9.0	4.4	
DR-70		13.4	12.5	3.1	
DR-71		13.0	11.5	0.9	
DR-73		13.0	11.7	1.0	
DR-80		11.0	5.5	2.1	
DR-83		8.7	3.7	2.7	
DR-86		10.3	4.4	5.3	
DR-91		9.9	3.3	2.7	

MK ≡ Mafic Komatiite

UK ≡ Ultramafic Komatiite

MTB ≡ mg tholeiitic basalt.

and that the variances of the two populations are equal (Davis, 1973). Presented in Table 15 are the statistics for a group variance and mean equivalence tests. At the 5% significance level, there is no difference between the variances of the komatiitic and Mg tholeiitic data. The group means were then tested for equivalence. At the 5% significance level, the computed statistic does not fall into the critical region, implying that the two sample groups do not come from populations having different means.

It is concluded that komatiitic and Mg tholeiitic volcanic rocks of the Upper Supergroup have equivalent gold abundances at the 5% significance level. Furthermore, these gold abundances (1 to 3 ppb) are comparable to reported (table 16) gold, background levels for mafic and ultramafic volcanic rocks in the Kirkland Lake (Tihor and Crocket, 1977) and Kakagi Lake areas (Kwong and Crocket, 1978). The komatiitic source bed concept apparently is not supported by the analytical data. Hence, the apparent, strong, spatial association between some gold deposits and komatiitic volcanic rocks (Pyke, 1975; Viljoen et al., 1970; Fripp, 1976; Keays, 1979) is somewhat paradoxical in light of the typical gold abundances of the komatiites. It is, however, impossible to to categorically disprove the source bed concept using analytical data because the "freshest" Archean komatiitic

TABLE 15

Variance And Mean Equivalance Test Of Gold Contents In Komatiitic And Magnesium Tholeiitic Flows Not Spatially Associated With Economic Gold Mineralization

Group 1 Komatiitic n=13	Group 2 Magnesium Tholeiitic Basalt n=34	Variance Equivalance Test			
		M Statistic	C^{-1} Transform	X^2 Statistic	$X^2_{.05(1)}$ Critical
		0.0103	0.9844	0.0101	3.84

Mean Equivalance Test

t Statistic	$t_{.05[45]}$ Critical
1.8912	2.0184

TABLE 16: GOLD CONTENT IN EARLY PRECAMBRIAN (ARCHEAN) METAVOLCANIC FLOWS OF THE CANADIAN SHIELD, NOT SPATIALLY ASSOCIATED WITH GOLD MINERALIZATION

AREA	RANGE	MEAN	# OF ANALYSES
TIMMINS (1)			
ULTRAMAFIC KOMATIITE	0.5 - 4.5	1.8	13
MG THOLEIITIC BASALT	0.2 - 5.3	2.6	34
KIRKLAND LAKE (2)			
ULTRAMAFIC KOMATIITE	1.8	1.8	1
THOLEIITES	-	3.0	3
SPINIFEX HILL, MONRO TWP (3)			
ULTRAMAFIC KOMATIITE	1.3 - 6.7	2.8	11
KAKAGI LAKE (4)			
THOLEIITES	0.3 - 8.1	2.0	17

REFERENCES:
1) THIS STUDY
2) TIHOR AND CROCKET (1977)
3) MACRAE AND CROCKET (UNPUBLISHED DATA)
4) KWONG AND CROCKET (1978)

rocks (Munro Township; Pyke et al., 1973; Arndt et al., 1977) are partially serpentinized. It has been demonstrated that during seafloor hydration of basalts gold is effectively leached from pillow basalt cores (Keays and Scott, 1976). This process undoubtedly affects komatiitic volcanic rocks to a similar, if not a greater, degree. Therefore, gold analyses of serpentinized, komatiitic volcanic rocks are likely representative of a base or residual gold content.

For exploration purposes, it must be emphasized that there exists a spectrum of gold deposit types which are associated with rock types ranging in composition from komatiitic to calc-alkalic (Doucet, 1979; Anhaeusser, 1976). The genetic link between these different types of deposits must be the mechanism by which gold is concentrated. This mechanism must be equally efficient at concentrating gold in a variety of volcanic terrains characterized by the presence of a variety of volcanic rock types. It has been documented that the convective circulation of seawater through recent and ancient oceanic crust is an integral part of the thermal and chemical evolution of submarine volcanic rocks (Hart, 1969; Hart and Nalwalk, 1970; Tómasson and Kristmannsdottir, 1972; Spooner et al., 1974; Keays and Scott, 1976; Humphris et al., 1978a,b; Dimroth and Lichtblau, 1979). This is proposed as the mechanism which concentrated precious (and

base) metals on, or near, the seafloor in the Timmins camp (Karvinen, 1978a; Fryer and Hutchinson, 1976; Fyon and Karvinen, 1978; Fyon and Crocket, 1979). In principle, any rock is a suitable source of gold. However, it is the volcanic environment, defined by a style of volcanism, the rate of local sedimentation and the complexity of the local, synvolcanic tectonic regime, rather than the presence of a specific rock type which dictates the viability of hydrothermal gold enrichment.

In the Deloro township study area (Map 1) such a suitable environment is characterized by numerous, more lengthy (?) volcanic hiatuses during episodic volcanic activity from komatiitic, tholeiitic and calc-alkalic sources (see Chapter 9). Auriferous, carbonate-rich sediments, genetically related to intense rock/seawater interaction, accumulated during local volcanic hiatuses without being diluted by either effusive or clastic volcanic material.

The synvolcanic, tectonic setting of these Archean gold deposits is as yet speculative. Ferguson et al. (1968) and Pyke (1978b) indicate that within the Timmins camp and on a regional scale, all gold deposits are located within 10 km (6 mi) of the Destor-Porcupine fault. This structure has been interpreted as part of a major fracture system in the Archean crust, possibly related to rifting (Pyke, 1978b).

The localization of felsic volcanic and hypabassal rocks and ore deposits by synvolcanic fracture systems has been demonstrated by Knuckey et al. (1978a,b) for the Corbet and Millenbach deposits of Noranda area, and by Scott (pers. comm., 1979) for the Japanese Kuroko deposits. In this regard, the regional, spatial association of Archean gold deposits with the Destor-Porcupine fault probably reflects a similar tectonic control of felsic to ultramafic volcanism, sedimentation and ore genesis. The fault zone probably represents a tectonic environment not unlike that of modern oceanic rift systems, where rock/seawater interaction, leading to the accumulation of base and precious metal enriched sediments (Spooner and Bray, 1977; Keays and Scott, 1976; Crocket et al.,1973; Bostrom et al., 1973) is an inherent aspect of the seafloor evolution.

In summary then, it is difficult to reconcile the validity of the komatiitic source bed concept using the available analytical data, but it must be acknowledged that these gold analyses might represent residual abundances because of the degree of rock alteration. Hence, Archean ultramafic komatiites may originally have been much richer in gold. However, regardless of the elevated gold abundances in a source rock, the fundamental control on ore genesis is the ease with which that gold can be mobilized from the source

and enriched elsewhere by hydrothermal solutions. It is emphasized that in the Timmins camp, this gold mobilization from the source and enrichment in interflow sediments took place in a volcanic environment characterized by episodic volcanism, related to a change from komatiitic to calc-alkalic volcanism. Rock/seawater interaction was most pervasive during these volcanic hiatuses. Gold (and base metal) exploration programs should concentrate on the definition or extension of stratigraphic sequences in which volcanism was episodic, rather than emphasize the delineation of a particular rock type without regard to the local volcanic environment. As was demonatrated in section 9, the presence of carbonatized rock does not itself define the optimum geological environment. Only by detailed mapping to define the stratigraphic relationships, is it possible to establish the subseafloor or seafloor environment of carbonate alteration.

10.2 TRACE ELEMENT SCREENS

Because of the extensive overburden cover in Canadian, Archean terrains, the field parameters which serve to define optimum gold deposit target areas, would, in all likelihood,

not be recognized. However, the carbonate alteration has affected a relatively large volume of rock and therefore, altered rock is likely to be exposed. Hence, a lithogeochemical study has been carried out on altered volcanic rock to evaluate its use as a gold exploration tool to augment geological parameters. Altered samples have been classified into "productive" and "unproductive" groups. "Productive" samples come from altered rock located within 30 m (100 ft) of ore grade material in the Aunor, Delnite and Buffalo Ankerite mines, whereas unproductive samples come from the numerous alteration zones in both study areas not associated with known gold mineralization. Whole rock samples, rather than mineral separates were used during this orientation study, because the objective was to identify trace element screens which could be applied routinely by industry engaged in gold exploration. Use of whole rock samples, rather than mineral separates, is not as labour intensive and therefore, the possibility of incorrect sample labelling, sample contamination and/or loss is minimized. Cost per sample is thus minimized, while sample turnaround time is maximized.

Because a group discrimination cannot be made on a basis of CO_2 content (Figure 37), some trace element screens

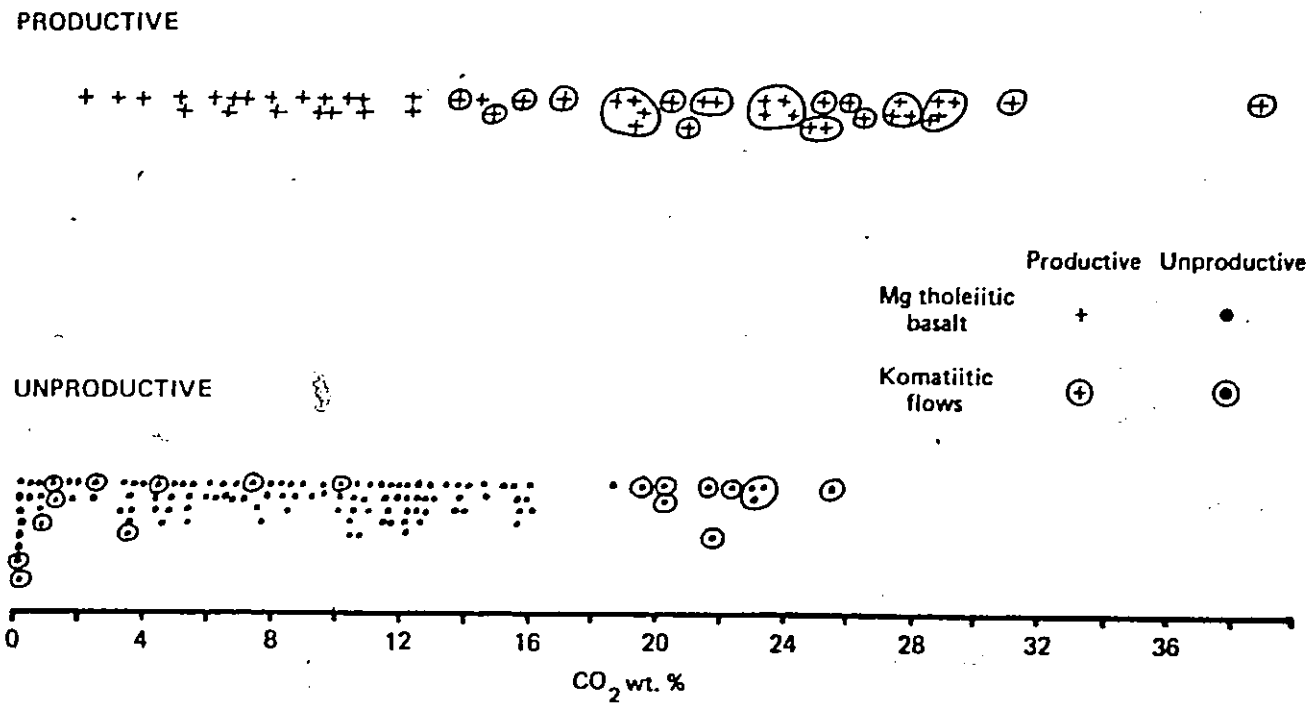

FIGURE 37 : Range of CO_2 content of Productive and Unproductive rock samples collected from both the Deloro and Tisdale study areas. See text for a definition of Productive and Unproductive samples.

were examined. Element abundances vary as a function of rock type (komatiitic versus tholeiitic), flow facies (pillowed, spinifex, cumulate), degree of rock alteration (see section 7.2), and sampling and analytical variability. Hence, a data file compiled on the basis of geographical location (i.e. proximity to ore) without regard to rock type, facies or degree of alteration, cannot be treated using simple statistical techniques (e.g. cumulative frequency plot) for which data variability is attributed to one factor. Hence, the trace element geochemical data, classified into productive and unproductive groups, have been plotted on binary diagrams as a function of alteration intensity, expressed at CO_2 wt %, rather than L.O.I.. CO_2 is used as an alteration index, because many of the trace element analyses presented in this section were carried out by the Ontario Geoscience Laboratory, and CO_2 and S were the only volatiles determined.

For convenience, komatiitic and Mg tholeiitic volcanic rocks have been distinguished on all diagrams. Threshold values were established to maximize the discrimination between productive and unproductive data groups.

Au

Background gold values range up to 5 ppb. Using a threshold of 4.5 ppb, 83% of productive samples are distinguished

from the unproductive group, while 91% of the unproductive samples contain less than 4.5 ppb gold (Figure 38).

S

Discrimination between productive and unproductive groups using sulfur is less efficient because pyrite is a ubiquitous accessory phase in all rocks. Using a threshold of 0.025 wt %, only 69% of the productive samples are classed as anomalous. Of the unproductive samples, 72% contain less than this threshold. Slightly better group discrimination is attained using the sulfur content of Mg tholeiitic rocks (threshold 0.045 wt %), although considerable group overlap exists. No effective discrimination is possible using sulfur content of altered komatiitic rocks (Figure 38).

As

Arsenic content of altered volcanic rock effectively discriminates between productive and unproductive groups. Using a threshold of 70 ppm As, better than 80% of the data from the two groups are distinguished (Figure 39).

Li

Group discrimination using Li is best achieved using altered tholeiitic basaltic samples (<18 wt % CO_2), although

FIGURE 38. Variation of Au and S as a function of alteration intensity, expressed as CO_2 content. See text for a definition of Productive and Unproductive samples.

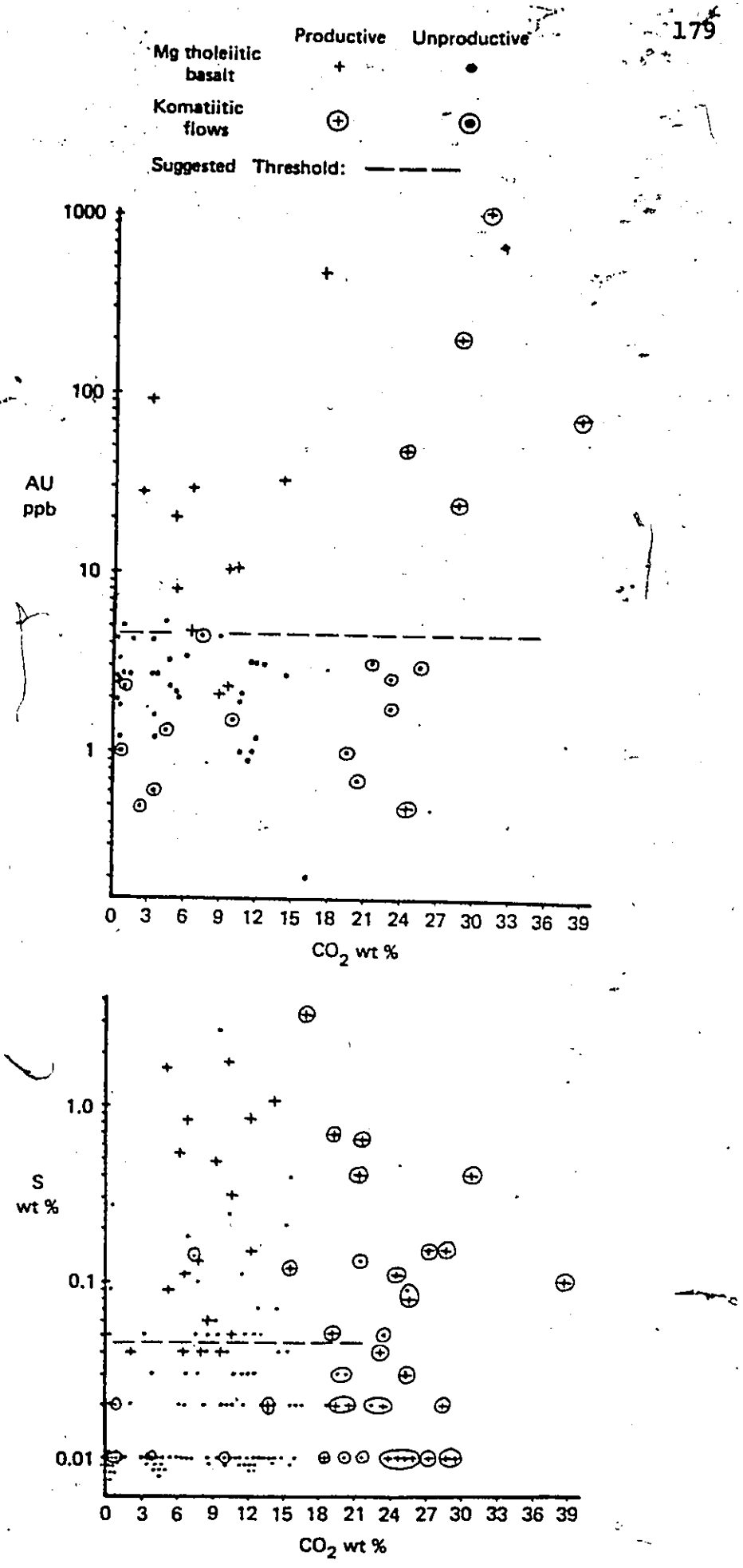
Productive
Unproductive
Mg tholeiitic basalt
Komatiitic flows
Suggested Threshold:
1000
100
10
1
AU ppb
0 3 6 9 12 15 18 21 24 27 30 33 36 39
CO_2 wt %
1.0
0.1
0.01
S wt %
0 3 6 9 12 15 18 21 24 27 30 33 36 39
CO_2 wt %

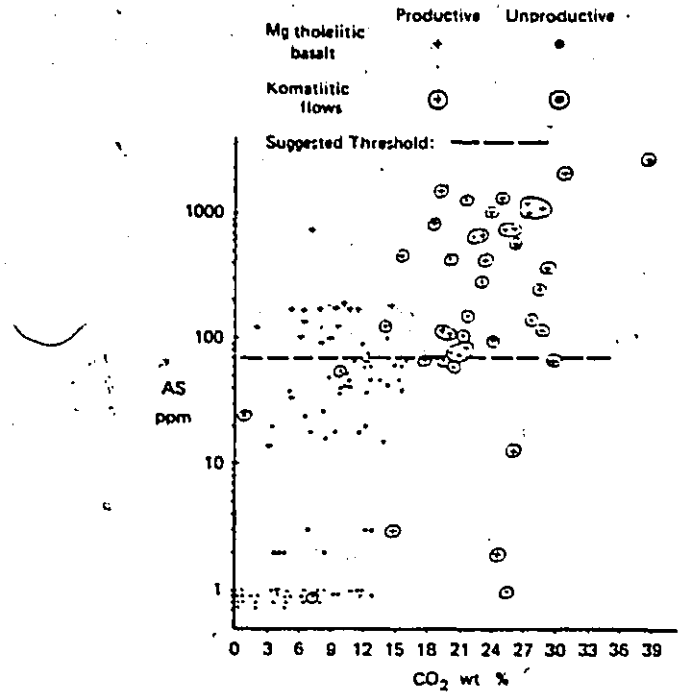

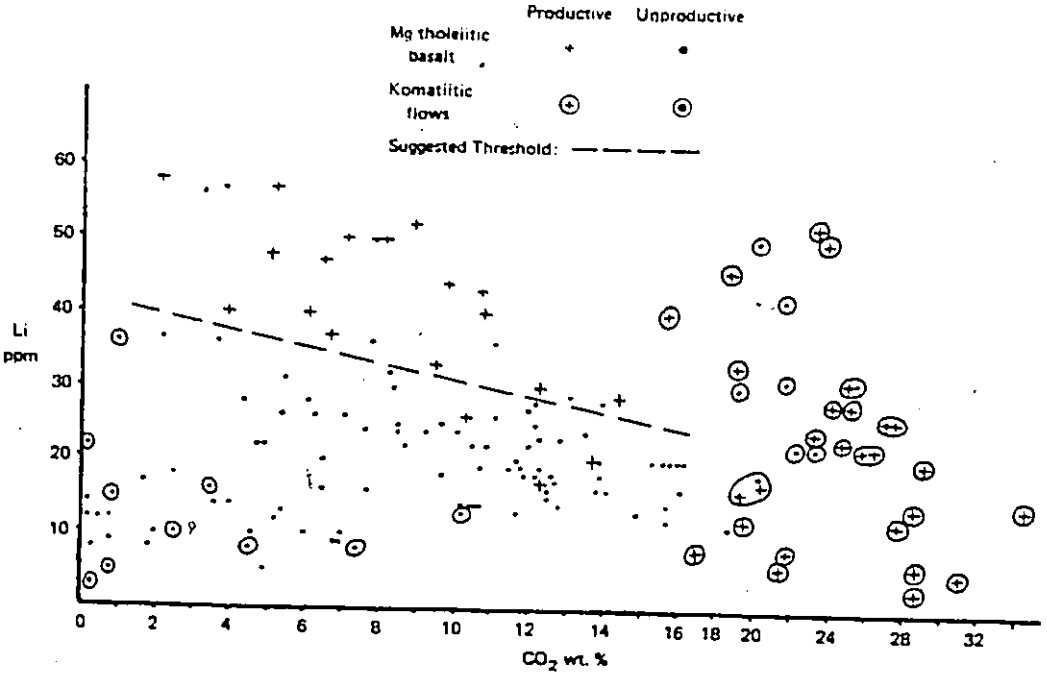

FIGURE 39 : Variation of As and Li as a function of alteration intensity, expressed as CO_2 content. See text for a definition of Productive and Unproductive samples.

the Li threshold varies as a function of alteration intensity. Approximately 85% of the productive and 94% of the unproductive samples exceed and fall below, respectively, the indicated Li threshold. No discrimination exists for altered komatiitic rocks (Figure 39).

Sb

Using a threshold of 0.35 ppm, 84% of the productive, altered tholeiitic samples are classed as anomalous, whereas 90% of the altered tholeiitic samples of the unproductive group contain less than this threshold. Insufficient data exists to determine the Sb threshold for the altered komatiitic rocks (Figure 40).

B

Effective discrimination between productive and unproductive Mg tholeiitic basalts is achieved using a threshold of 30 ppm. Komatiitic flows can not be screened using boron. Approximately 87% of the productive group exceed this value, whereas 98% of the unproductive group contain less boron (Figure 40).

Although it has been demonstrated that boron is enriched in altered Mg tholeiitic basalt not associated with gold ores (see section 7.2.2), it is apparent that altered

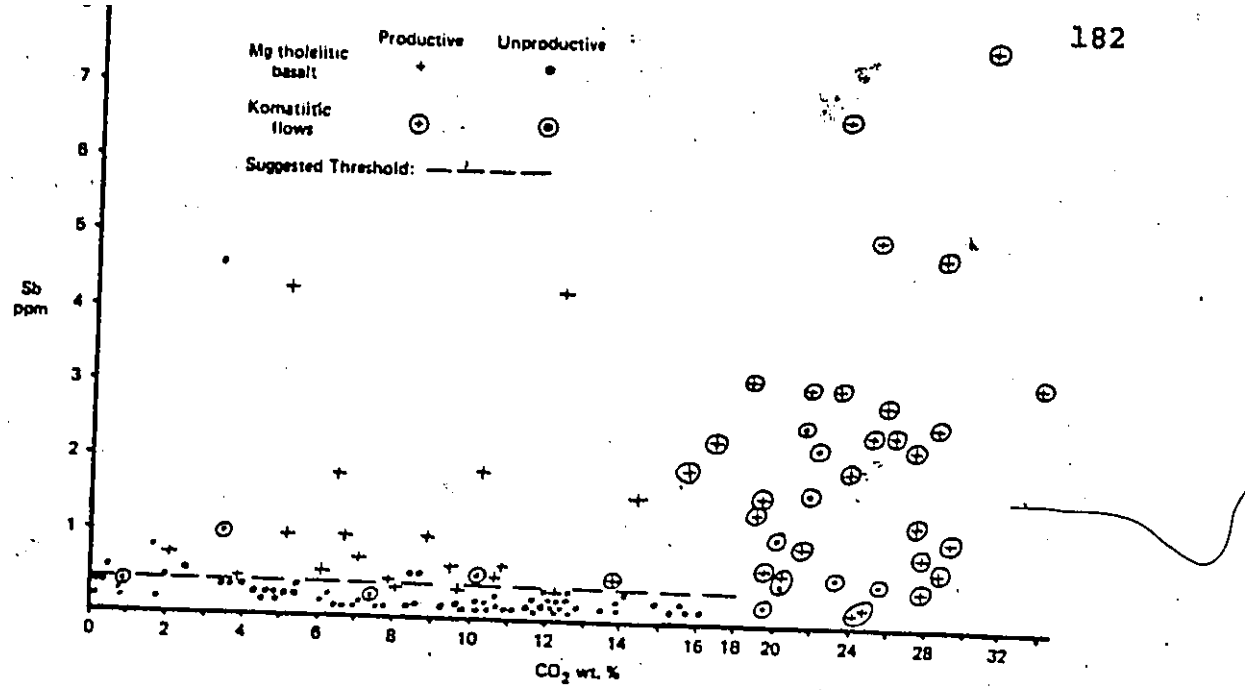

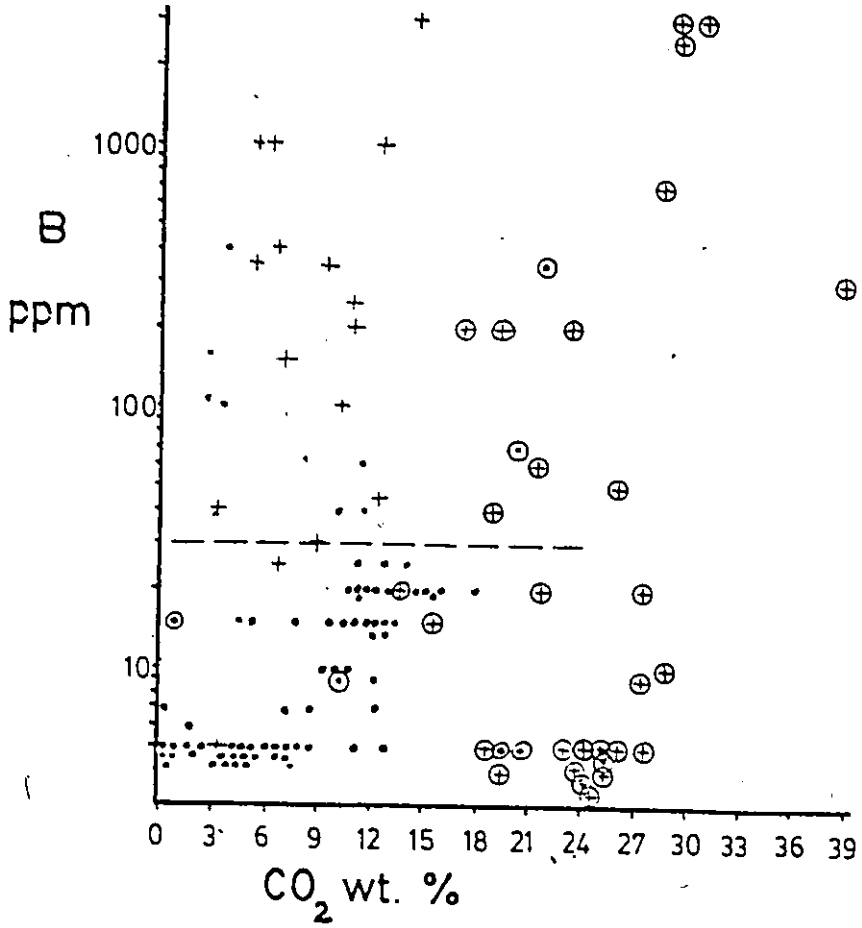

FIGURE 40 : Variation of Sb and B as a function of alteration intensity, expressed as CO_2 content. See text for a definition of Productive and Unproductive samples.

rocks proximal to gold deposits are enriched in boron to a greater extent. This implies that mineralized rock environment underwent a greater degree of seawater interaction, which incorporated more boron into the rock relative to the unmineralized environments. This, in turn, suggests that in the mineralized environment the volumes of seawater interacting with the rock were greater and/or the local volcanic hiatuses were longer with respect to the unmineralized environment.

Ba

No discrimination between productive and unproductive groups was found using barium. It is of interest to speculate that the apparent increase in barium content of altered rocks having 10 to 13 wt % CO_2 reflects the presence of a barium sulfate phase. No barite was identified in any of the XRD whole rock scans.

Zn

Like barium, no discrimination between productive and unproductive groups is achieved using zinc. Also there is an apparent increase of Zn abundance in altered rocks having 10 to 13 wt % CO_2 (Figure 41).

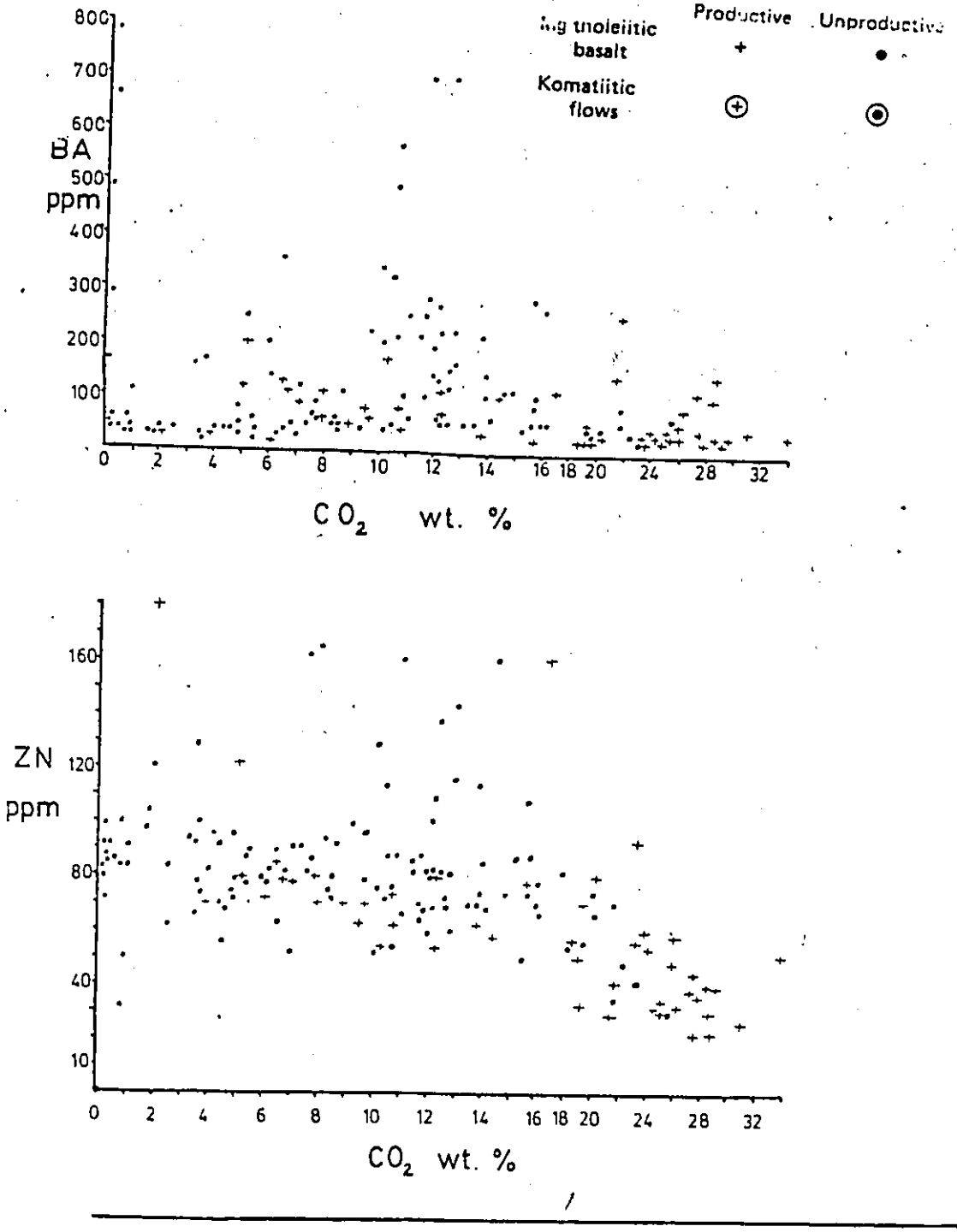

FIGURE 41 : Variation of Ba and Zn as a function of alteration intensity, expressed as CO_2 content. See text for a definition of Productive and Unproductive samples.

Cu

Copper depletion characterizes the "productive" Mg tholeiitic basalts. Using a threshold of 70 ppm copper, 89% of the "productive" tholeiitic samples fall below the value, whereas 89% of the "unproductive" tholeiitic samples exceed 70 ppm copper (Figure 42).

Too few komatiitic data exist to permit a reliable estimate to be made of a copper threshold characteristic of that rock type.

K_2O

No K_2O threshold exists which discriminates between ore and non-ore associated altered rock, although K_2O, hosted in sericite, is enriched in pervasively carbonatized tholeiitic basalts (Figure 42).

Bi

Although no "unproductive" Mg tholeiitic basalt samples contain in excess of 0.1 ppm bismuth, only 47% of the "productive" tholeiitic basalt samples exceed this threshold. Hence, bismuth does not reliably discriminate between altered rock groups. Too few intensely altered, "unproductive" komatiitic rocks exist to evaluate the efficiency of bismuth discrimination for that rock type (Figure 43).

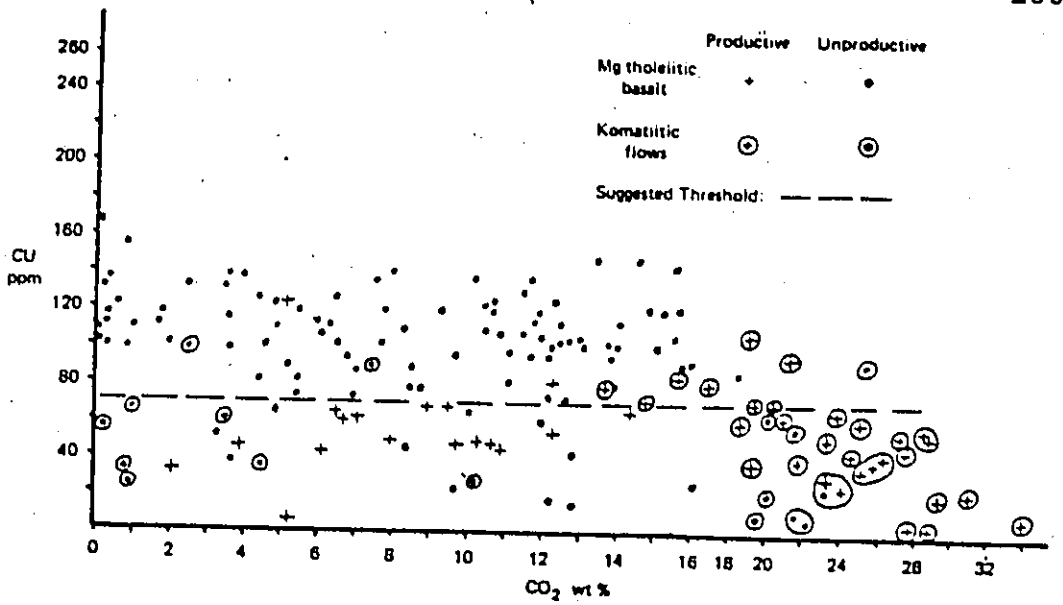

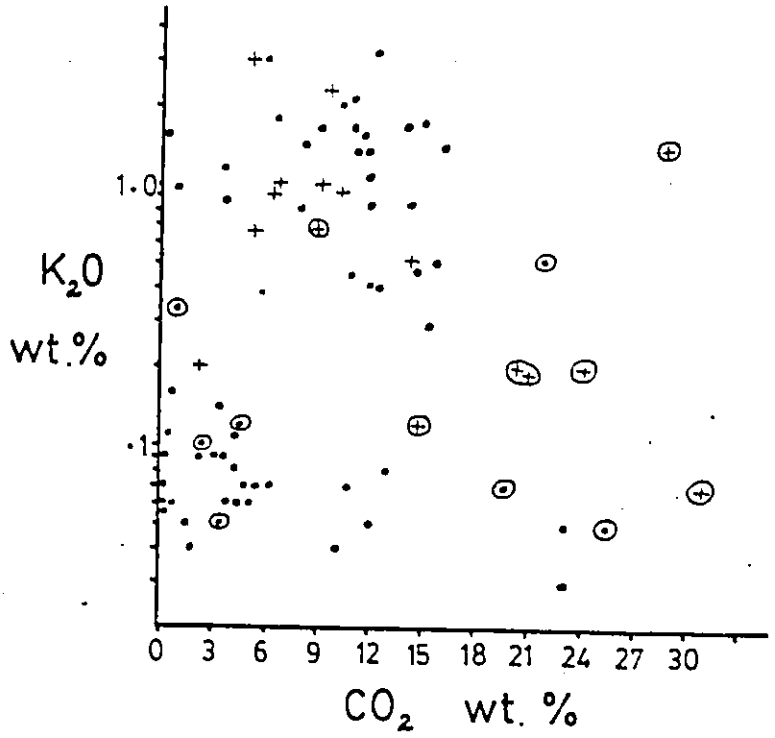

FIGURE 42 : Variation of Cu and K_2O as a function of alteration intensity, expressed as CO_2 content. See text for a definition of Productive and Unproductive samples.

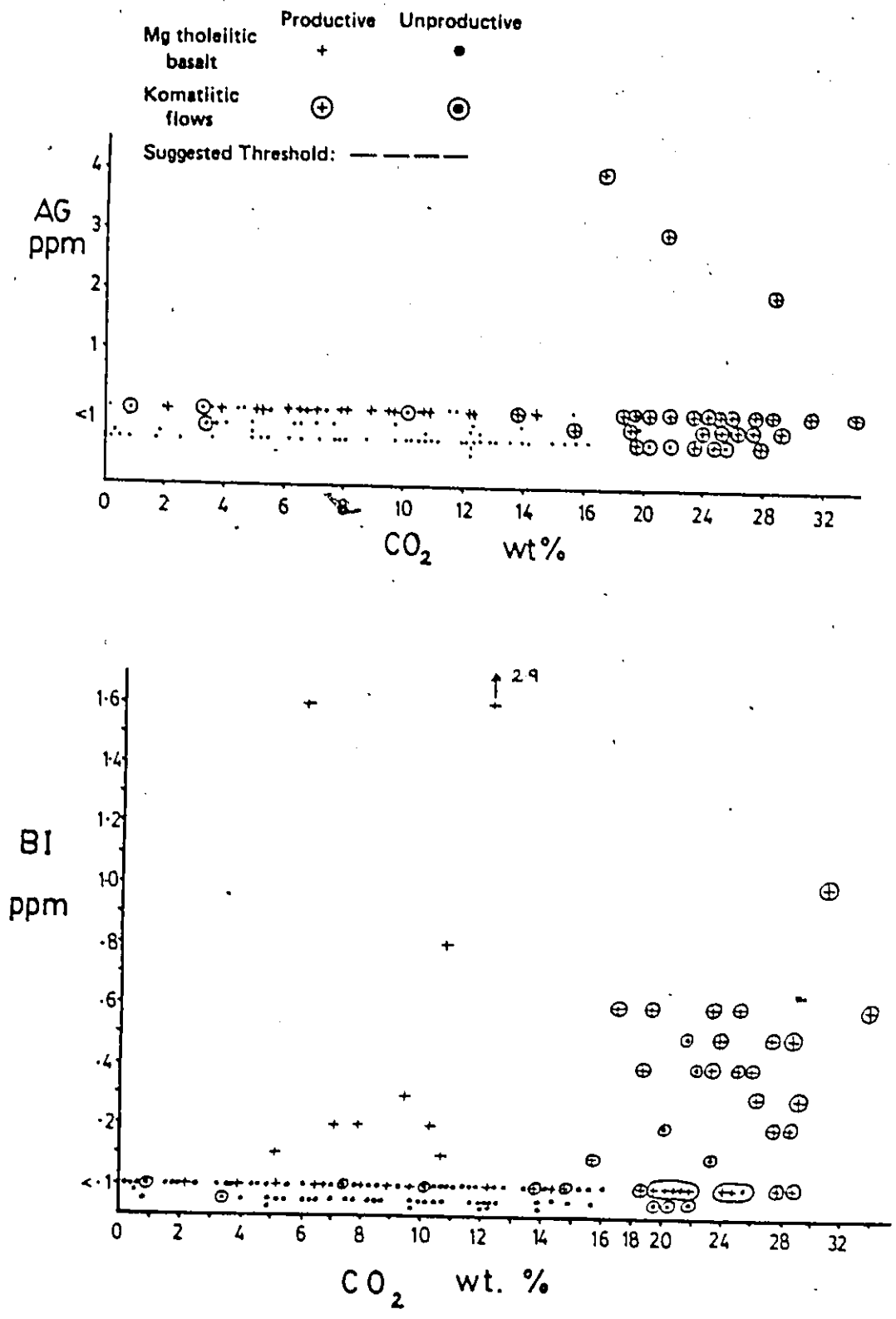

FIGURE 43: Variation of Ag and Bi in altered Mg tholeiitic and komatiitic flows as a function of alteration intensity, expressed as CO_2 content. See text for a definition of Productive and Unproductive samples.

Ag

Silver is not a useful lithogeochemical guide to gold ore in this geological environment, although silver is a byproduct and hence, is present in the ore material (Figure 43).

As-Au and B-Au

To reduce the possibility of geochemical "fliers" it is recommended that binary elemental screens be used (Figure 44). Using As-Au pair, 98% of the altered samples are discriminated. Only one productive sample lies within the unproductive field (Figure 44). A similar discriminatory effectiveness is obtained using the B-Au pair (Figure 44).

10.3 APPLICATION OF THE GEOCHEMICAL SCREENS

Illustrated on Map 8 is the surface geology of the Delnite Mine area and the sample locations. Depicted on Figures 45, 46 is a profile across this area on which the salient features of the surface geology and the relative location of samples are depicted. Element abundances across this profile are plotted to demonstrate the relationship between element abundance variations, the location of

FIGURE 44. Variation of As-Au and B-Au. To reduce the influence of an isolated geochemical "flier", usage of binary plots is recommended to screen altered rocks.

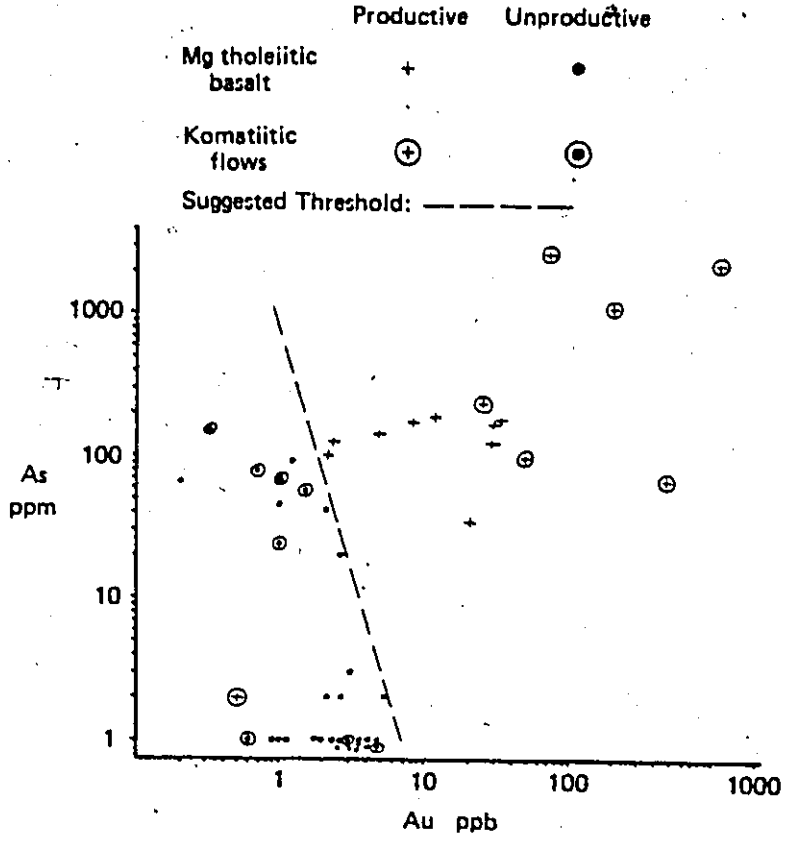
Productive
Unproductive
Mg tholeiitic basalt
Komatiitic flows
Suggested Threshold:
As ppm
1000
100
10
1
1
10
100
1000
Au ppb

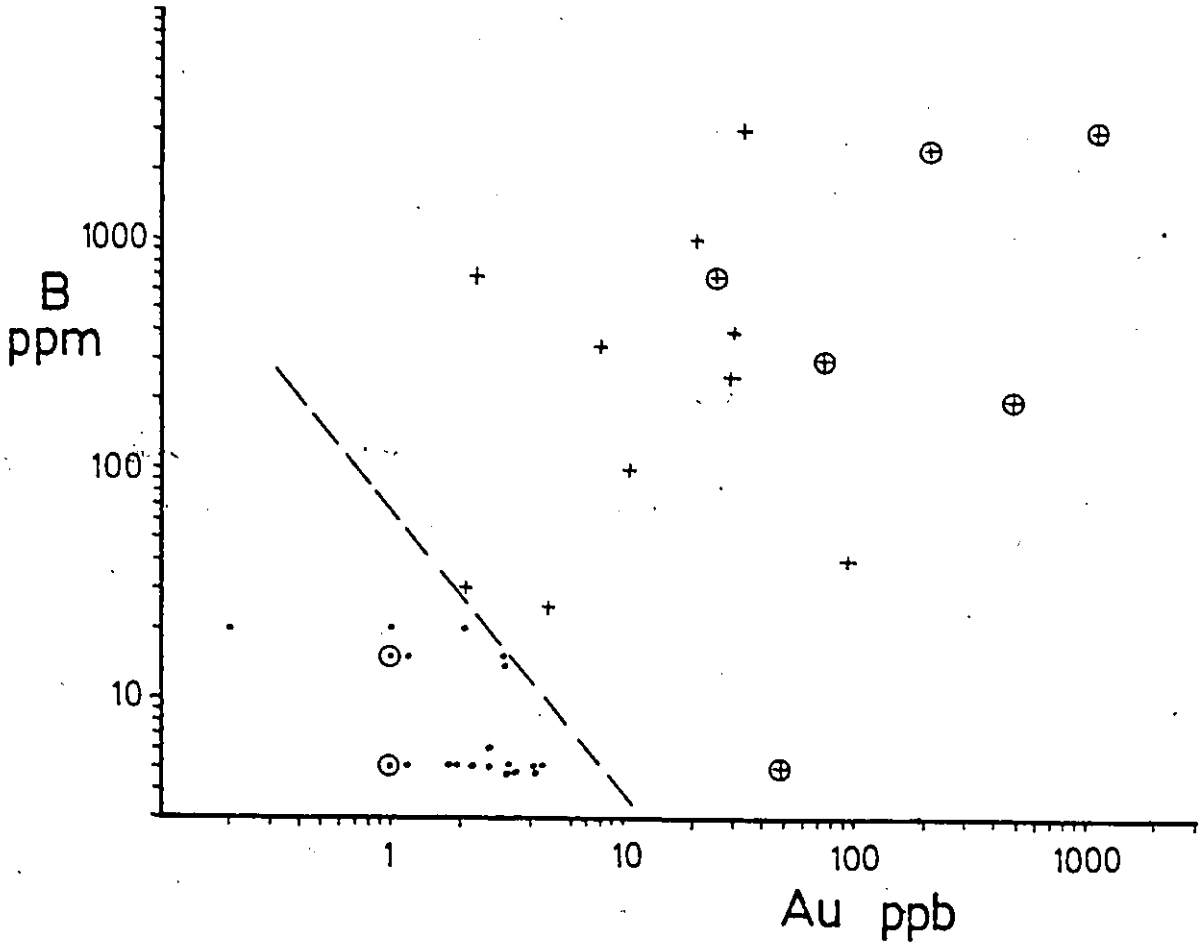
B ppm
1000
100
10
1
10
100
1000
Au ppb

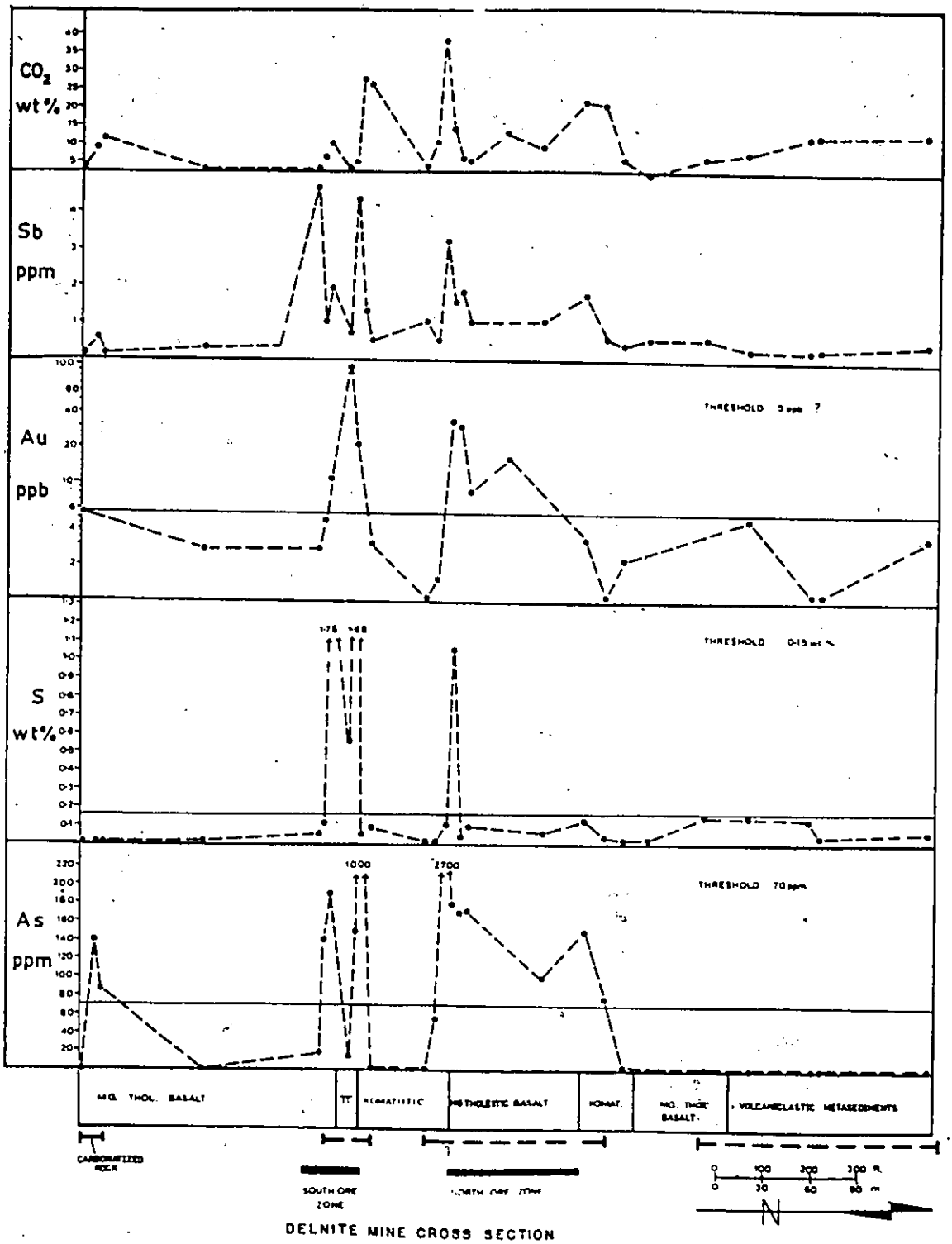

FIGURE 45 : Variation of CO_2, Sb, Au, S, As across the surface of the Delnite Mine property. The locations of carbonatized rock, and the two ore zones are indicated.

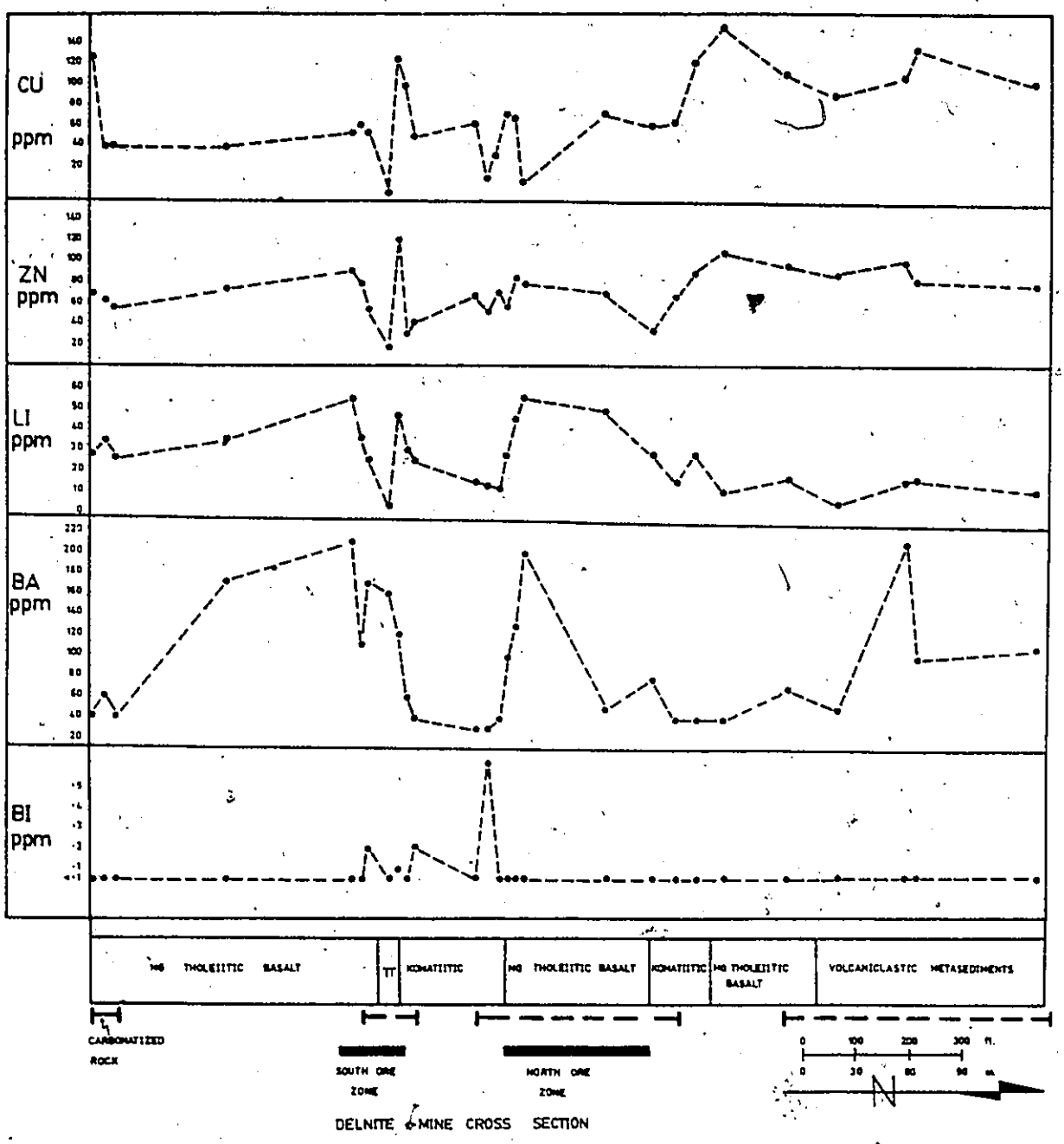

FIGURE 46 : Variation of Cu, Zn, Li, Ba, Bi across the surface of the Delnite Mine property. The location of carbonatized rock and the two ore zones is indicated.

carbonatized rock, and the two ore zones. Examination of Figures 45, 46 reveals that Sb, Au and As profiles outline the ore zones, whereas S, Li, Cu are not as effective in this regard. Ba and CO_2 attain maximum values in carbonatized rock, regardless of ore association, and Zn shows little variation over the ore zones.

For exploration purposes it is the presence of anomalous, trace element abundances which are of interest. Thresholds (Th) established in section 10.2 are used as a reference for each rock type, to establish if an element abundance (X) in a sample is anomalous. Anomalous samples have been subdivided into three classes:

1. low priority, X/Th = 1-2;
2. moderate priority, X/Th = 2-3;
3. high priority, X/Th = 3.

Illustrated on Figures 47-53 is the location of anomalous samples with respect to carbonatized rock and the ore zones of the Delnite Mine (Map 8). Sb, As, Au (Figures 47, 48, 49) effectively define the ore zones, although isolated As and Au anomalies occur in the southern most carbonate alteration zone and in the volcaniclastic metasediments. Cu and Li (Figures 50, 51) define low priority anomalies over the ore

FIGURE 47 : Location of anomalous Sb samples on the Delnite Mine property. See map 8 for the detail geology and the location of carbonatized rock. Symbols are as follows:

X : < threshold

⊙ : 1-2 times threshold

● : 2-3 times threshold

◉ : > 3 times threshold

DELNITE MINE SURFACE GEOLOGY
DELORO TOWNSHIP

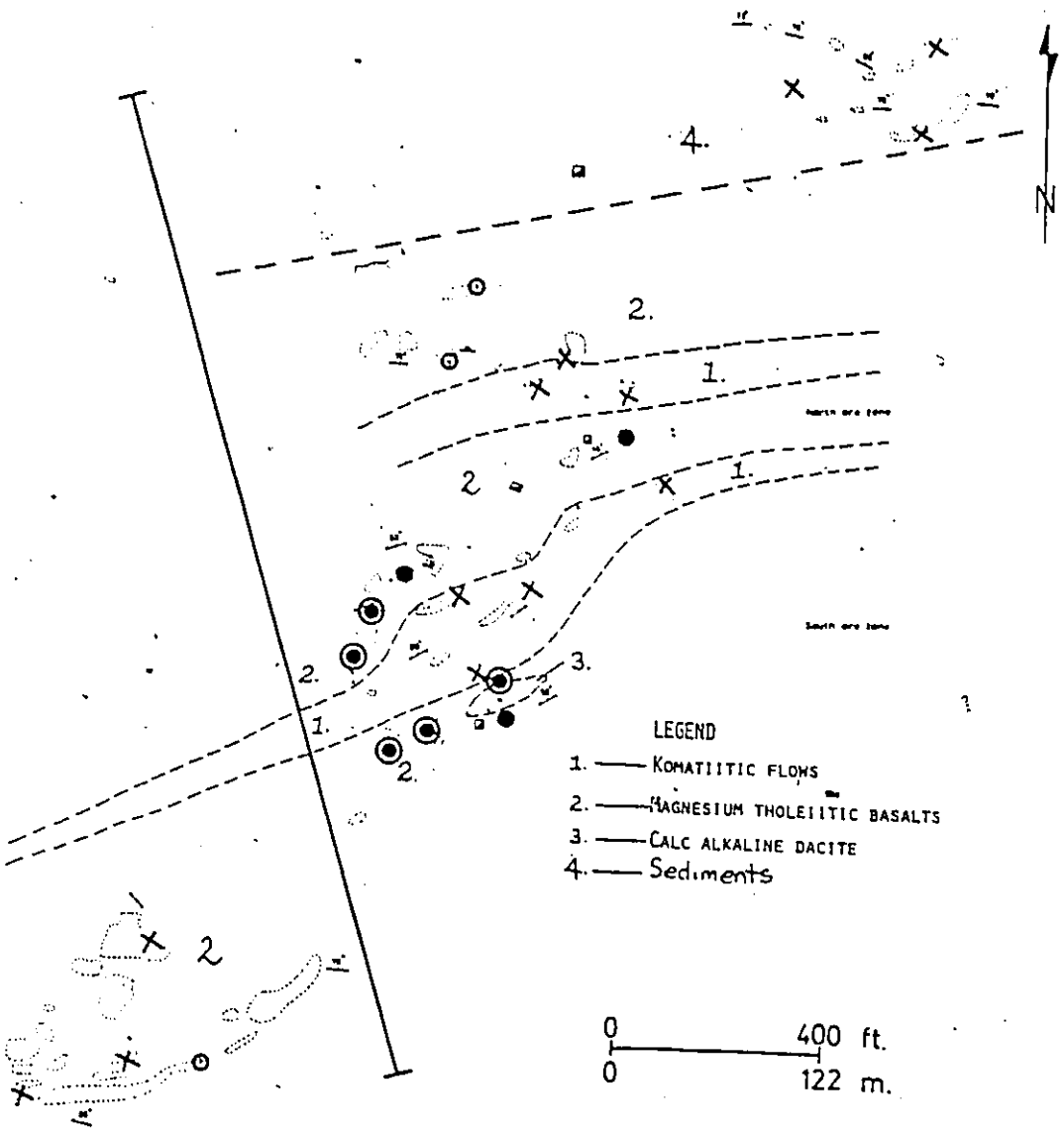

FIGURE 48 : Location of anomalous As samples on the Delnite Mine property. See map 8 for the detail geology and the location of carbonatized rock. Symbols are as follows:

X : < threshold

⊙ : 1-2 times threshold

● : 2-3 times threshold

◉ : >3 times threshold

DELNITE MINE SURFACE GEOLOGY
DELORO TOWNSHIP

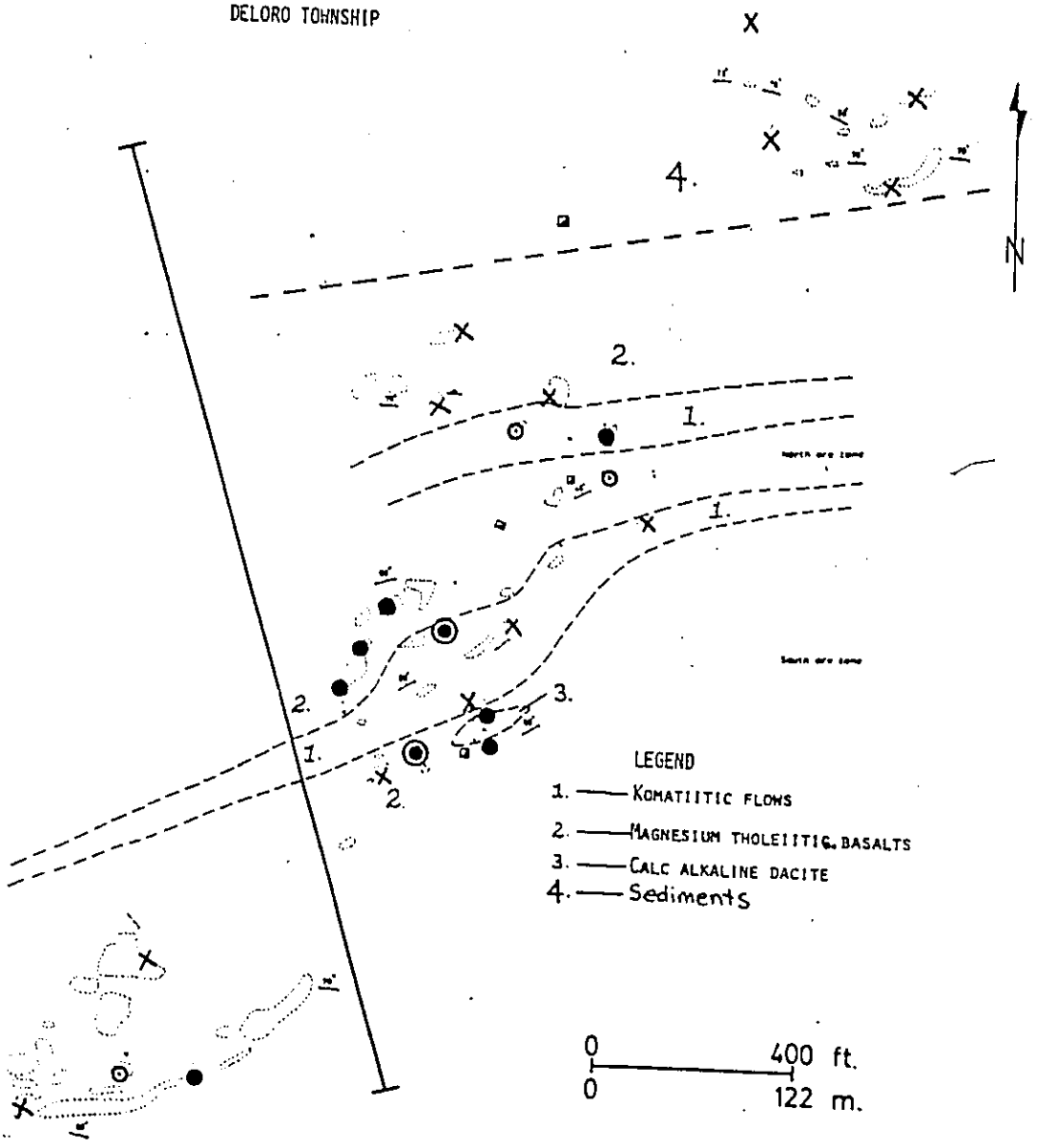

FIGURE 49 : Location of anomalous Au samples on the Delnite Mine property. See map 8 for the detail geology and the location of carbonatized rock. Symbols are as follows:

X : < threshold

⊙ : 1-2 times threshold

● : 2-3 times threshold

◉ : >3 times threshold

DELNITE MINE SURFACE GEOLOGY
DELORO TOWNSHIP

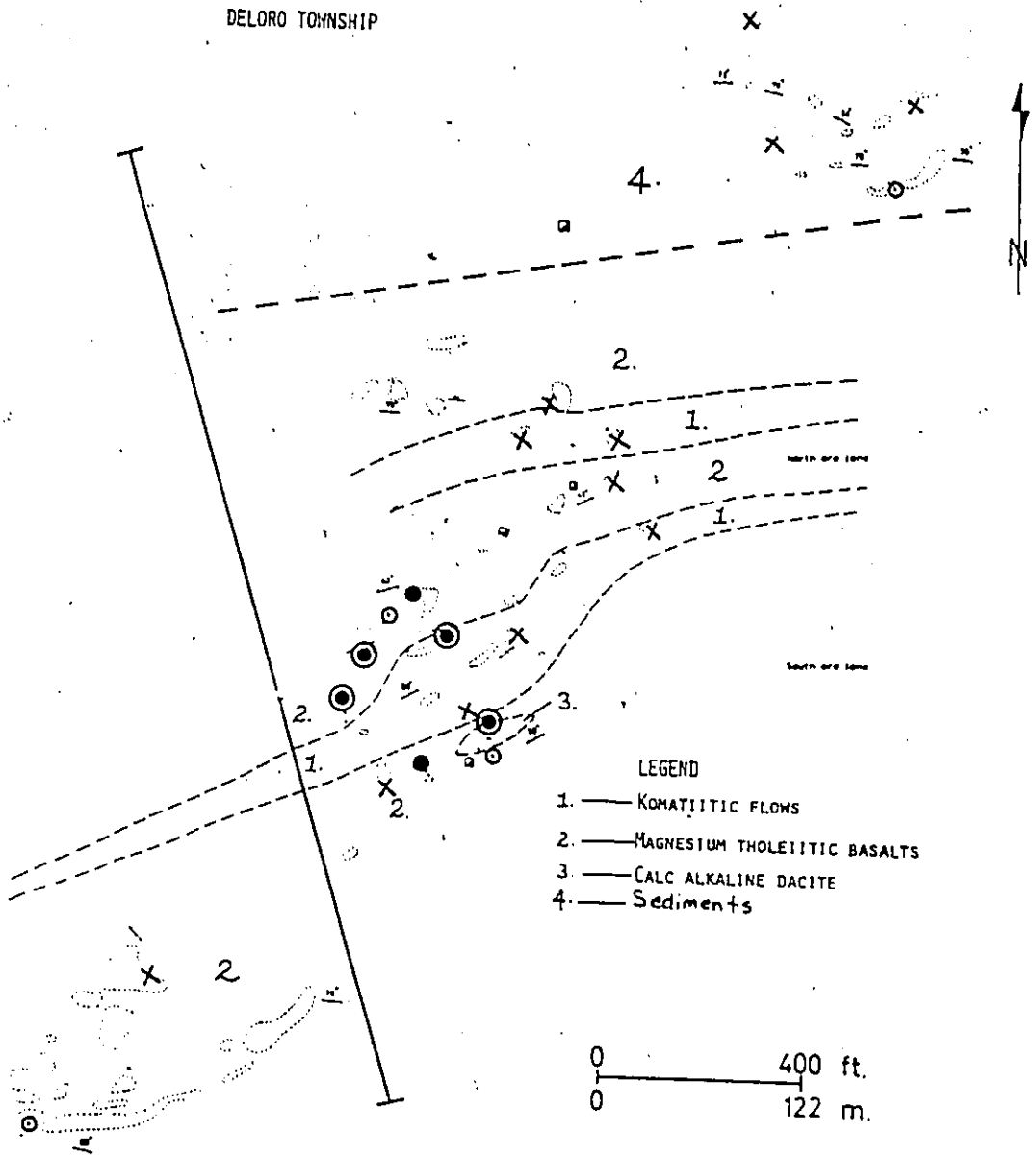

FIGURE 50 : Location of anomalous Cu samples on the Delnite Mine property. See map 8 for the detail geology and the location of carbonatized rock. Symbols are as follows:

X : <threshold

⊙ : 1-2 times threshold

● : 2-3 times threshold

◉ : >3 times threshold

DELNITE MINE SURFACE GEOLOGY
DELORO TOWNSHIP

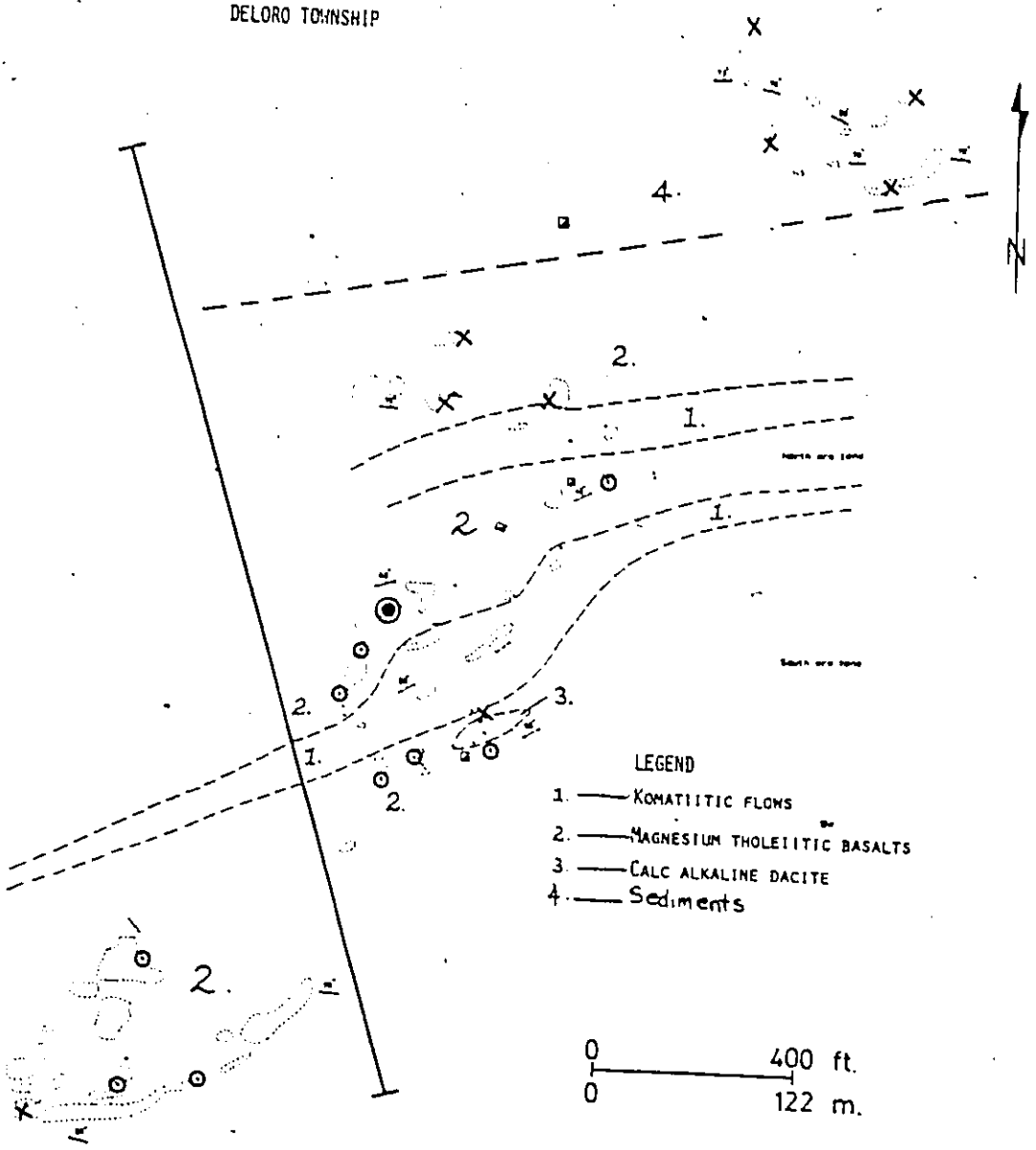

FIGURE 51 : Location of anomalous Li samples on the Delnite Mine property. See map 8 for the detail geology and the location of carbonatized rock. Symbols are as follows :

X : < threshold

⊙ : 1-2 times threshold

● : 2-3 times threshold

◉ : > 3 times threshold

DELNITE MINE SURFACE GEOLOGY
DELORO TOWNSHIP

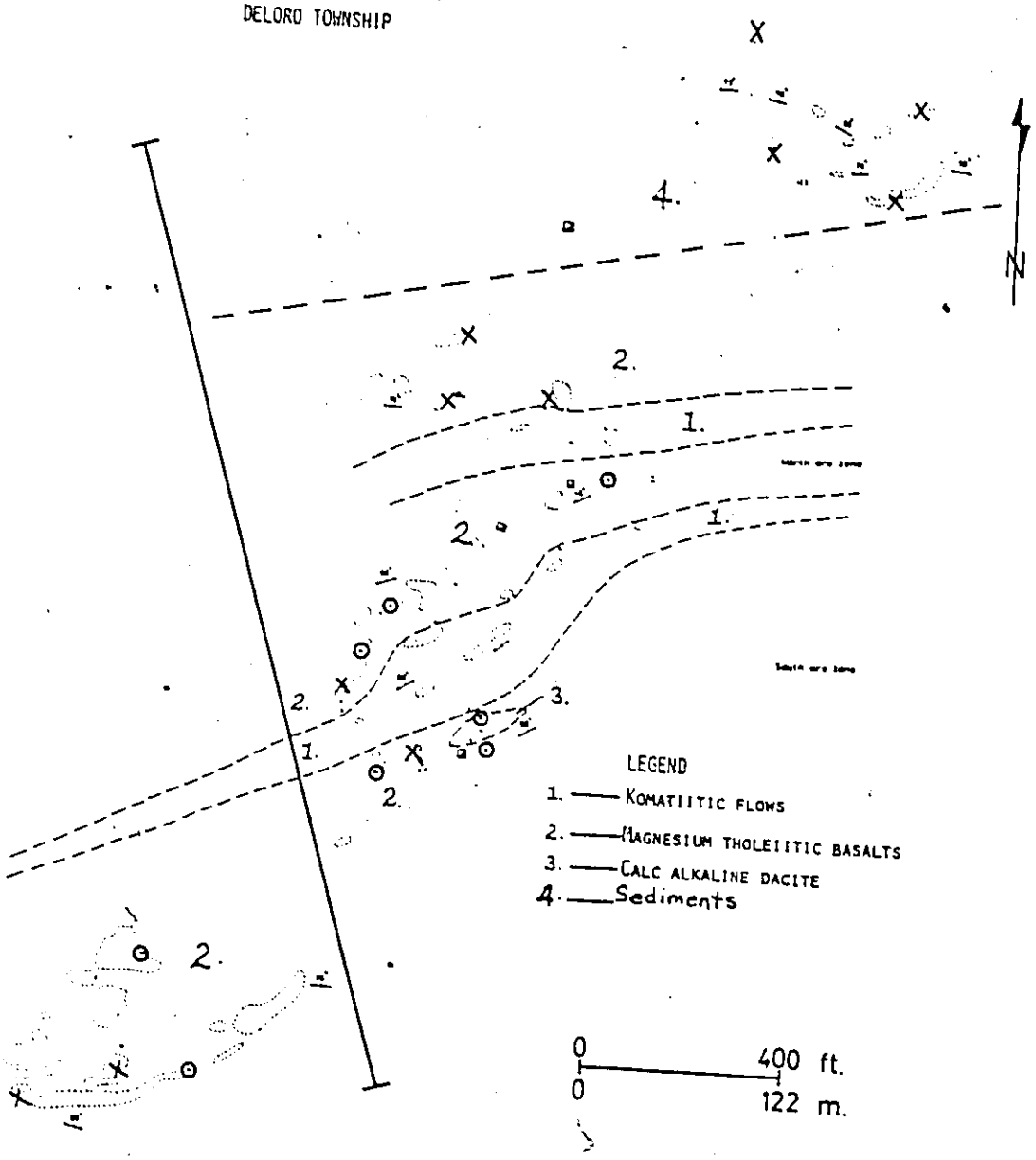

zones, but both show similar responses over the southern-most carbonate alteration zone. CO_2 (Figure 52) anomalies outline the zones of carbonatized rock. S anomalies (Figure 53) occur throughout the stratigraphy, reflecting the ubiquitous distribution of pyrite. The two ore zones are outlined using boron (Figure 54); however, three anomalous samples occur to the southwest where no known gold mineralization exists.

The lateral extent of this primary dispersion halo is impossible to evaluate at the Delnite Mine, because outcrop is absent. However, because the Aunor Mine ore zone lies approximately 3 km from both the Buffalo Ankerite and Delnite porphyries, an estimate of the lateral dispersion is attained by examining the frequency of anomalous samples which occur in the Aunor Mine ore zone (Figures 55-62). Unfortunately, Au anomalies are not presented because of insufficient data. The rocks at the east end of the ore zone are richer in CO_2 (Figure 55), with respect to the rest of the ore zone. Similarly, As, Bi, S and Sb (Figures 56, 57, 58, 59) define high priority anomalies in the east block. B (Figure 60), on the other hand, defines a high priority anomaly throughout the ore zone. Cu and Li (Figures 61, 62) define only a low priority anomaly in the ore zone. Production figures are

FIGURE 52 : Location of anomalous CO_2 in samples on the Delnite Mine property. See map 8 for the detail geology and the location of carbonatized rock. Symbols are as follows :

X : < threshold

⊙ : 1-2 times threshold

● : 2-3 times threshold

◉ : > 3 times threshold

DELNITE MINE SURFACE GEOLOGY
DELORO TOWNSHIP

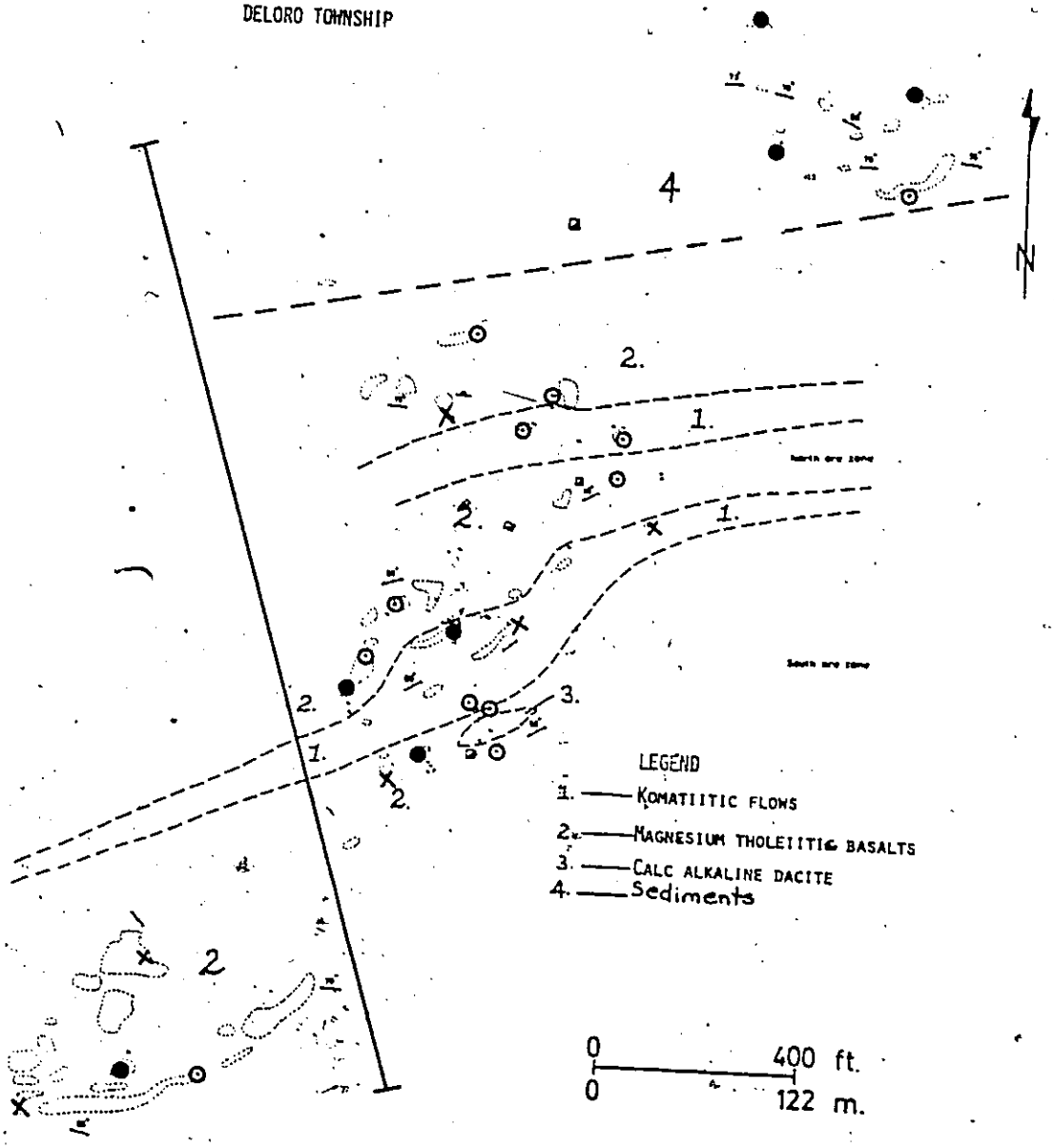

FIGURE 53 : Location of anomalous S samples on the Delnite Mine property. See map 8 for the detail geology and the location of carbonatized rock. Symbols are as follows :

X : < threshold

⊙ : 1-2 times threshold

● : 2-3 times threshold

◉ : > 3 times threshold

DELNITE MINE SURFACE GEOLOGY
DELORO TOWNSHIP

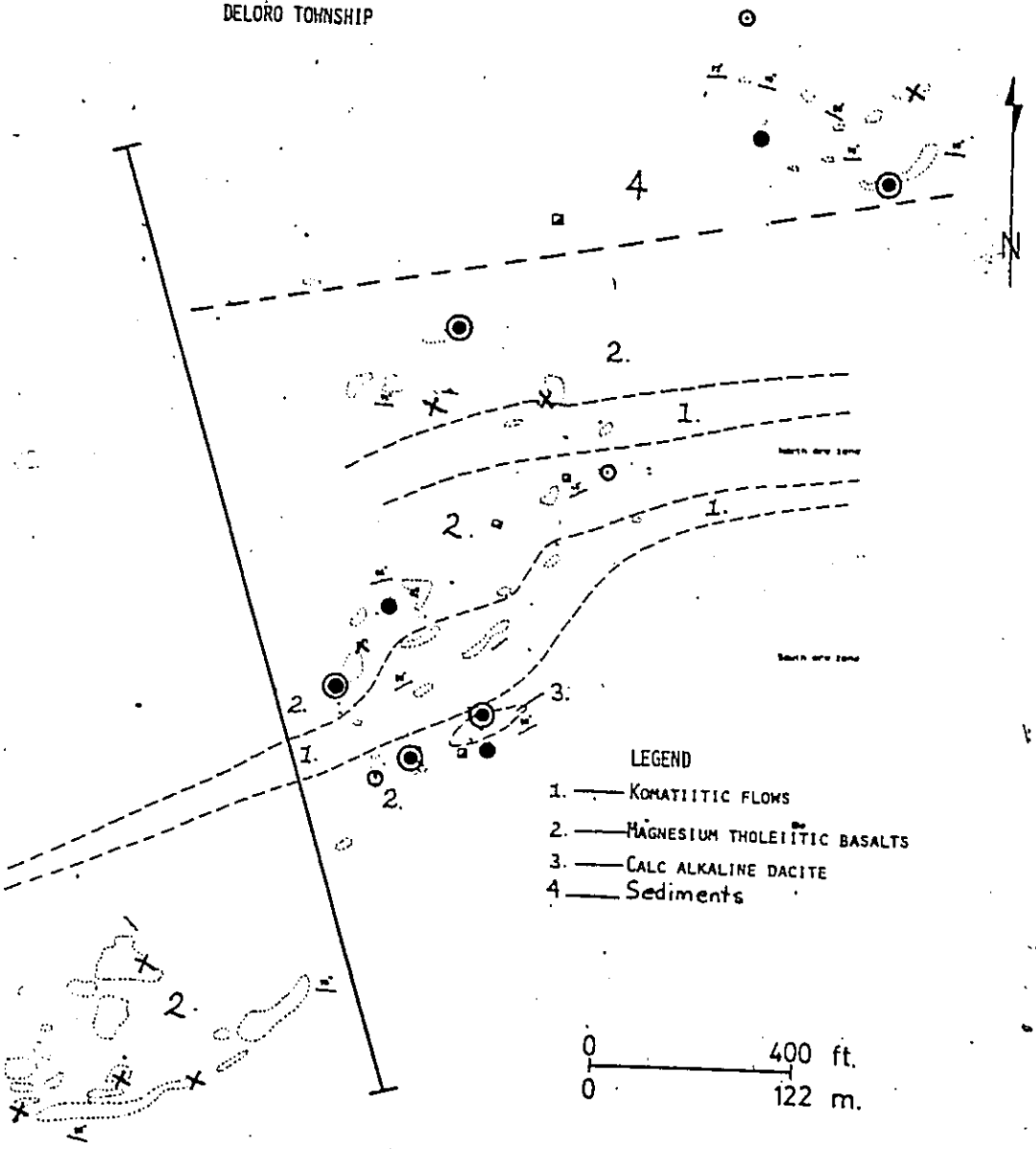

FIGURE 54: Location of B anomalies on the Delnite Mine property. See map 8 for the detail geology and the location of carbonatized rock. Symbols are as follows:

X : threshold

⊙ : 1-2 times threshold

● : 2-3 times threshold

◉ : 3 times threshold

DELNITE MINE SURFACE GEOLOGY
DELORO TOWNSHIP

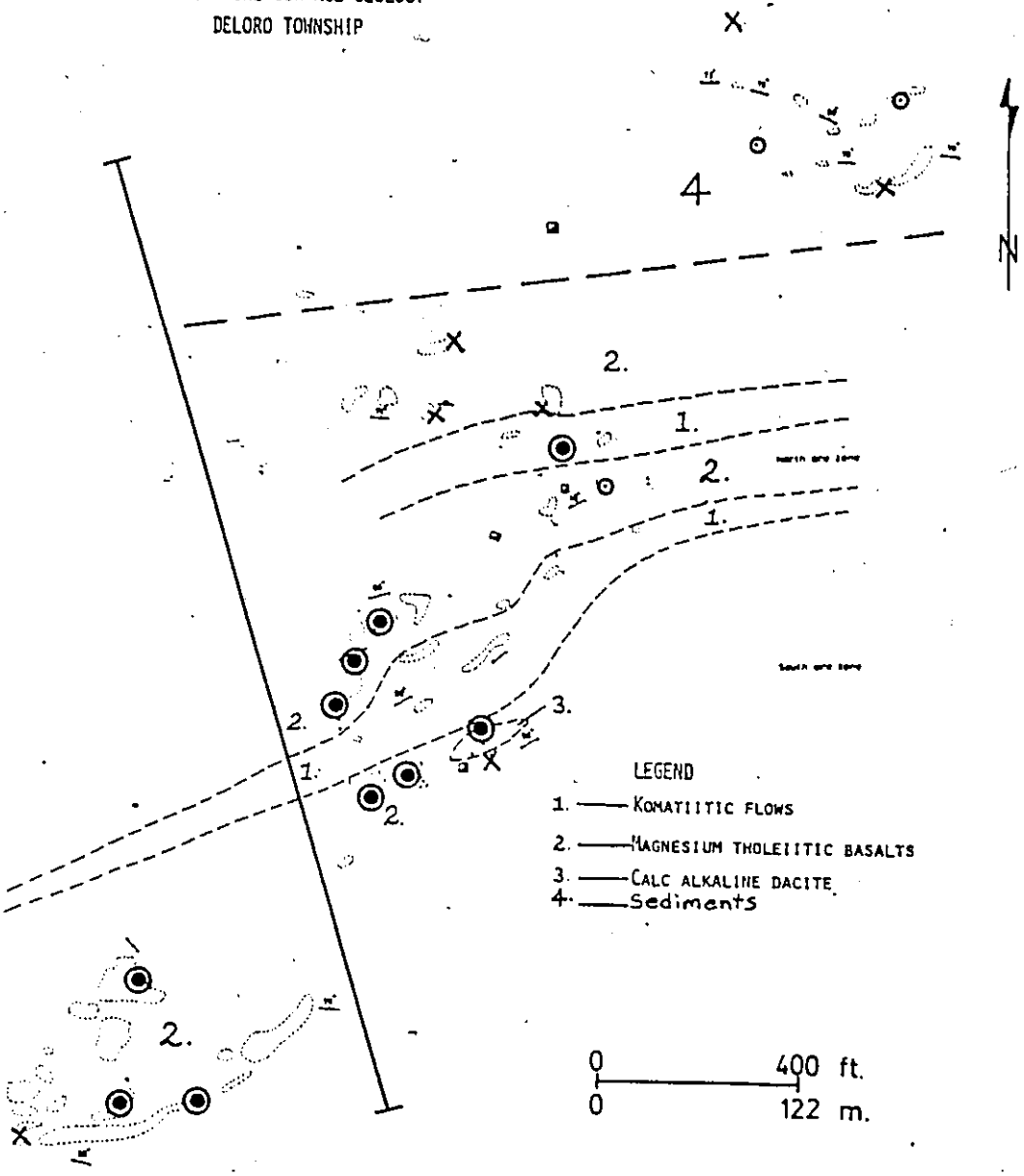

FIGURE 55. Location of anomalous CO_2 in tholeiitic and komatiitic samples from the 1000 level of the Aunor Mine. Symbols are as follows:

X : < threshold

⊙ : 1-2 times threshold

● : 2-3 times threshold

⊗ : > 3 times threshold

GEOLOGICAL PLAN OF AUNOR MINE, 1000 LEVEL
DELORO TWP STUDY AREA

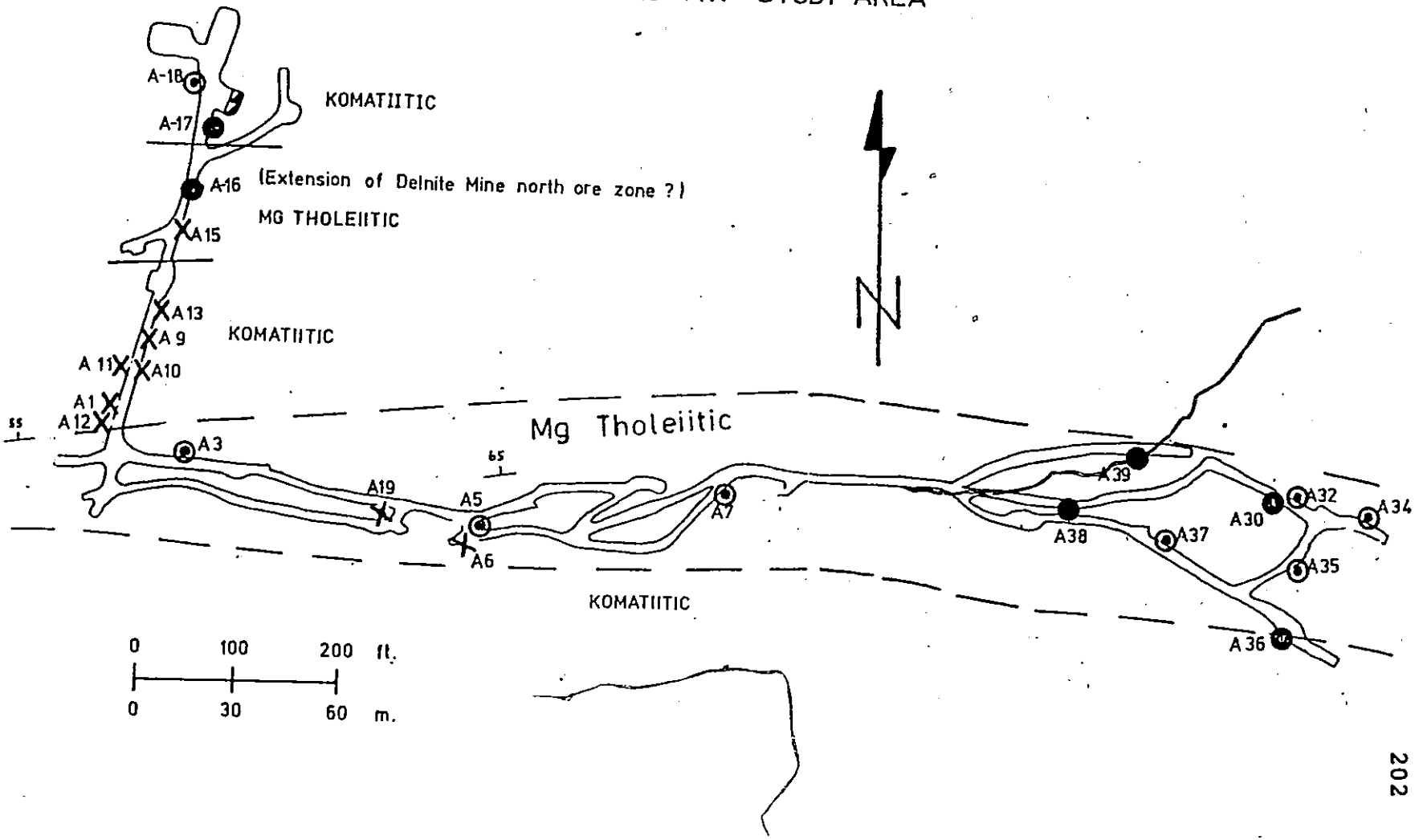

FIGURE 56. Location of anomalous As in tholeiitic and komatiitic samples from the 1000 level of the Aunor Mine. Symbols are as follows:

X : < threshold

⊙ : 1-2 times threshold

● : 2-3 times threshold

⊗ : > 3 times threshold

GEOLOGICAL PLAN OF AUNOR MINE, 1000 LEVEL
DELORO TWP STUDY AREA

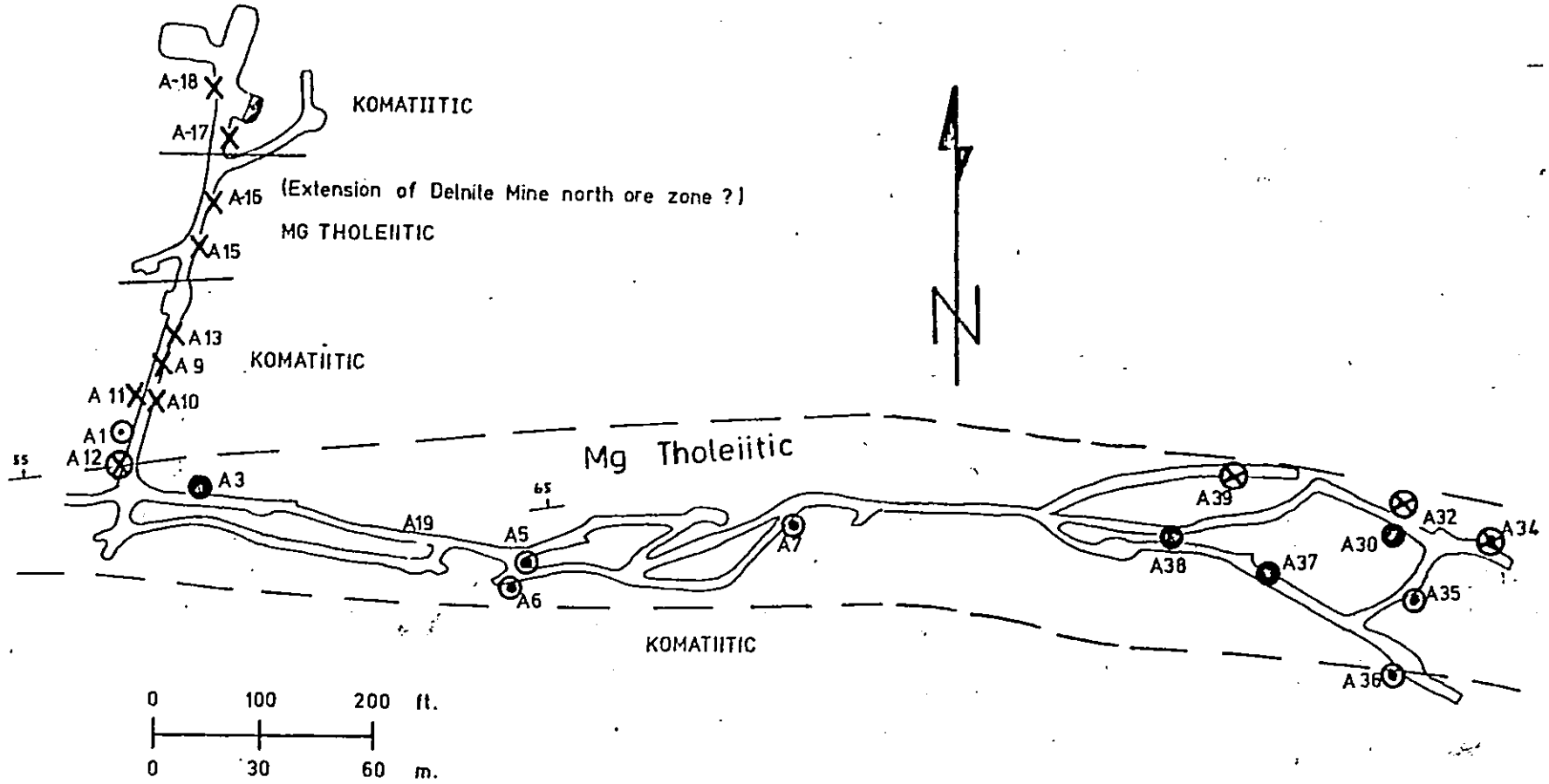

FIGURE 57. Location of anomalous Bi in tholeiitic and komatiitic samples from the 1000 level of the Aunor Mine. Symbols are as follows:

X : < threshold

⊙ : 1-2 times threshold

● : 2-3 times threshold

⊗ : > 3 times threshold

GEOLOGICAL PLAN OF AUNOR MINE, 1000 LEVEL
DELORO TWP STUDY AREA

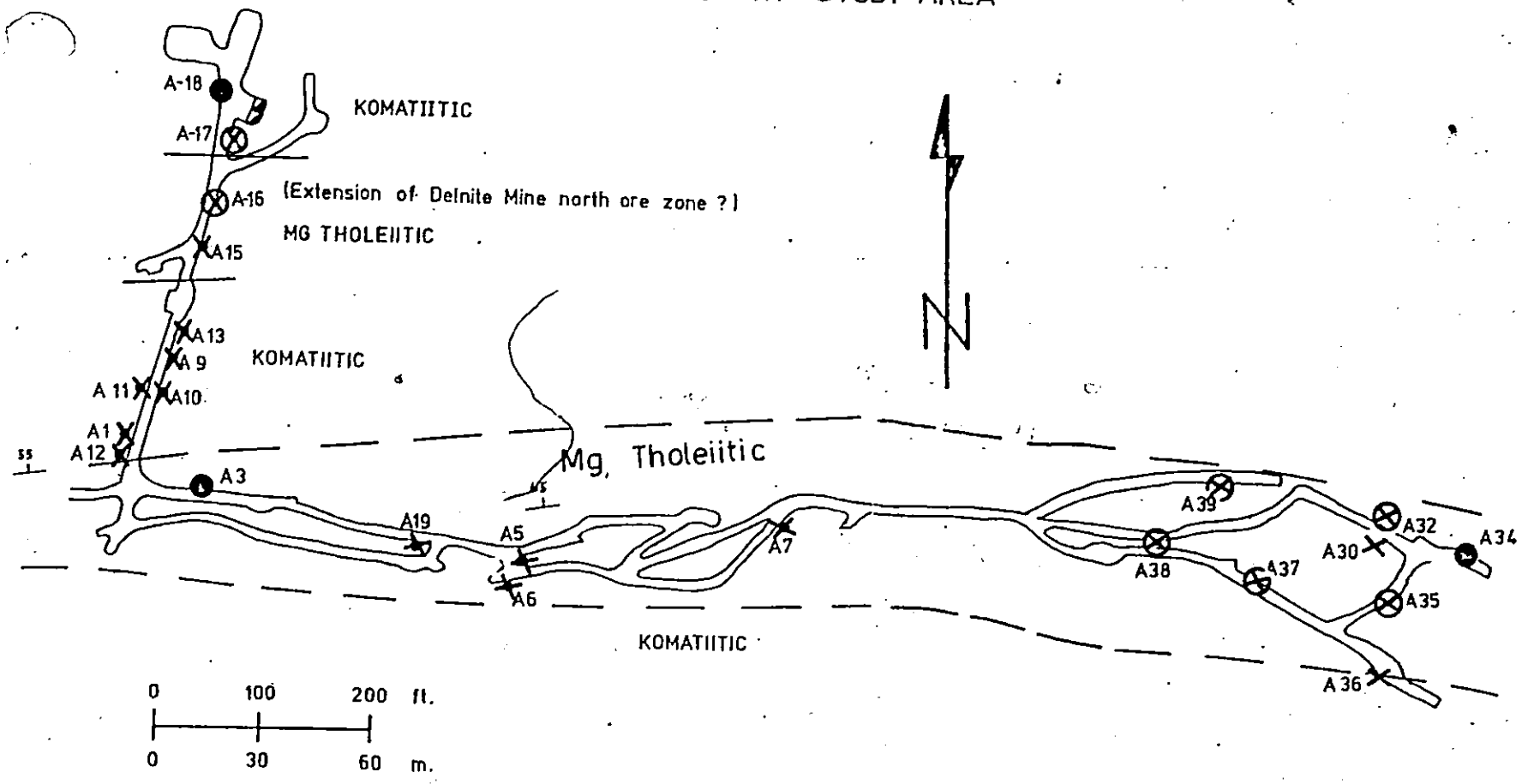

FIGURE 58. Location of anomalous S in Mg tholeiitic basalt samples from the 1000 level of the Aunor Mine. Symbols are as follows:

X: < threshold

⊙: 1-2 times threshold

●: 2-3 times threshold

⊗: > 3 times threshold

GEOLOGICAL PLAN OF AUNOR MINE, 1000 LEVEL
DELORO TWP STUDY AREA

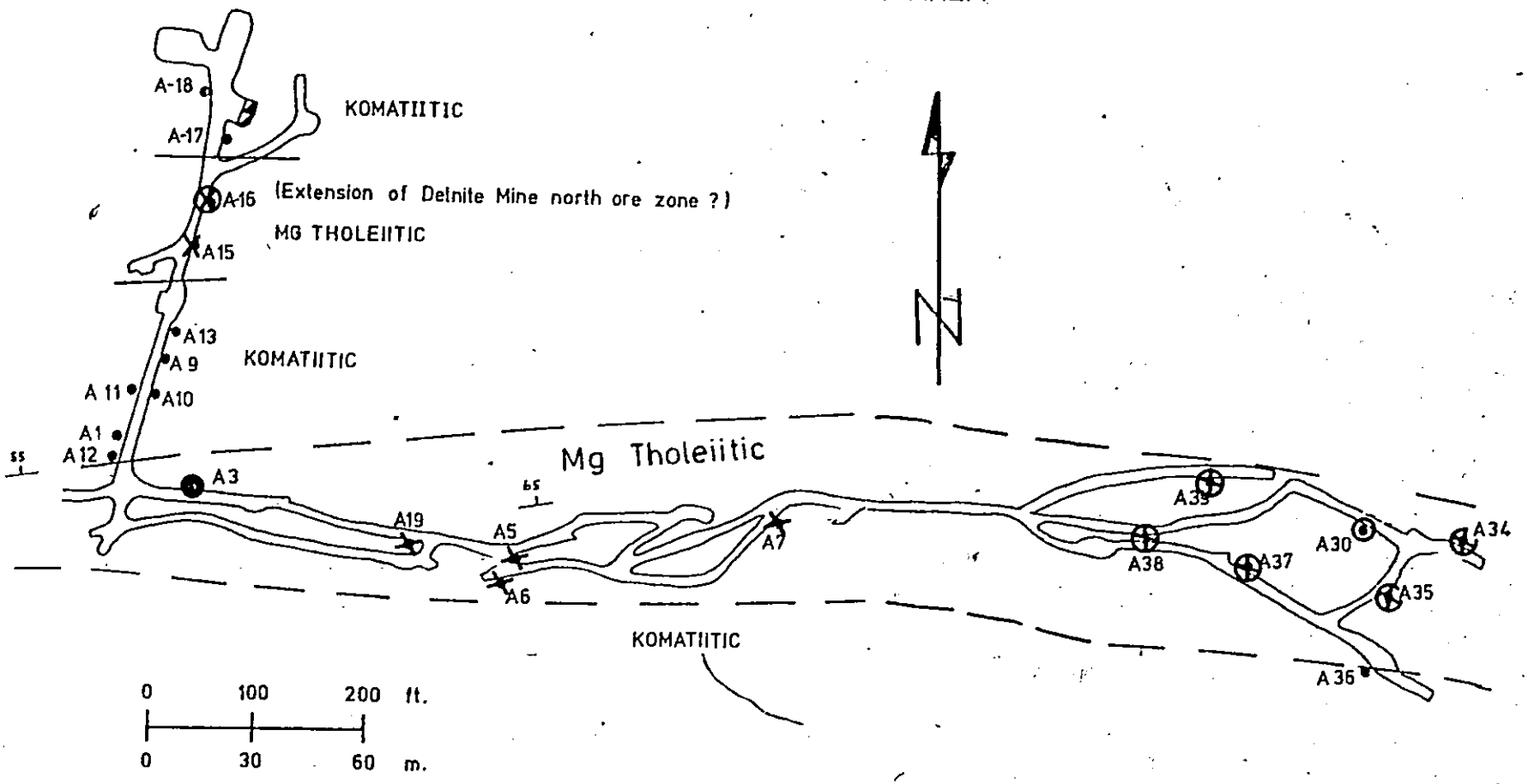

FIGURE 59. Location of anomalous Sb in Mg tholeiitic basalt samples from the 1000 level of the Aunor Mine. Symbols are as follows:

X : < threshold

⊙ : 1-2 times threshold

● : 2-3 times threshold

⊗ : > 3 times threshold

GEOLOGICAL PLAN OF AUNOR MINE, 1000 LEVEL
DELORO TWP STUDY AREA

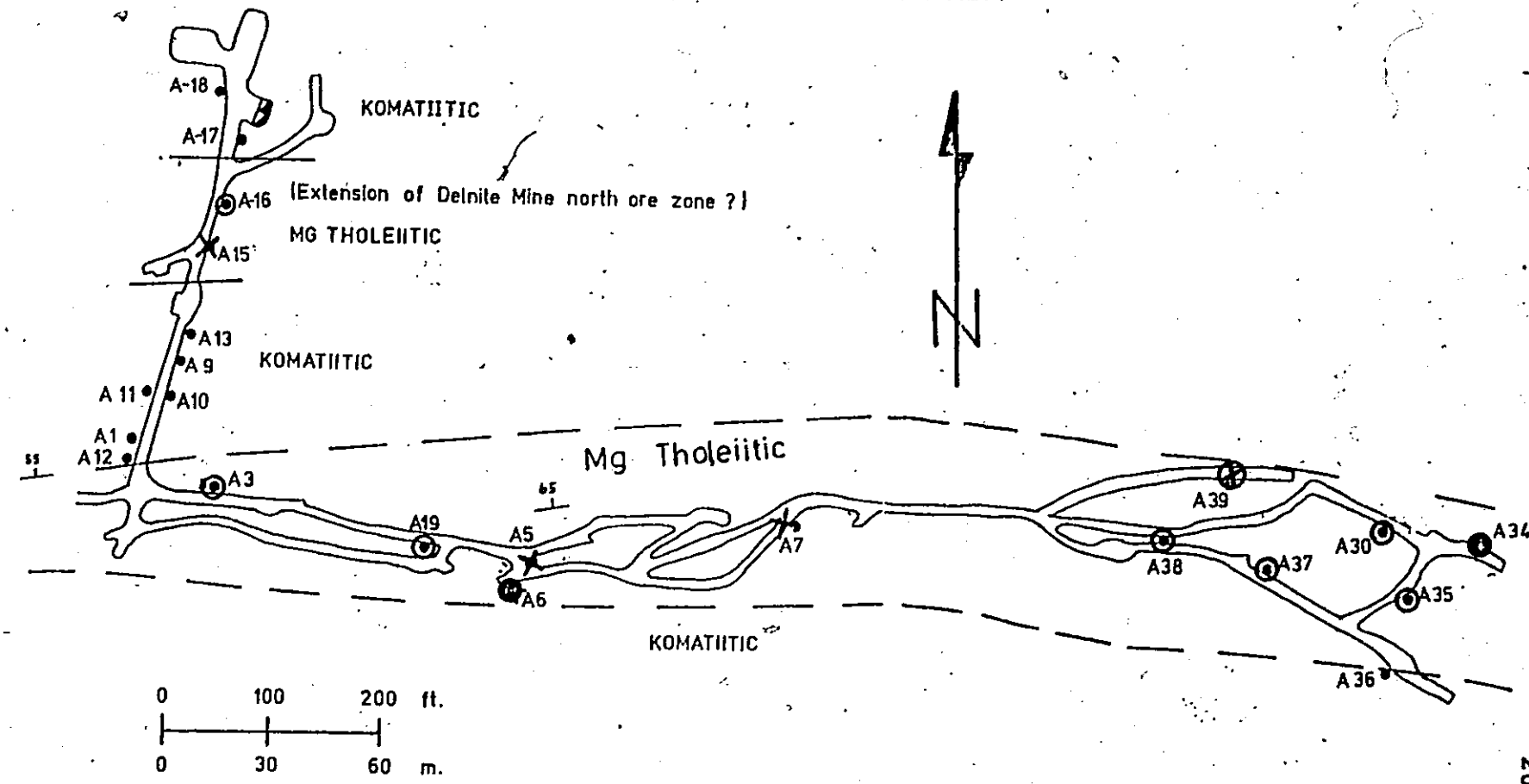

FIGURE 60. Location of anomalous B in Mg tholeiitic basalt samples from the 1000 level of the Aunor Mine. Symbols are as follows:

X: < threshold

⊙: 1-2 times threshold

●: 2-3 times threshold

⊗: > 3 times threshold

GEOLOGICAL PLAN OF AUNOR MINE, 1000 LEVEL
DELORO TWP STUDY AREA

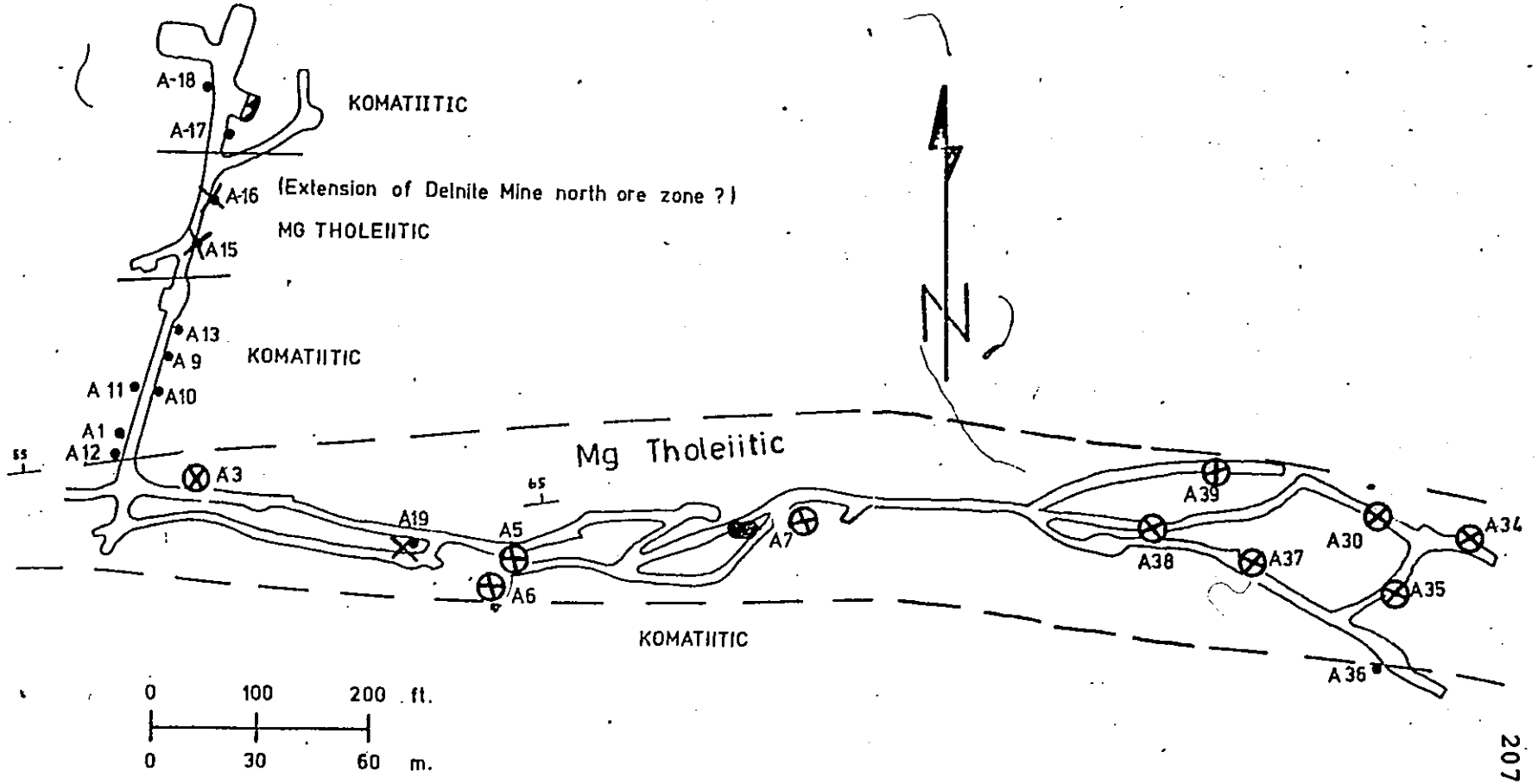

FIGURE 61. Location of anomalous Cu in Mg tholeiitic basalt samples from the 1000 level of the Aunor Mine. Symbols are as follows:

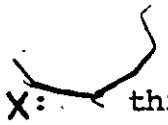

X: < threshold

⊙: 1-2 times threshold

●: 2-3 times threshold

⊗: > 3 times threshold

GEOLOGICAL PLAN OF AUNOR MINE, 1000 LEVEL
DELORO TWP STUDY AREA

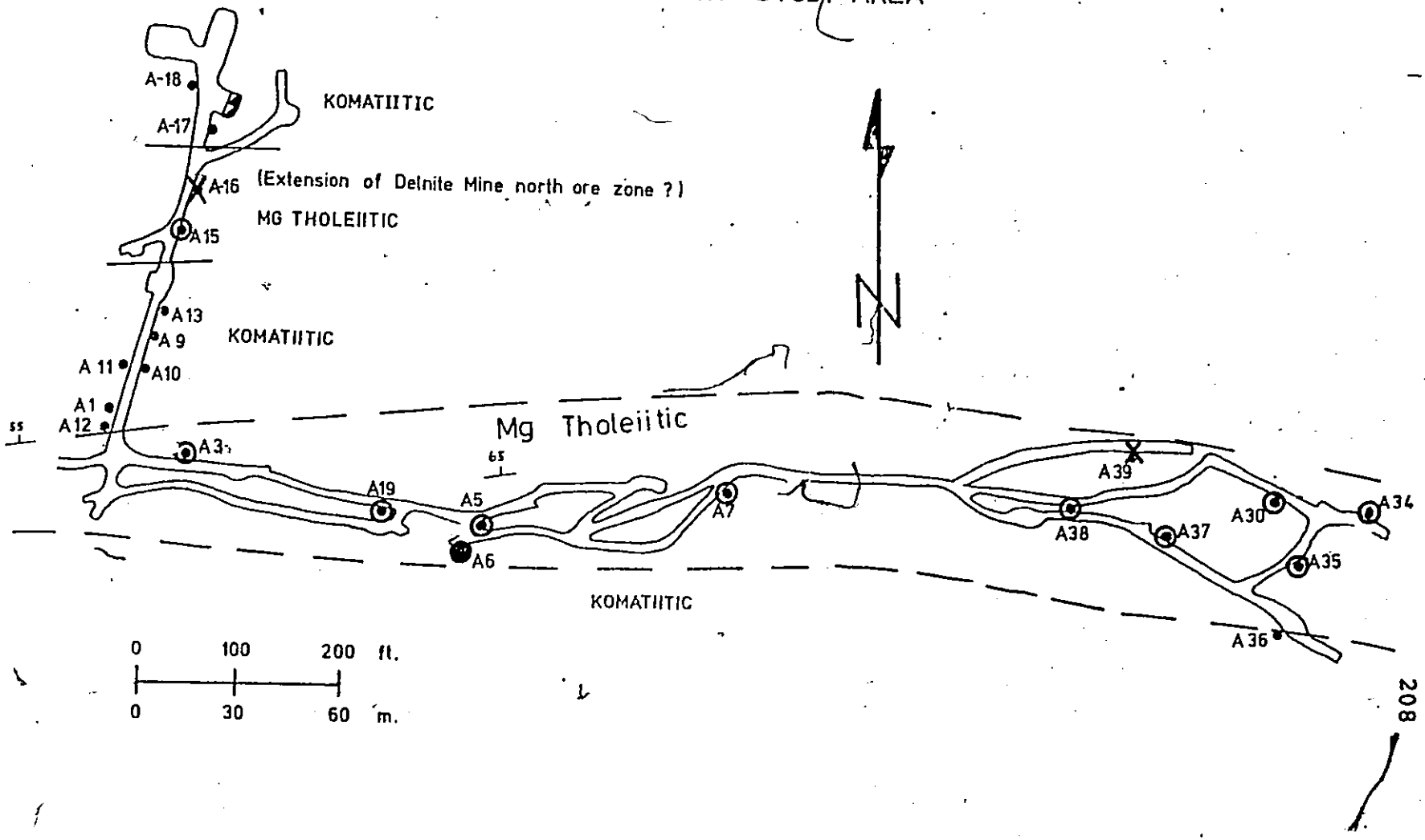

FIGURE 62. Location of anomalous Li in Mg tholeiitic basalt samples from the 1000 level of the Aunor Mine. Symbols are as follows:

X: < threshold

⊙: 1-2 times threshold

●: 2-3 times threshold

⊗: > 3 times threshold

GEOLOGICAL PLAN OF AUNOR MINE, 1000 LEVEL
DELORO TWP. STUDY-AREA

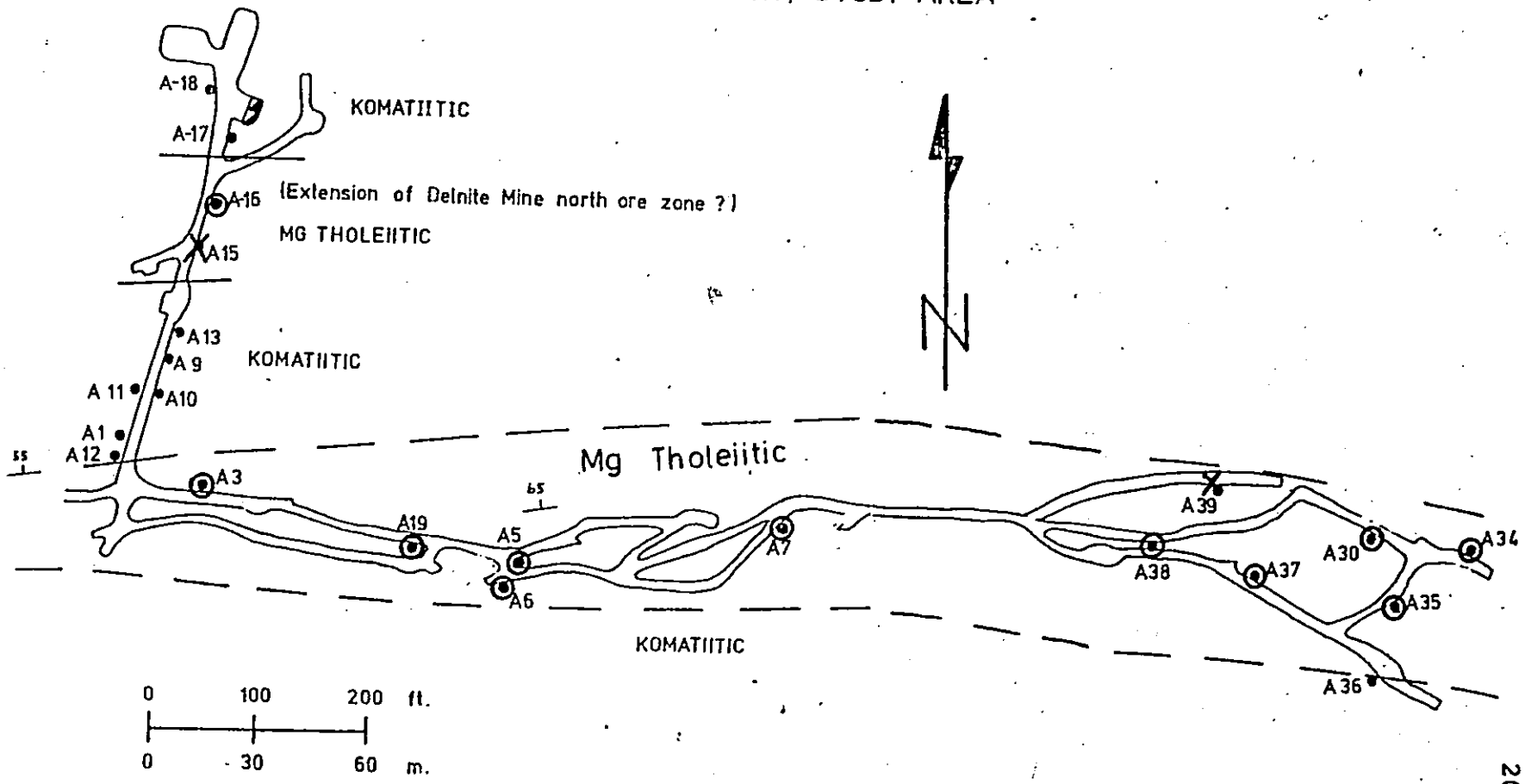

unavailable and hence it is not possible to establish if the ore material in the east end was of higher grade with respect to the rest of the ore zone. However, the east end is much closer to the Buffalo Ankerite porphyry, which is interpreted as a site of a major volcanic/hydrothermal vent zone, and hence, the enrichments of As, Bi, S, CO_2 and Sb in this area might reflect a more intense, hydrothermal alteration imprint. Boron anomalies define excellent, large scale target areas, as indicated by the presence of high priority anomalies throughout the ore zone.

Hence, altered Mg tholeiitic basalt flows which lie in close proximity (<30 m, 100 ft) to auriferous, cherty dolomites, are screened from altered flows not associated with "economic" gold mineralization using B, Bi, Sb and Au. Lateral dispersions of 1-3 km are identifiable only in flows associated with cherty dolomitic mineralization. During drill programs, systematic sampling and analysis for B, As, Sb, and Au will most effectively define high priority target areas.

10.4 SUMMARY

Volcanic rock is not enriched in gold by virtue of

the carbonatization process itself, and therefore carbonatized zones do not a priori represent anomalously enriched gold source rocks for tectonic or structurally controlled, epigenetic, gold deposits. Gold is however enriched in carbonatized rocks which are spatially associated with auriferous, cherty dolomites. This gold enrichment is attributed to the ore forming process.

There is no statistical difference at the 5% significance level between the mean gold abundances of komatiitic and Mg tholeiitic flows in the study areas, or in those reported in the literature for similar rock types. However, considering the extent to which seawater has interacted with the rocks, it must be assumed that this gold abundance represents a residual or base level (c.f. Keays and Scott, 1976). It is therefore impossible to evaluate the viability of the komatiitic source bed concept using the analytical data from the Porcupine camp. Intense carbonate alteration extracts virtually all gold from Mg tholeiitic basalts. Considering the relative ease of mobilizing gold from the hydrated basalts (Keays and Scott, 1976) and from intensely carbonatized rocks, it is apparent that in principle, any volcanic rock could act as a source of gold if that rock was subjected to a suitable hydrothermal process.

The gold deposit/komatiitic rock association is only one from a spectrum of gold deposit associations, which formed in a common or similar volcanic environment which was suitable for gold enrichment. Typically the onset of komatiitic volcanism is contemporaneous with the waning, volcanic activity of the older, underlying, volcanic pile, characteristically of felsic, calc-alkalic composition. This intermittent felsic/ultramafic volcanic activity and the inherent volcanic hiatuses define an optimum volcanic environment conducive to prolonged, intense rock/seawater interaction.

Those trace elements and their thresholds which most effectively identify altered rock which is spatially associated with auriferous, cherty dolomites are:

1. Au - >4.5 ppm
2. As - >70 ppm
3. Li - >30 ppm (Mg tholeiitic basalt only)
4. Sb - >0.35 ppm (Mg tholeiitic basalt only)
5. B - >30 ppm (Mg tholeiitic basalt only)
6. Cu - <70 ppm (Mg tholeiitic basalt only)

Of these elements, Bi, Li, Sb and Cu are useful only for Mg tholeiitic basalts. Hence, to use these elemental screens the rock type must be identified using field and petrochemical

parameters. Of general application are Au and As, whose use is not rock type dependent. To minimize the effects of geochemical "fliers", it is recommended that binary, element plots be used (e.g. Au-As or B-Au).

Primary dispersion haloes are restricted to the immediate ore zone environment. Lateral dispersion haloes on the order of 1-3 km are developed in altered, volcanic rocks which lie within 30 m (100 ft) of economic, auriferous, cherty dolomitic sediments.

The inability of boron and lithium to screen altered komatiitic flows, which are spatially associated with gold mineralization, reflects the process by which these elements are enriched in the flows. Because of their bulk composition, komatiitic rocks are chemically "reactive" and would alter readily to a clay-chlorite stable assemblage when exposed to seawater. Since B and Li are concentrated in these secondary clays (Schwarcz et al., 1969) an altered rock having a high modal proportion of clay minerals would consequently be enriched in boron and lithium.

CHAPTER 11

CONCLUSIONS

1. Synvolcanic, rock alteration which is present throughout the Lower Metavolcanic Group of the Upper Supergroup is characterized by two principle features: an initial palagonitization of hyaloclastite granules and flows which produced a regionally extensive, zeolite-clay type alteration assemblage; and localized, intensely altered, chlorite/carbonate assemblages. The localized, alteration zones occur parallel and discordant to flow contacts and consist of an outer chlorite-rich subzone which encloses a dolomitic core.

2. Per unit volume, the chloritized rocks are enriched in Li, Au, As, H_2O, CO_2 and are depleted in Sr, Ni, Cr, Co, Cu, Zn, Rb, Sb, SiO_2, Al_2O_3, Fe_2O_3 (total iron), MgO, and CaO with respect to the least altered samples. The pervasively carbonatized rocks are enriched in CaO, K_2O, P_2O_5, CO_2, Rb, As, Li, B, and Ba but are depleted in Sb, Au, Ni, Cr, Co, Cu, Zn, SiO_2, Al_2O_3, Fe_2O_3 (total iron), MgO,

TiO_2, MnO, and H_2O per unit volume with respect to the least altered rocks.

3. No element examined, specifically TiO_2 or Al_2O_3, is immobile during this type of alteration.

4. Because of the chemical variations induced by the intense carbonate alteration, the chemical composition of altered rock (>4 wt % L.O.I.) is statistically different from that of the least altered or spilitic samples at the 5% significance level. Chemical classifications of altered rocks using either the Jensen Cation Plot or the Al_2O_3-MgO-CaO plot must be interpreted with caution, particularly when field relations are not known.

5. Textural, structural and sedimentalogical data support the contention that the carbonatization of tholeiitic and komatiitic volcanic rock was synvolcanic and was localized by porosity factors such as the presence of flow top breccias or joint systems.

6. The elevated abundances of Ba, Li, B, Rb, H_2O, K_2O, CO_2, ferrous/ferric ratio and whole rock oxygen 18/16 isotopic ratios in the altered volcanic rock are consistent with a lower temperature (<200°C) seawater/rock interaction

model. It follows that the composition of the Archean ocean was not drastically different from the present day composition. However, the abundance of carbonate-rich altered rock of Archean age has no modern analogue which suggests that the partial pressure of CO_2 in the Archean atmosphere was greater than that of the present atmosphere.

7. Subsequent to the initial, low temperature, seawater/rock interaction, the volcanic pile was metamorphosed to greenschist facies in response to burial and intrusive activity.

8. Carbonatized volcanic rock which was altered in a subseafloor, volcanic environment is not associated with either auriferous, cherty dolomite, or felsic extrusive/hypabyssal rocks (Q.F.P.). Conversely, carbonate alteration zones which formed at or very near the seafloor/seawater interface are spatially associated with extrusive, felsic volcanic rocks and exhalative, auriferous sediments.

9. The seafloor environment in which the auriferous, cherty dolomites precipitated was characterized by localized felsic volcanism and synchronous but episodic tholeiitic and komatiitic volcanism. This environment facilitated pervasive, seafloor alteration by CO_2 charged, aqueous solutions of sea-

water origin, solution mass transport to the oceanfloor/seawater interface and areally widespread, chemical sedimentation.

10. Altered volcanic rock is not enriched in gold by virtue of the carbonatization process itself; therefore carbonatized rock does not a priori represent an anomalously enriched source rock for tectonic or structurally controlled epigenetic gold deposits. Rather, gold is effectively leached from the volcanic rock during the most intense stages of carbonate alteration.

11. Gold is enriched in altered volcanic rocks which are spatially associated with auriferous, cherty dolomites. This enrichment is attributed to the ore forming process.

12. At the 5% significance level, there is no statistical difference between the gold content of komatiitic and Mg tholeiitic volcanic rock. However, considering the degree of rock/seawater interaction, these analytical means of 1.8 and 2.6 ppb, respectively, probably represent residual or base levels. It is therefore impossible to evaluate the viability of the komatiitic, source-bed concept using analytical data as no fresh, komatiitic, volcanic rock of Archean age exists. Gold deposits are associated with volcanic rock of

widely varying composition (komatiitic to calc-alkalic) and the unifying genetic link is the volcanic environment and the extent to which seawater interacted with the seafloor.

13. Whole rock, single element screens, using the following trace elements and respective thresholds, discriminate between carbonate alteration zones which are spatially associated with auriferous, cherty dolomites and those altered rocks which have no associated gold mineralization.

a. Au - >4.5 ppb
b. As - >70 ppm
c. B - >30 ppm (Mg tholeiitic basalt only)
d. Li - >30 ppm (Mg tholeiitic basalt only)
e. Sb - >0.35 ppm (Mg tholeiitic basalt only)
f. Cu - <70 ppm (Mg tholeiitic basalt only)

Of these elements B, Li, Sb and Cu are effective only for Mg tholeiitic basalt; hence, rock type must be established. Of general application are Au and As, whose use is not rock type dependent.

14. Binary element screens, such as Au-As or Au-B should be used routinely to minimize the effect of geochemical "fliers".

15. Primary dispersion haloes are restricted to the immediate, ore bearing rocks, within 30 m (100 ft) of auriferous, cherty dolomite type mineralization.

REFERENCES

Andrews, A.J. (1977). Low temperature fluid alteration of oceanic layer 2 basalts, D.S.D.P. Leg 37. Can. Jour. Earth Sci., 14, 911-926.

Anhaeusser, C.R. (1976). Nature and distribution of Archean gold mineralization in Southern Africa. Minerals Sci. Engineering, 8, #1, 46-83.

Arndt, N.T., Naldrett, A.J. and Pyke, D.R. (1977). Komatiitic and iron-rich tholeiitic lavas of Munro Township, Northeast Ontario. Jour. Petrol., 18, 319-369.

Arndt, N.T., Francis, D. and Hynes, A.J. (1979). The field characteristics and petrology of Archean and Proterozoic komatiites. Can. Mineral., 17, 147-165.

Aumento, F., Loncarevic, B.D. and Ross, D.I. (1970). Hudson geotraverse, geology of the mid-Atlantic ridge at 45°N. Phil. Trans. Roy. Soc. London, A268, 623-650.

Babcock, R.S. (1973). Computational models of metasomatic processes. Lithos, 6, 279-290.

Backman, O.L. (1948). Broulan Mine: in Structural Geology of Canadian Ore Deposits. Can. Inst. Min. Met., 554-558, Jubilee Volume, 948p.

Baragar, W.R.A. (1968). Major element geochemistry of the Noranda volcanic belt, Quebec-Ontario. Can. Jour. Earth Sci., 5, 733-790.

Baragar, W.R.A., Plant, A.G., Pringle, G.J. and Schau, M. (1977). Petrology and alteration of selected units of mid-Atlantic ridge basalts samples from sites 332 and 335, D.S.D.P. Can. Jour. Earth Sci., 14, 837-874.

Baragar, W.R.A., Plant, A.G., Pringle, G.J. and Schau, M. (1979). Diagenetic and postdiagenetic changes in the composition of an Archean pillow. Can. Jour. Earth Sci., 16, 2102-2121.

Bell, A.M. (1948). Hallnor Mine: in Structural Geology of Canadian Ore Deposits. Can. Inst. Min. Met., 547-553, Jubilee Volume, 948p.

Beswick, A.E. and Soucie, G. (1978). A correction procedure for metasomatism in an Archean greenstone belt. Precambrian Research, 6, 235-248.

Beswick, A.E. and Nichol, I. (1979). Alteration in Precambrian volcanic rocks and relations to metallic mineral deposits: in Geoscience Research Seminar, Abstracts, (E.G. Pye, ed.), p.3. Ontario Geological Survey, 23p.

Bostrom, K., Kraemer, T. and Gartner, S. (1973). Provenance and accumulation rates of opaline silica, Al, Ti, Fe, Mn, Cu, Ni and Co in Pacific pelagic sediments. Chem. Geol., 11, 123-148.

Brown, C.L. (1967). The golden Porcupine. Can. Geographic Jour., 1, 1-17.

Buffam, B.S.W. (1948a). Aunor Mine: in Structural Geology of Canadian Ore Deposits. Can. Inst. Min. Met., 507-515, Jubilee Volume, 948p.

Buffam, B.S.W. (1948b). Moneta Porcupine Mine: in Structural Geology of Canadian Ore Deposits. Can. Inst. Min. Met., 457-464, Jubilee Volume, 948p.

Burrows, A.G. (1924). The Porcupine gold area: accompanied by Map 33a. Ontario Dept. Mines, 33, pt. 2, 1-84 (published 1925).

Carlson, H.D. (1967). The geology of Ogden, Deloro, and Shaw Townships, District of Cochrane, Ontario: accompanied by Maps P.341, P.342, scale 1 inch to 1/4 mile. Ontario Dept. Mines, OFR 5012, 117p.

Carter, O.F. (1948). Coniaurum Mine: in Structural Geology of Canadian Ore Deposits. Can. Inst. Min. Met., 497-503, Jubilee Volume, 948p.

Chayes, F. (1964). Variance-covariance relations in some published Harher diagrams of volvanic suites. Jour. Petrology, 5, 219-237.

Clifton, H.E., Hunter, R.E., Swanson, F.J. and Phillips, R.L. (1969). Sample size and meaningful gold analyses. U.S. Geol. Surv. Prof. Paper 625-C, 17p.

Cloud, P.E. (1973). Paleoecological significance of the banded iron-formations. Econ. Geol., 68, 1135-1143.

Crocket, J.H., MacDougall, J.D. and Harriss, R.C. (1973). Au, Pd, Ir in marine sediments. Geochim. Cosmochim. Acta, 37, 2547-2556.

Croudace, I.W. (1979). Errors in instrumental neutron activation analysis caused by matrix absorption. Chem. Geol., 25, 175-177.

Davis, J.C. (1973). Statistics and Data Analysis in Geology. John Wiley and Sons, Inc., Toronto, 550p.

Davies, J.F. (1977). Structural interpretation of the Timmins mining area, Ontario. Can. Jour. Earth Sci., 14, 1046-1053.

Davies, J.F., Grant, R.W.E. and Whitehead, R.E.S. (1979). Immobile trace elements and Archean volcanic stratigraphy in the Timmins mining area, Ontario. Can. Jour. Earth Sci., 16, 305-311.

Davies, J.F. and Luhta, L.E. (1978). An Archean "porphyry type" disseminated copper deposit, Timmins, Ontario. Econ. Geol., 73, 383-396.

Dear, W.A., Howie, R.A. and Zussman, J. (1974). An Introduction to the Rock Forming Minerals. Longman Group Ltd., London, 7th Edition, 528p.

Dimroth, E. and Rocheleau, M. (1979). Volcanology and sedimentology of the Rouyn-Noranda area, Quebec. Field Excursions Guidebook, Part A-1, Joint Meeting of Geol. Assoc. Can., Mineral. Assoc. Can., 199p.

Dimroth, E. and Lichtblau, A.P. (1979). Metamorphic evolution of Archean hyaloclastites, Noranda area, Quebec, Canada. Part 1: Comparison of Archean and Cenozoic sea-floor metamorphism. Can. Jour. Earth Sci., 16, 1315-1340.

Doucet, R.J.P. (1979). Mine de Bousquet, un gisement d'Or different, historique et geologie, Quebec: in Program with Abstracts, p.47. Ann. Meeting Geol. Assoc. Can., Mineral. Assoc. Can., Quebec City, May 1979.

Dunbar, W.R. (1948). Structural relations of the Porcupine ore deposits: in Structural Geology of Canadian Ore Deposits, Can. Inst. Min. Met., 442-456.

Eckstrand, O.R. (1975). The Dumont serpentinite: a model for control of nickeliferous opaque mineral assemblages by alteration reactions in ultramafic rocks. Econ. Geol., 70, 183-201.

Evans, J.F.L. (1944). Porphyry of the Porcupine District. Geol. Soc. Amer. Bull., 55, 1115-1142.

Ferguson, S.A. (1958a). Deloro Township, northwest quarter, District of Cochrane. Ontario Dept. Mines, Prelim. Map P.11, scale 1 inch to 500 feet.

Ferguson, S.A. (1958b). Deloro Township, northeast quarter, District of Cochrane. Ontario Dept. Mines, Prelim. Map P.12, scale 1 inch to 500 feet.

Ferguson, S.A. (1958c). Whitney Township, northwest quarter, District of Cochrane. Ontario Dept. Mines, Prelim. Map P.9, scale 1 inch to 500 feet.

Ferguson, S.A. (1960). Tisdale Township, northeast quarter, District of Cochrane. Ontario Dept. Mines, Prelim. Map P.6 (revised edition), scale 1 inch to 500 feet.

Ferguson, S.A., Buffam, B.S.W., Carter, O.F., Griffis, A.T., Holmes, T.C., Hurst, M.E., Lones, W.A., Lane, H.C. and Longley, C.S. (1968). Geology and ore deposits of Tisdale Township, District of Cochrane. Ontario Dept. Mines, GR 58, 177p. Accompanied by Map 2075, scale 1 inch to 1000 feet.

Fripp, R.E.P. (1976). Gold metallogeny in the Archean of Rhodesia: in Early History of the Earth (B.F. Windley, ed.), 455-466. John Wiley and Sons, Toronto, 619p.

Fritze, K. and Robertson, R. (1969). Precision in the neutron activation analysis for gold in standard rocks G-1 and W-1: in Modern Trends in Activation Analysis (J.R. DeVoe, ed). N.B.S. Spec. Pub. #312, 2, 1279-1283.

Fryer, B.J. and Hutchinson, R.W. (1976). Generation of metal deposits on the sea floor. Can. Jour. Earth Sci., 13, 126-135.

Fryer, B.J., Kerrich, R., Hutchinson, R.W., Peirce, M.G. and Rogers, D.S. (1979). Archean precious-metal hydrothermal systems, Dome Mine, Abitibi greenstone belt. 1. Patterns of alteration and metal distribution. Can. Jour. Earth Sci., 16, 421-439.

Fryer, B.J., Fyfe, W.S. and Kerrich, R. (1979b). Archean volcanogenic oceans. Chem. Geol., 24, 25-33.

Furse, G.D. (1948). McIntyre Mine: in Structural Geology of Canadian Ore Deposits. Can. Inst. Min. Met., 482-496, Jubilee Volume, 948p.

Fyon, J.A. and Karvinen, W.O. (1978). Volcanic environment of gold mineralization in the Timmins area: in Summary of Field Work, 1978, by the Ontario Geological Survey (V.G. Milne, O.L. White, R.B. Barlow and J.A. Robertson, eds.), 202-205. Ontario Geol. Survey, MP 82, 235p.

Fyon, J.A. and Crocket, J.H. (1979). Geological and geochemical guides to gold mineralization of the Porcupine camp, Timmins area: in Summary of Field Work, 1979, by the Ontario Geological Survey (V.G. Milne, O.L. White, R.B. Barlow and C.R. Kustra, eds.), 192-198. Ontario Geol. Survey, MP 90, 245p.

Garlick, G.D. and Dymond, J.R. (1970). Oxygen isotope exchange between volcanic materials and ocean water. Geol. Soc. Amer. Bull., 81, 2137-2142.

Gélinas, L., Brooks, C., Perrault, G., Carignan, J., Trudel, P. and Grasso, F. (1977). Chemo-stratigraphic divisions within the Abitibi volcanic belt, Rouyn-Noranda District, Quebec: in Volcanic Regimes in Canada (W.R.A. Baragar, L.C. Coleman and J.M. Hall, eds.), 265-295. Geol. Assoc. Canada Spec. Paper #16, 476p.

Gibson, H.L. and Watkinson, D.H. (1979). Silicification in the Amulet "rhyolite" formation, Turcotte Lake section, Noranda area, Quebec. Geol. Survey Canada Paper 79-1B, 111-118.

Goodwin, A.M. (1977). Archean volcanism in the Superior Province, Canadian Shield: in Volcanic Regimes in Canada (W.R.A. Baragar, L.C. Coleman and J.M. Hall, eds.), 205-241. Geol. Assoc. Canada Spec. Paper #16, 476p.

Graton, L.C. and McKinstry, H.E. (1933). Outstanding features of Hollinger geology. Can. Inst. Min. Met. Trans., 33, 1-20.

Gresens, R.L. (1967). Composition-volume relationships of metasomatism. Chem. Geol., 2, 47-65.

Griffis, A.T. (1962). A geological study of the McIntyre mine. Can. Inst. Min. Met. Trans., 65, 47-54.

Griffis, A.T. (1978). An Archean "porphyry-type" disseminated copper deposit, Timmins, Ontario - a discussion. Geology, 74, 695-696.

Hart, S.R. (1969). K, Rb, Cs contents and K/Rb, K/Cs ratios of fresh and altered submarine basalts. Earth Planet. Sci. Letters, 6, 295-303.

Hart, S.R. and Nalwalk, A.J. (1970). K, Rb, Cs, and Sr relationships in submarine basalts from the Puerto Rico trench. Geochim. Cosmochim. Acta, 34, 145-155.

Hawley, J.E. and Hart, R.C. (1948). Preston East Dome Mine: in Structural Geology of Canadian Ore Deposits. Can. Inst. Min. Met., 528-538, Jubilee Volume, 948p.

Holland, H.D. (1967). Gangue minerals in hydrothermal deposits: in Geochemistry of Hydrothermal Ore Deposits (H.L. Barnes, ed.), 382-436. Holt, Rinehart and Winston, Inc., Toronto, 670p.

Holmes, T.C. (1944). Some porphyry sediment contacts at the Dome mine, Ontario. Econ. Geol., 39, 133-141.

Holmes, T.C. (1948). Dome mine: in Structural Geology of Canadian Ore Deposits. Can. Inst. Min. Met., 539-547, Jubilee Volume, 948p.

Hopwood, T.P. (1976). "Quartz-eye"-bearing porphyroidal rocks and volcanogenic massive sulfide deposits. Econ. Geol., 71, 589-612.

Hopwood, T.P. (1977). "Quartz-eye"-bearing porphyroidal rocks and volcanogenic massive sulfide deposits - a reply. Econ. Geol., 72, 701-703.

Humphris, S.E. and Thompson, G. (1978a). Hydrothermal alteration of oceanic basalts by seawater. Geochim. Cosmochim. Acta, 42, 107-125.

Humphris, S.E. and Thompson, G. (1978b). Trace element mobility during hydrothermal alteration of oceanic basalts. Geochim. Cosmochim. Acta, 42, 126-136.

Hurst, M.E. (1936). Recent studies in the Porcupine area. Can. Inst. Min. Met. Trans., 39, 448-458, Jubilee Volume, 948p.

Hyndman, D.W. (1972). Petrology of Igneous and Metamorphic Rocks. McGraw-Hill Book Co., New York, 533p.

Jensen, L.S. (1976). A new cation plot for classifying subalkalic volcanic rocks. Ontario Div. Mines, MP 66, 22p.

Jensen, L.S. (1978a). Geology of Thackeray, Elliott, Tannahill and Dokis Townships, District of Cochrane. Ontario Div. Mines, GR 165, 71p. Accompanied by Maps 2367 and 2368, scale 1:31680 (1 inch to 1/2 mile).

Jensen, L.S. (1978b). Regional stratigraphy and structure of the Timmins-Kirkland Lake area, Districts of Cochrane and Timiskaming and the Kirkland Lake-Larder Lake area, District of Timiskaming: in Summary of Field Work, 1978, by the Ontario Geological Survey (V.G. Milne, O.L. White, R.B. Barlow and J.A. Robertson, eds.), 67-72. Ontario Geol. Survey, MP 82, 235p.

Jolly, W.T. (1975). Subdivision of the Archean lavas of the Abitibi area, Canada, from Fe-Mg-Ni-Cr relations. Earth Planet. Sci. Letters, 27, 200-210.

Jolly, W.T. (1978). Metamorphic history of the Archean Abitibi belt. Geol. Survey Canada Paper 78-10, 63-77.

Jones, W.A. (1948). Hollinger mine: in Structural Geology of Canadian Ore Deposits. Can. Inst. Min. Met., 464-481, Jubilee Volume, 948p.

Kanaris-Sotiriou, R., Gibb, F.G.F., Carswell, D.A. and Curtis, C.D. (1978). Trace-element distribution and ore formation in vein-metasomatized peridotite at Kalskaret, near Tafjord, South Norway. Contrib. Mineral. Petrol., 67, 289-295.

Karvinen, W.O. (1976). Distribution of carbonate-rich rocks, porphyries and gold deposits, Timmins area: in Summary of Field Work, 1976, by the Geological Branch (V.G. Milne, W.R. Cowan, K.D. Card and J.A. Robertson, eds.), 182-183. Ontario Div. Mines, MP 67, 183p.

Karvinen, W.O. (1978a). The Porcupine camp - a model for gold exploration in the Archean. Can. Min. Jour., September, 48-53.

Karvinen, W.O. (1978b). Structural interpretation of the Timmins mining area - a discussion. Can. Jour. Earth Sci., 15, 854.

Keays, R.R. and Scott, R.B. (1976). Precious metals in ocean ridge basalts: implications for basalts as source rocks for gold mineralization. Econ. Geol., 71, 705-720.

Keays, R.R. (1979). Gold deposits and ultramafic rocks: the link with nickel sulfide deposits; in Program with Abstracts, Ann. Meeting Geol. Assoc. Can., Mineral. Assoc. Can., p.60. Quebec City, May 1979.

Kerrich, R. and Fryer, B.J. (1979). Archean precious metal hydrothermal systems, Dome mine, Abitibi greenstone belt. II. REE and oxygen isotope relations. Can. Jour. Earth Sci., 16, 440-458.

Kinkel, A.R. (1948). Buffalo Ankerite mine: in Structural Geology of Canadian Ore Deposits. Can. Inst. Min. Met., 515-519, Jubilee Volume, 948p.

Knauth, L.P. and Epstein, S. (1976). Hydrogen and oxygen isotope ratios in nodular and bedded cherts. Geochim. Cosmochim. Acta, 40, 1095-1108.

Knuckey, M.J. and Watkins, J.J. (1978a). The Corbet mine and its environment of ore deposition, Noranda, Quebec: in Abstracts with Programs, Ann. Meeting Geol. Assoc. Can., Mineral. Assoc. Can., Geol. Soc. Amer., p436, Toronto, October 1978.

Knuckey, M.J., Comba, C.D.A. and Riverin, G. (1978b). The Millenback deposit, Noranda District, Quebec - an update on structure, metal zoning and wallrock alteration: in Abstracts with Programs, Ann. Meeting Geol. Assoc. Can., Mineral. Assoc. Can., Geol. Soc. Amer., p.436, Toronto, October 1978.

Kwong, Y-T.J. (1975). Distribution of Gold in an Archean Greenstone Belt as Exemplified by the Kakagi Lake Area, Northwestern Ontario. Unpub. M.Sc. thesis, McMaster Univ., Hamilton, Ont., 82p.

Kwong, Y-T.J. and Crocket, J.H. (1978). Background and anomalous gold in rocks of an Archean greenstone assemblage, Kakagi Lake area, Northwestern Ontario. Econ. Geol., 73, 50-63.

Longley, C.S. and Lazier, T.A. (1948). Paymaster mine: in Structural Geology of Canadian Ore Deposits. Can. Inst. Min. Met., 520-528, Jubilee Volume, 948p.

Lorsong, J. (1975). Stratigraphy and Sedimentology of the Porcupine Group (Early Precambrian), Northeastern Ontario. Unpub. B.Sc. thesis, Univ. Toronto, Toronto, Ont.

MacLean, W.H. (1977). Sulfides in Leg 37 drill core from the mid-Atlantic ridge. Can. Jour. Earth Sci., 14, 674-683.

Marchand, M. (1973). Determination of Rb, Sr, and Rb/Sr by XRF. Tech. Memo 73-2, Dept. Geology, McMaster Univ., Hamilton, Ont., Canada.

Middleton, R.S. (1976). Gravity survey of geological structures in the Timmins and Matheson area, District of Cochrane, Timiskaming, and Sudbury. Ontario Div. Mines, GR 135, 45p. Accompanied by Maps 2321 and 2322, scale 1 inch to 4 miles (1:253440).

Moore, E.S. (1954). Porphyries of the Porcupine area, Ontario. Roy. Soc. Can. Trans., 3rd series, 48, Sec. 4, 41-57.

Muehlenbachs, K. and Clayton, R.N. (1972a). Oxygen isotope studies of fresh and weathered submarine basalts. Can. Jour. Earth Sci., 9, 172-

Muehlenbachs, K. and Clayton, R.N. (1972b). Oxygen isotope geochemistry of submarine greenstones. Can. Jour. Earth Sci., 9, 471-478.

Muehlenbachs, K. and Clayton, R.N. (1976). Oxygen isotope composition of the oceanic crust and its bearing on seawater. Jour. Geophys. Res., 81, 4365-4369.

Muehlenbachs, K. (1977). Oxygen isotope geochemistry of rocks from D.S.D.P. Leg 37. Can. Jour. Earth Sci., 14, 771-776.

Nesbitt, R.W., Sun, S.S. and Purvis, A.C. (1979). Komatiites: geochemistry and genesis. Can. Mineral., 17, 165-186.

Norrish, K. and Hutton, J.T. (1969). An accurate X-ray spectrographic method for the analysis of a wide range of geological samples. Geochim. Cosmochim. Acta, 33, 431-453.

Nunes, P.D., Pyke, D.R. and Jensen, L.S. (1978). Toward an absolute age stratigraphy for the Abitibi greenstone belt, Eastern Ontario - zircon ages from the Timmins and Kirkland Lake areas: in Abstracts with Programs, p. , Ann. Meeting Geol. Assoc. Can., Mineral. Assoc. Can., Geol. Soc. Amer., Toronto 1978.

Pearce, T.H. (1968). A contribution to the theory of variation diagrams. Contrib. Mineral. Petrol., 19, 142-157.

Pearce, T.H. and Birckett, T.C. (1974). Archean metavolcanic rocks from Thackeray Township, Ontario. Can. Mineral., 12, 509-519.

Perry, E.C., Ahmad, S.N. and Swulius, T.M. (1978). The oxygen isotope composition of 3800 M.Y. old metamorphosed chert and iron formation from Isukasia, West Greenland. Jour. Geol., 86, 223-239.

Perry, E.C. (1967). The oxygen isotope chemistry of ancient cherts. Earth Planet. Sci. Letters, 3, 62-66.

Pineau, F., Javoy, M., Hawkins, J.W. and Craig, H. (1976). Oxygen isotope variations in marginal basin and oceanic ridge basalts. Earth Planet. Sci. Letters, 28, 299-307.

Price, P. and Byers, A.R. (1948). Pamour mine: in Structural Geology of Canadian Ore Deposits. Can. Inst. Min. Met., 558-565, Jubilee Volume, 948p.

Pyke, D.R. (1974). Timmins area, Districts of Cochrane and Timiskaming. Ontario Div. Mines, Prelim. Map P.941, Geological Series, scale 1 inch to 1 mile. Geology and compilation, 1973.

Pyke, D.R. (1975). On the relationship of gold mineralization and ultramafic volcanic rocks in the Timmins area. Ontario Div. Mines, MP 62, 23p.

Pyke, D.R. (1978a). Geology of the Redstone River area, District of Timiskaming. Ontario Div. Mines, GR 161, 75p. Accompanied by Maps 2363 and 2364, scale 1:31,680 (1 inch to 1/2 mile).

Pyke, D.R. (1978b). Regional geology of the Timmins-Matachewan area, Districts of Cochrane and Timiskaming: in Summary of Field Work, 1978, by the Ontario Geological Survey (V.G. Milne, O.L. White, R.B. Barlow and J.A. Robertson, eds.), 73-77. Ontario Geol. Survey, MP 82, 235p.

Pyke, D.R. and Middleton, R.S. (1971). Distribution and characteristics of the sulfide ores of the Timmins area. Can. Inst. Min. Met. Trans., 74, 157-168.

Pyke, D.R., Naldrett, A.J. and Eckstrand, O.R. (1973). Archean ultramafic flows in Munroe Township, Ontario. Geol. Soc. Amer. Bull., 84, 955-978.

Pyke, D.R., MacVeigh, J.G. and Middleton, R.S. (1978). Volcanic stratigraphy and geochemistry in the Timmins mining area: in Toronto '78 Field Excursions Guidebook (A.L. Currie and W.O. Mackasey, eds.), 160-184. Geol. Assoc. Can., Mineral. Assoc. Can., Geol. Soc. Amer. Ann. Meeting, Toronto, October 1978.

Roberts, R.G., Carnevali, J. and Harris, J.D. (1978). The volcanic-tectonic setting of gold-quartz vein systems in the Timmins district, Ontario: in Current Research, Part b, Geol. Surv. Canada, Paper 78-1B.

Roberts, R.G. and Spiteri, J.C. (1979). Volcanic-tectonic setting of gold deposits in the Timmins district: in Geoscience Research Grant Program, Summary of Research, 1978-1979 (E.G. Pye, ed), Grant 32, 37-41. Ontario Geol. Survey, MP 87, 152p.

Scarfe, C.M. and Smith, D.G.W. (1977). Secondary minerals in some basaltic rocks from D.S.D.P. Leg 37. Can. Jour. Earth Sci., 14, 903-910.

Schidlowski, M., Eichmann, R. and Junge, C. (1975). Precambrian sedimentary carbonates: carbon and oxygen isotope geochemistry and implications for the terrestrial oxygen budget. Precambrian Research, 2, 1-69.

Schwarcz, H.P., Agyei, E.K. and McMullen, C.C. (1969). Boron isotopic fractionation during clay adsorption from seawater. Earth Planet. Sci. Letters, 6, 1-5.

Spooner, E.T.C., Beckinsale, R.D., Fyfe, W.S. and Smewing, J.D. (1974). Oxygen-18 enriched ophiolitic metabasaltic rocks from E. Liguria (Italy), Pindos (Greece), and Troodos (Cyprus). Contrib. Mineral. Petrol., 47, 41-62.

Spooner, E.T.C. and Bray, C.J. (1977). Hydrothermal fluids of seawater salinity in ophiolitic sulfide ore deposits in Cyprus. Nature, 266, 808-812.

Taylor, R.B. (1948). Delnite mine: in Structural Geology of Canadian Ore Deposits. Can. Inst. Min. Met., 504-507, Jubilee Volume, 948p.

Thompson, J.E. (1943). Geology of McGarry and McVittie townships, Larder Lake area. Ontario Dept. Mines, 50, pt. 7, 1-99. Accompanied by Maps 50a,b, scale 1 inch to 1000 feet and Map 50d, scale 1 inch to 400 feet.

Thompson, M. and Howarth, R.J. (1976). Duplicate analyses in geochemical practice. Part 1. Theoretical approach and estimation of analytical reproducibility. Analyst, 101, 690-698.

Thompson, G. and Melson, W.G. (1970). Boron contents of serpentinites and metabasalts in the oceanic crust: implications for the boron cycle in the oceans. Earth Planet. Sci. Letters, 8, 61-65.

Tihor, L.A. and Crocket, J.H. (1977). Gold distribution in the Kirkland Lake-Larder Lake area with emphasis on Kerr Addison-type ore deposits - a progress report. Report of Activities, Part A, Geol. Surv. Canada Paper 77-1A.

Tomasson, J. and Kristmannsdottir, H. (1972). High temperature alteration minerals and thermal brines, Rekjanes, Iceland. Contrib. Mineral. Petrol., 36, 123-134.

Veizer, J. and Hoefs, J. (1976). The nature of O^{18}/O^{16} and C^{13}/C^{12} secular trends in sedimentary carbonate rocks. Geochim. Cosmochim. Acta, 40, 1387-1395.

Vernon, R.H. and Flood, R.H. (1977). "Quartz-eye" bearing porphyroidal rocks and volcanogenic massive sulfide deposits - a discussion. Econ. Geol., 72, 698-701.

Viljoen, R.P., Saager, R. and Viljoen, M.J. (1970). Some thoughts on the origin and processes responsible for the concentration of gold in the Early Precambrian of Southern Africa. Mineral. Deposita, 5, 164-180.

Weber, J.N. (1965). Evolution of the oceans and the origin of fine-grained dolomites. Nature, 207, 930-933.

Whitehead, R.E.S., Cameron, R.A. and Davies, J.F. (1979). The relation of gold deposits to concentrations of CO_2 in volcanic rocks: in Geoscience Research Grant Program, Summary of Research, 1978-1979 (E.G. Pye, ed.), Grant 30, 108-116. Ontario Geol. Survey, MP 87, 152p.

Wicks, F.J., Whittaker, J.W. and Zussman, J. (1977). An idealized model for serpentine textures after olivine. Can. Mineral., 15, 446-458.

Winkler, H.F.G. (1976). Petrogenesis of Metamorphic Rocks. Springer-Verlag, New York, 4th edition, 334p.

APPENDIX 1

RADIOCHEMICAL NEUTRON ACTIVATION PROCEDURE FOR GOLD

1. Pipette 2.00 ml gold carrier solution into a zirconium crucible. Add 3 NaOH pellets. Evaporate to dryness. Gold carrier should contain about 10 mg gold per ml.

2. Add rock powder when carrier is dry.

3. Add Na_2O_2-NaOH flux. Total flux is about 5 gms (4 to 4.45 gm Na_2O_2, rest NaOH).

4. Fuse for 2 minutes over low heat (burner) and 3 minutes in melted state. Swirl while molten. Let cool for 3 to 5 minutes.

5. Transfer crucible to 400 ml beaker and cover with watchglass. Dissolve cake in H_2O-HCl by first adding 15 ml H_2O. Add 15 ml concentrated HCl to produce 6 M solution. Remove and rinse zirconium crucible.

6. Transfer beaker to hot plate, set at 3 and warm for 0.5 hours or until solution reaches 80 to 90°C.

7. Centrifuge.

8. Transfer clear solution to 250 ml separatory funnel. Volume should be 50 to 100 ml of 6 M HCl.

9. Add equal volume of ethyl acetate to residual in centrifuge tube, mix and centrifuge. Transfer clear solution to respective 250 ml separatory funnel.

10. Add equal volume of ethyl acetate to separatory funnel, shake for 2 minutes and drain off aqueous phase.

11. Scrub organic phase with about 50 ml of 6 M HCl and shake for 2 minutes. Drain off aqueous phase.

12. Drain organic into 250 ml beaker, add about 50 ml 2 M HCl, place on hot plate and evaporate organic.

13. After organic has evaporated, turn heat to 3, evaporate to 15 to 20 ml and transfer to 50 ml centrifuge tube.

14. Precipitate gold by adding about 1 gm hydroquinine. Allow to sit for 20 minutes, dilute with hot 2 M HCl to about 40 ml and centrifuge.

15. Wash twice with alcohol-H_2O, then with about 5 ml of pure alcohol.

16. Transfer gold to .25 dram counting vial and dry.

APPENDIX 2

EQUALITY OF VARIANCE-COVARIANCE MATRICES

The following is condensed from Davis (1973).

For the data involved in this study, two groups of observations (K) each with "m" measured variables on each sample are treated at a time. For each group, a variance-covariance matrix $[Si^2]$ is computed. The null hypothesis is tested:

$$H_0: \quad [\Sigma_1^2] = [\Sigma_2^2]$$

against

$$H_1: \quad [\Sigma_1^2] \neq [\Sigma_2^2]$$

Each variance-covariance matrix $[Si^2]$ is an estimate of a population matrix $[\Sigma_i^2]$. Because the alteration groups are derived from the fresh rock group, that is, the parent populations of the groups are identical, a pooled estimate of the population variance-covariance matrix is created by:

$$[S_p^2] = \sum_{i=1}^{K} \frac{(n_i - 1)\,[S_i^2]}{\left(\sum_{i=1}^{K} n_i\right) - K}$$

where n_i = number of samples in the i^{th} group

Σn_i = total number of all samples in all K groups.

Because in this case K = 2 (at any one time - fresh vs. altered).

$$[Si^2] = \frac{[SPi]}{(n_i - 1)}$$

where [SPi] matrix of sums of squares and cross-products for sample group i.

From the pooled estimate of the population variance-covariance matrix, test statistic M is computed:

$$M = \left(\sum_{i=1}^{K} n_i\right) - K \quad \ln|Sp^2| - \sum_{i=1}^{K} (n_i - 1)\ln|Si^2|$$

The test is based on the difference between the logarithm of the determinant of the pooled variance-covariance matrix and the average of the logarithms of the determinants of the sample variance-covariance matrices. If the sample matrices are the same, this difference will be small, but the

test statistic increases as the variances and covariances of the samples deviate from one another.

The following transformation is used to convert M to an approximate χ^2 statistic:

$$C^{-1} = 1 - \frac{2m^2 + 3m - 1}{6(m+1)(K-1)} \sum_{i=1}^{K} \frac{1}{n_i - 1} - \frac{1}{\left(\sum_{i=1}^{K} n_i\right) - K}$$

$$\chi^2 = MC^{-1}$$

χ^2 has ν degrees of freedom

$$\nu = 0.5\,(K-1)\,(m)\,(m+1)$$

The χ^2 approximation is good if K and m do not exceed 5 and each variance-covariance estimate is based on at least 20 observations.

Map 1

REGIONAL GEOLOGY DELORO TOWNSHIP STUDY AREA

LEGEND

5 Iron Tholeiitic Metavolcanics
- a Unsubdivided

4 Magnesium Tholeiitic Metavolcanics
- a Massive
- b Pillowed

3 Clastic and Chemical Metasediments
- a Conglomerate
- b Argillite
- c Auriferous cherty dolomite
- d Siliceous limestone
- e Chert

2 Calc Alkalic Metavolcanics
- a Quartz-feldspar-sericite schist
- b Andesitic tuff

1 Komatiitic Metavolcanics
- a Ultramafic
- b Mafic

c Pillow attitude

1 of

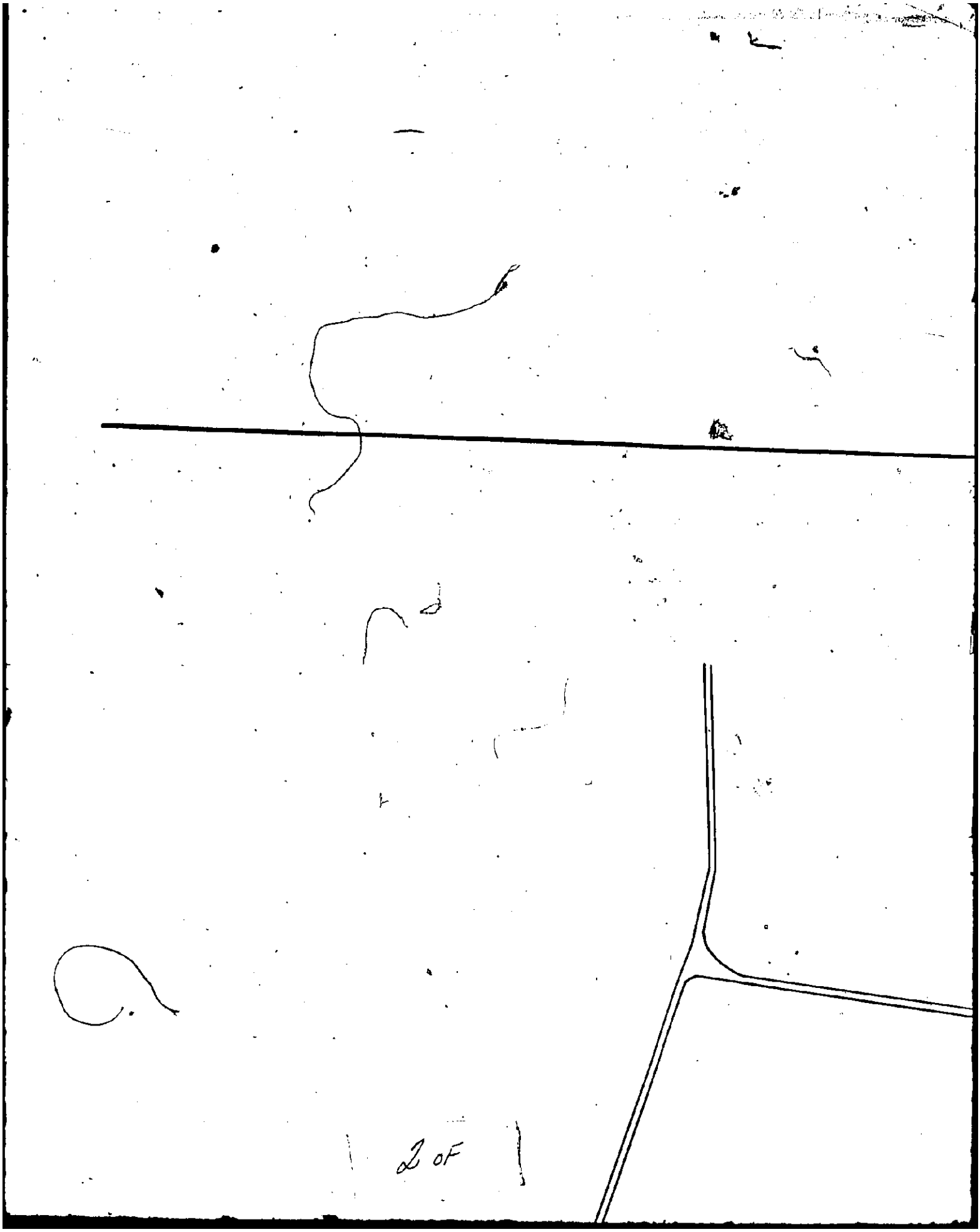
2 OF

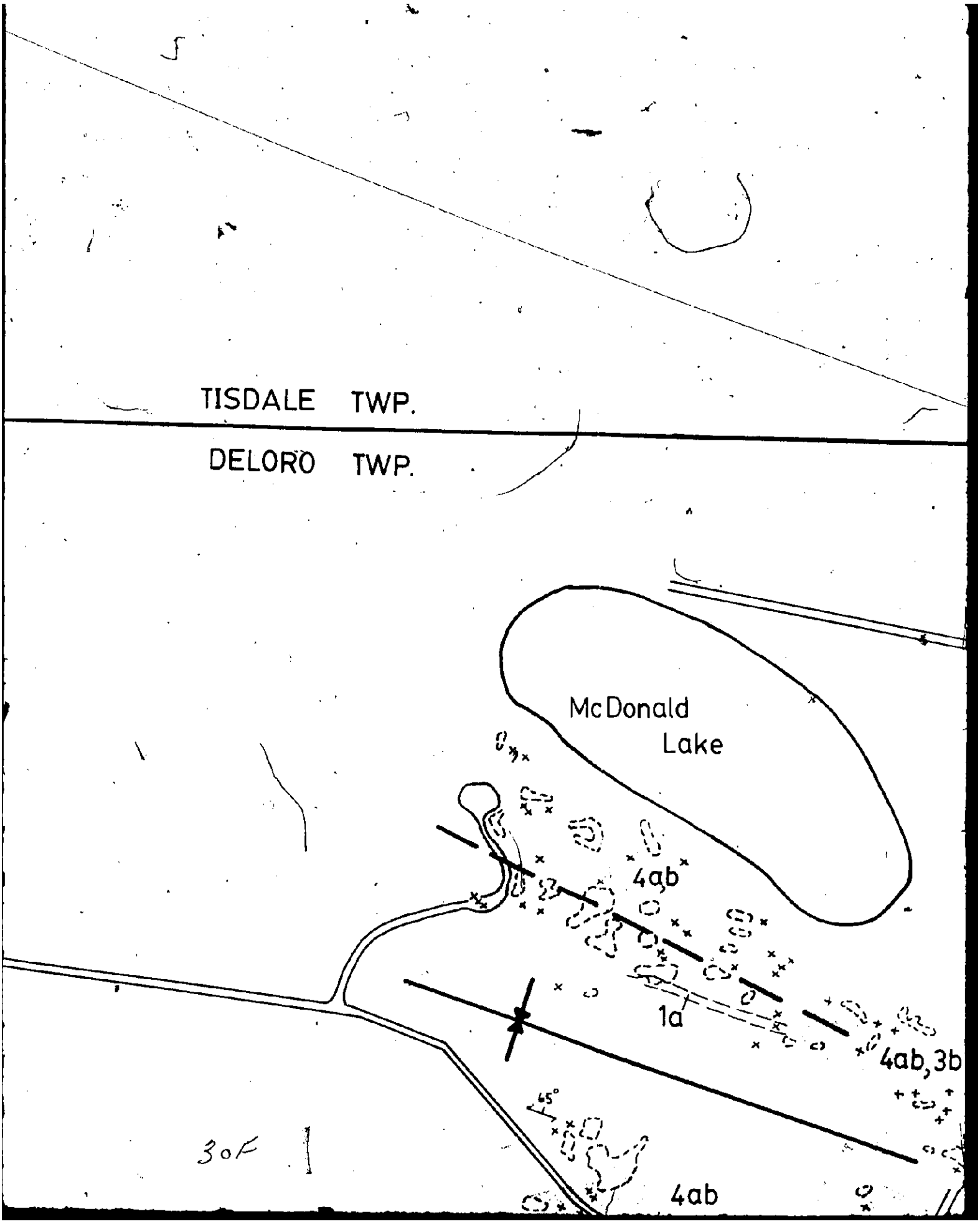
TISDALE TWP.
DELORO TWP.
McDonald
Lake
4ab
1a
4ab, 3b
45°
4ab

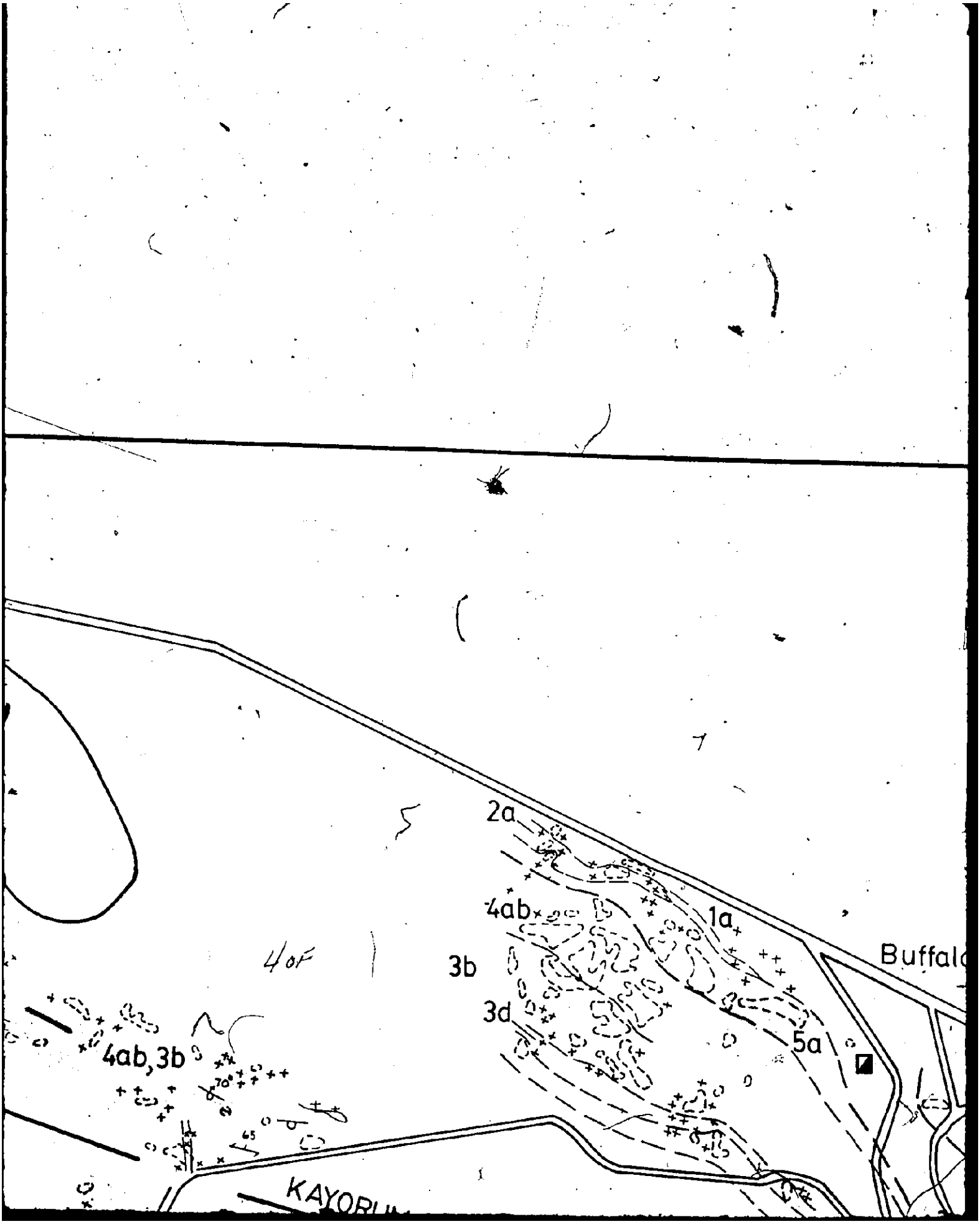
2a
4ab
1a
3b
3d
5a
4ab, 3b
Buffalo
KAYORU

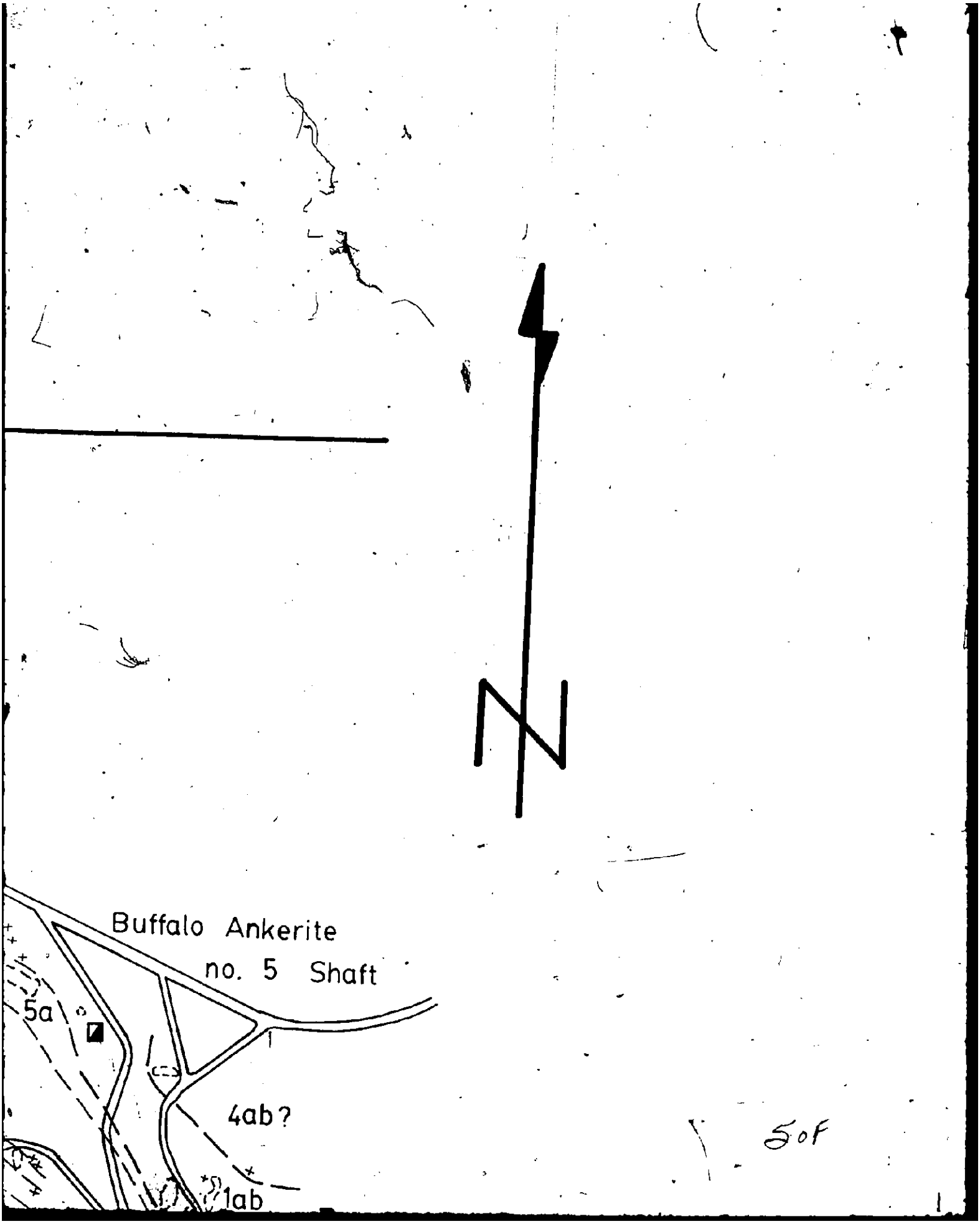

5 of

1 Komatiitic Metavolcanics

a Ultramafic

b Mafic

Pillow attitude

Bedding

Foliation

Lineation

Geological contact

Fault

Synclinal axis

Anticlinal axis

Drag fold

Shaft

Open pit

δ Diorite

Pervasive carbonatization

qv Quartz vein

py,cpy Pyrite, chalcopyrite

V.G. Visible gold

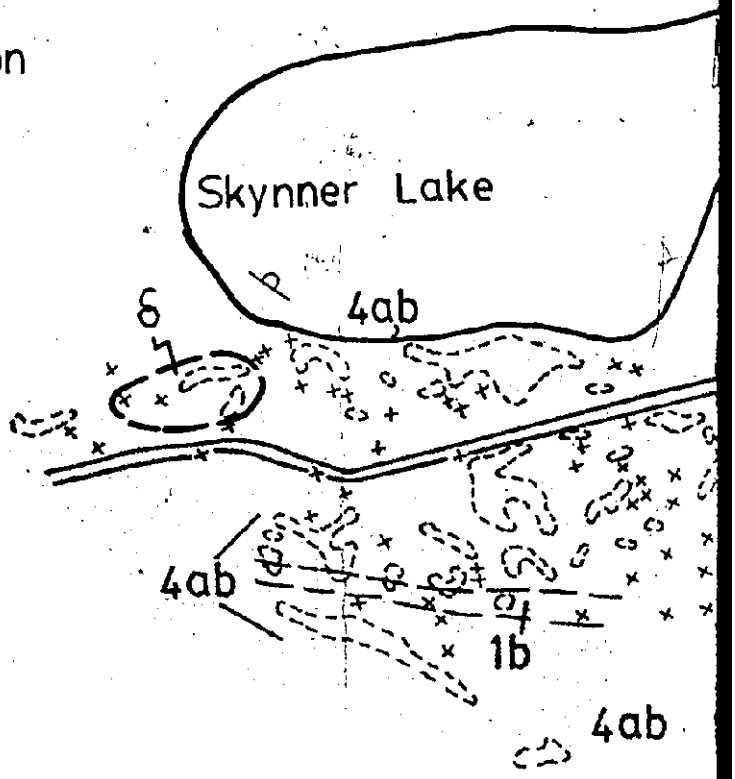

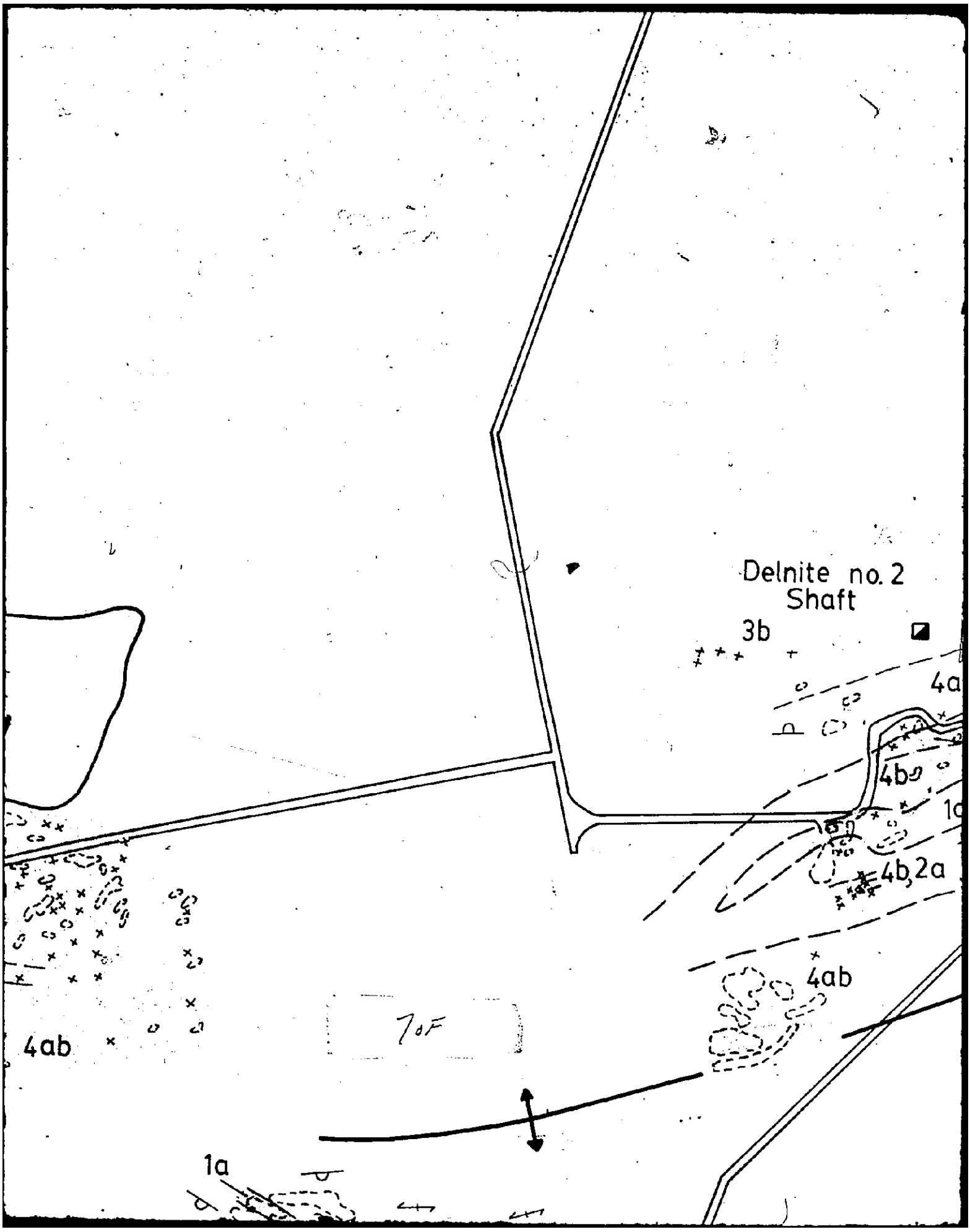
Delnite no. 2
Shaft
3b
4a
4b
1a
4b, 2a
4ab
4ab
7 of
1a

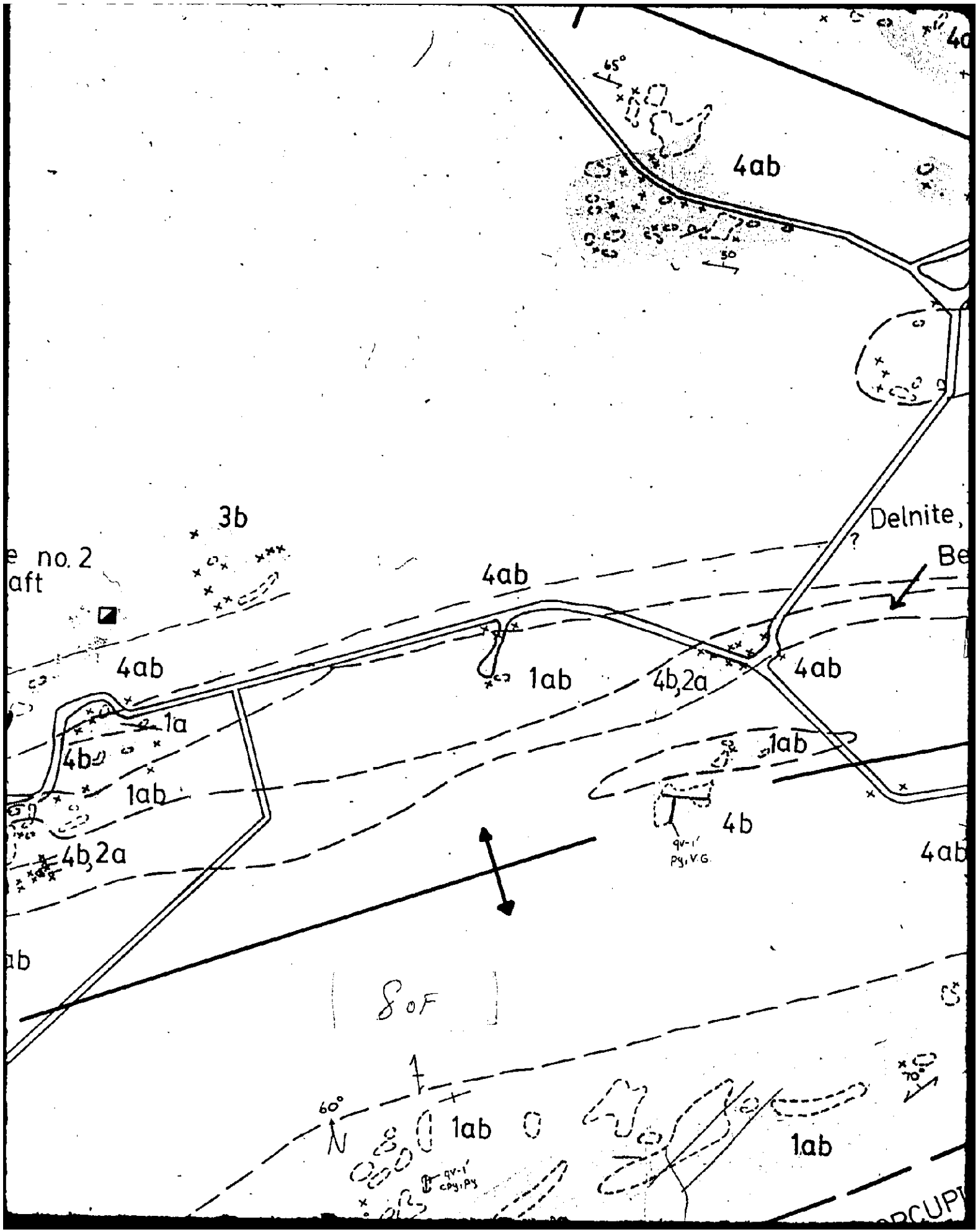
4ab
65°
50
3b
e no. 2
aft
Delnite,
Be
4ab
4ab
1ab
4b,2a
4ab
1a
4b
1ab
1ab
4b
qv-1'
Py, V.G.
4ab
4b,2a
ab
8 OF
60°
N
1ab
qv-1'
cpy, Py
1ab
70°

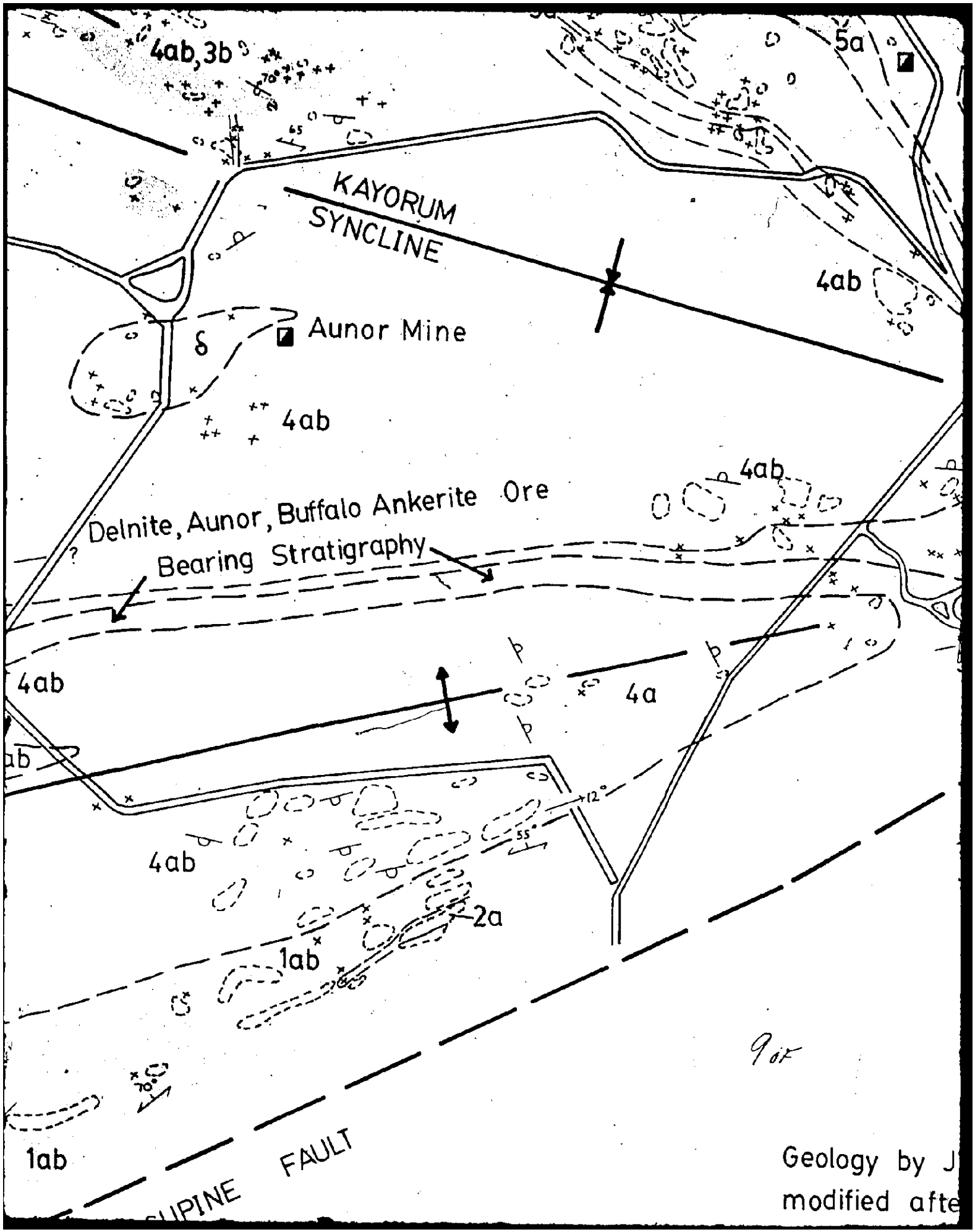
4ab, 3b
5a
KAYORUM
SYNCLINE
4ab
Aunor Mine
δ
4ab
4ab
Delnite, Aunor, Buffalo Ankerite Ore
Bearing Stratigraphy
4ab
4a
ab
12°
55°
4ab
2a
1ab
1ab
FAULT
Geology by J
modified afte

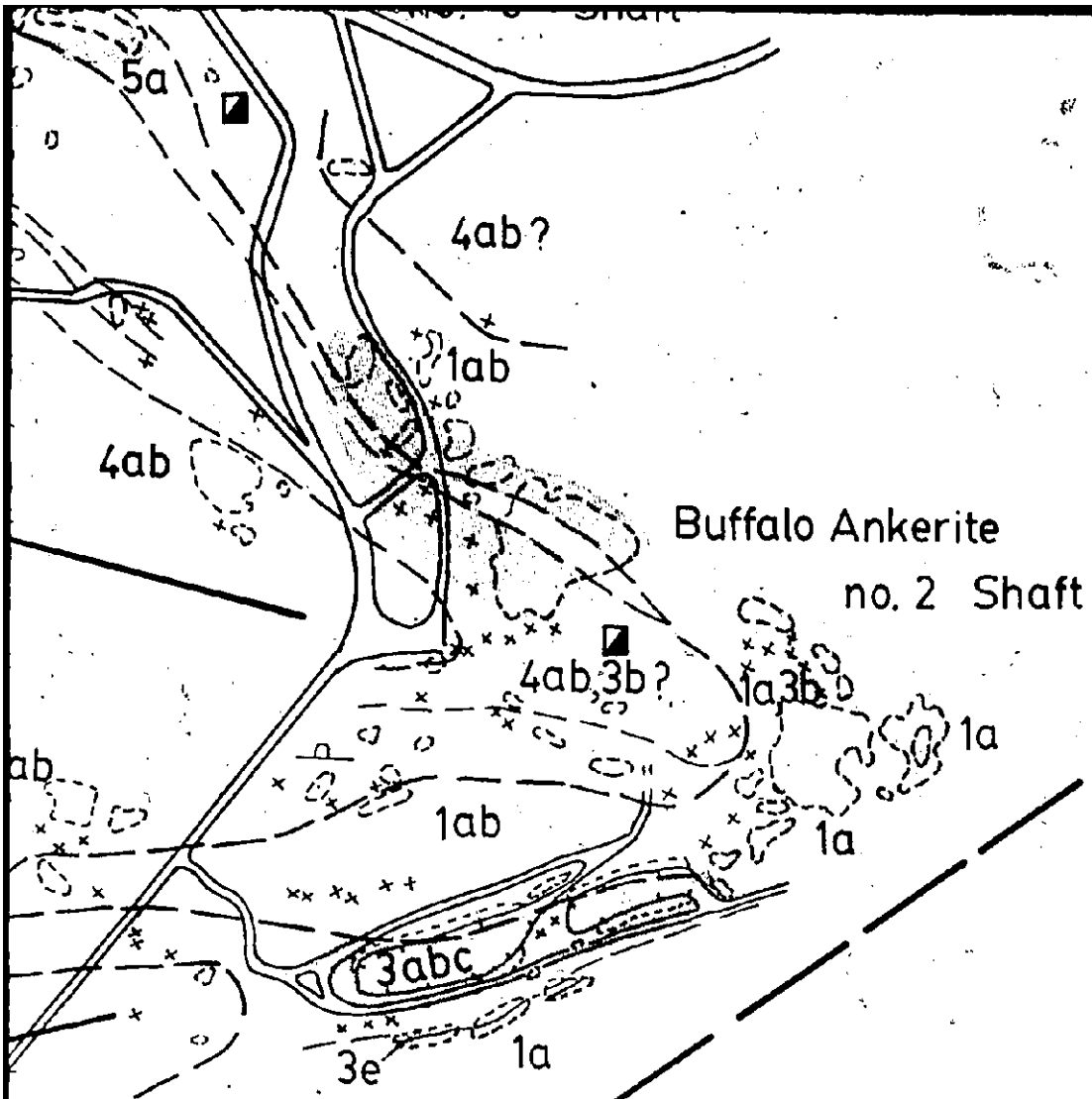

Geology by J A Fyon 1977-78
modified after Ferguson (1958 ab)

10 of

py,cpy Pyrite, chalcopyrite
V.G. Visible gold

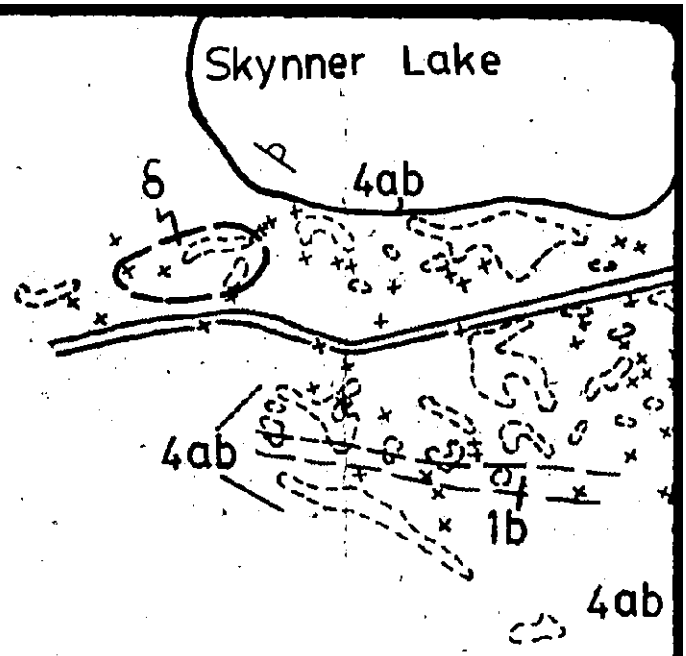

0 161 322 483 m
0 528 1056 1584 ft

McBine

Upper Supergrou

Lower Su

11 of

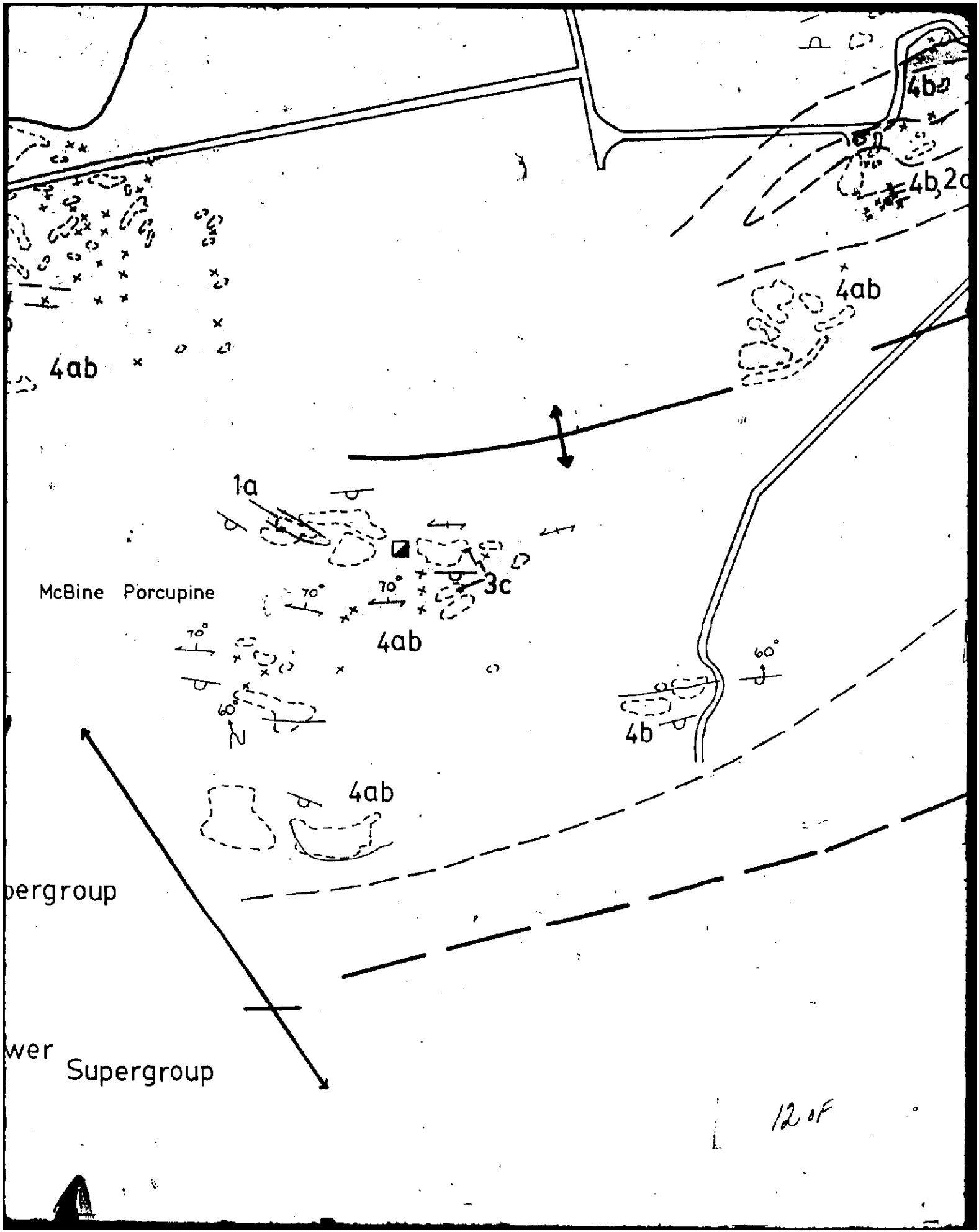
4b
4b,2c
4ab
4ab
1a
3c
McBine Porcupine
70°
70°
70°
60°
N
4ab
60°
4b
4ab
pergroup
wer
Supergroup
12 of

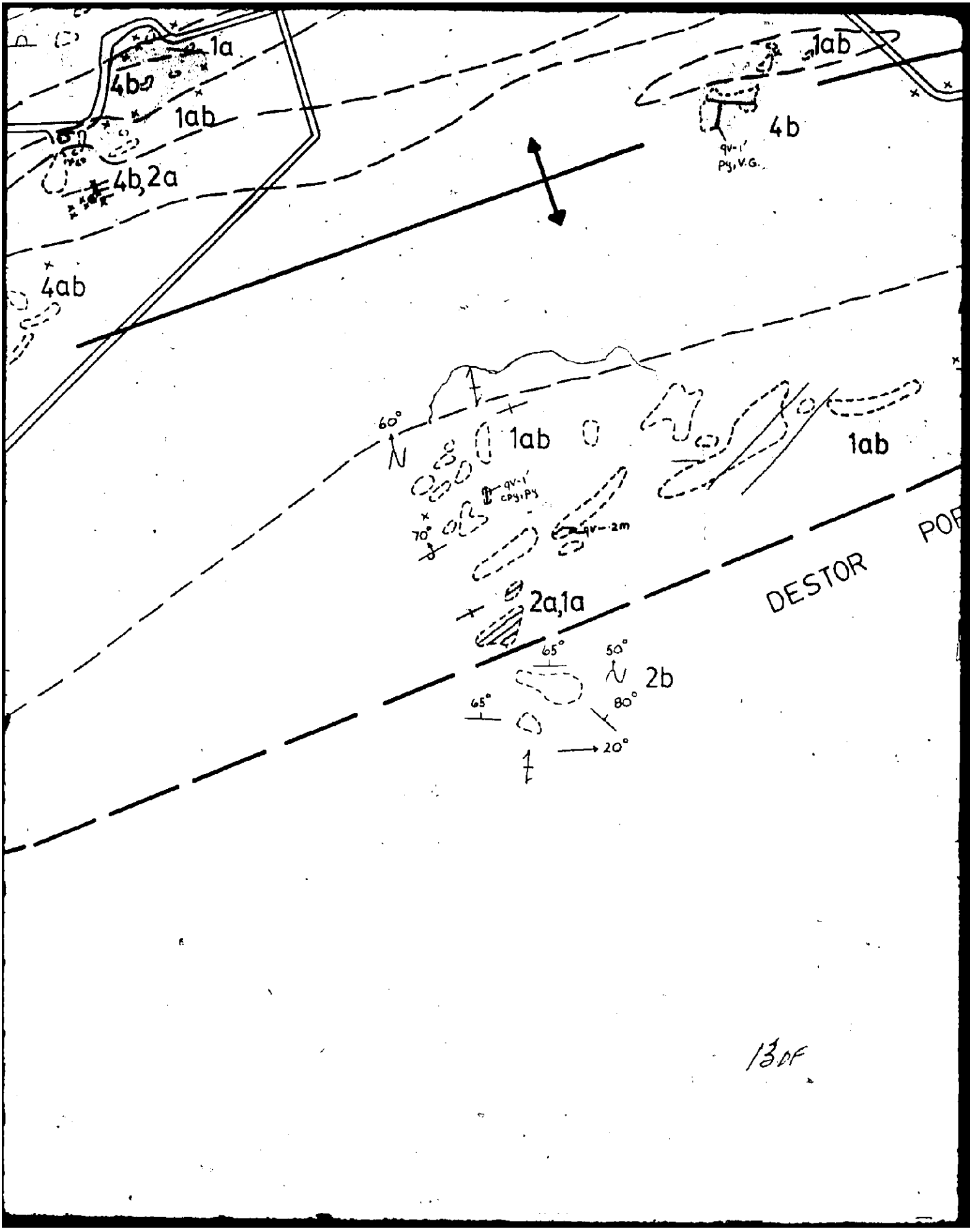
1a
4b
1ab
4b,2a
4ab
1ab
4b
qv-1'
Py, V.G.
60°
1ab
1ab
qv-1'
cPy, Py
70°
qv-2m
DESTOR
2a,1a
65°
50°
2b
65°
80°
20°

13 DF

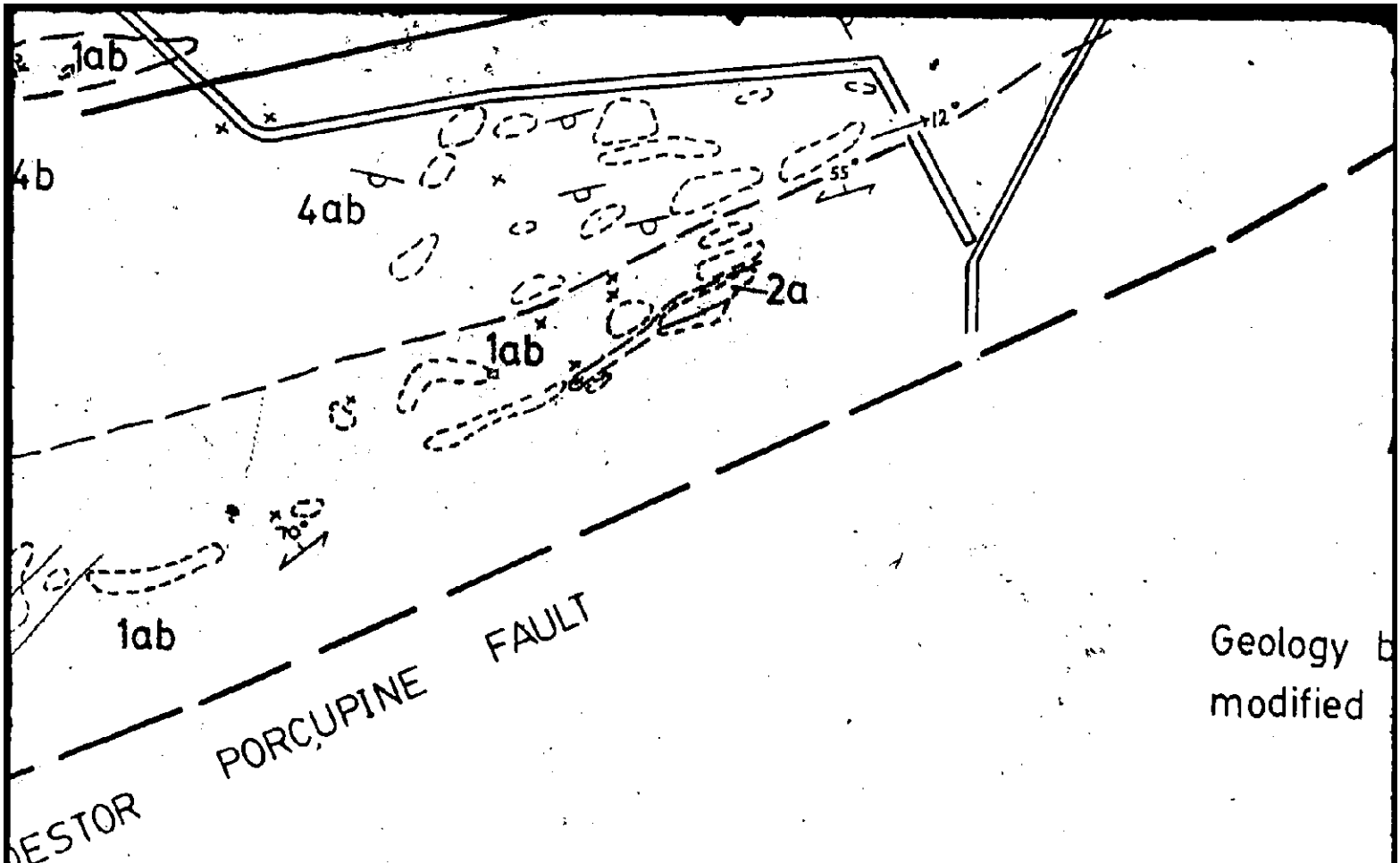

Geology b
modified

14 of

Geology by J A Fyon 1977-78
modified after Ferguson (1958 a,b)
Pyke (1975)

15 of 15

Lower Volcanic Domain
N
1a,b
2a,b
3a,b
1 of

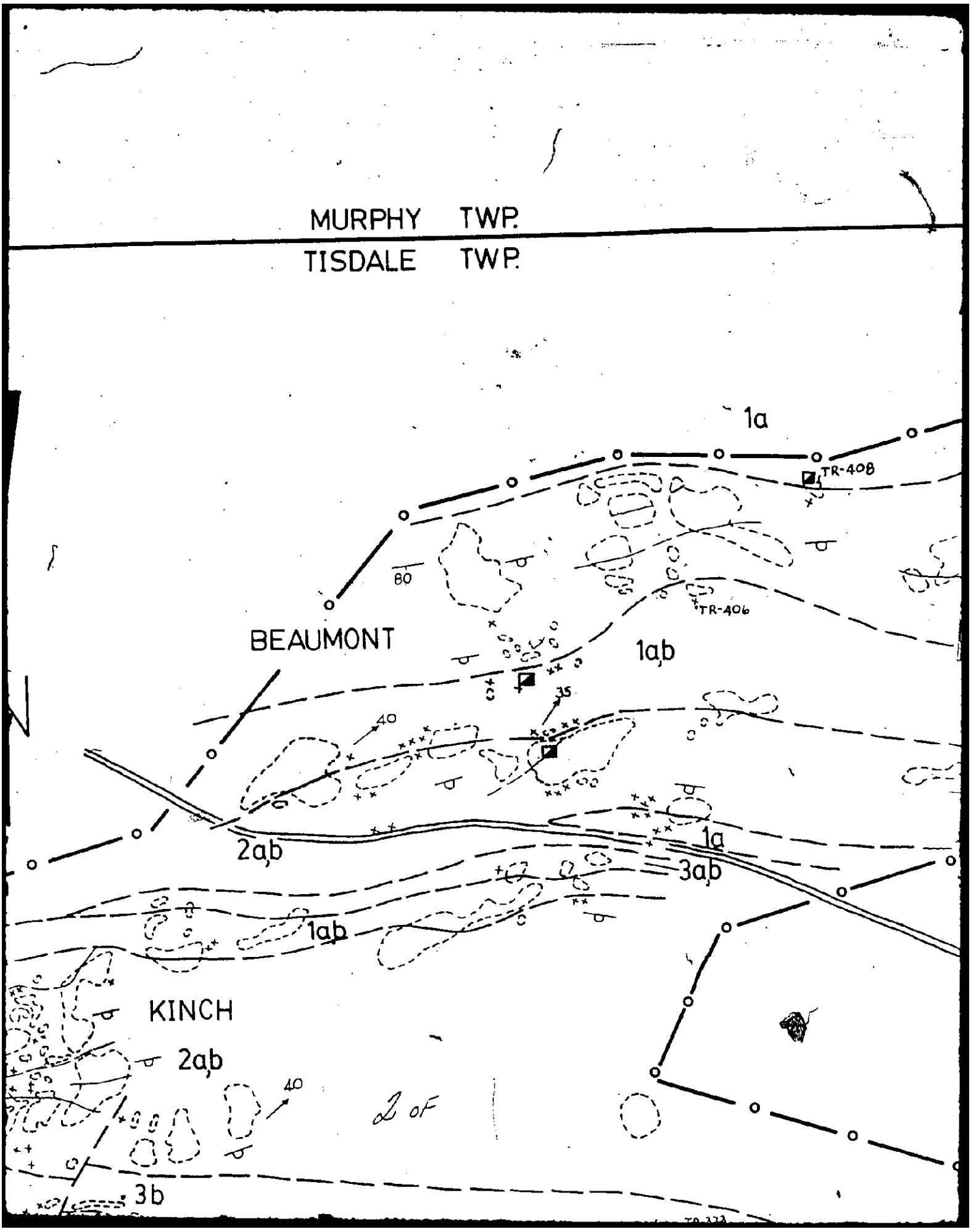
MURPHY TWP.
TISDALE TWP.
1a
TR-408
80
TR-406
BEAUMONT
1a,b
35
40
2a,b
1a
3a,b
1a,b
KINCH
2a,b
40
2 of
3b

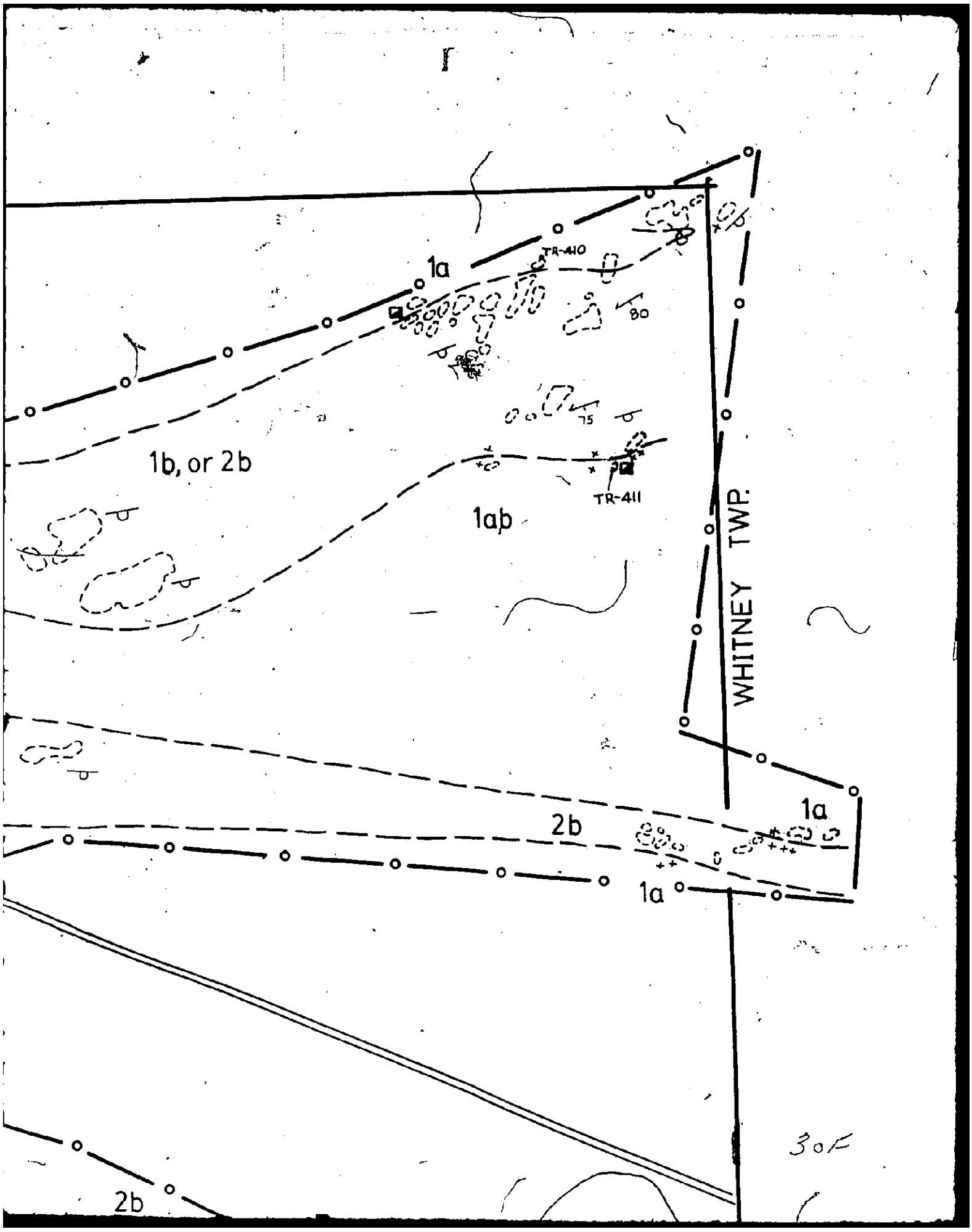
1a
TR-410
80
75
1b, or 2b
TR-411
1ab
WHITNEY TWP.
1a
2b
1a
2b
30F

Map 2

REGIONAL GEOLOGY TISDALE TOWNSHIP STUDY AREA

LEGEND

4 Turbidite Metasediments
- a Argillite

3 Iron Tholeiitic Metavolcanics
- a Massive
- b Pillowed

2 Magnesium Tholeiitic Metavolcanics
- a Massive
- b Pillowed
- c Flow top breccia

1 Komatiitic Metavolcanics
- a Ultramafic
- b Mafic

 Pillow attitude

 Foliation

 Bedding

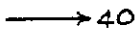 Lineation

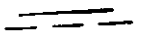 Flow contact

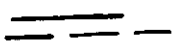 Flow unit contact

 Fault

4 of

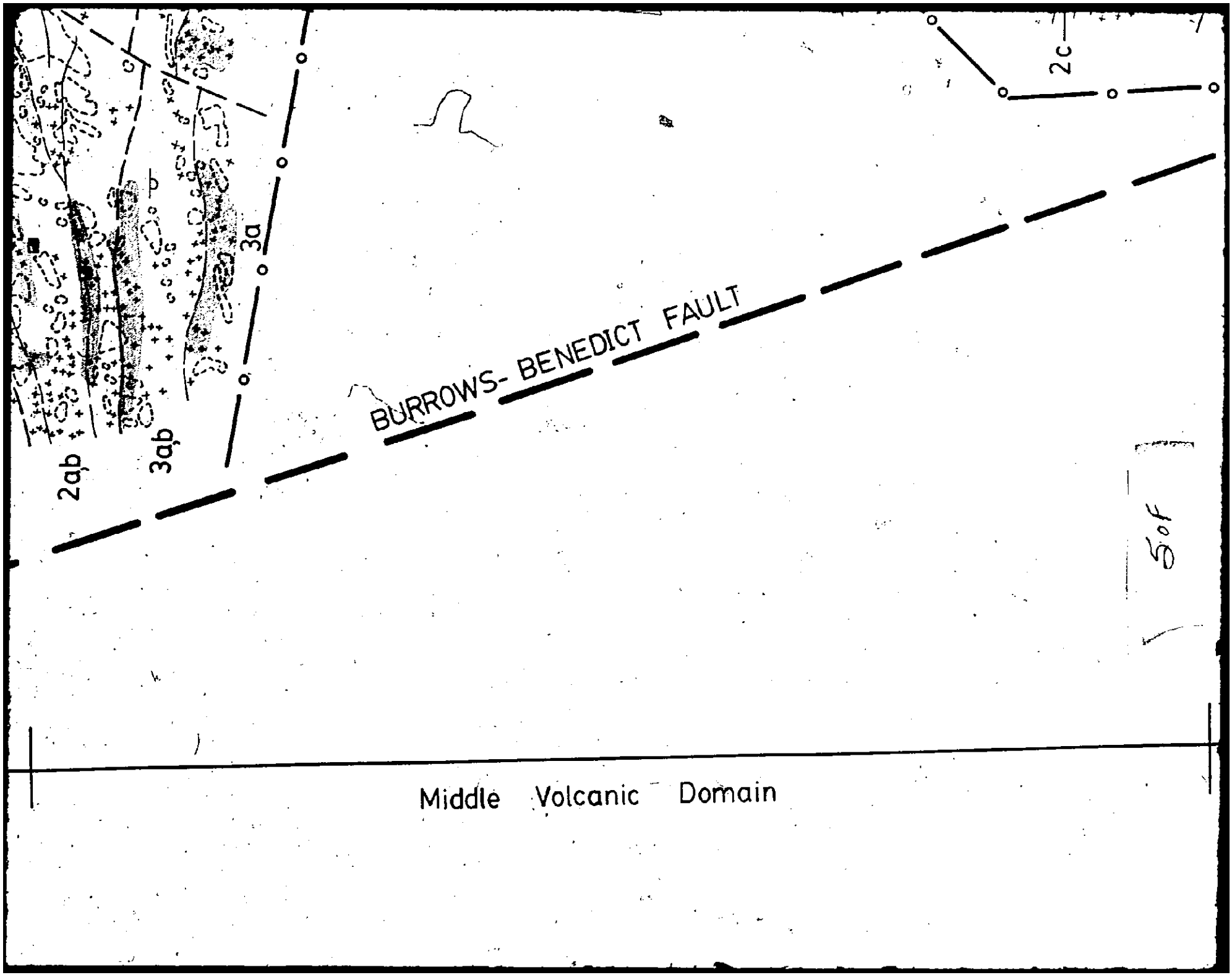
2c
3a
BURROWS- BENEDICT FAULT
2ab
3ab
Middle Volcanic Domain

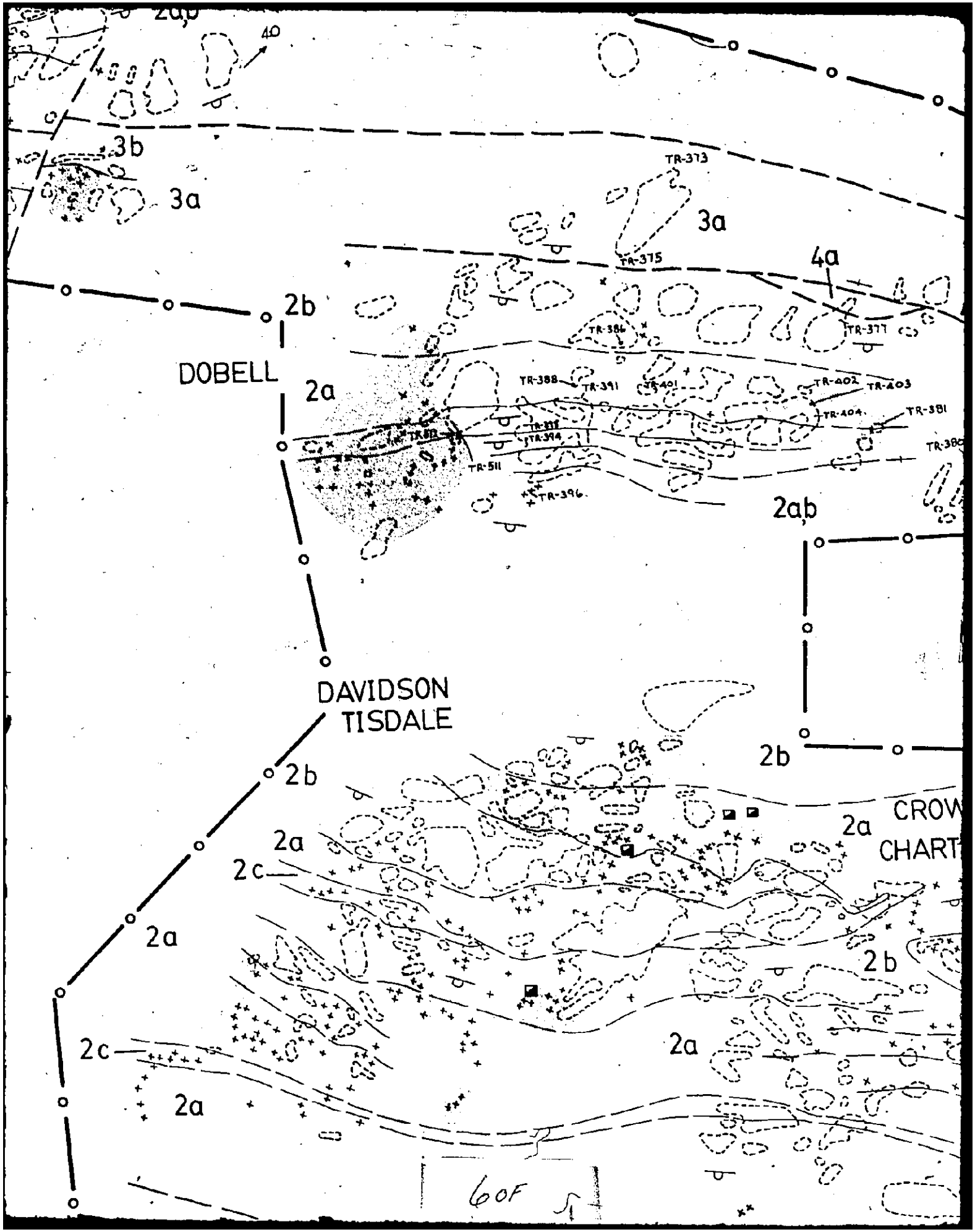
2a,b
40
3b
3a
TR-373
3a
TR-375
4a
2b
TR-384
TR-377
DOBELL
2a
TR-388
TR-391
TR-401
TR-402
TR-403
TR-404
TR-381
TR-511
TR-396
2a,b
DAVIDSON
TISDALE
2b
2b
2a
CROW
CHART
2c
2a
2b
2c
2a
2a
60F

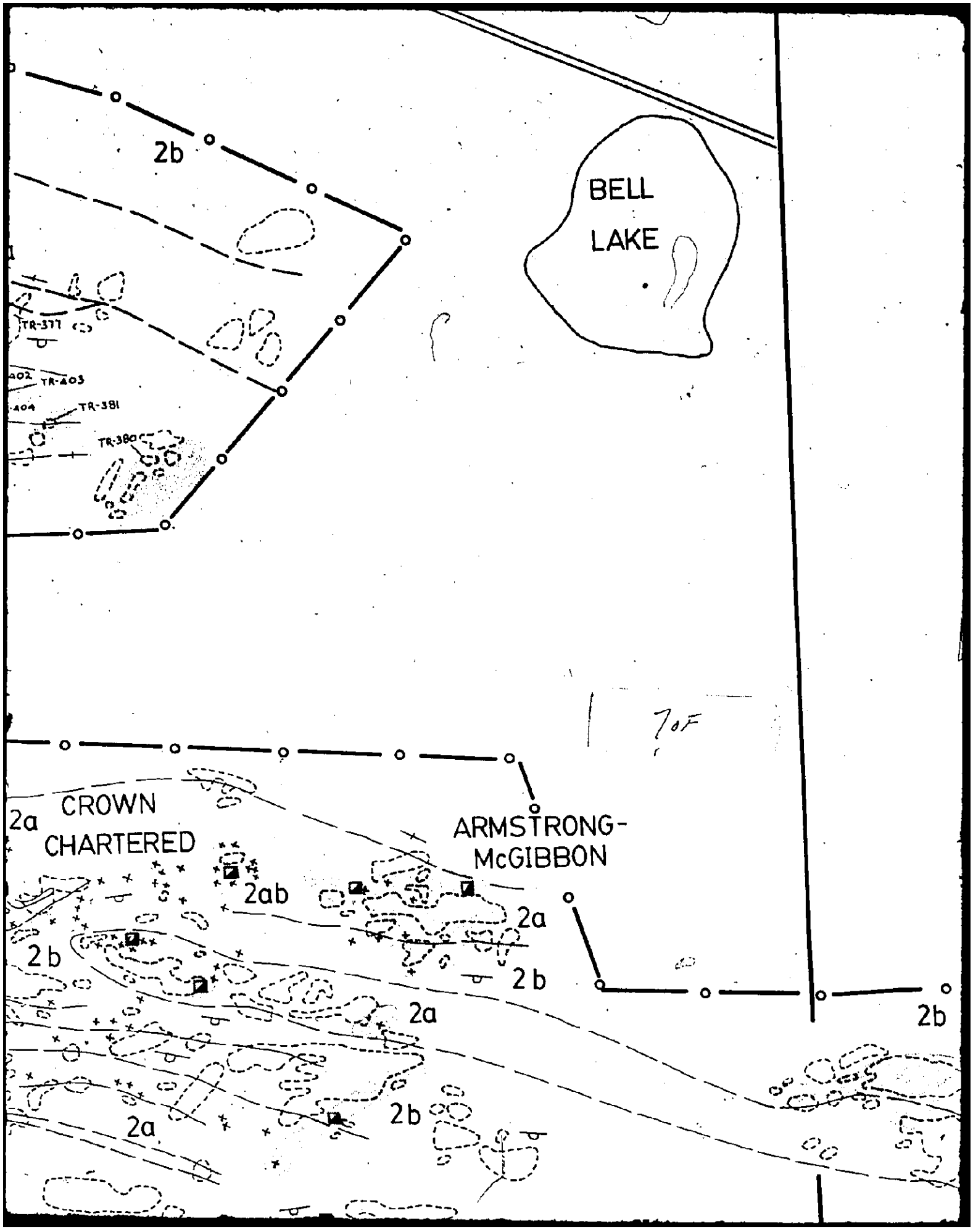
2b
BELL
LAKE
TR-377
TR-403
TR-381
TR-380
7 of
2a
CROWN
CHARTERED
ARMSTRONG-
McGIBBON
2ab
2a
2b
2b
2a
2b
2a
2b

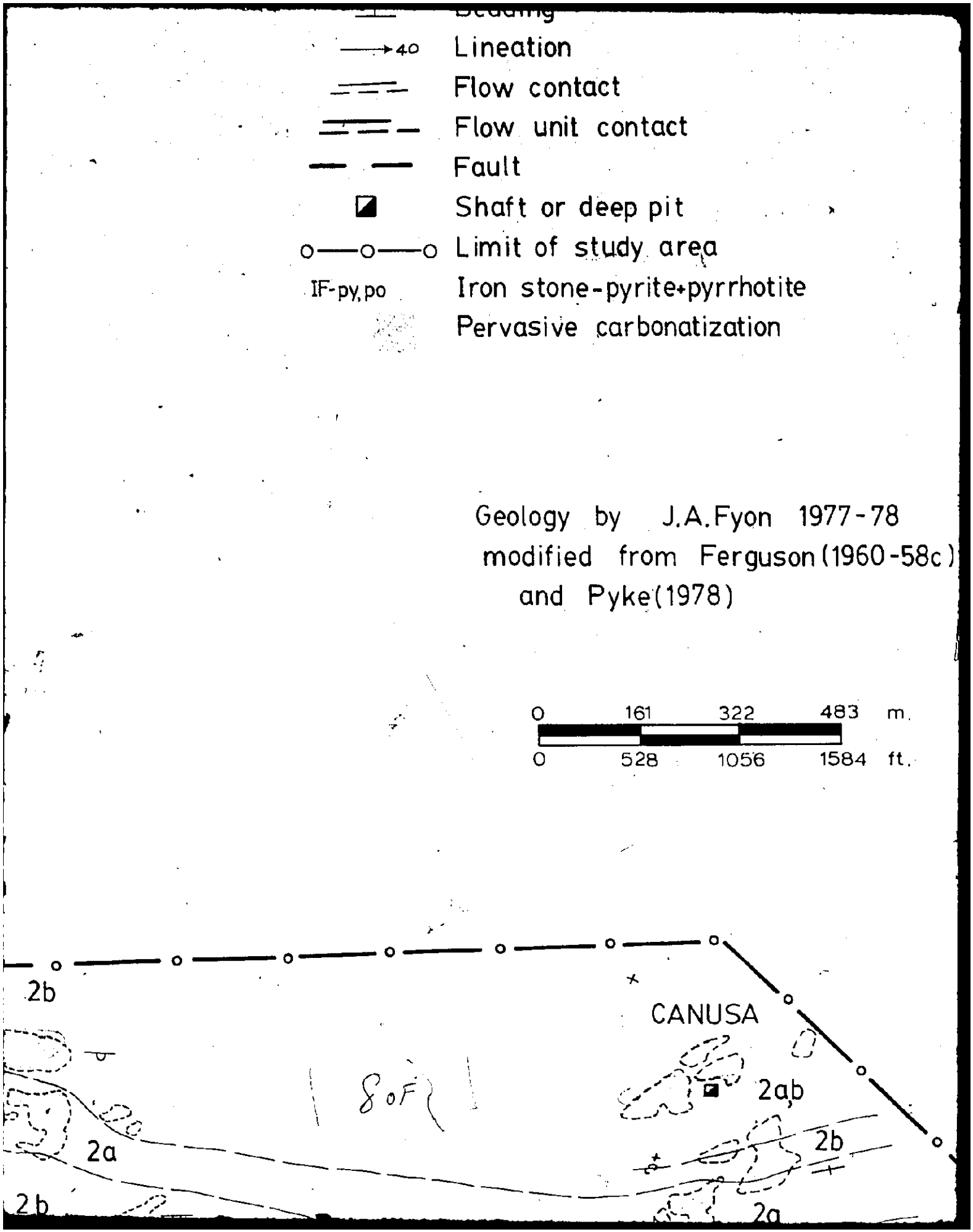
Bedding
40
Lineation
Flow contact
Flow unit contact
Fault
Shaft or deep pit
Limit of study area
IF-py,po
Iron stone-pyrite+pyrrhotite
Pervasive carbonatization
Geology by J.A.Fyon 1977-78
modified from Ferguson (1960-58c)
and Pyke (1978)
0 161 322 483 m.
0 528 1056 1584 ft.
2b
CANUSA
2a,b
2b
2a
2b
2a

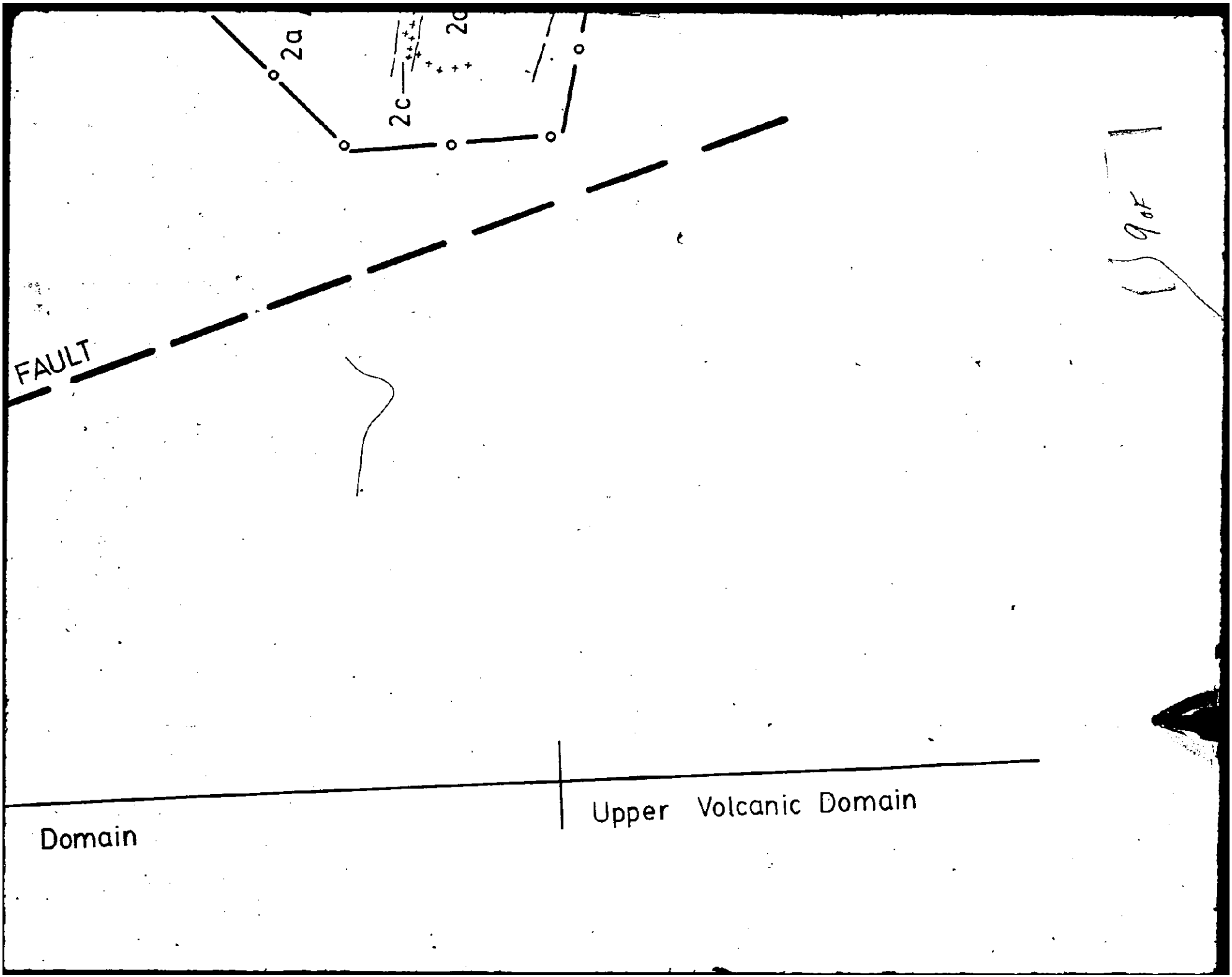
2a
2c
FAULT
Upper Volcanic Domain
Domain

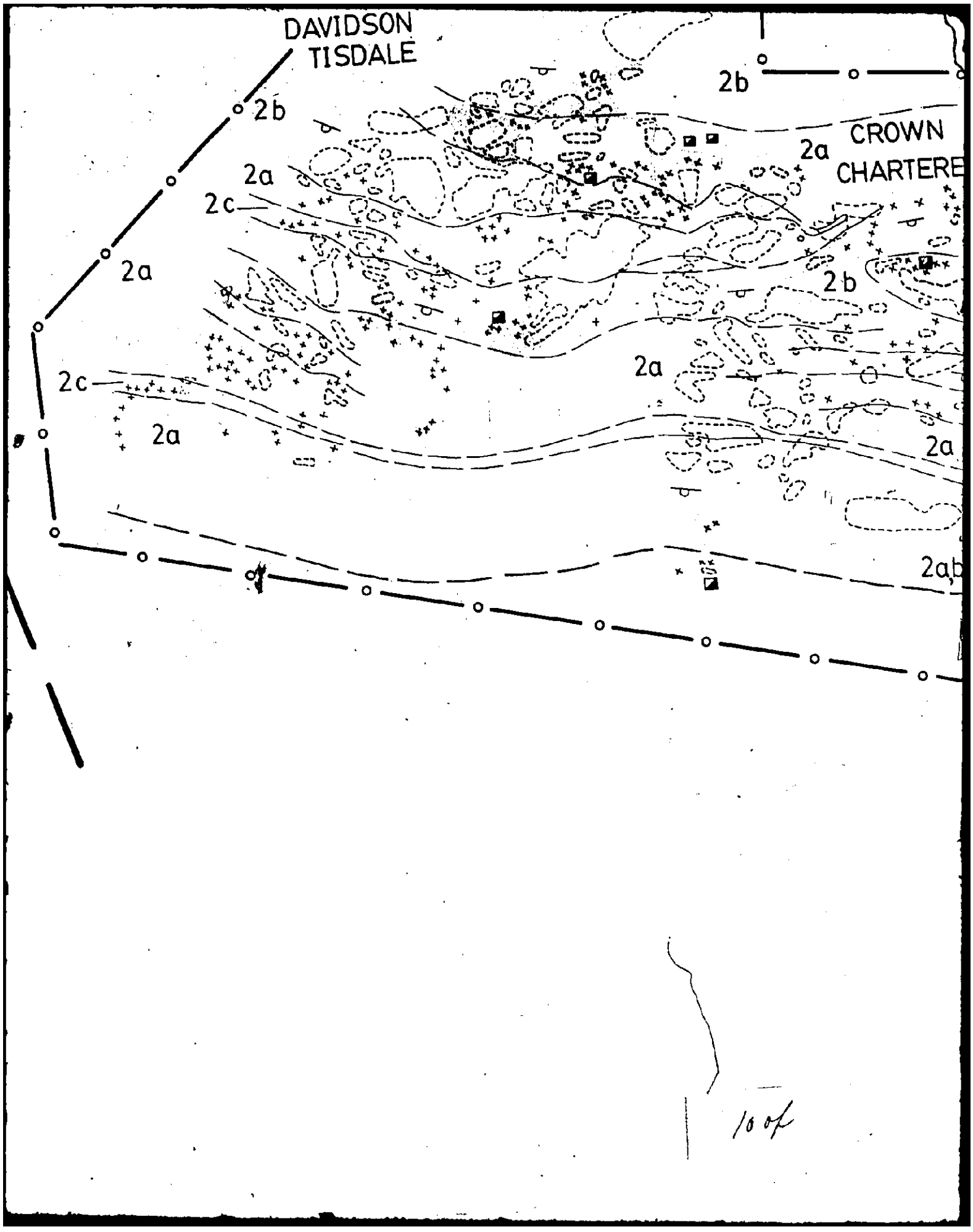
DAVIDSON
TISDALE
2b
2a
2c
2a
2c
2a
2b
2a
CROWN
CHARTERE
2a
2b
2a
2a
2a,b

10 of

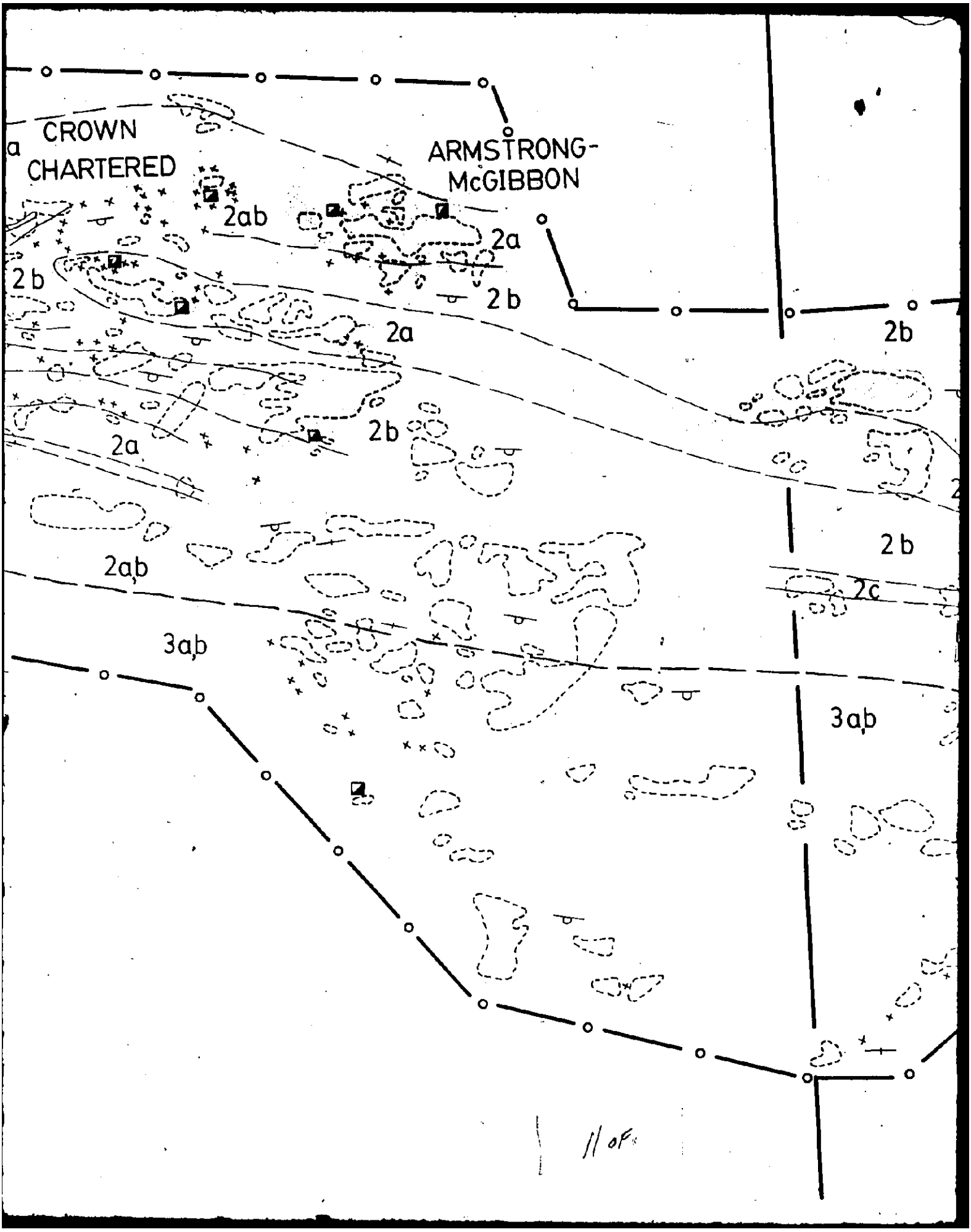
CROWN
CHARTERED
ARMSTRONG-
McGIBBON
2ab
2a
2b
2b
2a
2b
2b
2a
2ab
2b
2c
3ab
3ab

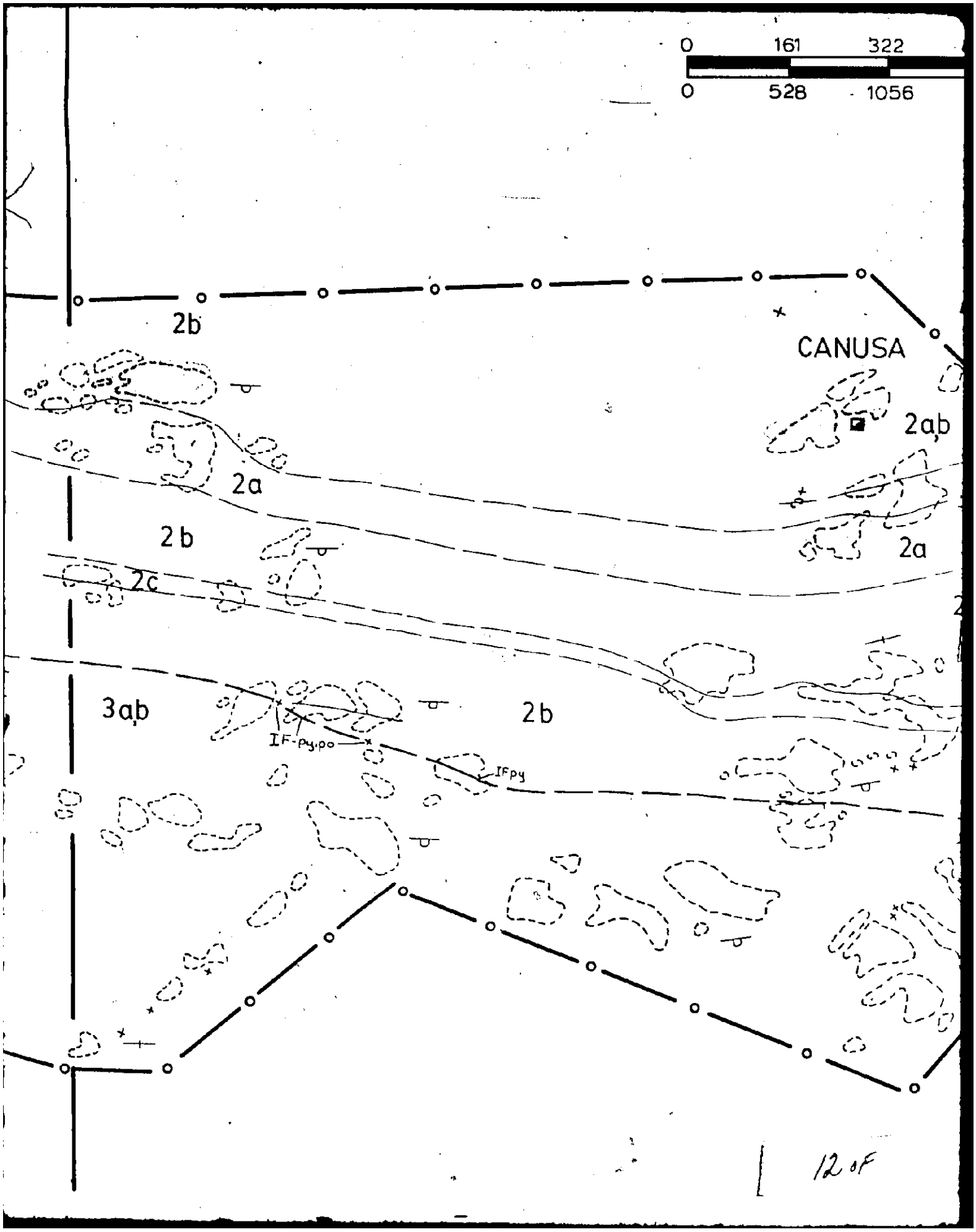
0 161 322
0 528 1056
2b
CANUSA
2a,b
2a
2b
2a
2c
3a,b
2b
IF-Py,po
IFpy
12 of

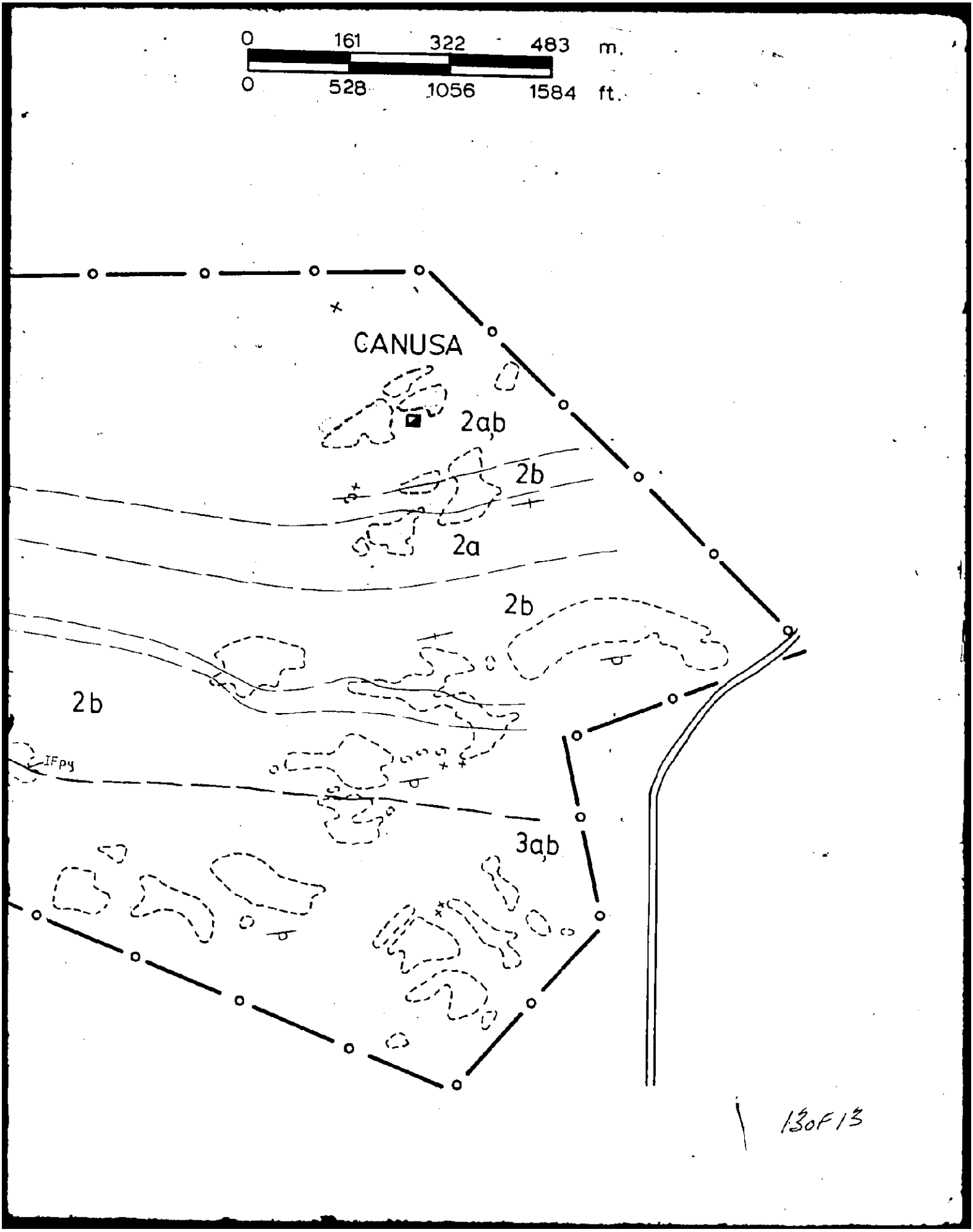

13 OF 13

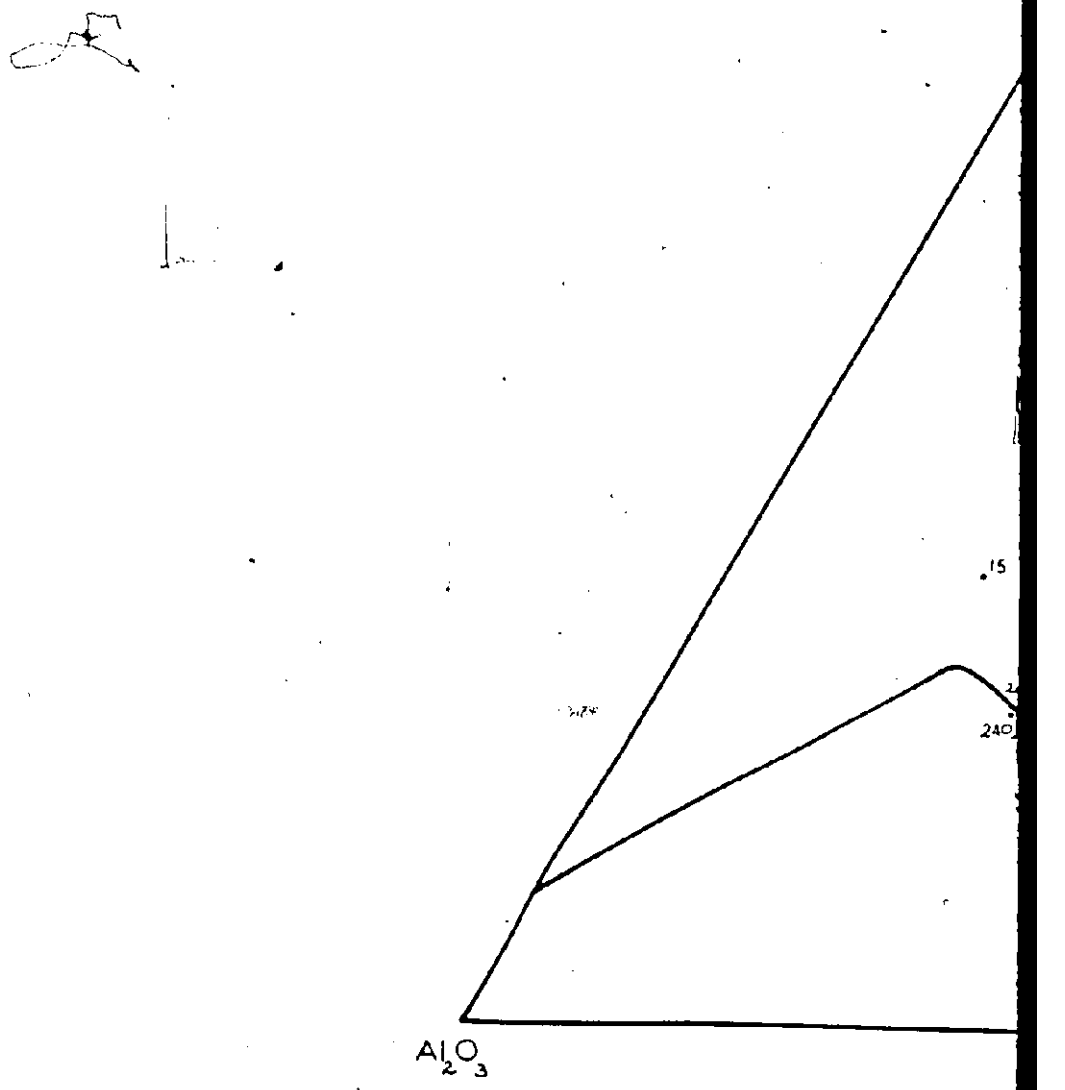

1 of

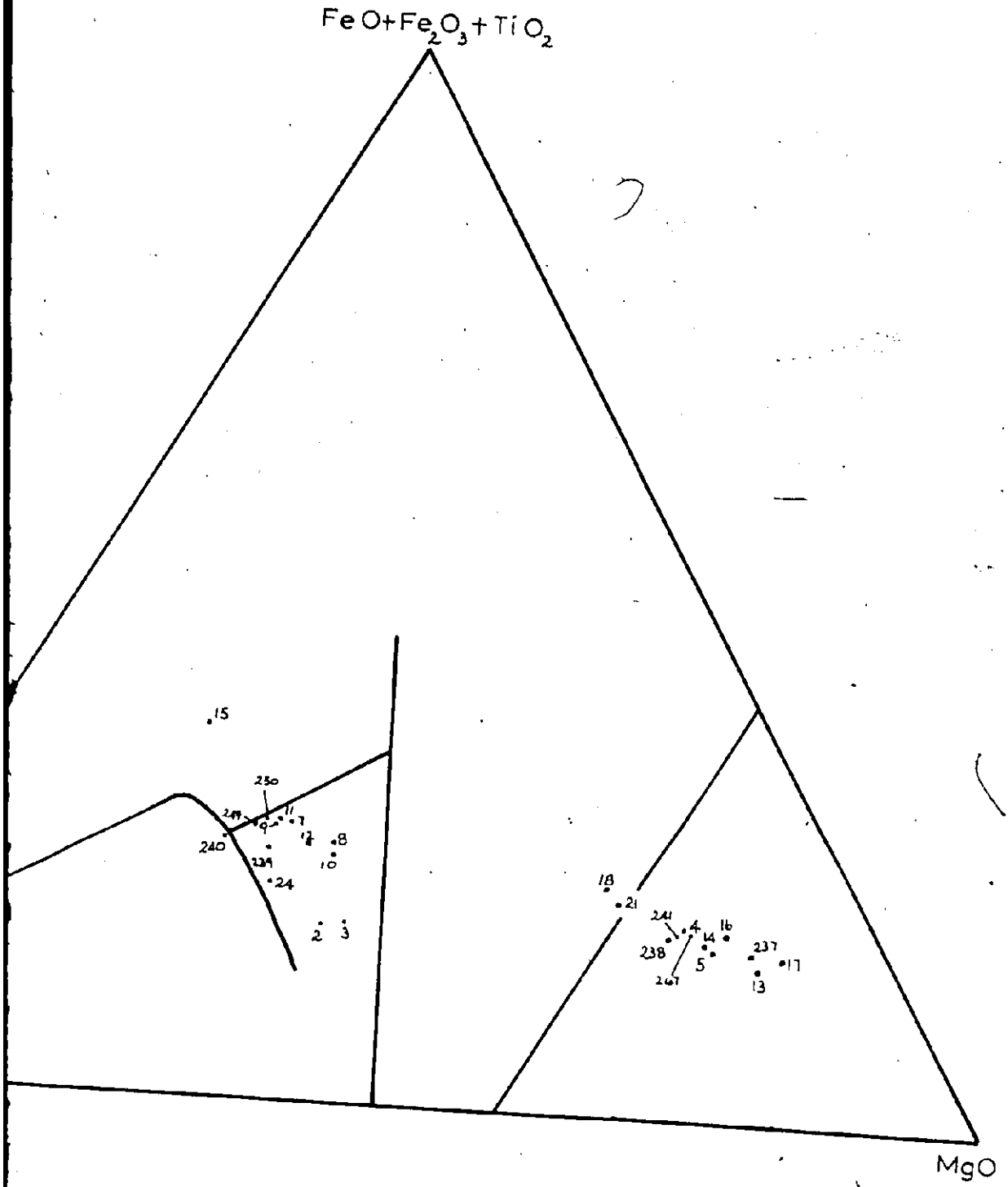
FeO+Fe2O3+TiO2
MgO
15
250
241
11
9
7
12
8
240
239
10
24
2
3
18
21
241
4
16
14
238
5
237
17
240
13

2 of

A D.

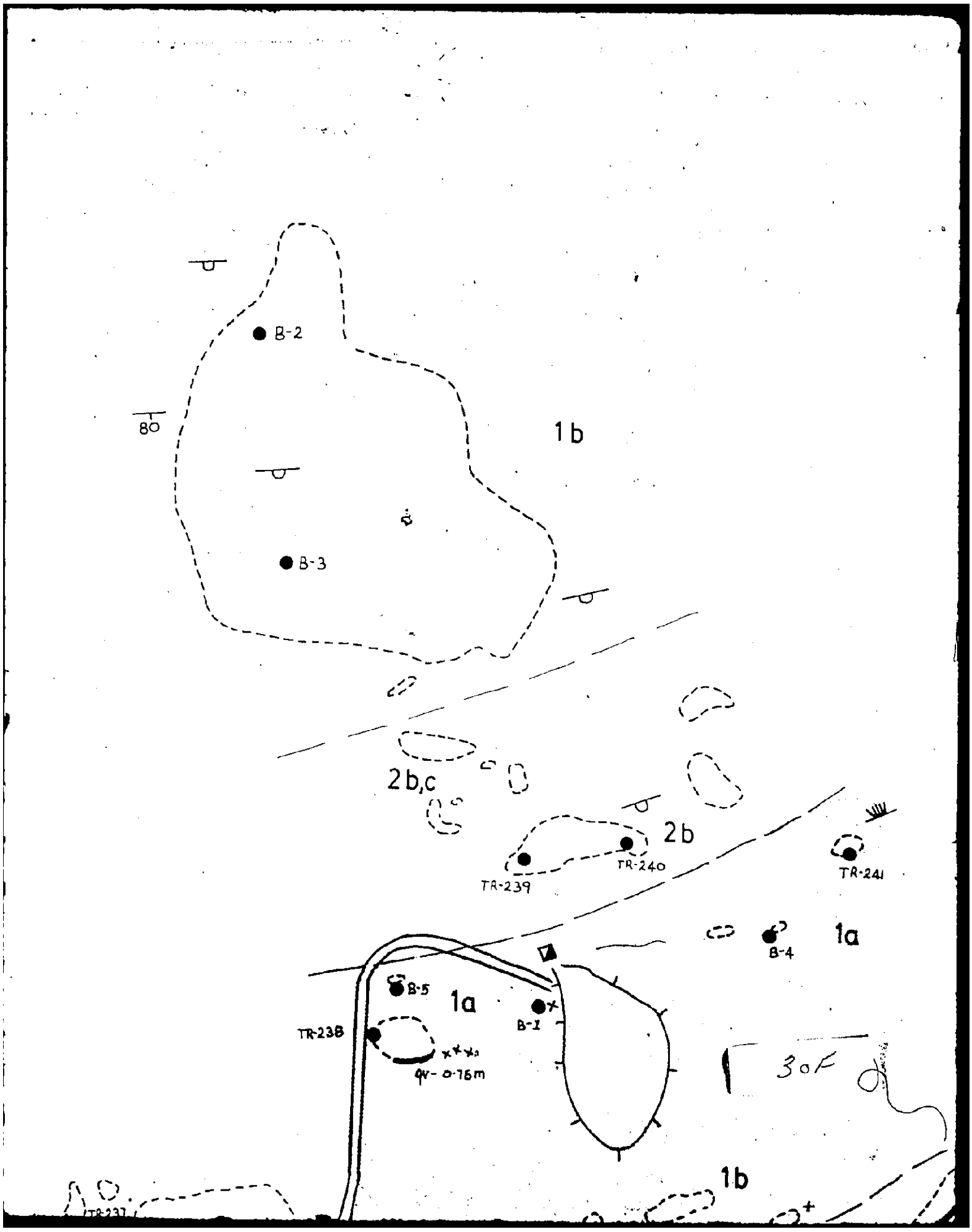
B-2
80
1b
B-3
2b,c
2b
TR-239
TR-240
TR-241
1a
B-4
B-5
1a
B-1
TR-238
qv- 0.76m
3 of
1b
TR-237

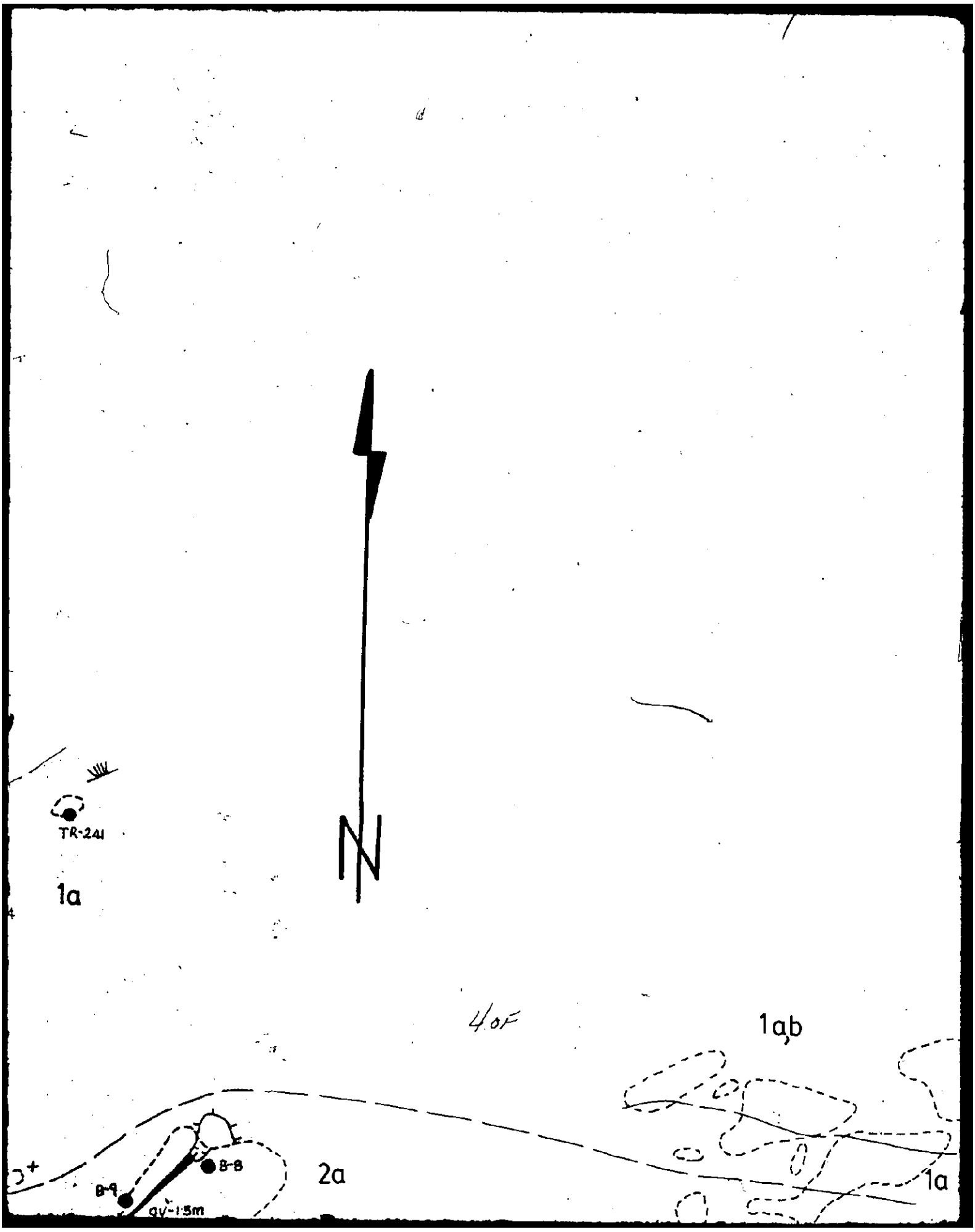
TR-241
1a
4 of
1a,b
B-8
B-9
av-1.5m
2a
1a

Map 3

BEAUMONT MINE AREA
TISDALE TWP. STUDY AREA

LEGEND

3 Iron Tholeiitic Metavolcanics
- a Massive
- b Pillowed

2 Magnesium Tholeiitic Metavolcanics
- a Massive
- b Pillowed
- c Microvariolitic

1 Komatiitic Metavolcanics
- a Ultramafic
- b Mafic

- Pillow attitude
- Bedding attitude
- Foliation
- Geological contact
- Spinifex, bar to top
- Sample location
- Pit
- Dump
- Shaft
- Pervasive carbonatization
- Intraflow facies contact

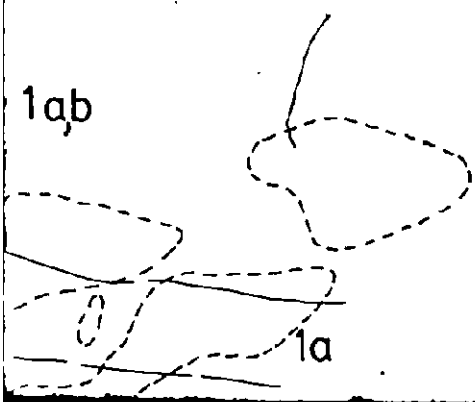

5 of

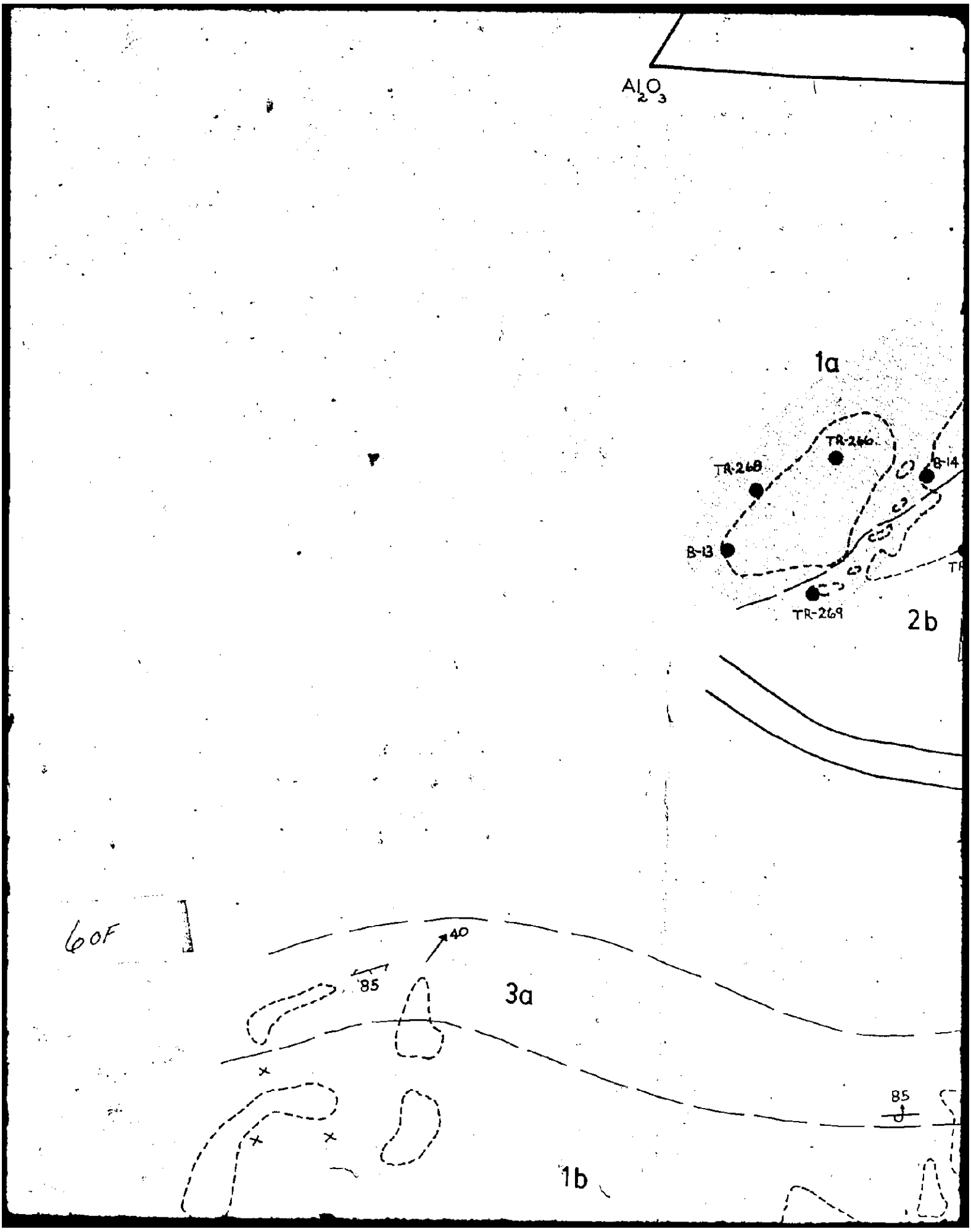
Al_2O_3
1a
TR-266
TR-268
B-14
B-13
TR-269
2b
60F
40
85
3a
85
1b

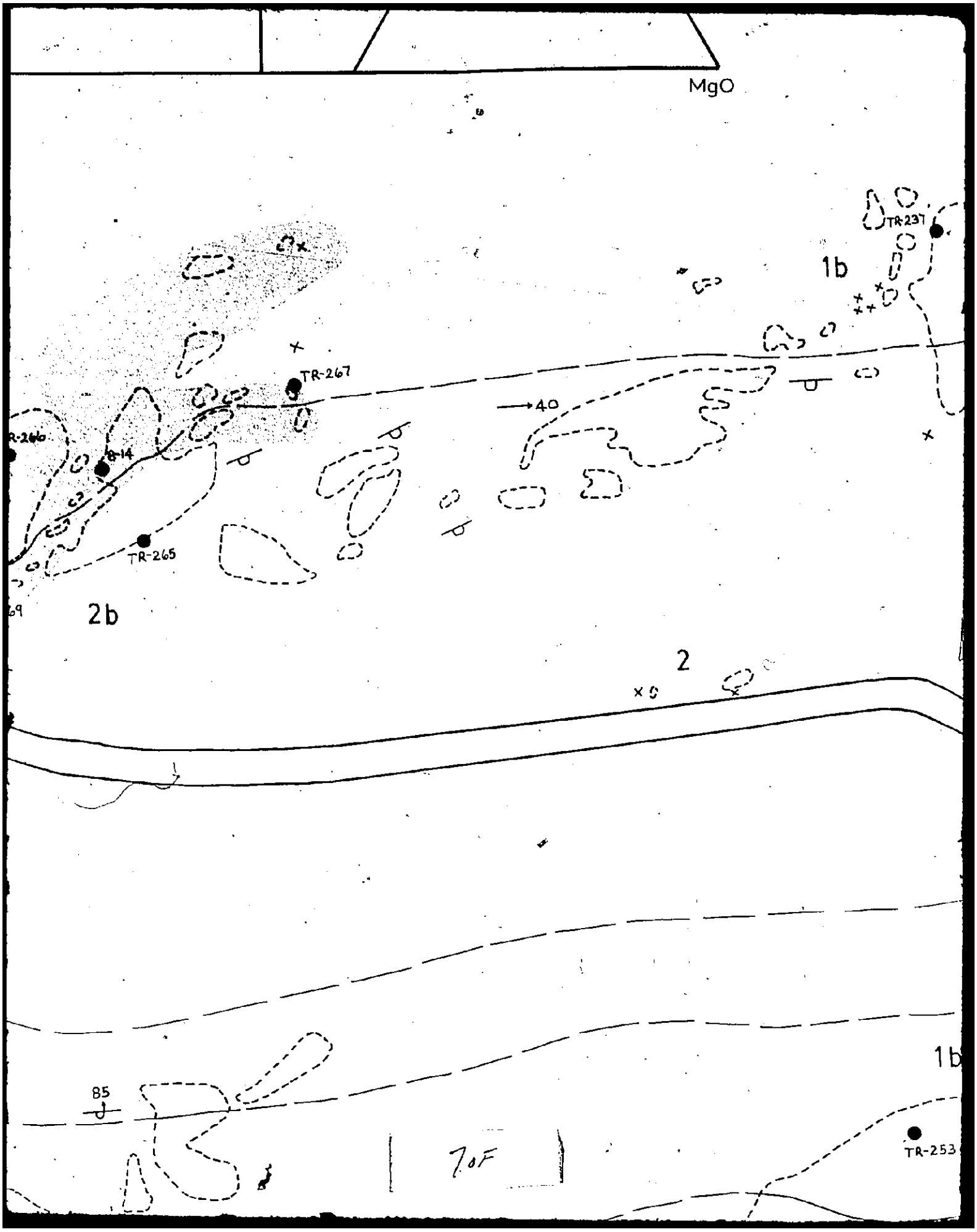
MgO
TR-237
1b
TR-267
40
TR-266
B-14
TR-265
2b
2
1b
85
TR-253
7 of

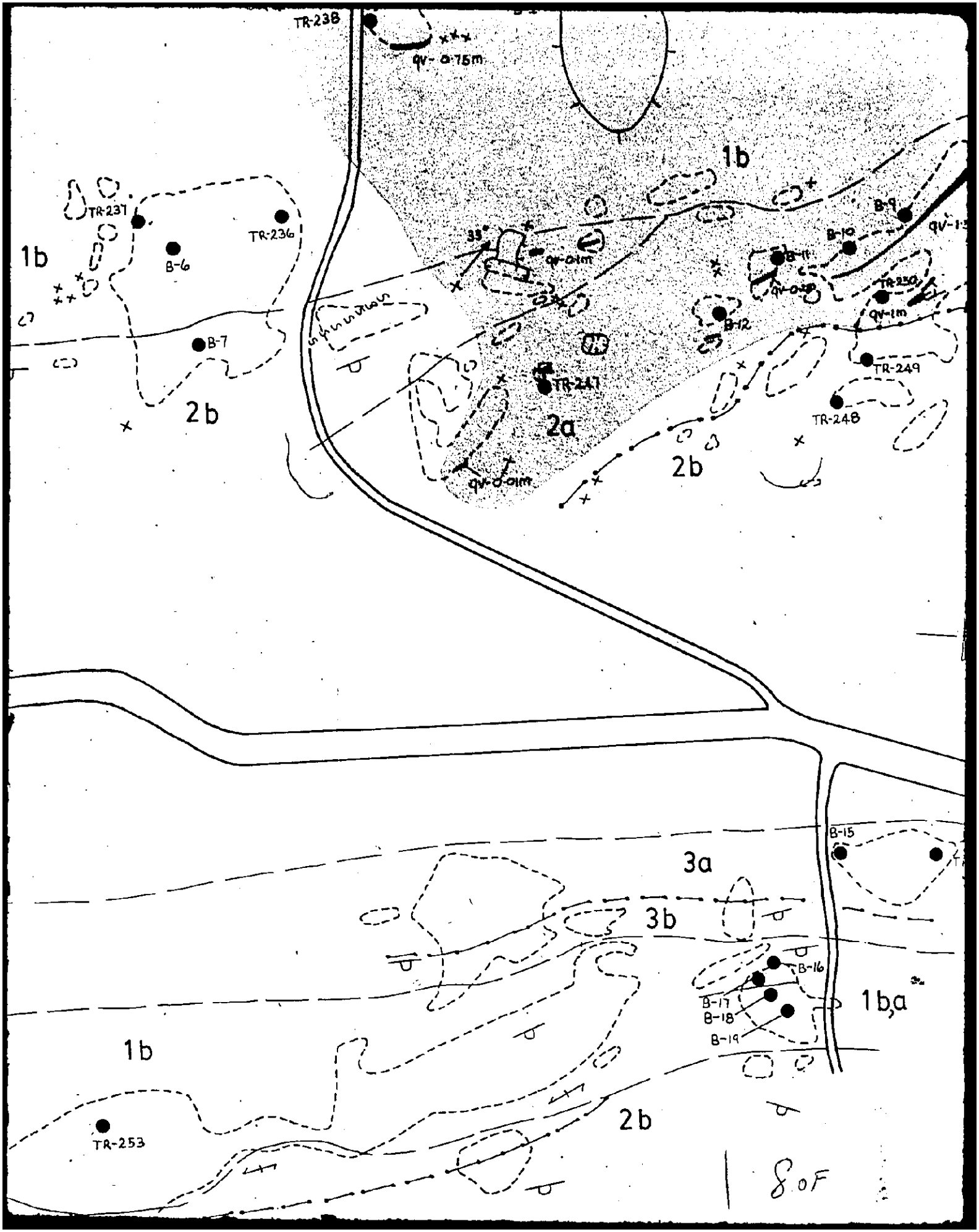
TR-238
qv- o·75m
1b
TR-237
TR-236
B-6
B-7
2b
35°
qv-o·1m
B-9
B-10
B-11
qv-o·1m
TR-250
qv-1m
B-12
TR-249
TR-247
2a
TR-248
qv-o·1m
2b
B-15
3a
3b
B-16
B-17
B-18
B-19
1b,a
1b
TR-253
2b
8 of

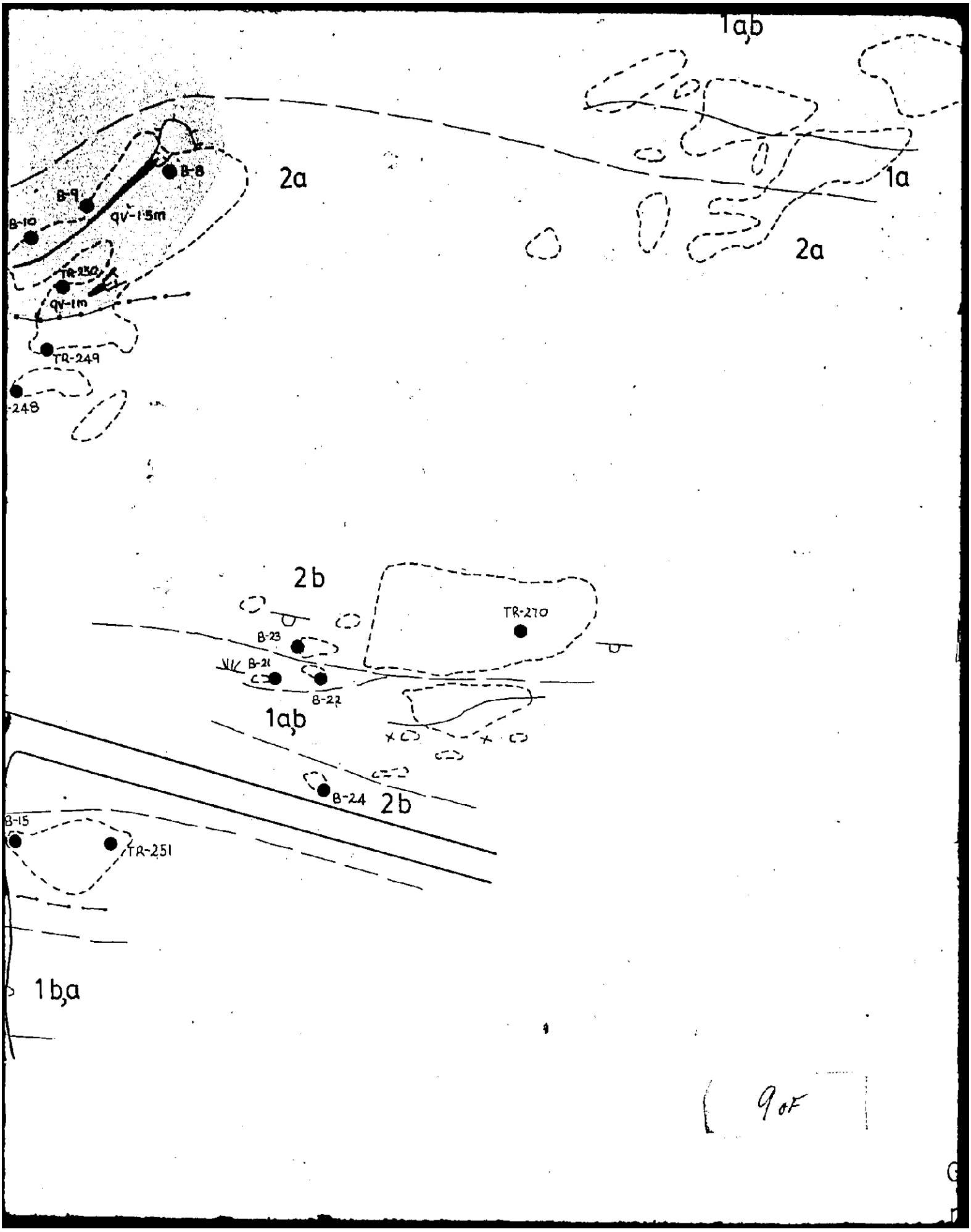
1a,b
1a
2a
2a
B-8
B-9
B-10
qv-1.5m
TR-250
qv-1m
TR-249
-248
2b
TR-270
B-23
B-21
B-22
1a,b
B-24
2b
B-15
TR-251
1b,a

9 of

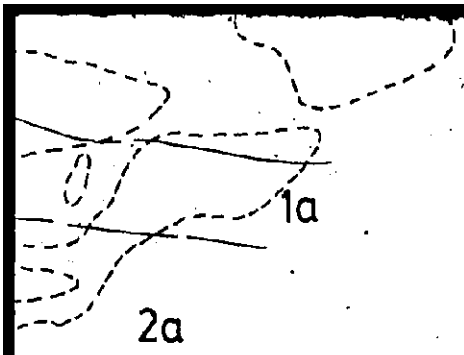

■ Shaft

Pervasive carbonatization

Intraflow facies contact

qv-1m Quartz vein-thickness

Lineation

Geology by J.A. Fyon 1978
modified after Ferguson (1960)
Pyke (pers. com., 1979)

10 of

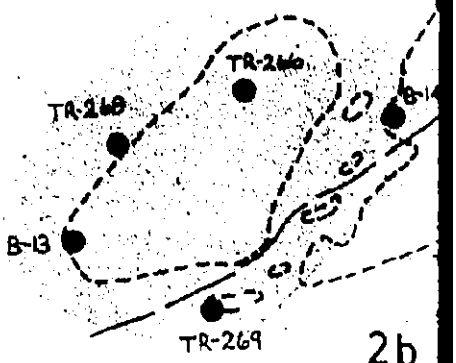

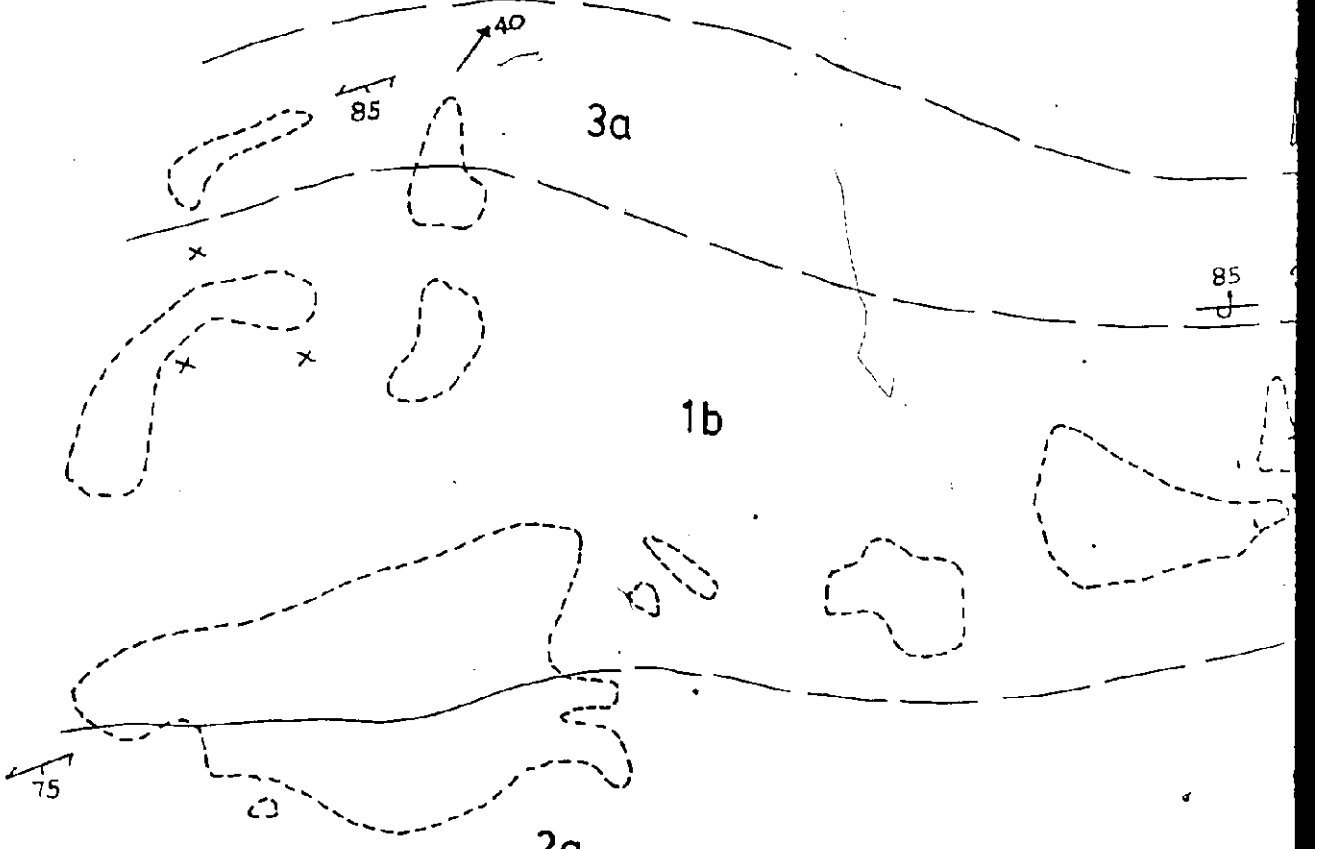

11 of

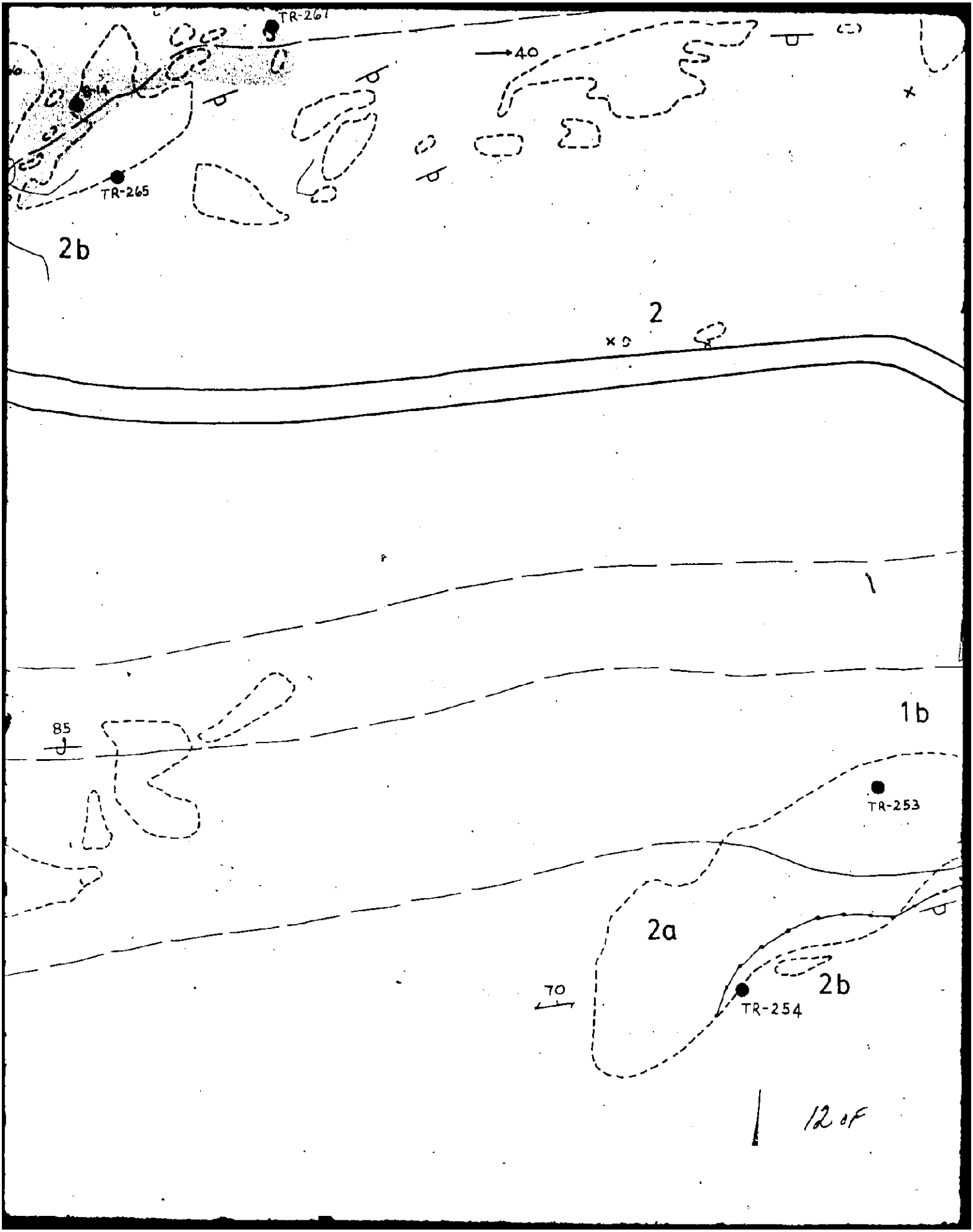

12 of

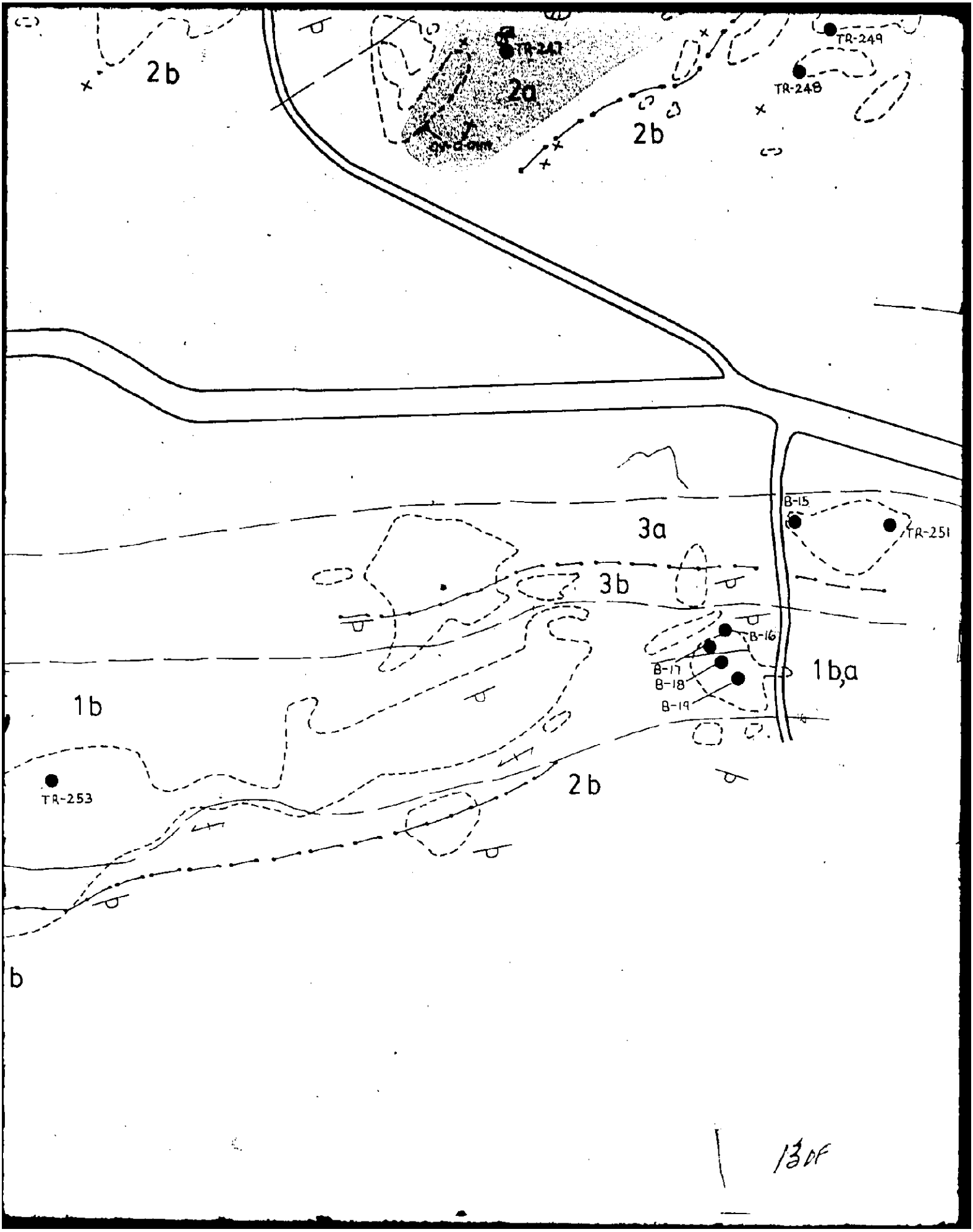
2b
TR-247
2a
TR-249
TR-248
2b
3a
B-15
TR-251
3b
B-16
B-17
B-18
B-19
1b,a
1b
TR-253
2b
b

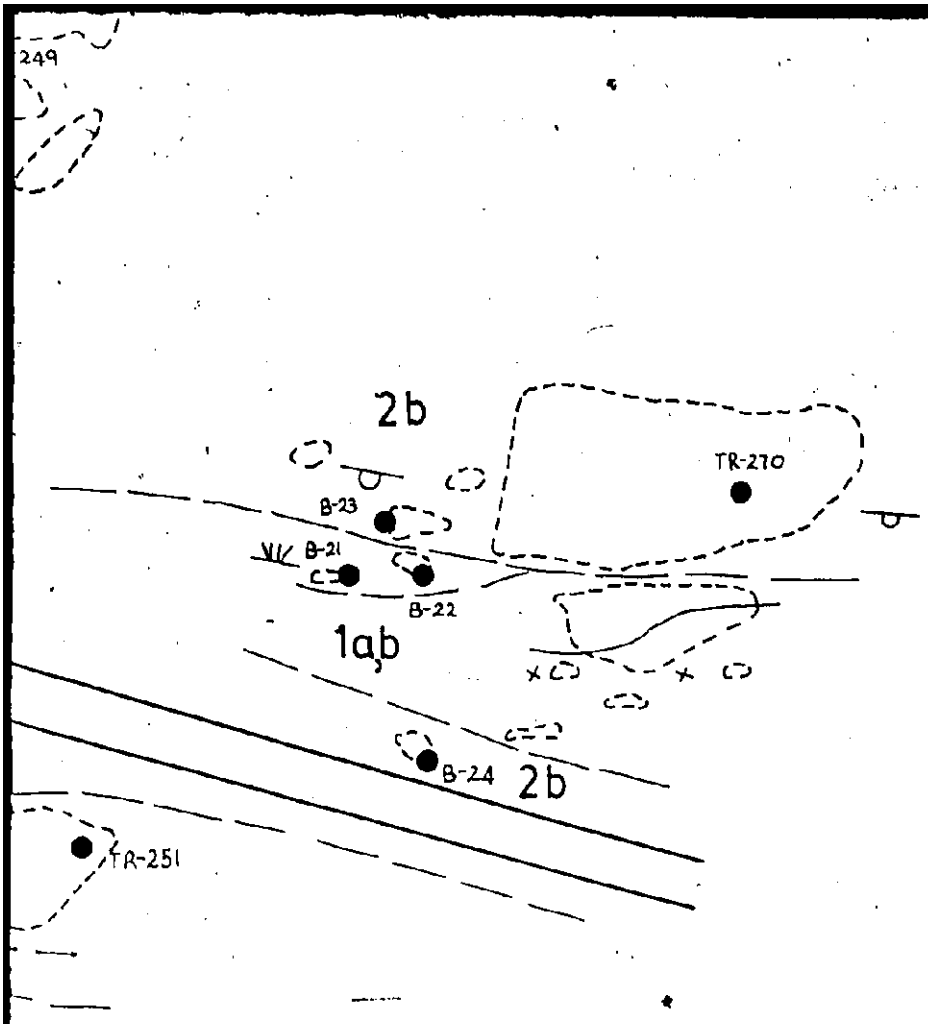

a

Geolo
modif

Geology by J.A. Fyon 1978
modified after Ferguson (1960)
Pyke (pers. com., 1979)

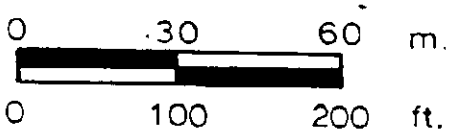

Map 4

KINCH PROPERTY
TISDALE TWP. STUDY AREA

LEGEND

3 Iron Tholeiitic Metavolcanics
- a Massive
- b Pillowed
- c Variolitic
- d Flow top breccia

2 Magnesium Tholeiitic Metavolcanics
- a Massive
- b Pillowed
- c Flow top breccia

1 Komatiitic Metavolcanics
- a Ultramafic
- b Mafic

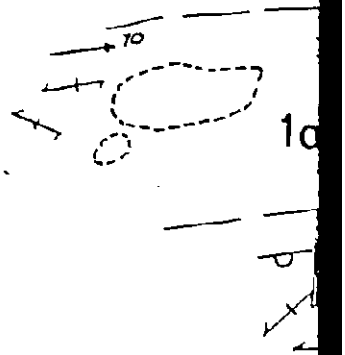

- Pillow attitude
- Bedding
- Foliation
- Lineation
- Joint attitude
- Flow contact
- Intraflow facies contact

1 of

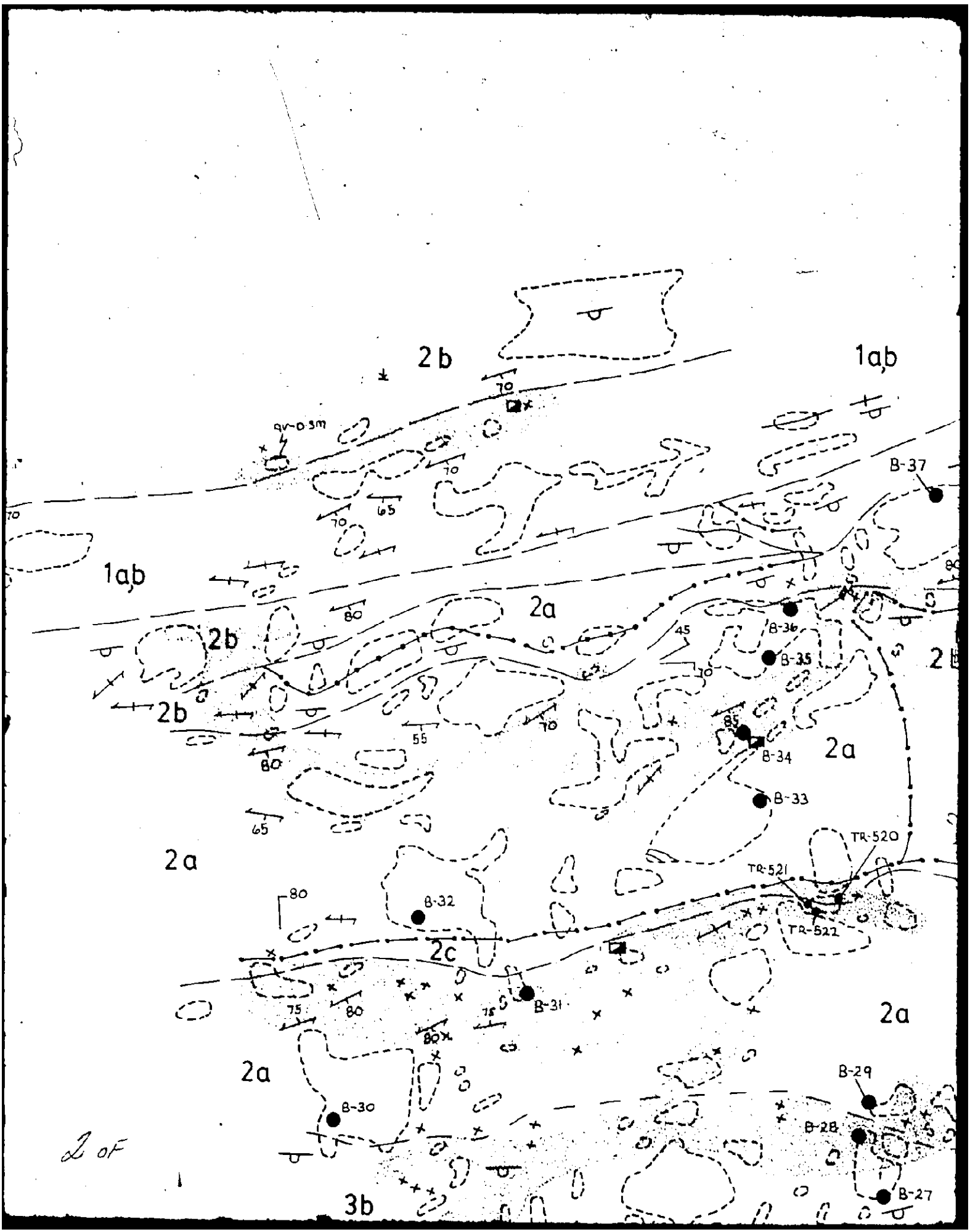
2b
1a,b
qv-0.3m
70
70
70
65
B-37
1a,b
80
2a
2b
45
B-36
B-35
2b
55
70
85
B-34
2a
80
B-33
65
2a
TR-520
TR-521
80
B-32
TR-522
2c
75
80
B-31
75
80
2a
2a
B-29
B-30
B-28
B-27
3b

2 of

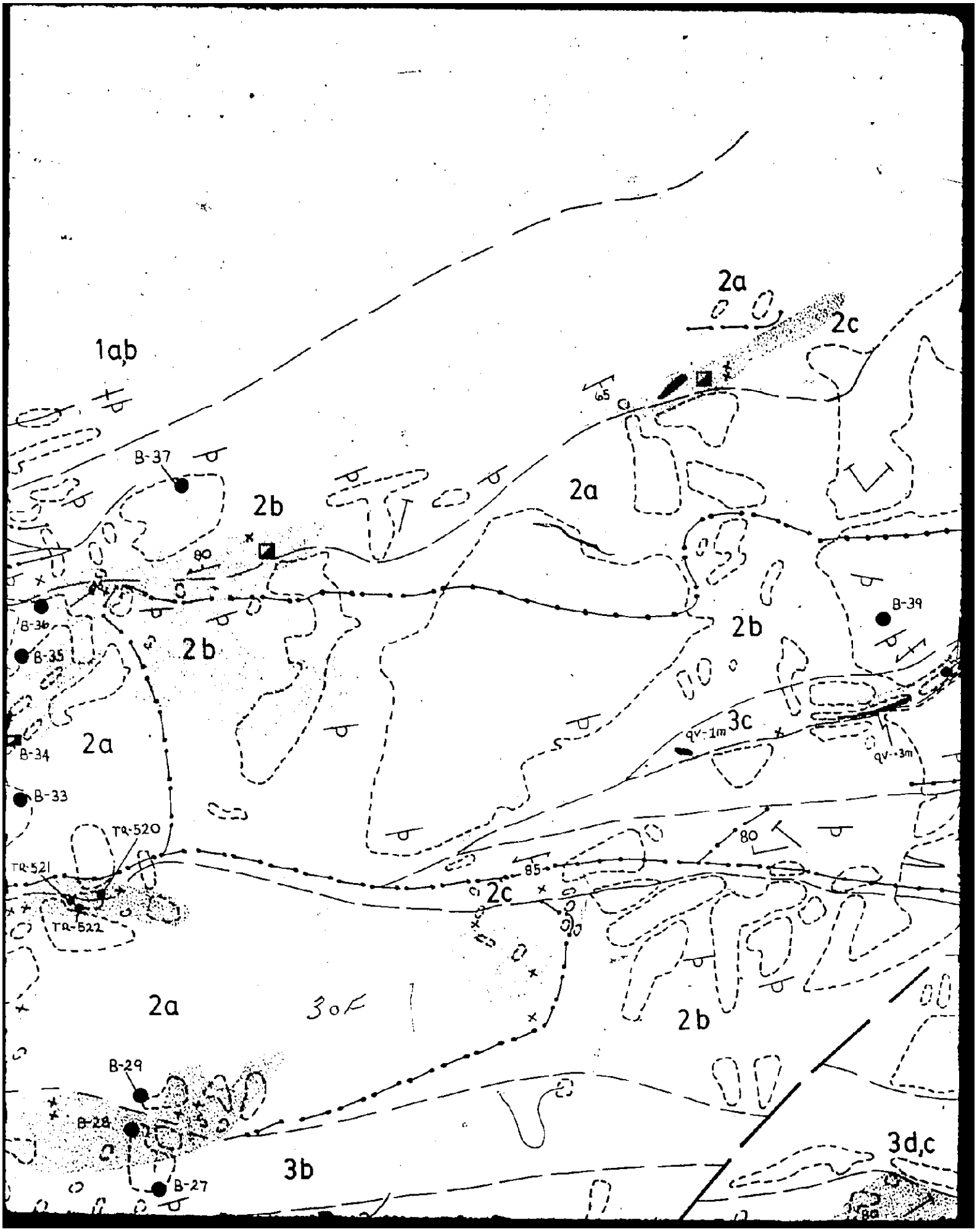
1a,b
2a
2c
2b
3c
3b
3d,c
B-37
B-36
B-35
B-34
B-33
B-39
B-29
B-28
B-27
TR-520
TR-521
TR-522
qv-1m
qv-3m
65
80
85
30

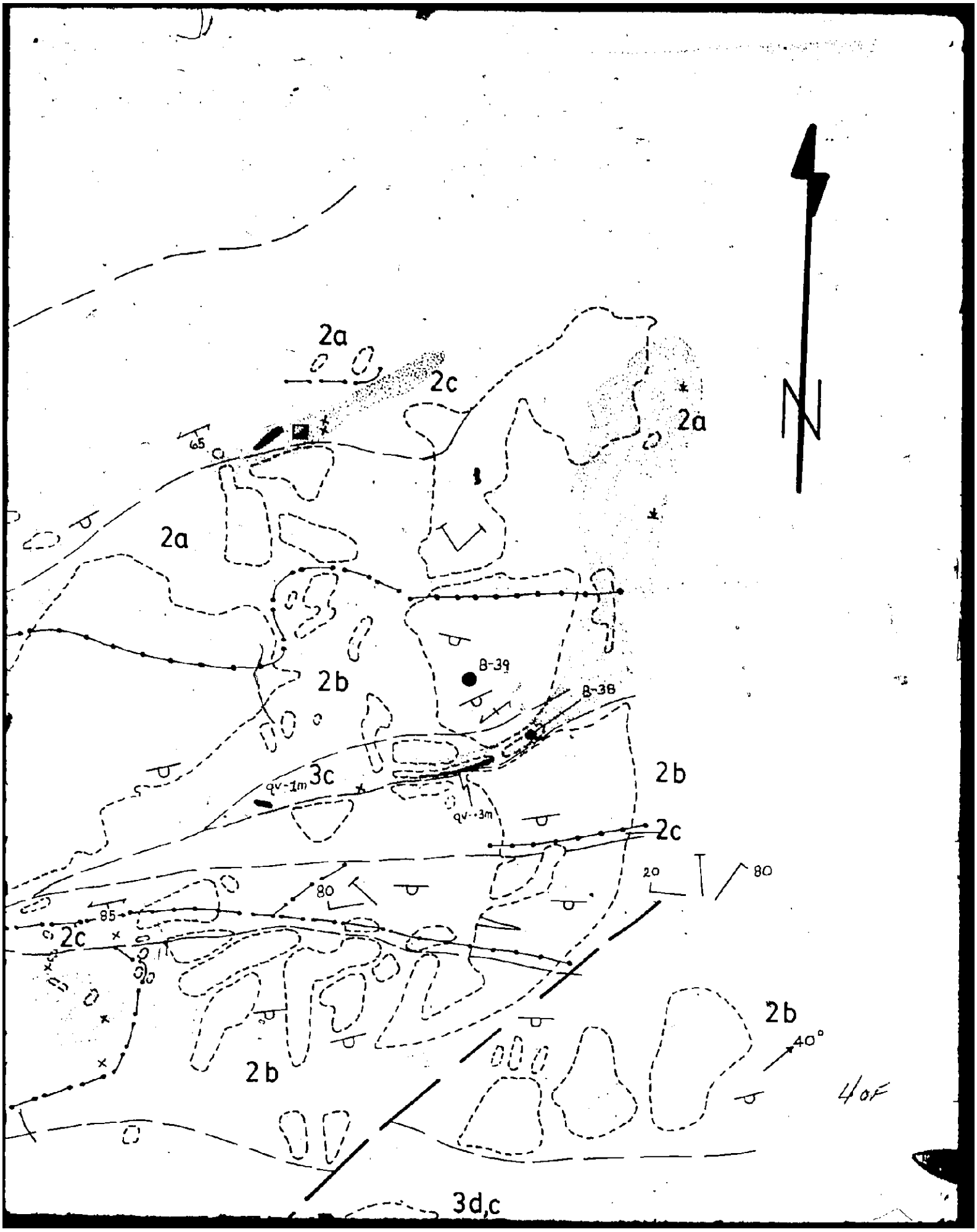
2a
2c
2a
65
2a
2b
B-39
B-38
3c
qv-1m
qv-3m
2b
2c
20
80
80
85
2c
2b
2b
40°
4 of
3d,c

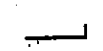
Lineation

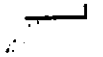
Joint attitude

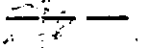
Flow contact


Intraflow facies contact

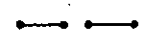
Fault

Shaft

Sample location


Pervasive carbonatization

qv Quartz vein

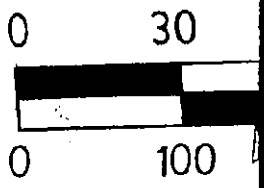

5 of

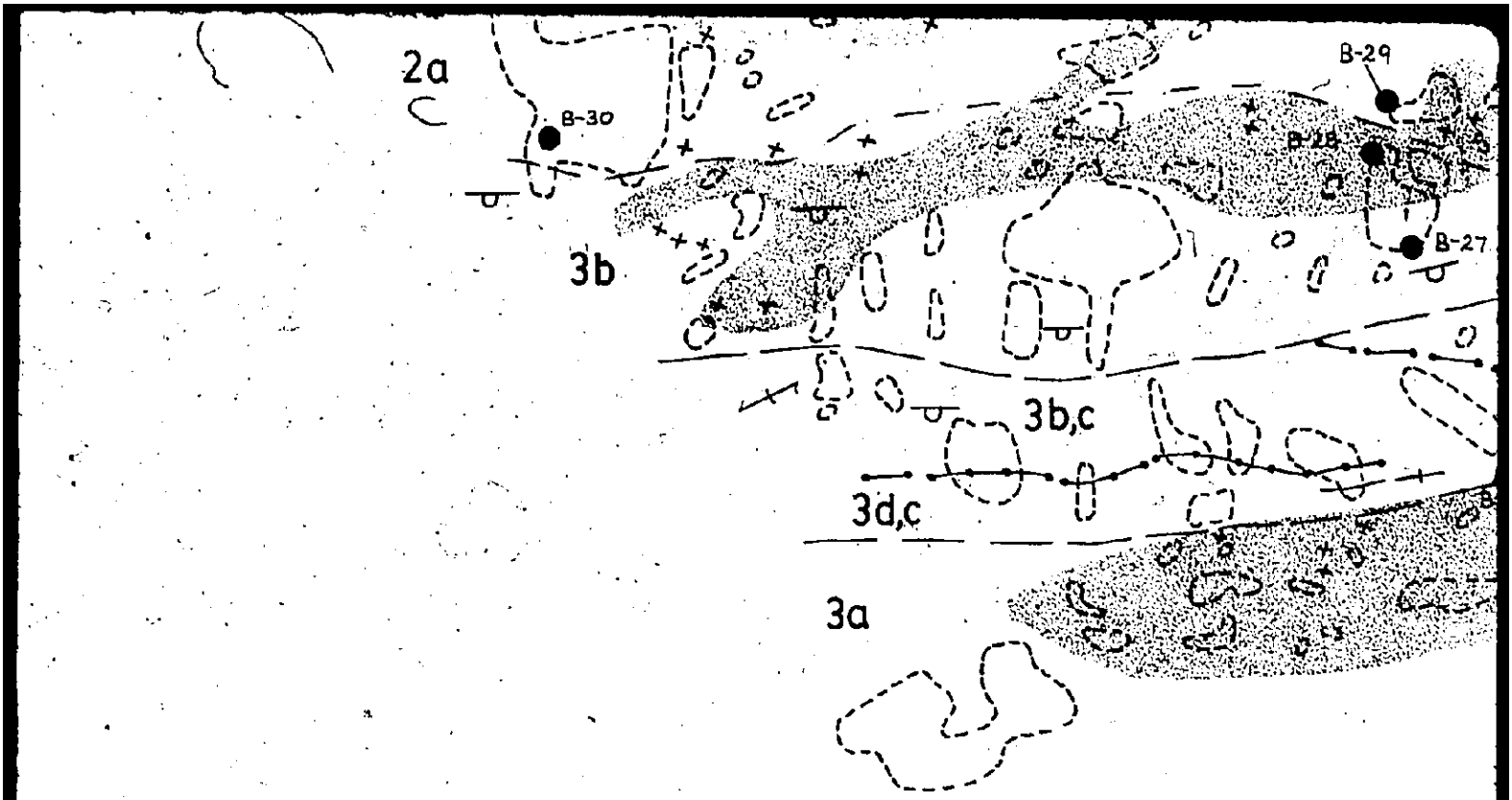

30 60 90 m.

100 200 300 ft.

Geology by J.A. Fyon 197
modified after Ferguson

6 OF

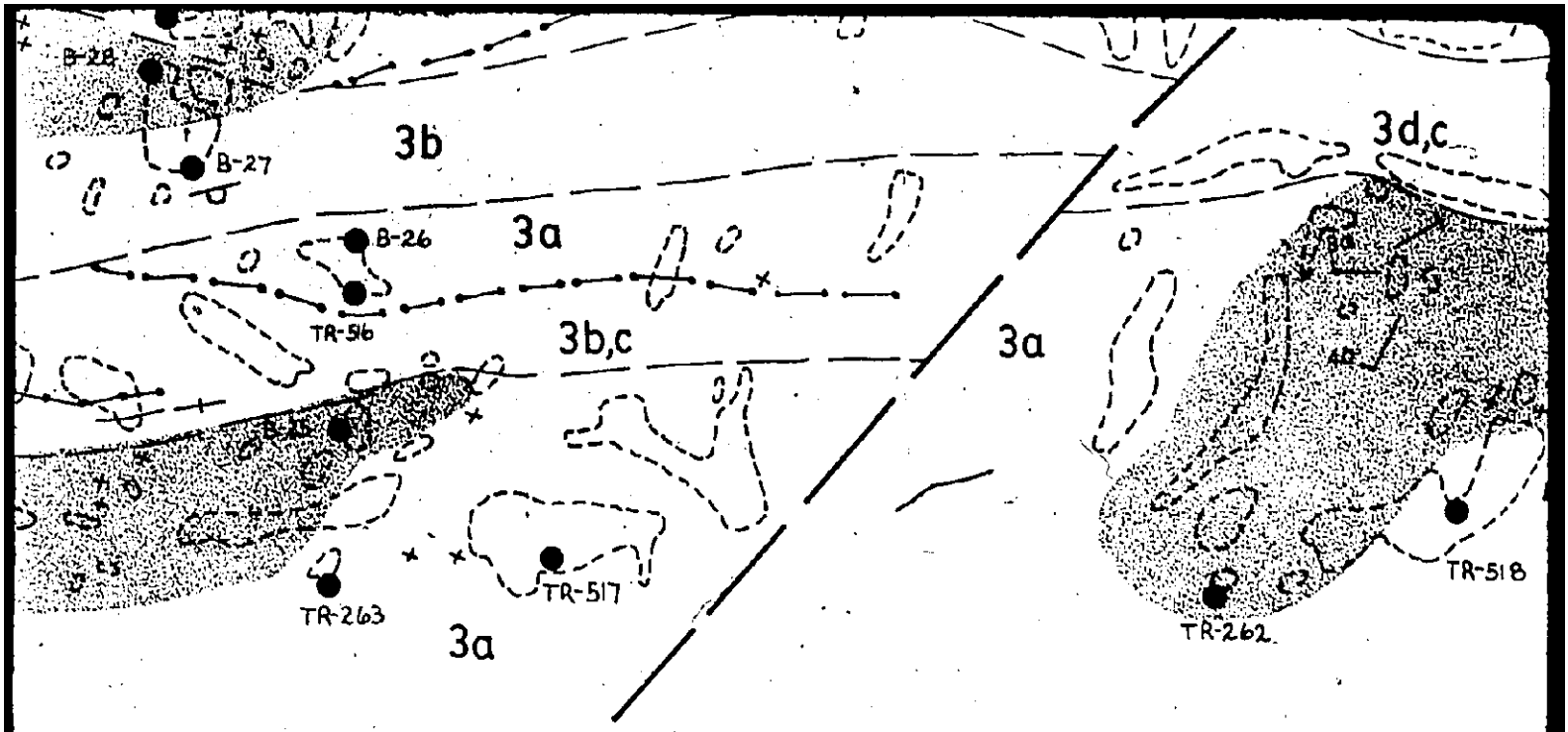

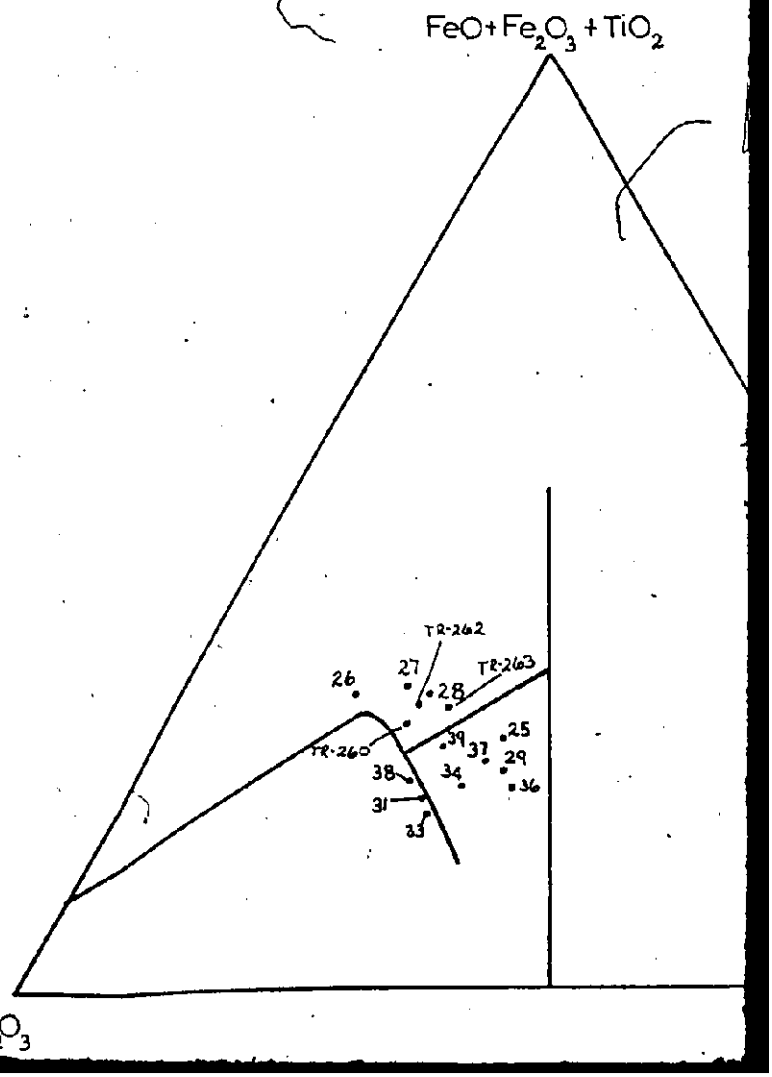

J. A. Fyon 1978

r Ferguson (1960)

7 of

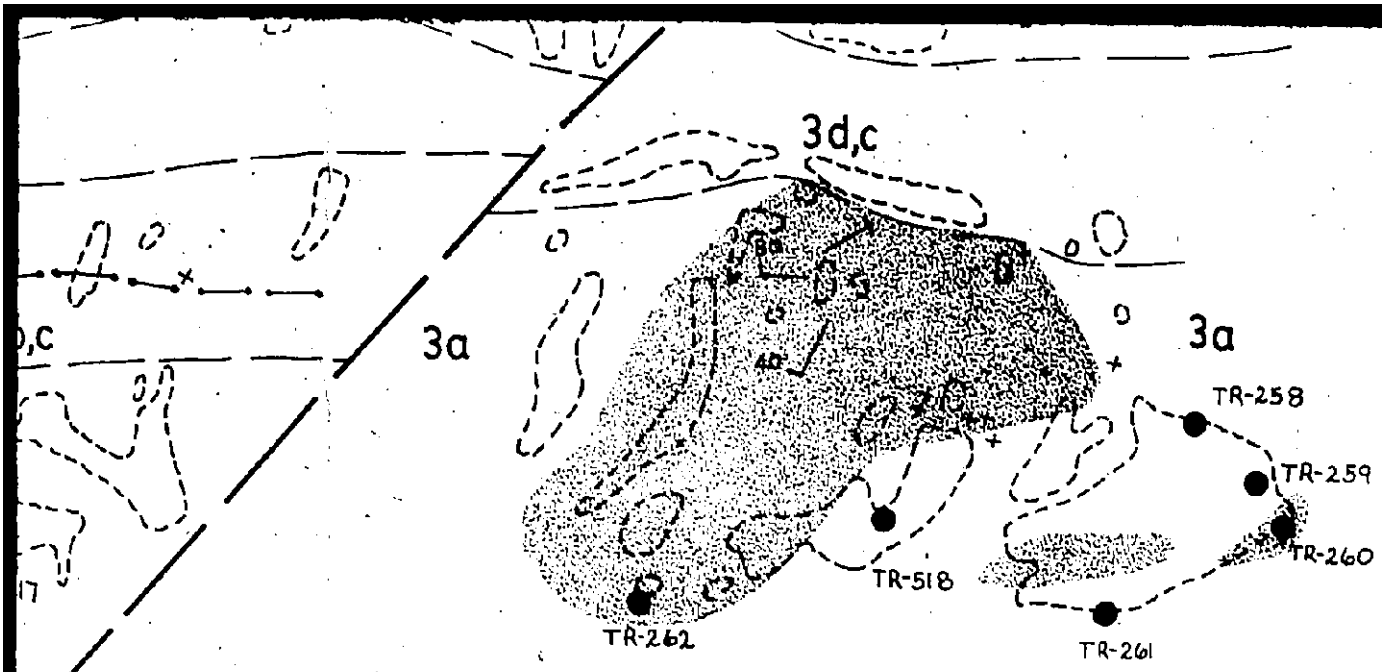
3d,c
3a
3a
TR-258
TR-259
TR-260
TR-518
TR-262
TR-261

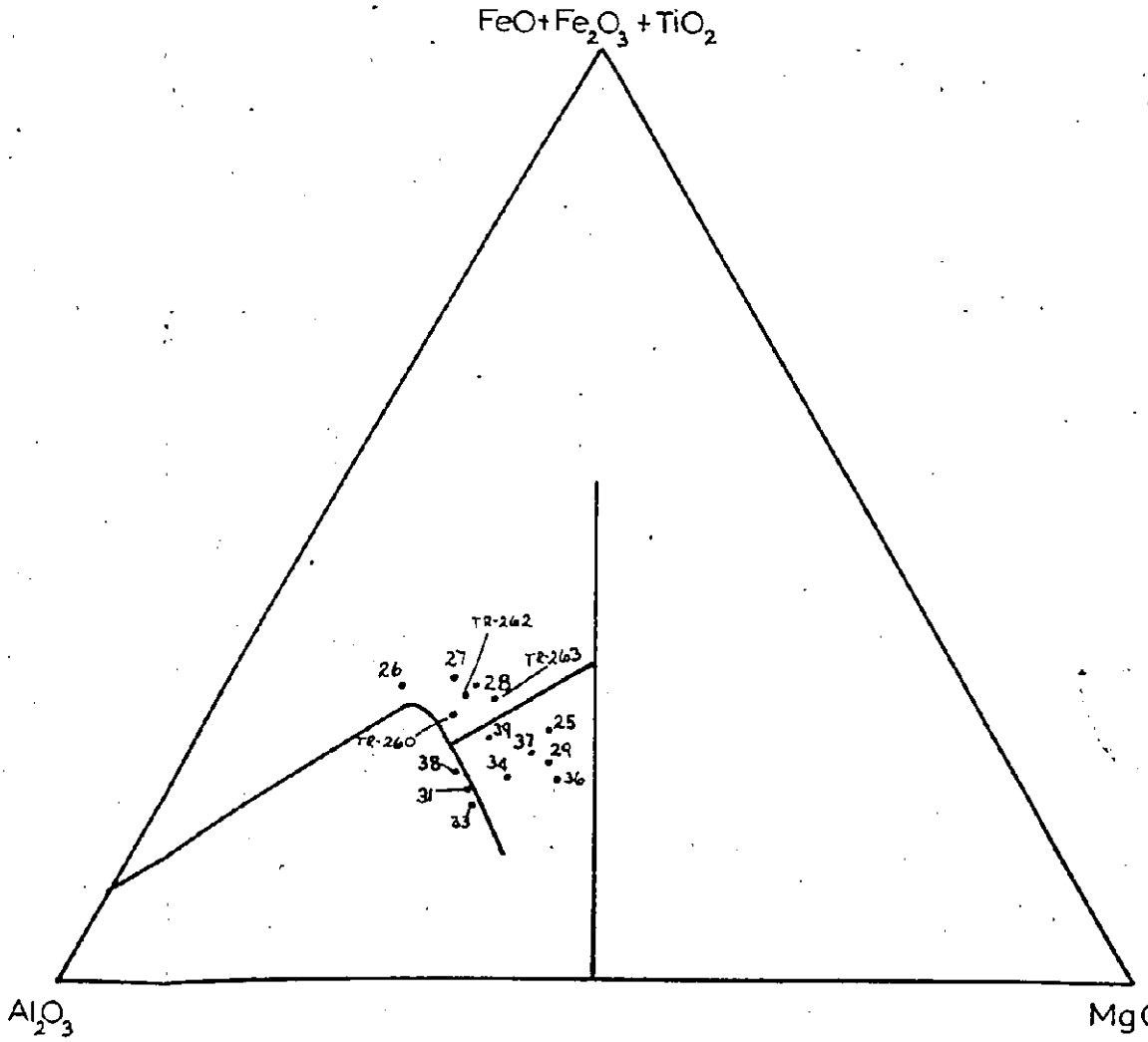
FeO+Fe2O3 +TiO2
Al2O3
MgO
TR-262
TR-263
TR-260
26
27
28
39
37
25
29
38
34
36
31
33

8 OF 8

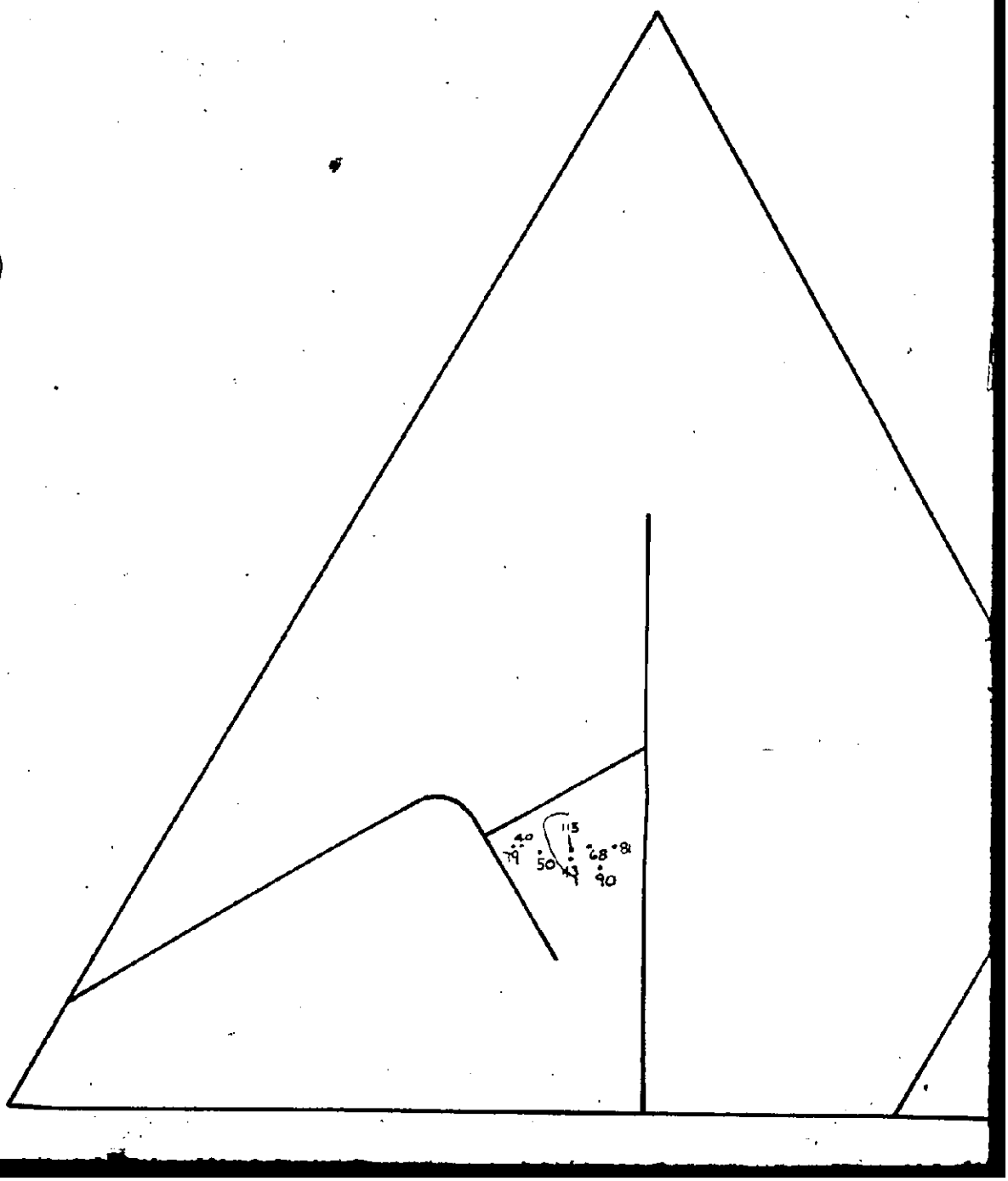

1 of

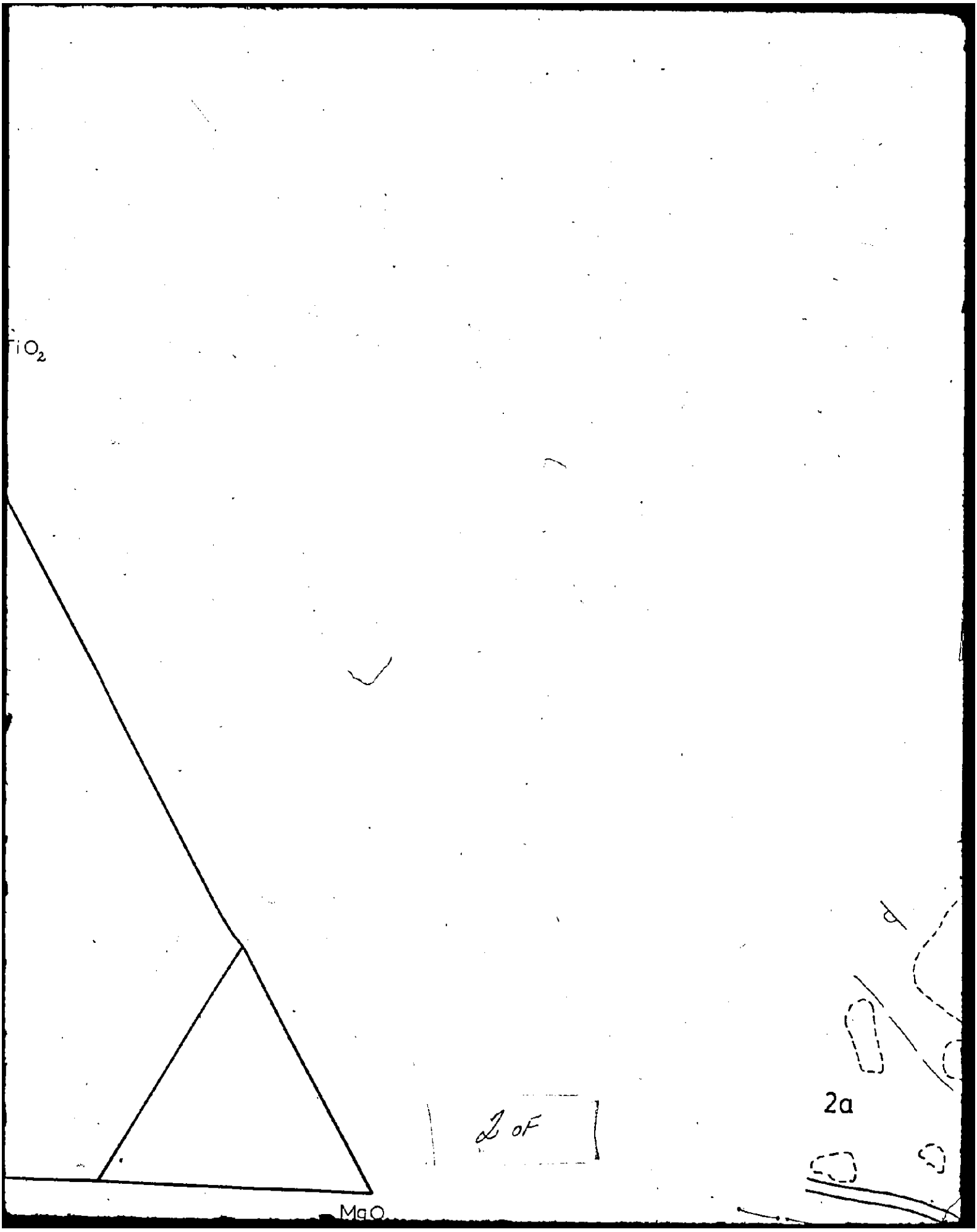
TiO2
MgO
2 OF
2a

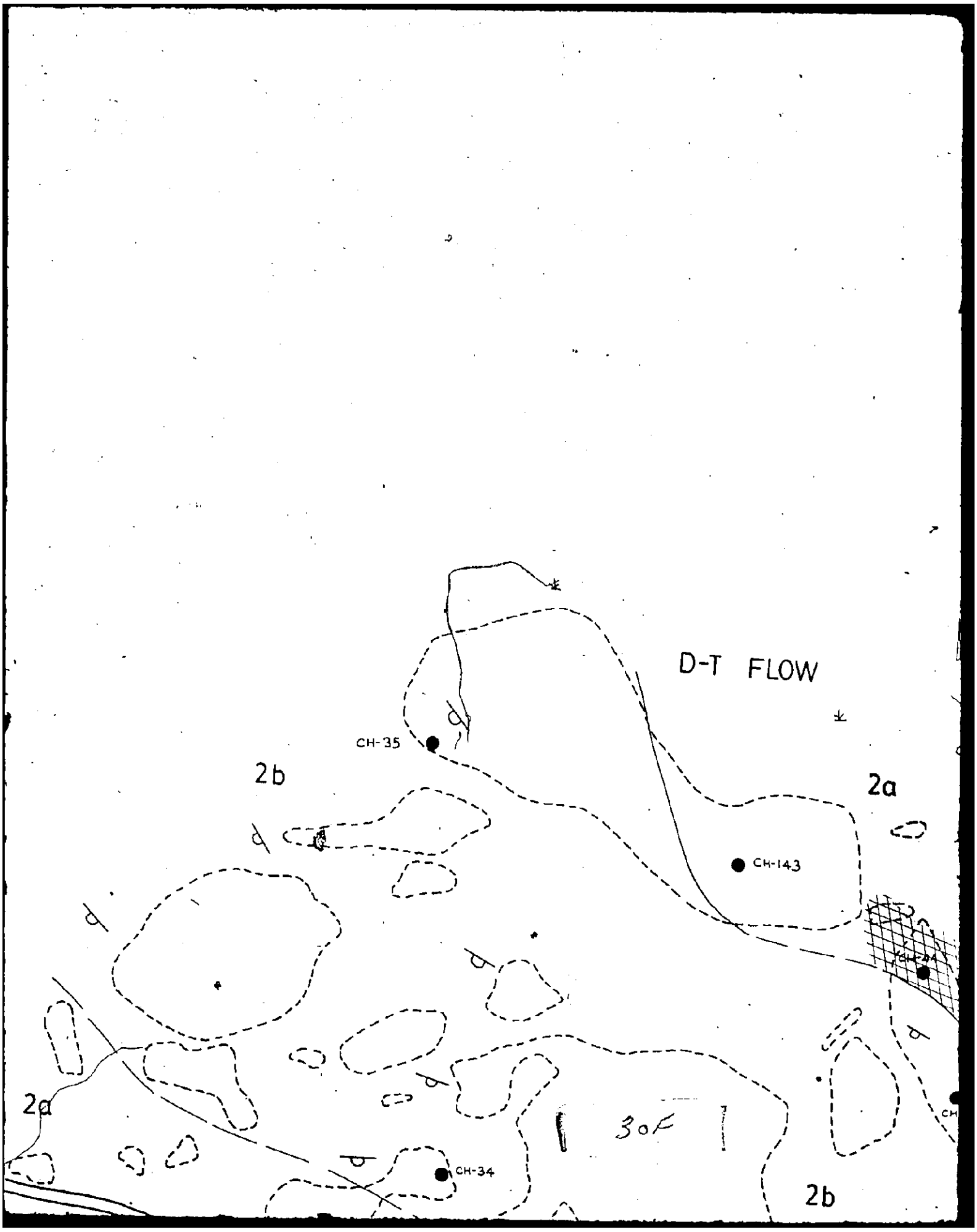
D-T FLOW
CH-35
CH-143
CH-34
2a
2b
2a
2b
3 of

DAVIDSON - TISDALE MINE ARE
TISDALE TWP STUDY AREA
Map 5

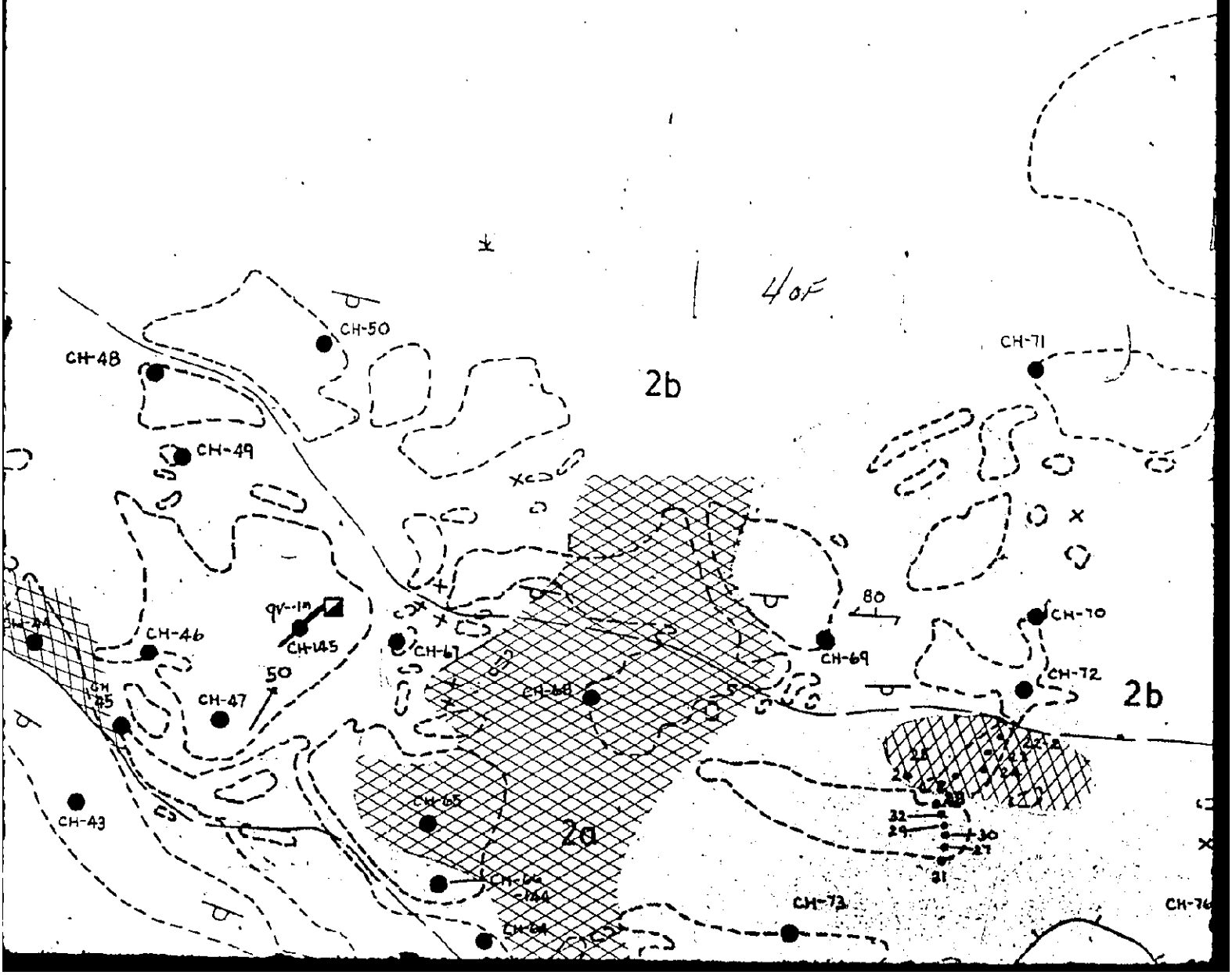

ALE MINE AREA

STUDY AREA

5

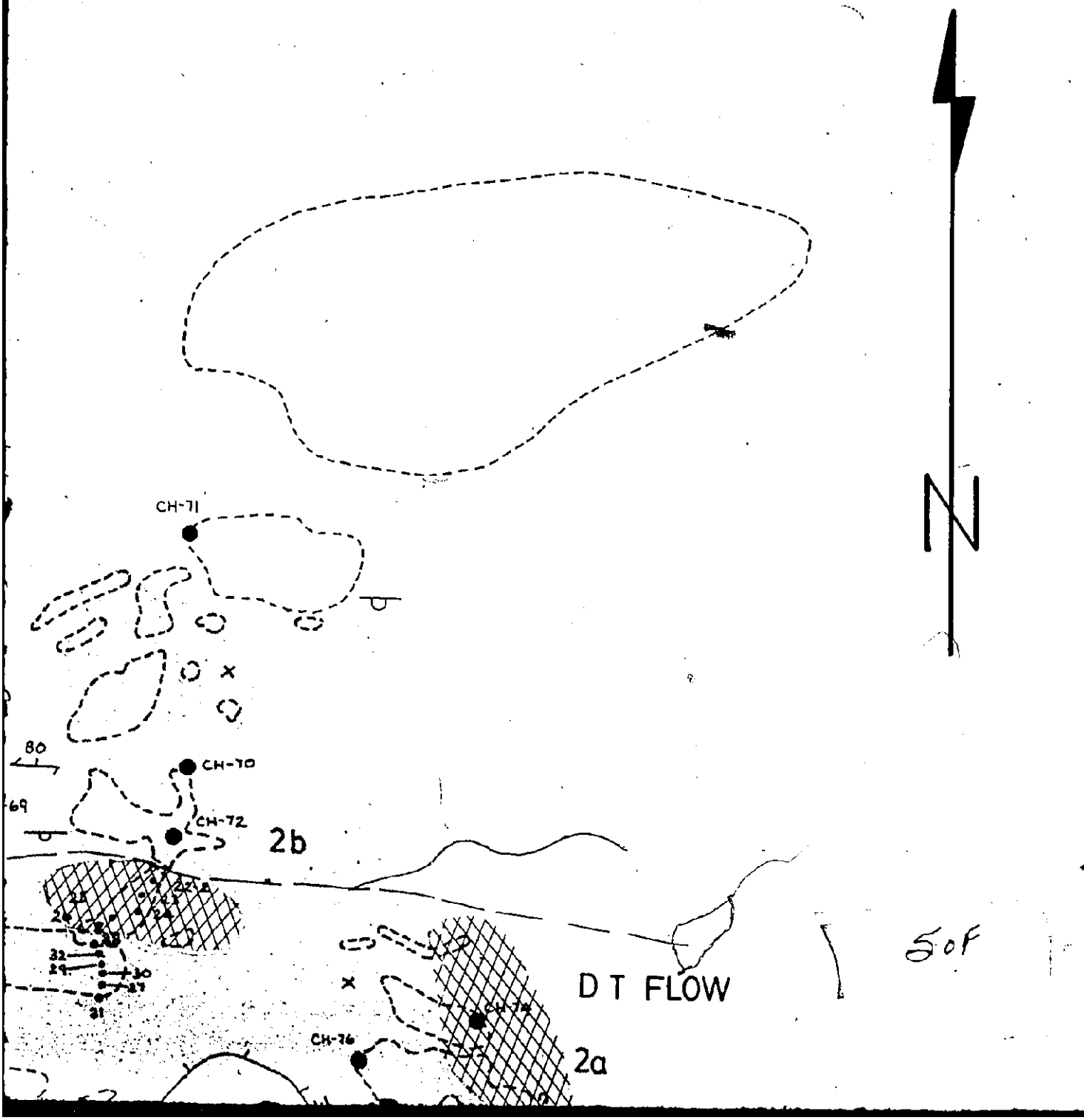

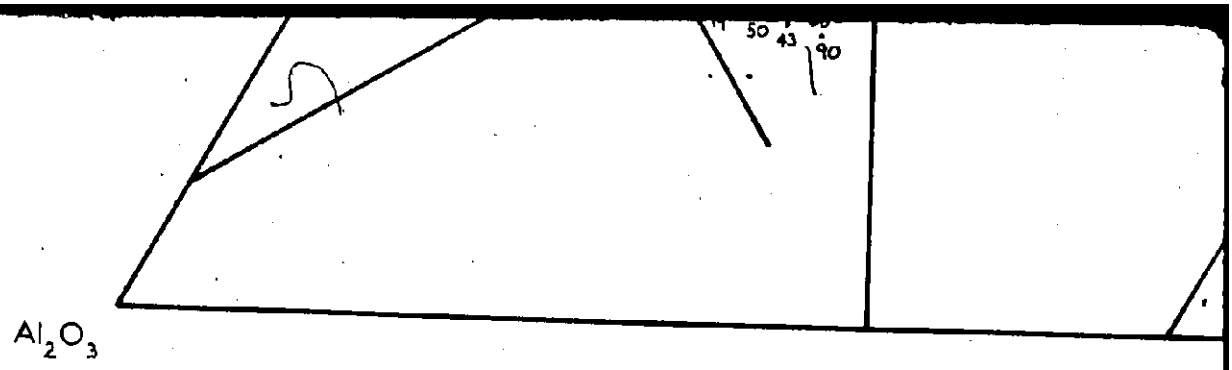

LEGEND

2 Magnesium Tholeiitic Metavolcanics

- a Massive
- b Pillowed
- c Megapillow or lava tube
- d Flow top breccia

- Pillow attitude
- Bedding
- Foliation
- 10° Lineation
- Flow contact
- Intraflow facies contact
- Sample location
- Shaft
- Pit
- Pervasive carbonatization
- Chloritic alteration
- qv Quartz vein

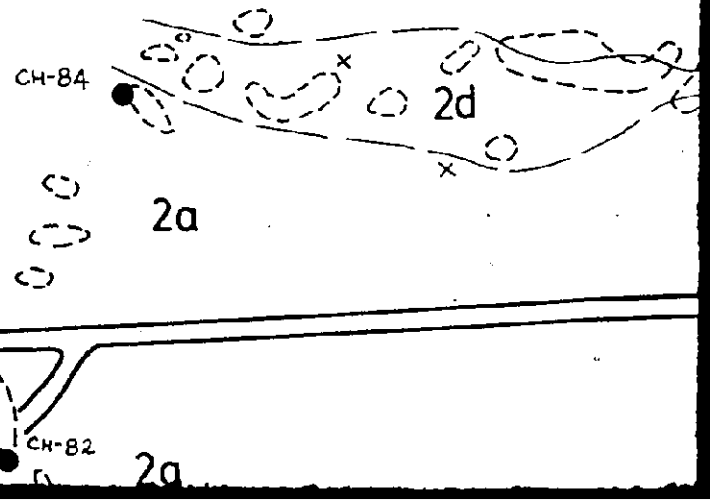

6 of 1

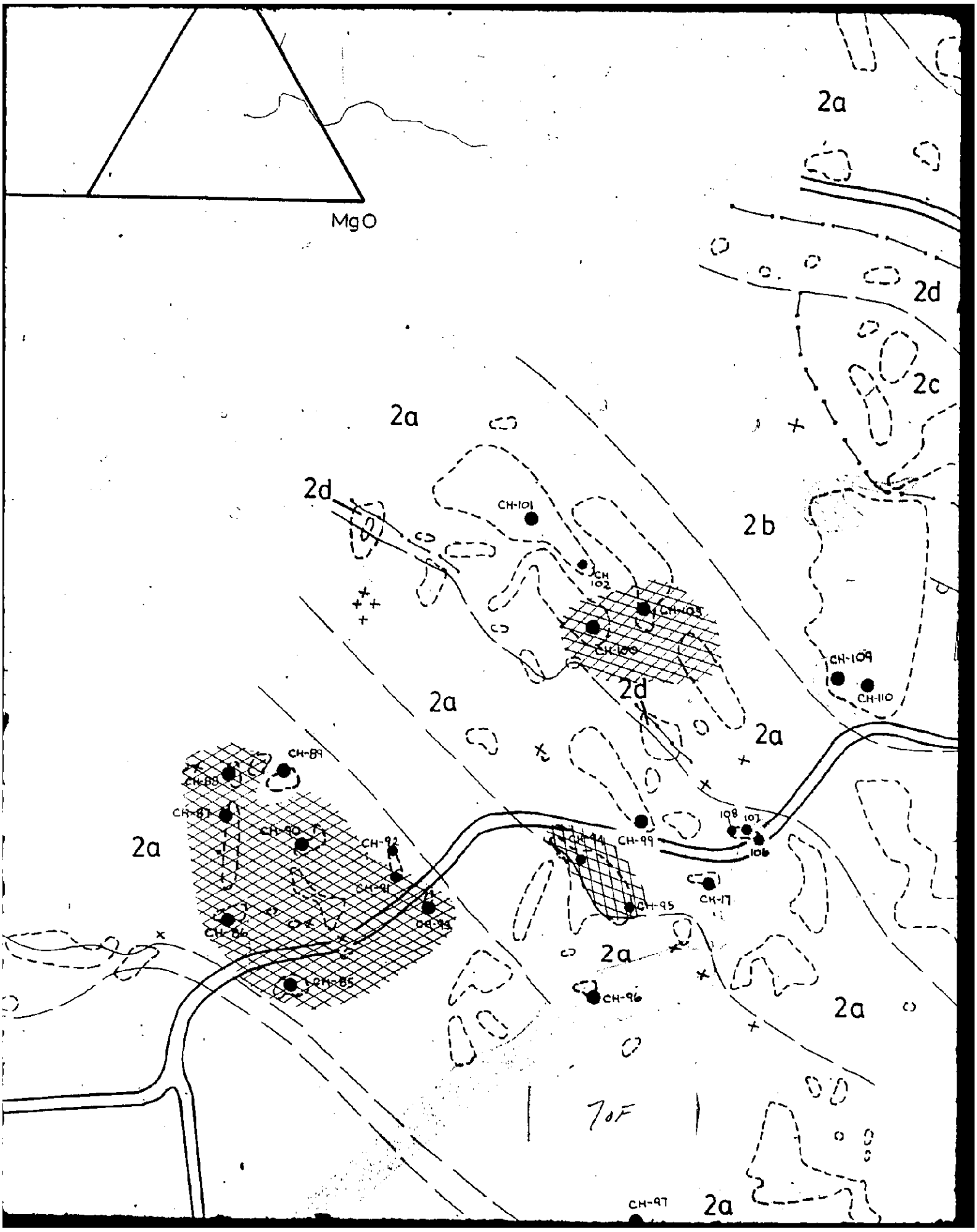
MgO
2a
2d
2c
2b
CH-101
CH-102
CH-103
CH-100
CH-109
CH-110
CH-89
CH-88
CH-87
CH-90
CH-92
CH-91
CH-86
CH-85
CH-94
CH-99
108
107
106
CH-17
CH-95
CH-96
CH-97
7 of

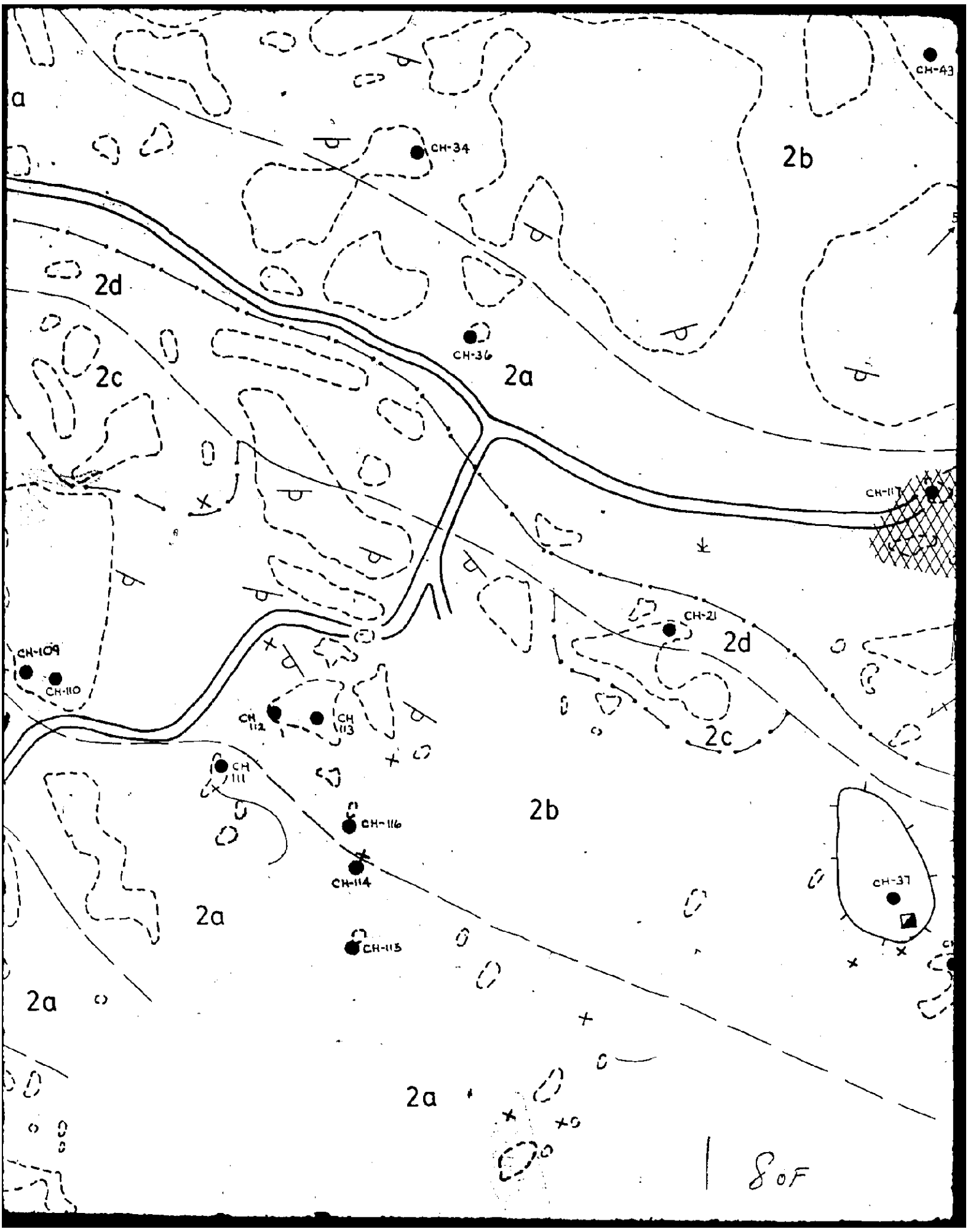
a
CH-43
CH-34
2b
2d
CH-36
2a
2c
CH-117
CH-21
2d
CH-109
CH-110
CH 112
CH 113
2c
CH 111
2b
CH-116
CH-114
CH-37
2a
CH-115
2a
2a
18 OF

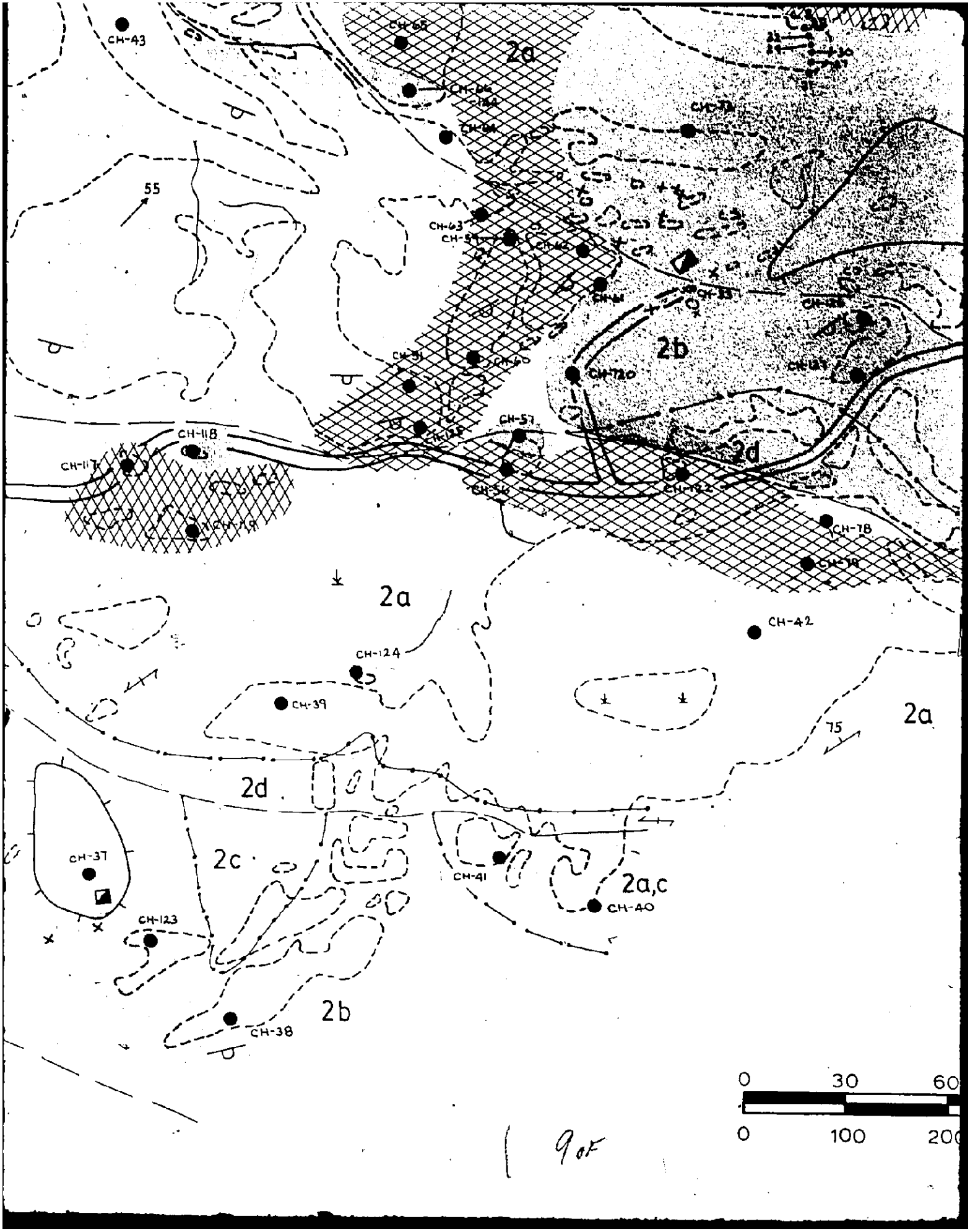
CH-43
CH-65
CH-66
CH-64
CH-72
CH-63
CH-62
CH-61
CH-33
CH-126
CH-51
CH-60
CH-120
CH-121
CH-57
CH-118
CH-117
CH-119
CH-122
CH-78
CH-79
CH-42
CH-124
CH-39
CH-37
CH-123
CH-38
CH-41
CH-40
2a
2b
2c
2d
2a,c
55
75
0
30
60
100
200
1 of

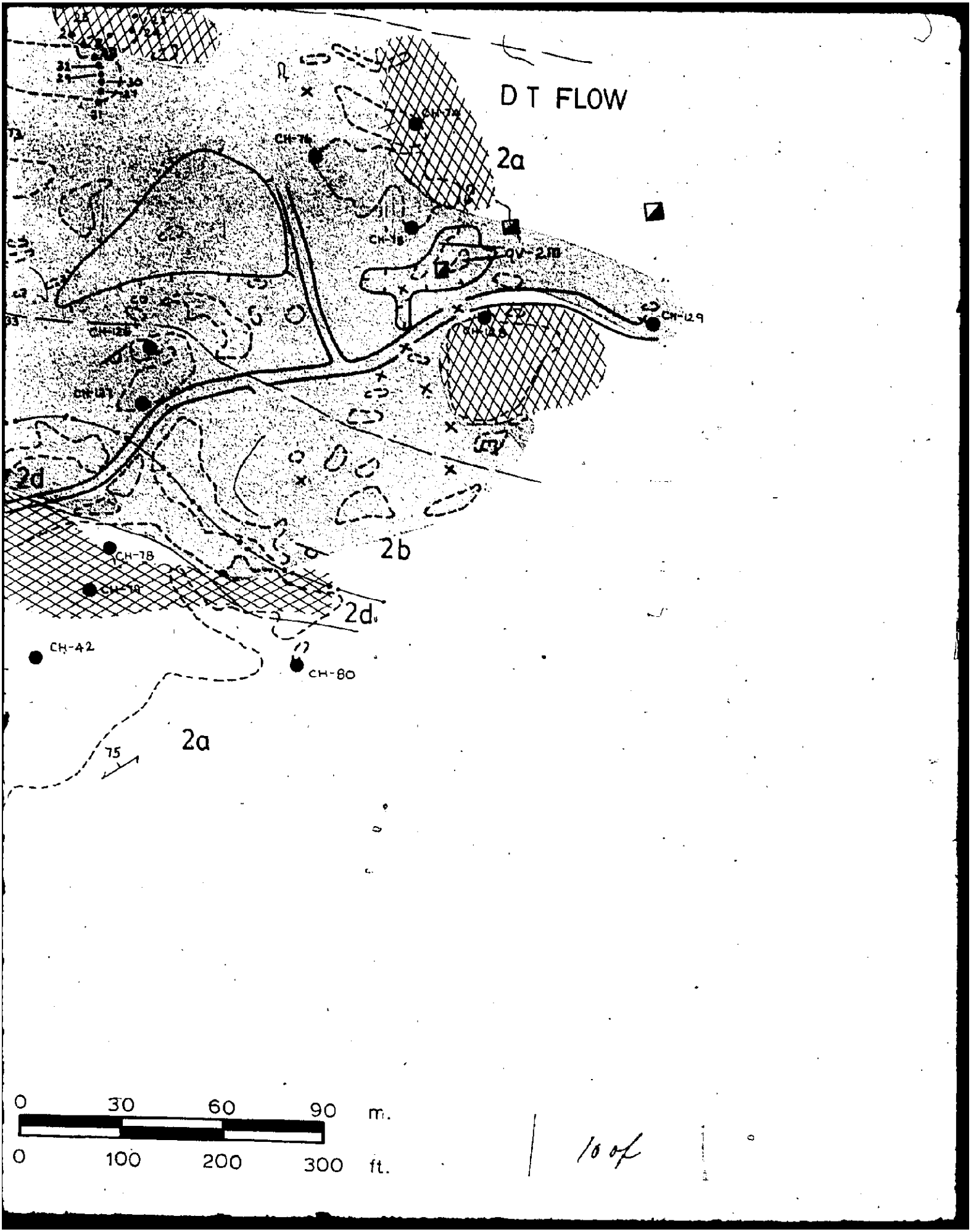
D T FLOW
2a
2d
2b
2d
2a
CH-74
CH-76
CH-18
CV-2B
CH-129
CH-128
CH-127
CH-78
CH-19
CH-42
CH-80
75
0
30
60
90
m.
0
100
200
300
ft.

10 of

a Massive
b Pillowed
c Megapillow or lava tube
d Flow top breccia

Pillow attitude
Bedding
Foliation
10° Lineation
Flow contact
Intraflow facies contact
Sample location
Shaft
Pit
Pervasive carbonatization
Chloritic alteration
qv Quartz vein

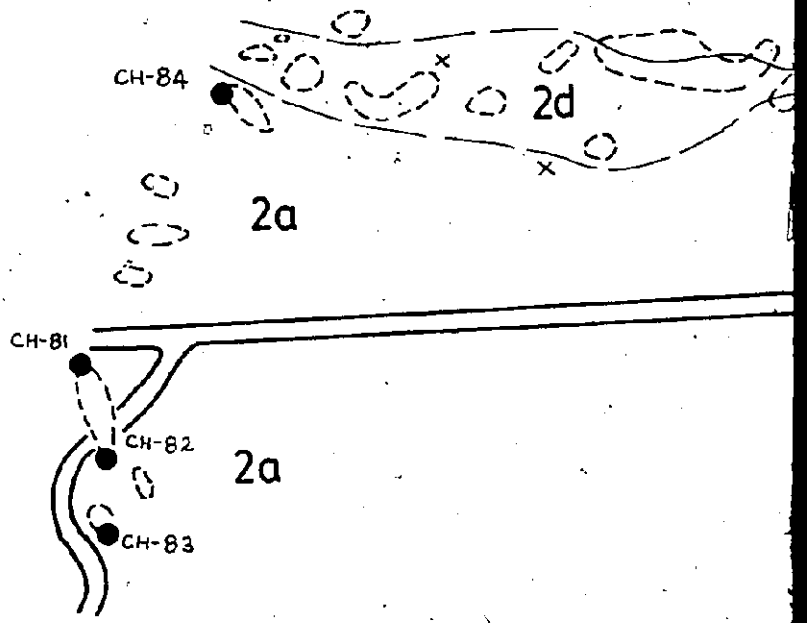

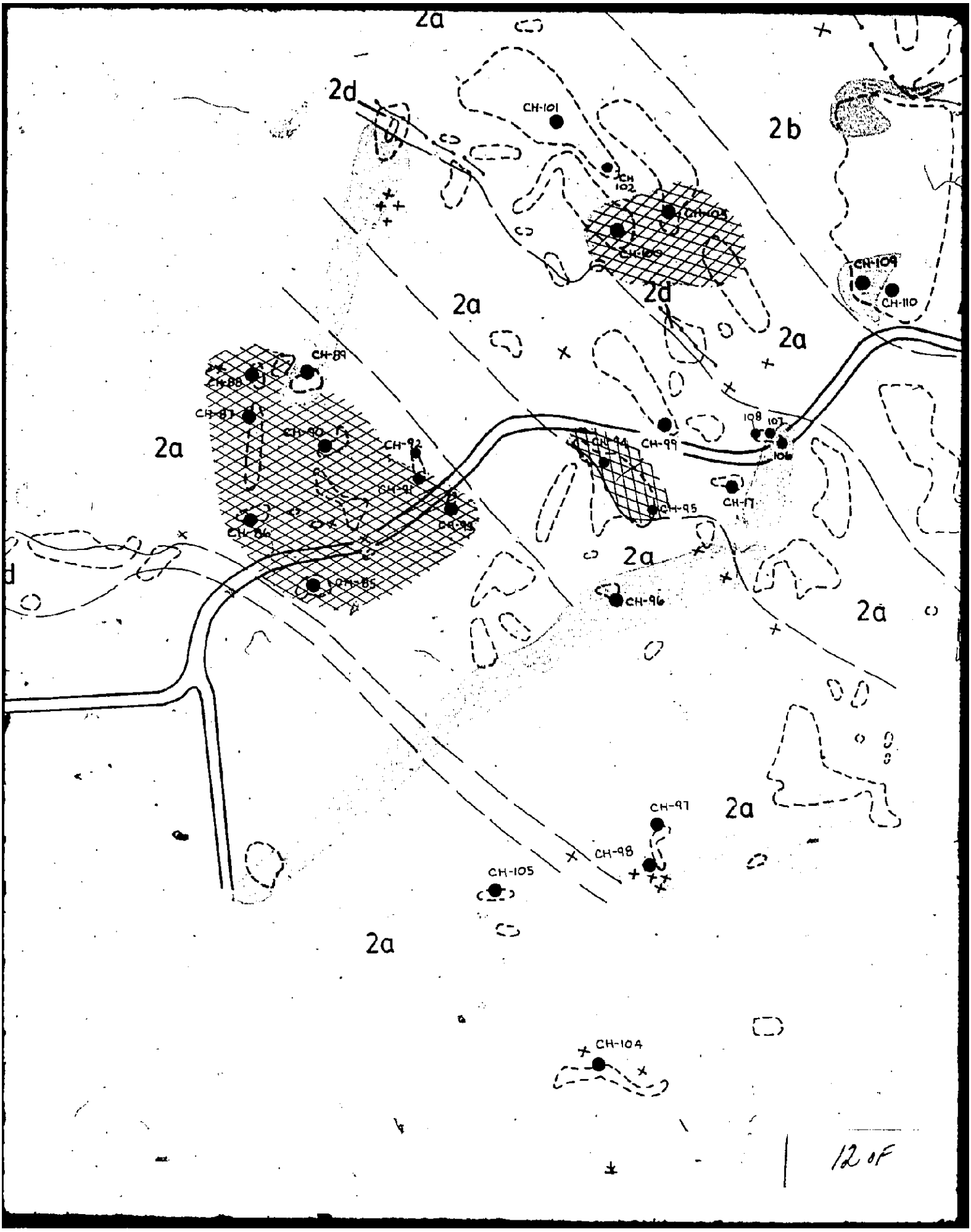
2a
2d
2b
CH-101
CH 102
CH-103
CH-100
2d
CH-109
CH-110
2a
2a
CH-89
CH-88
CH-87
CH-90
CH-92
CH-91
CH-86
CH-85
2a
CH-99
108
107
106
CH-94
CH-95
CH-17
2a
CH-96
2a
CH-97
2a
CH-98
CH-105
2a
CH-104
12 of

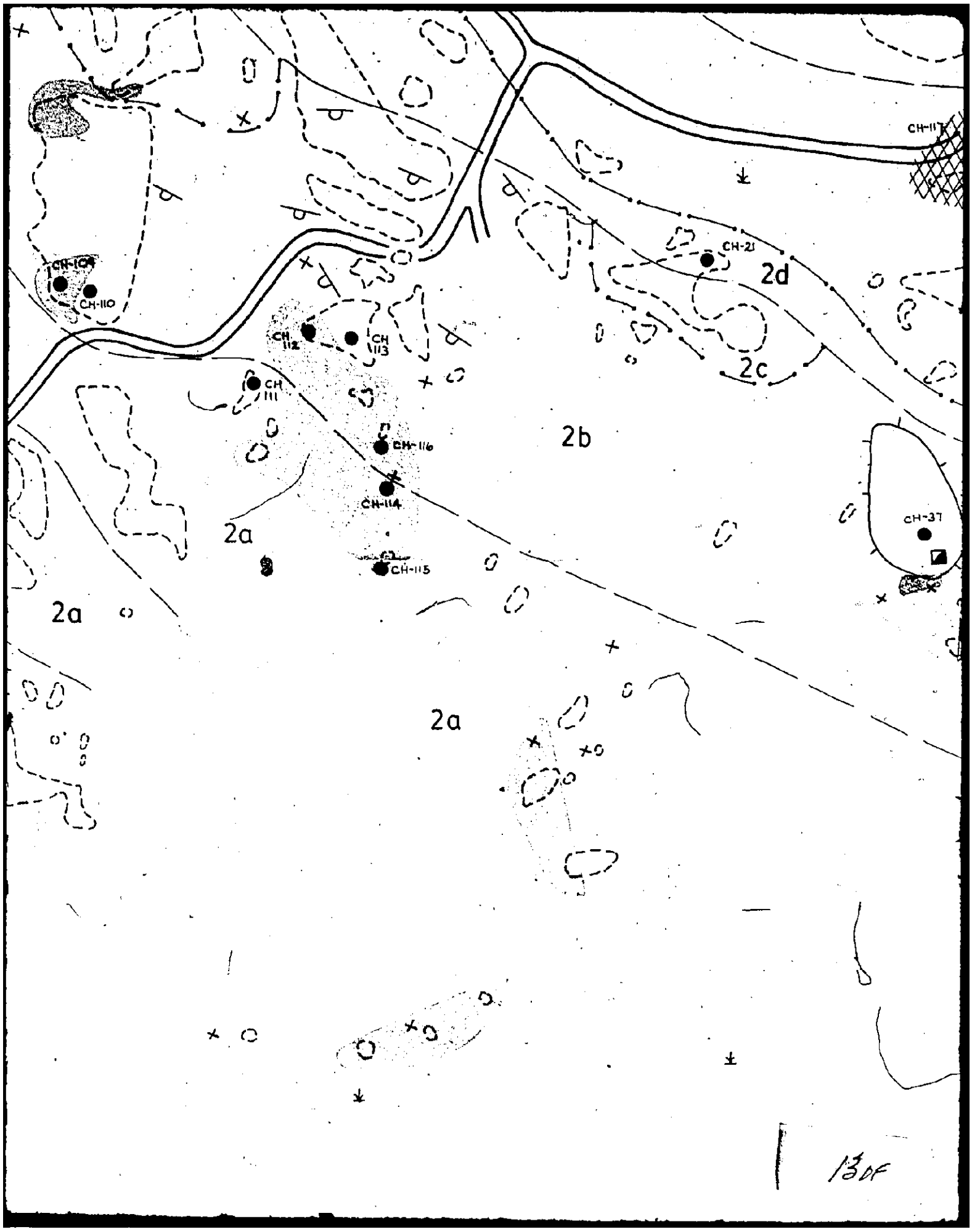
CH-109
CH-110
CH 112
CH 113
CH 111
CH-116
CH-114
CH-115
CH-21
CH-37
2a
2a
2a
2b
2c
2d

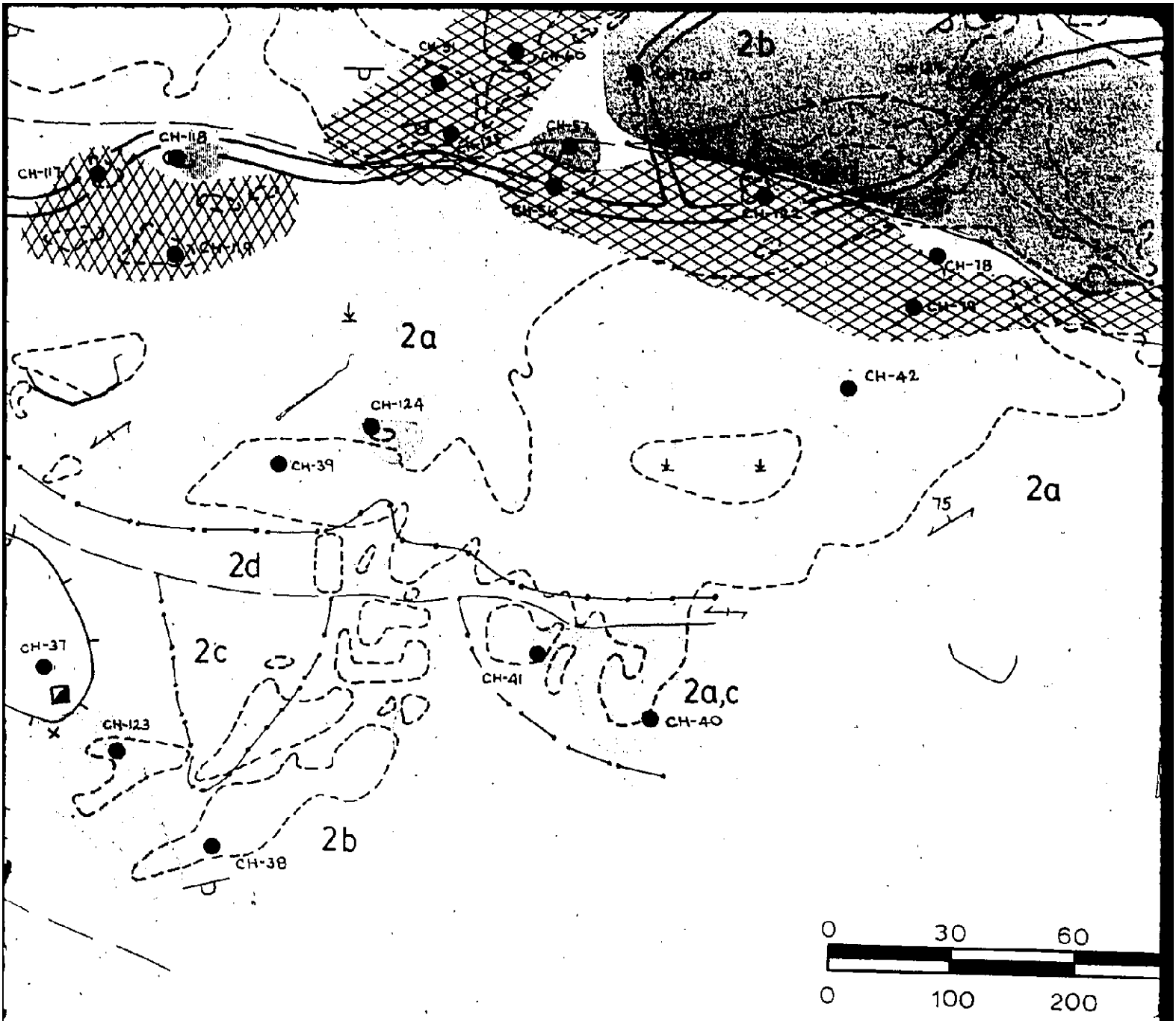

Geology by J.A. Fyon
modified after Fergus

14 of

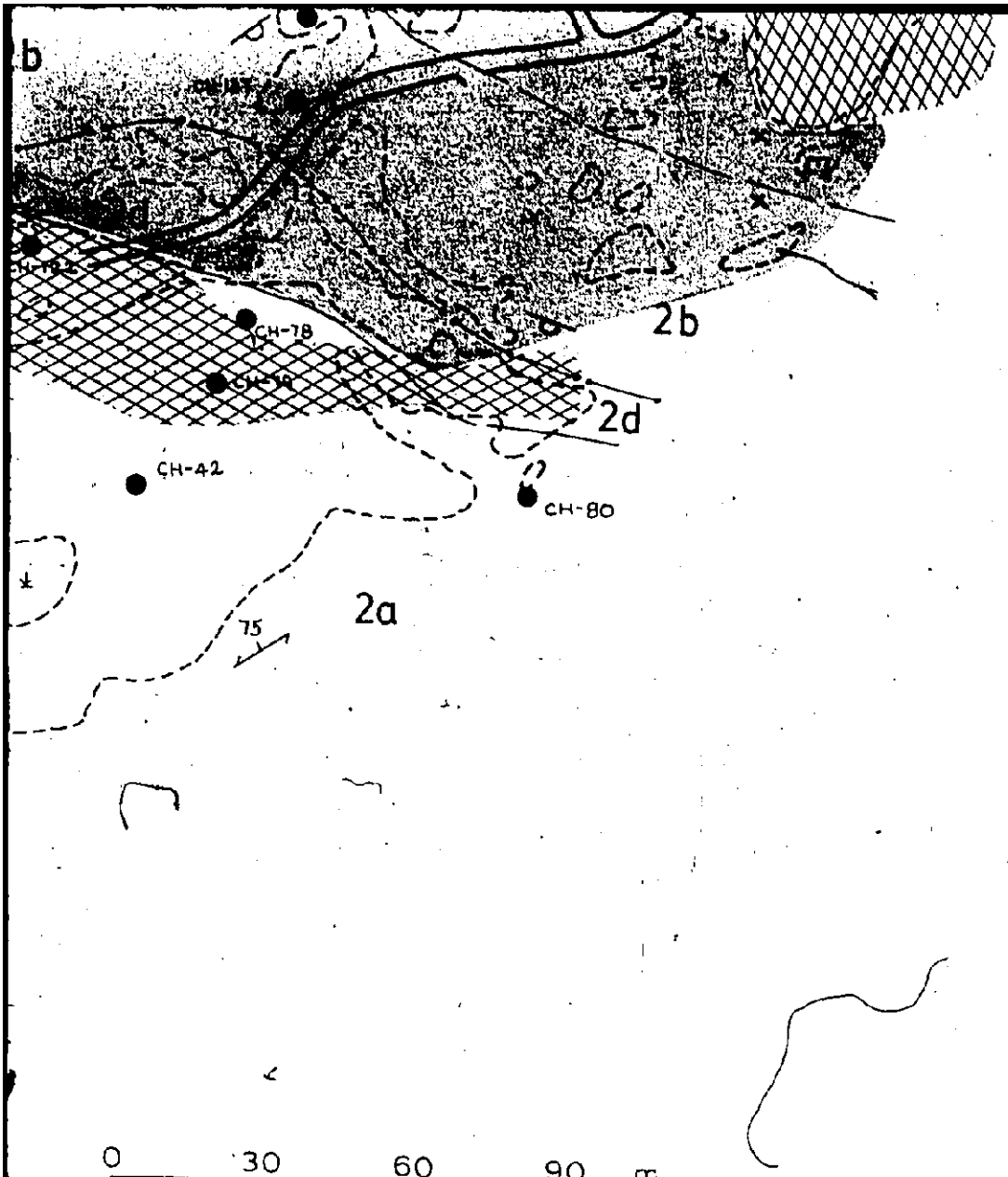

Geology by J.A. Fyon 1978
modified after Ferguson (1960)

15 OF 15

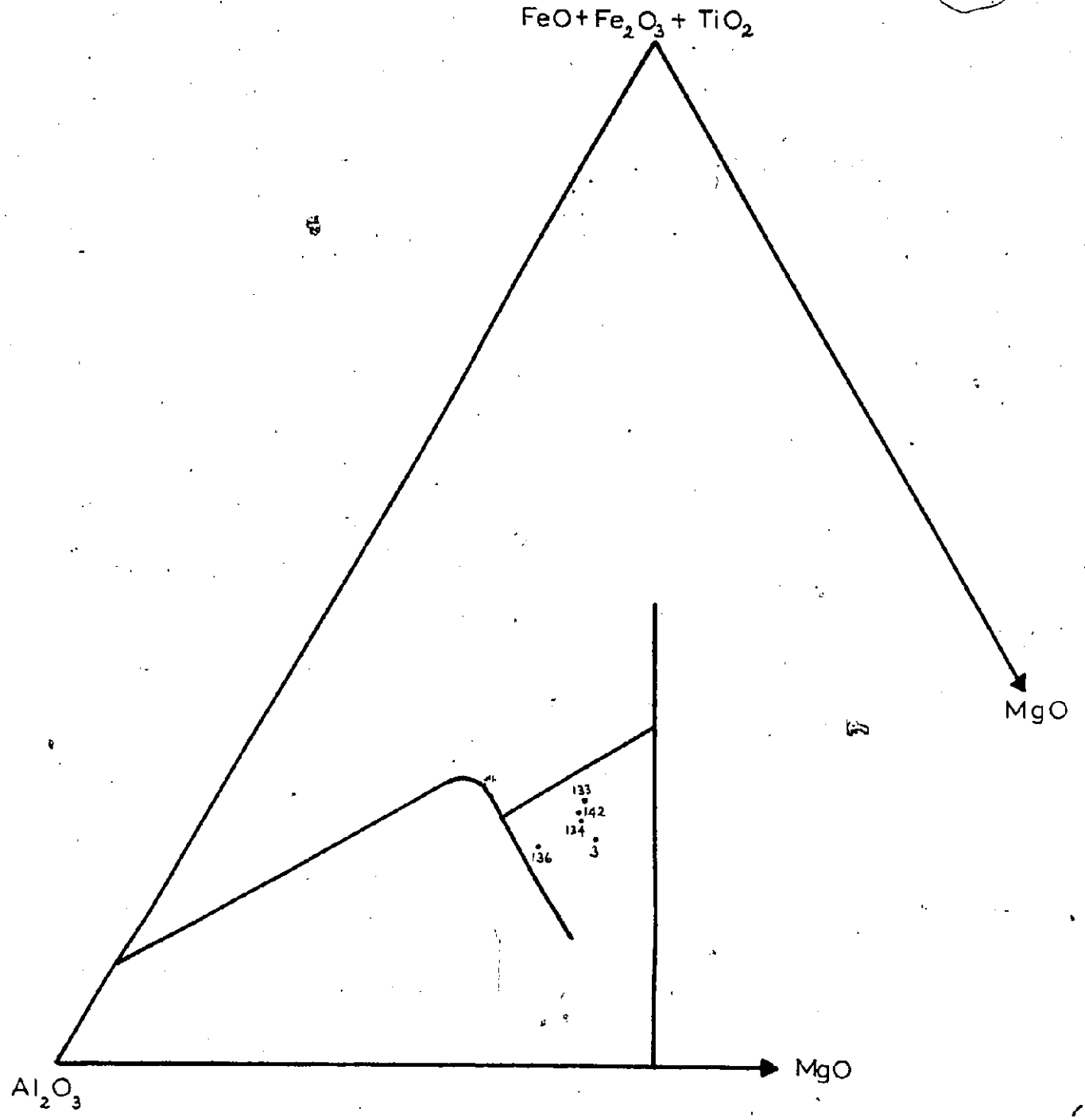

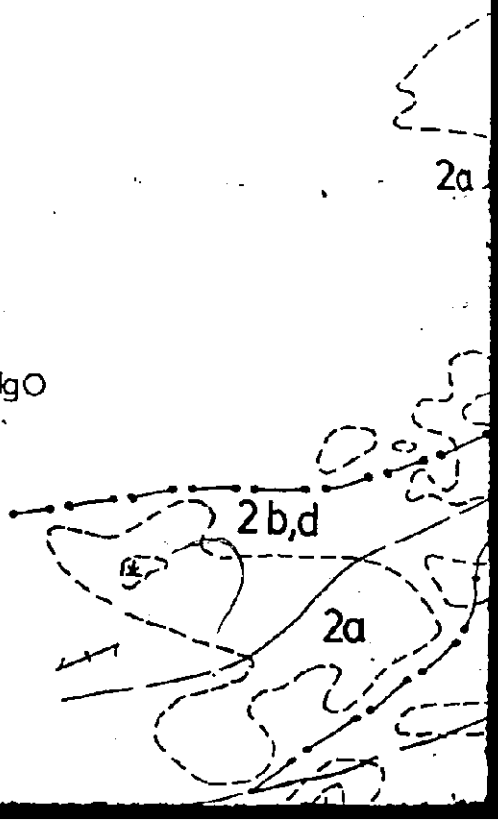

1 of F

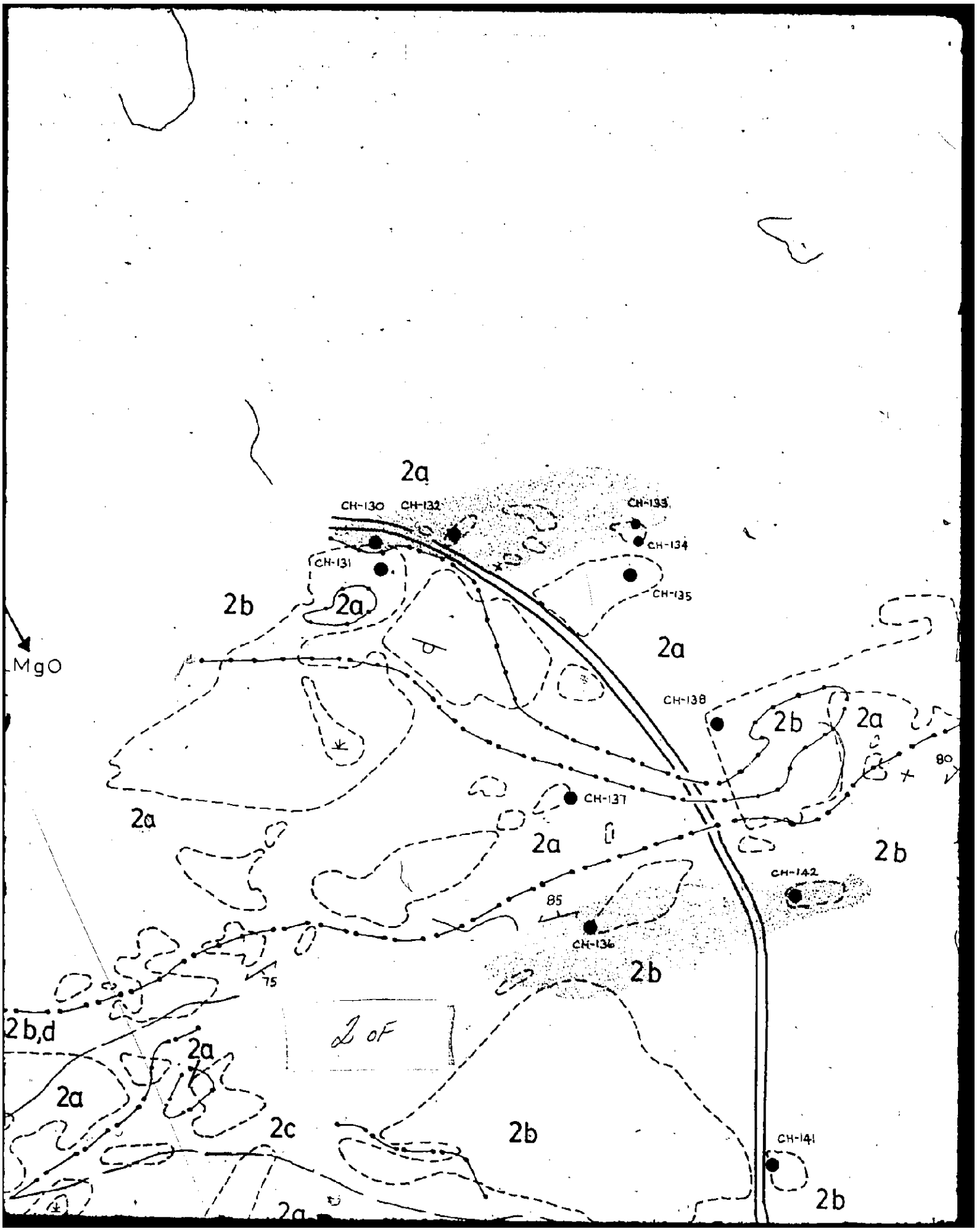
2a
CH-130
CH-132
CH-133
CH-134
CH-131
CH-135
2b
2a
MgO
2a
CH-138
2b
2a
80
CH-137
2a
2a
2b
CH-142
85
CH-136
2b
75
2b,d
2a
2a
2c
2b
CH-141
2b
2a

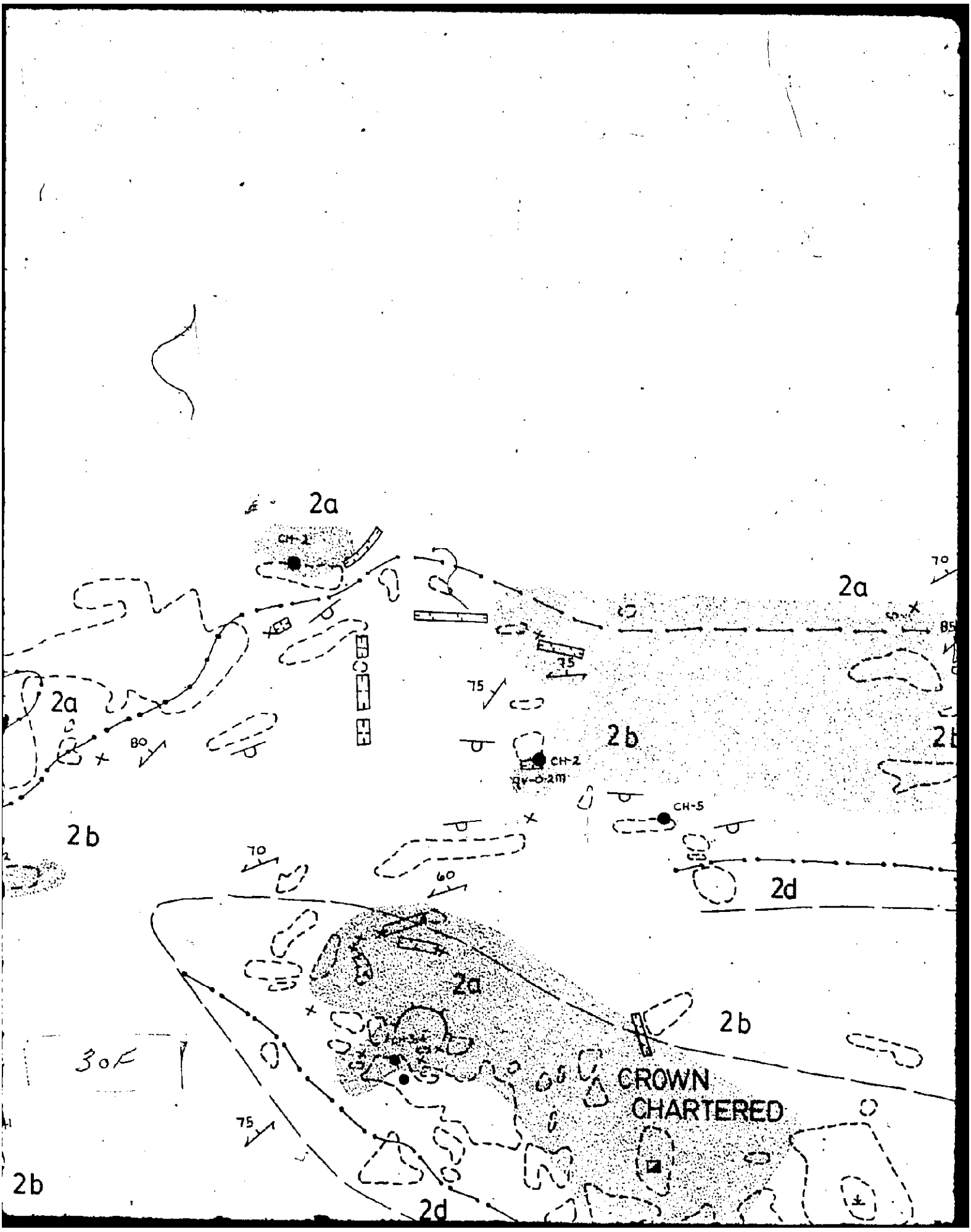
2a
CH-1
2a
70
2a
75
75
2b
CH-2
av-0.2m
CH-5
2b
2b
70
60
2d
2a
CH-3,4
2b
30F
CROWN
CHARTERED
75
2b
2d

Map 6

ARMSTRONG McGIBBON

SHAF

TISDALE TW

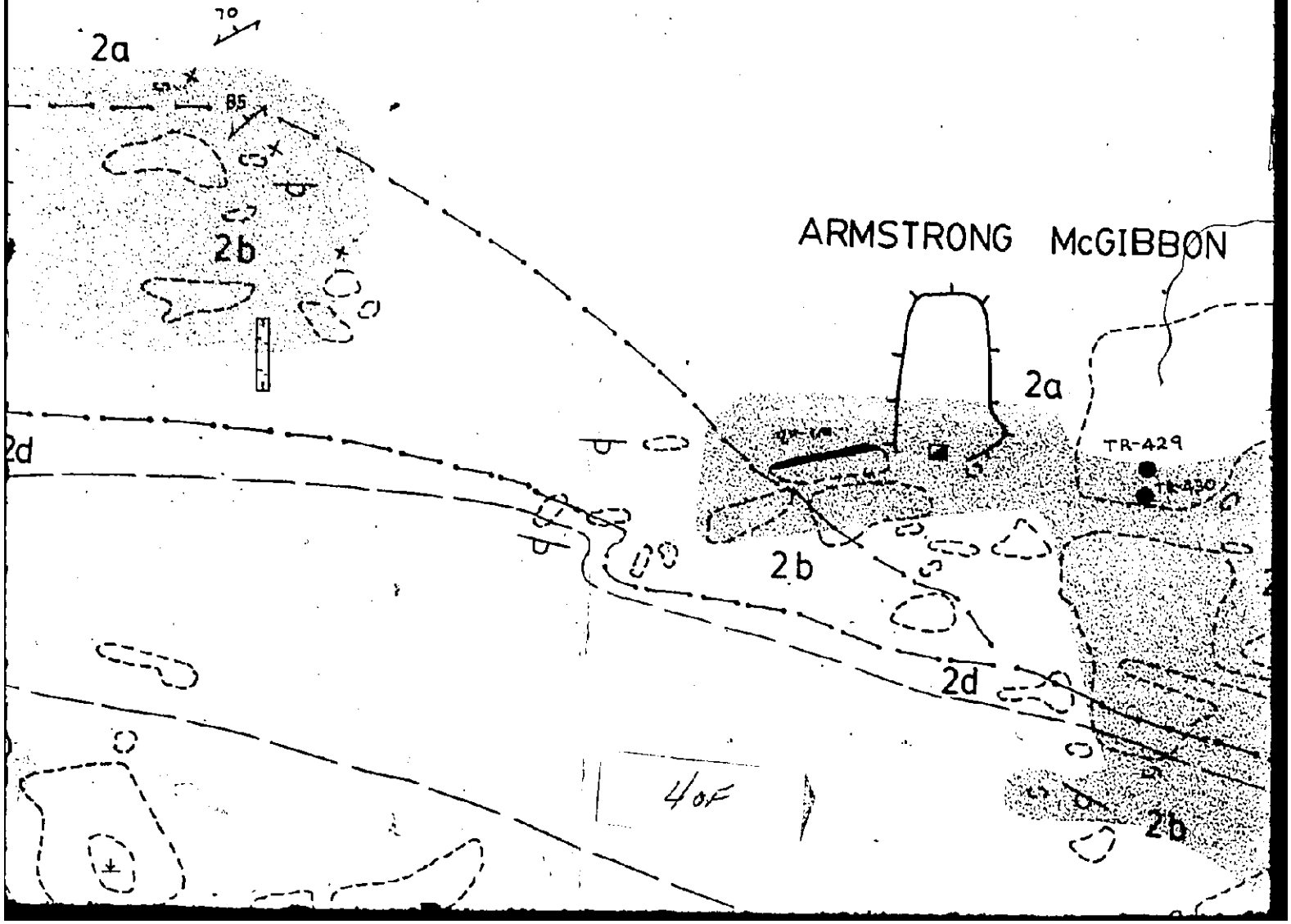

4 of

Map 6

NG McGIBBON CROWN CHARTERED SHAFT AREAS TISDALE TWP STUDY AREA

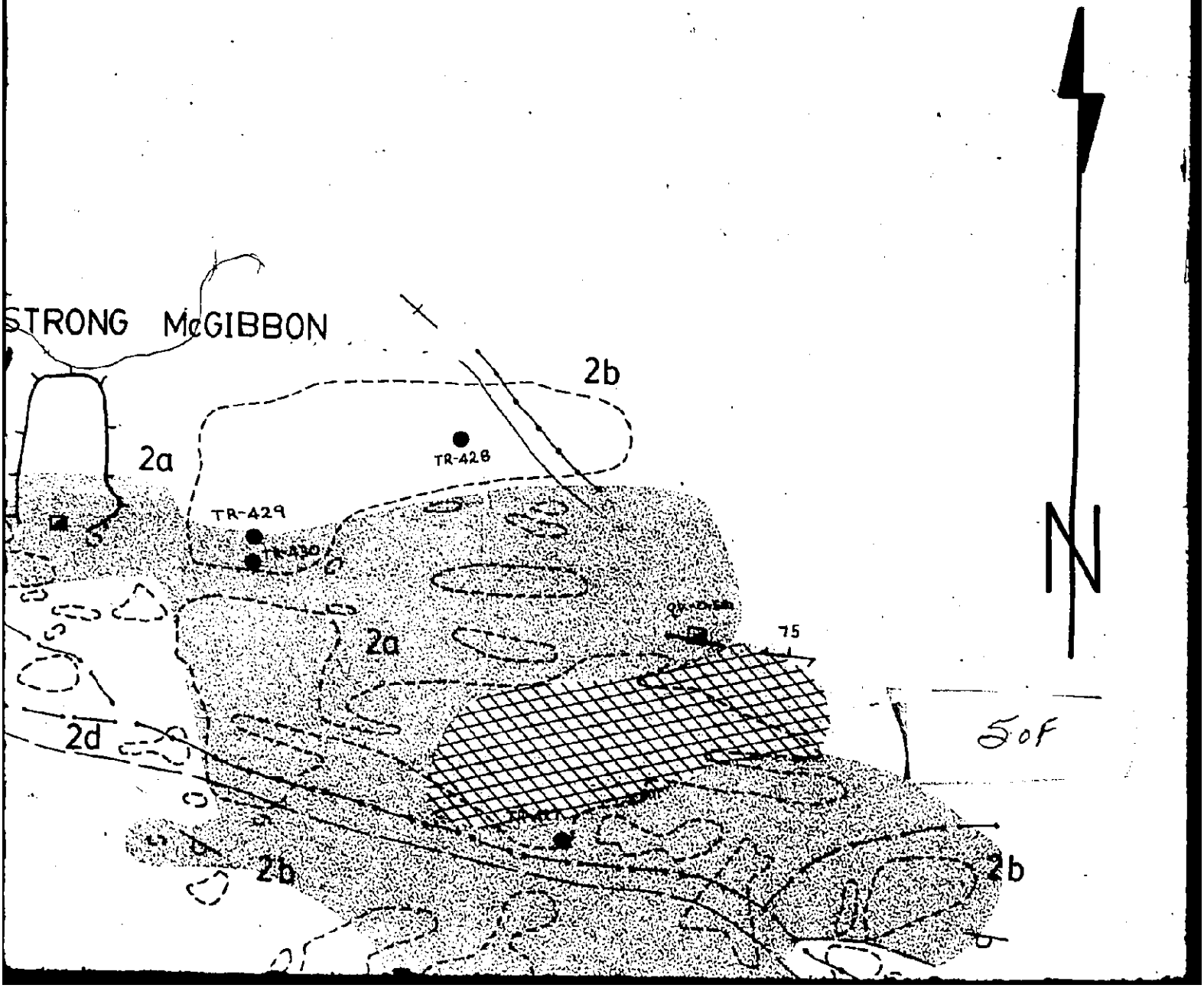

5 of

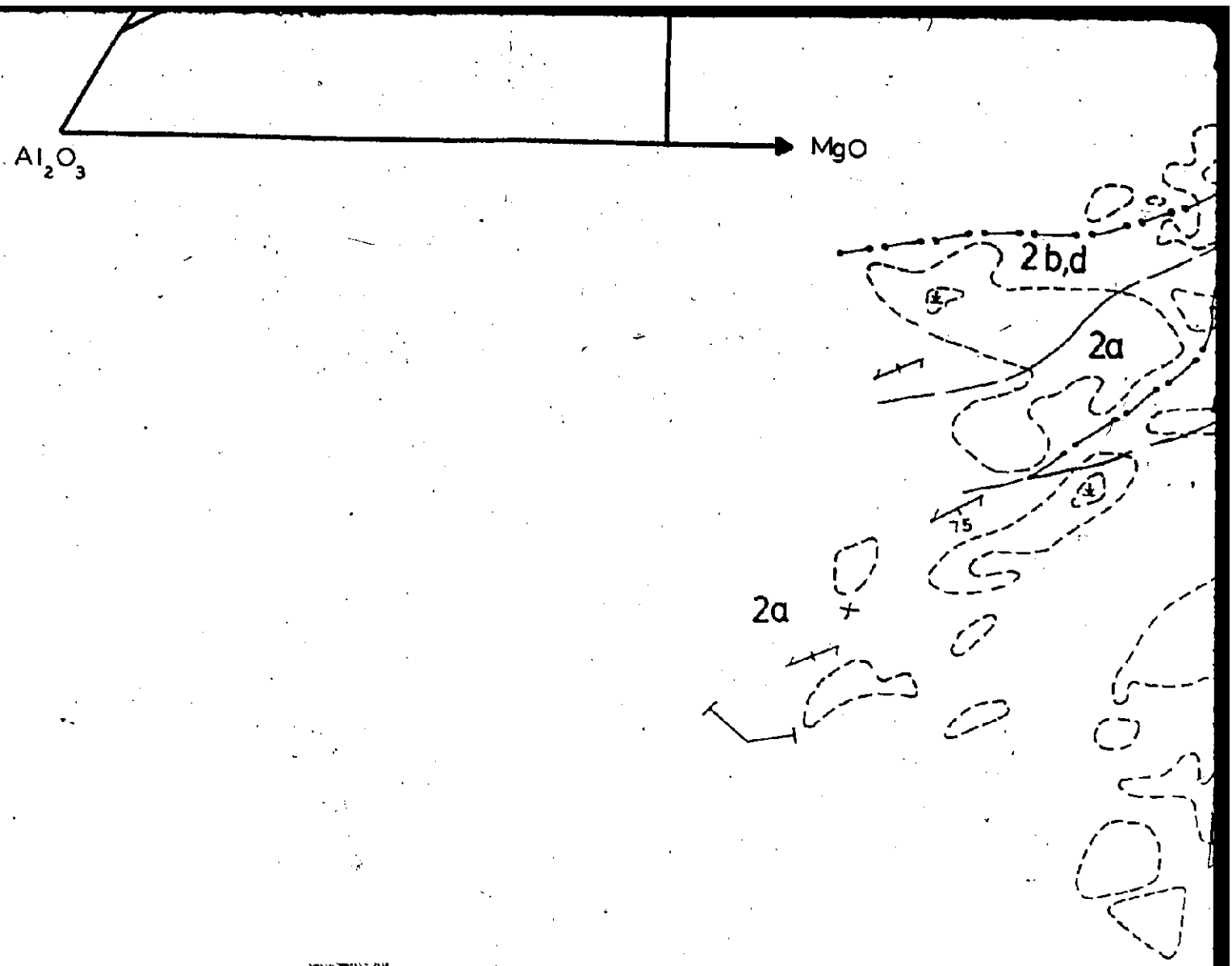

Pervasive carbonatization

Chloritic alteration

Geology
modifie

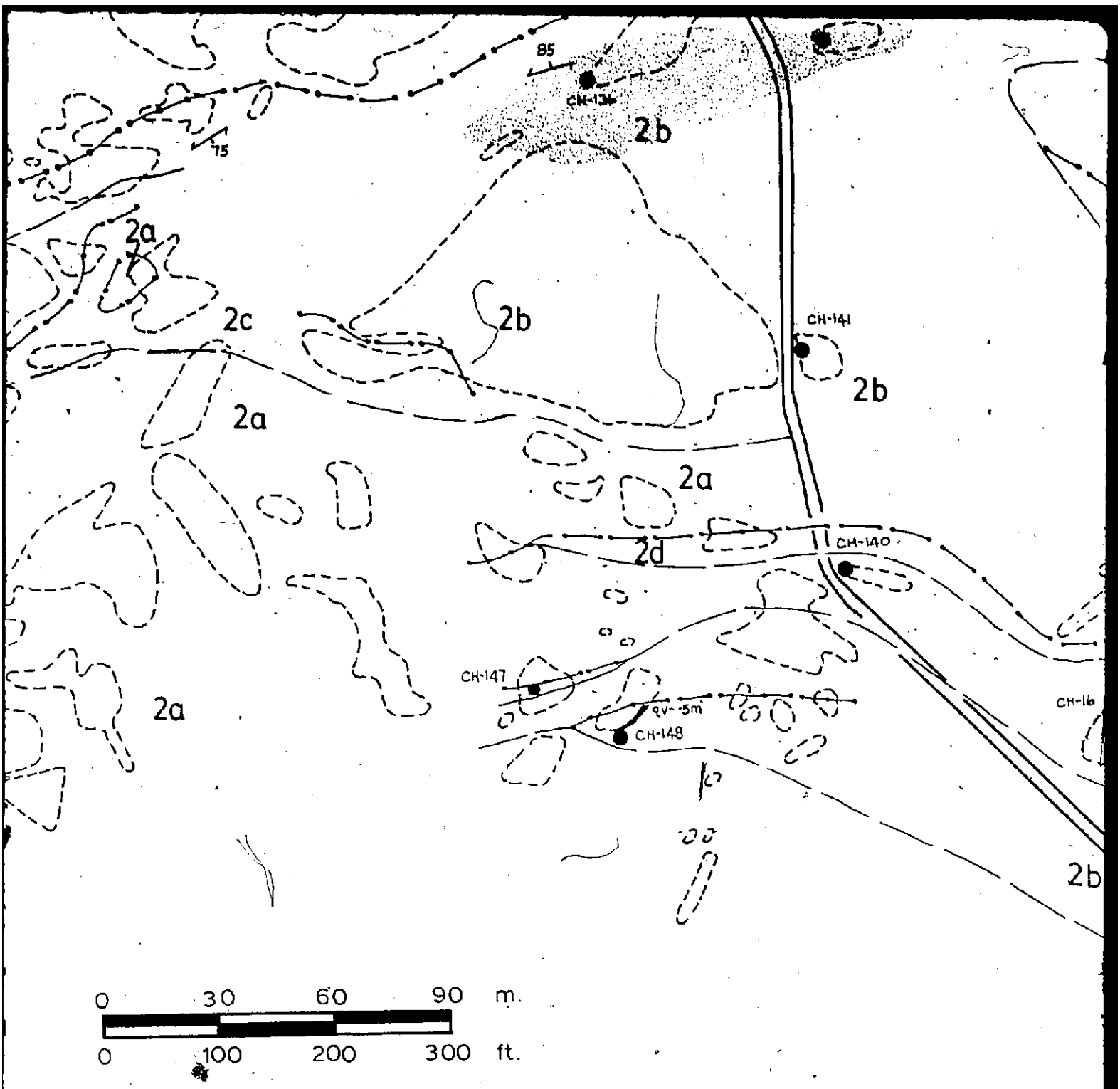

eology by J.A. Fyon 1978
odified after Ferguson(1960)

7 of

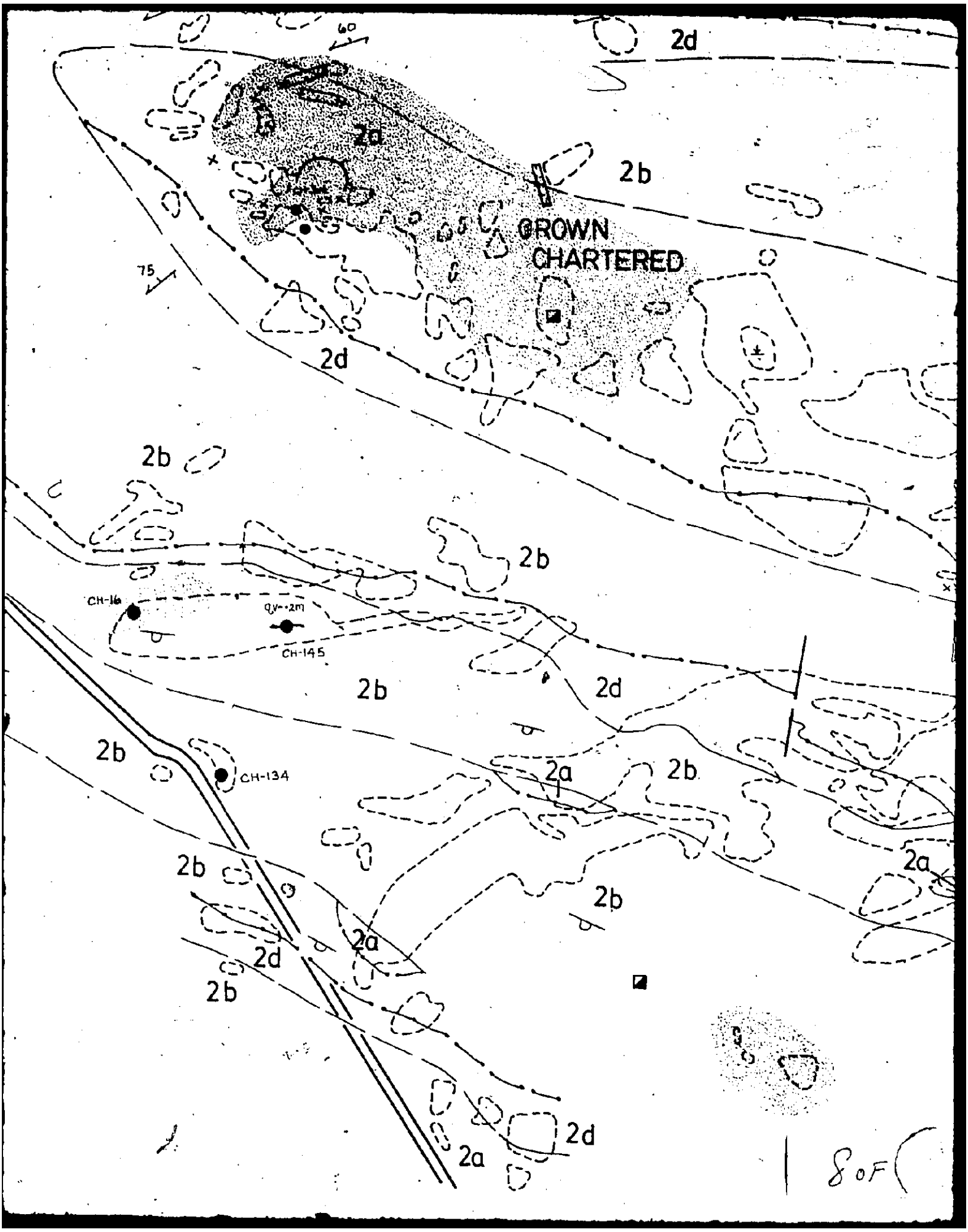
60
2d
2d
2b
CROWN
CHARTERED
75
2d
2b
2b
CH-16
QV-+2m
CH-145
2b
2d
2b
2a
2b
CH-134
2a
2b
2b
2d
2a
2b
2d
2a
8 OF

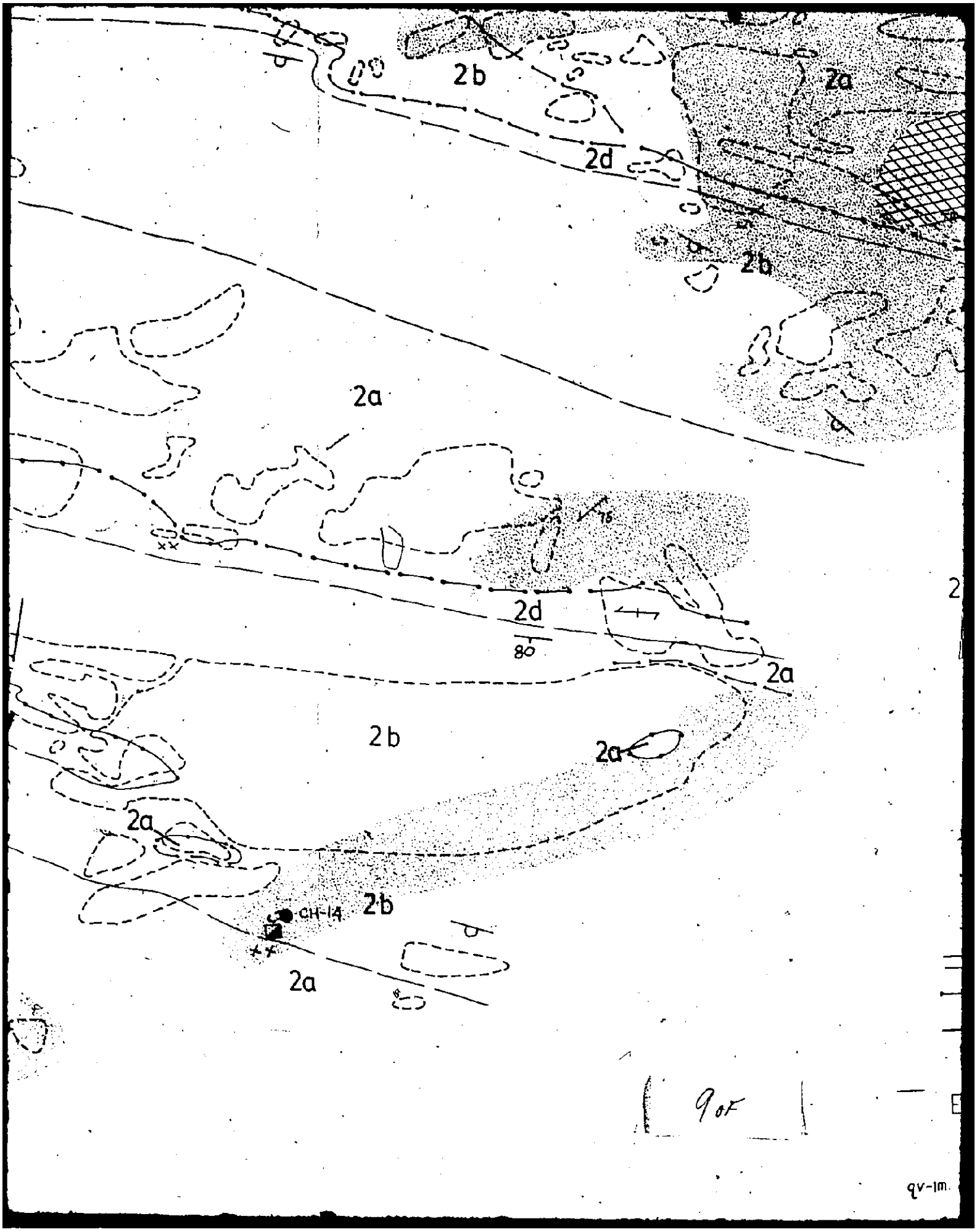
2b
2a
2d
2b
2a
2d
80
2a
2b
2a
2a
CH-14
2b
2a
9 of

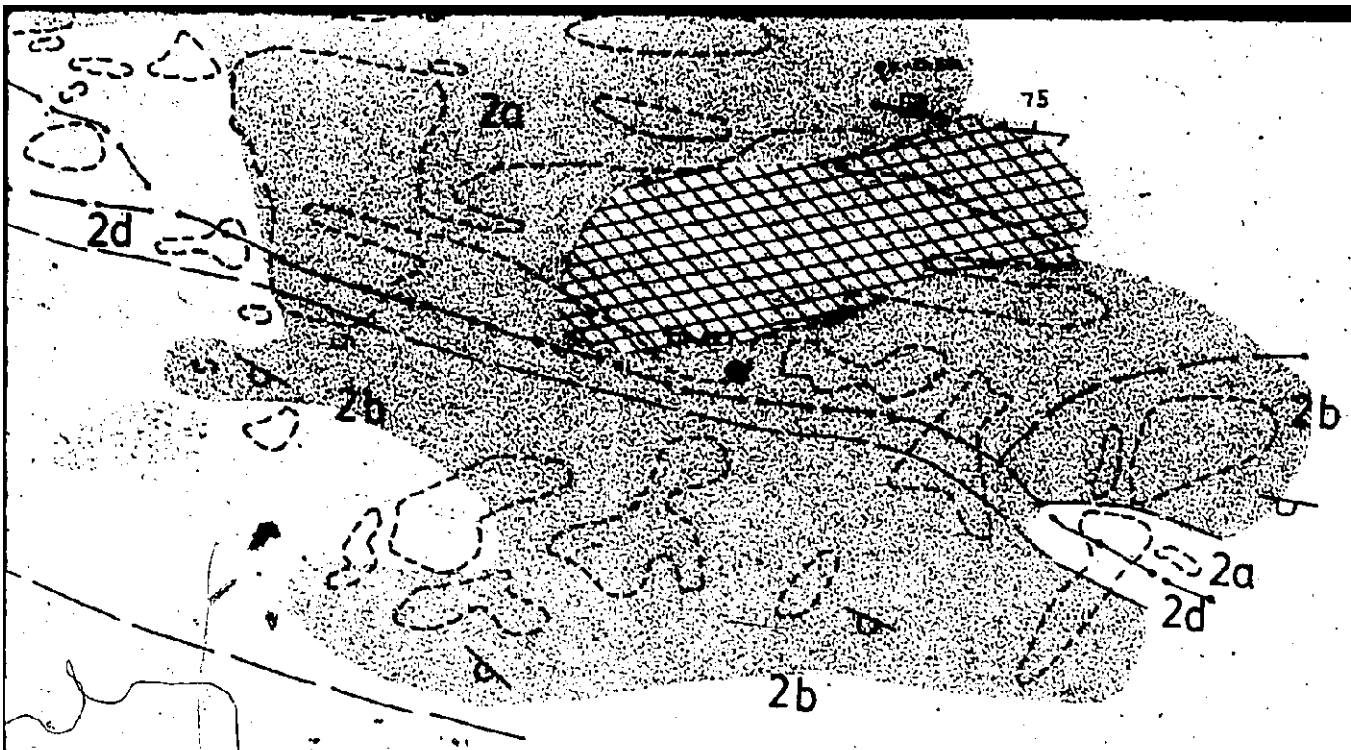

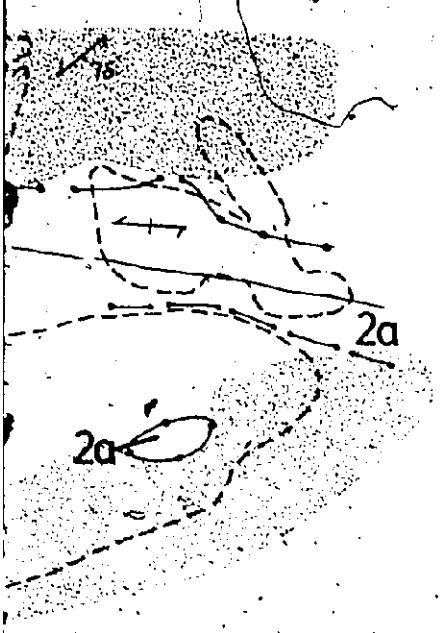

LEGEND

2 Magnesium Tholeiitic Metavolcanics

- a Massive
- b Pillowed
- c Megapillows
- d Flow top breccia

Pillow attitude

70 Foliation

80 Bedding

20 Joint attitude

Flow contact

Intraflow facies contact

Fault

Sample location

Pit

Shaft

qv-lm. Quartz vein

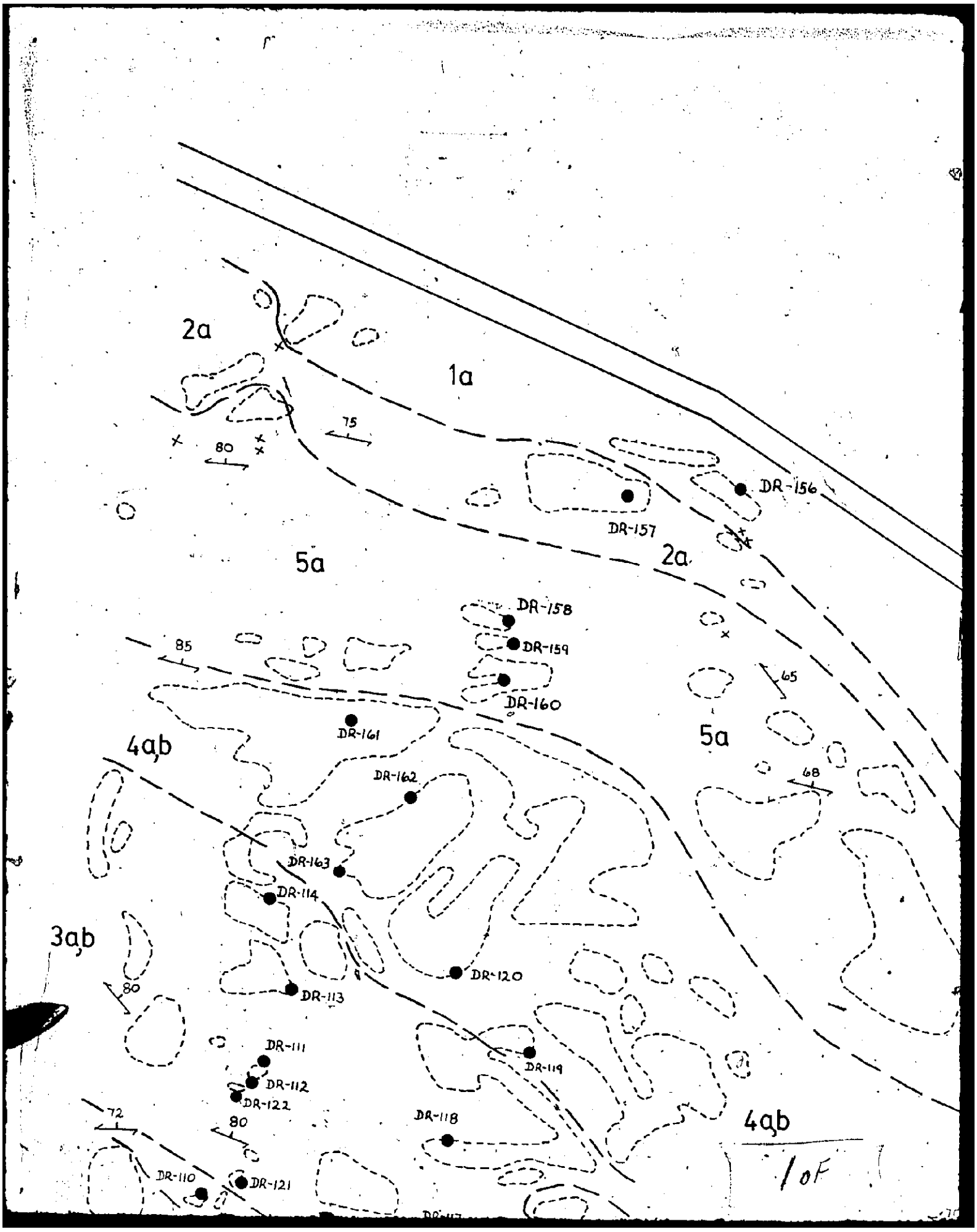
2a
1a
75
80
DR-156
DR-157
5a
2a
DR-158
DR-159
DR-160
85
65
DR-161
4ab
5a
DR-162
68
DR-163
DR-114
3ab
80
DR-120
DR-113
DR-111
DR-112
DR-122
DR-119
72
80
DR-118
4ab
DR-110
DR-121
1 of

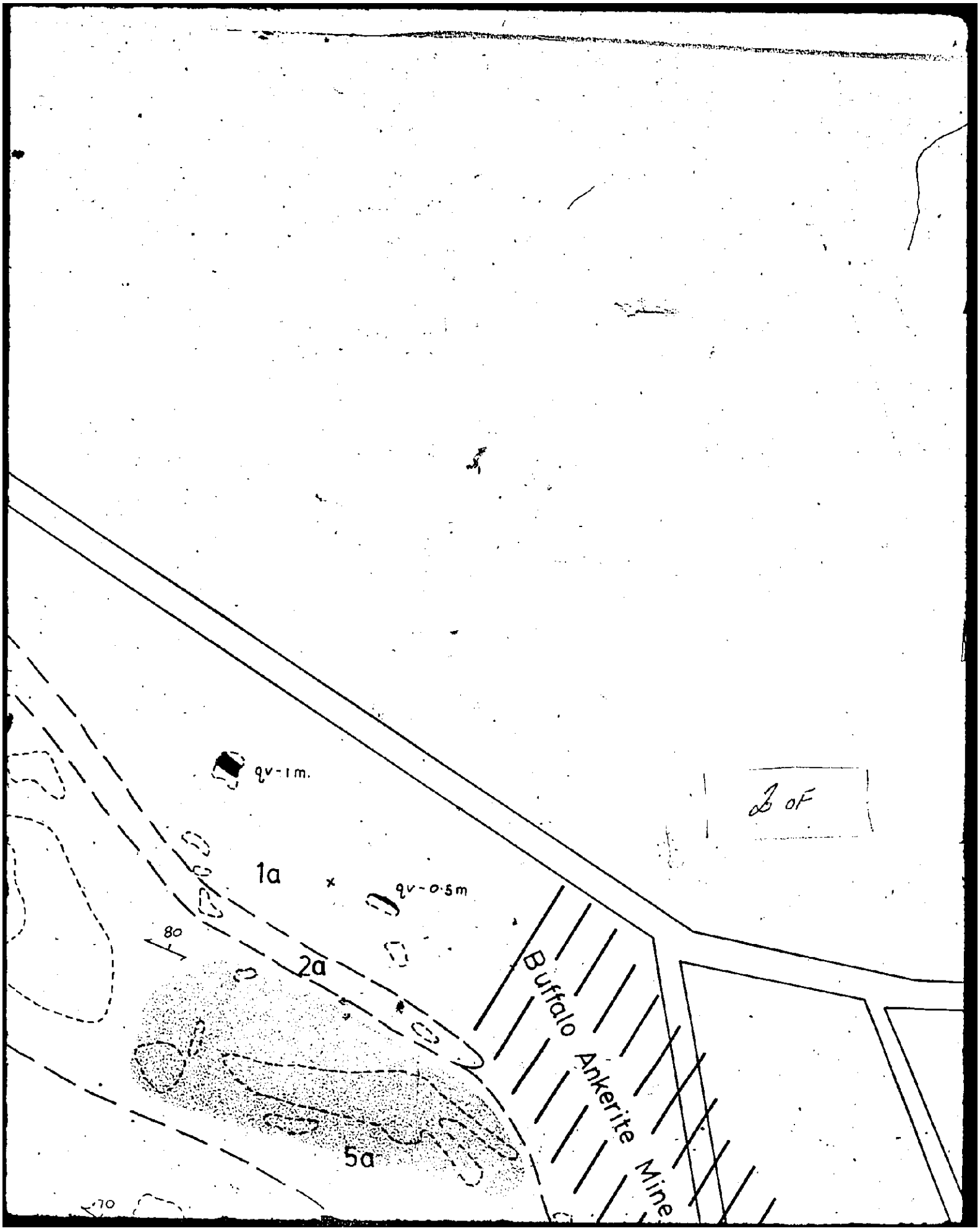
qv-1m.
1a
qv-0.5m
80
2a
5a
70
Buffalo Ankerite Mine
2 OF

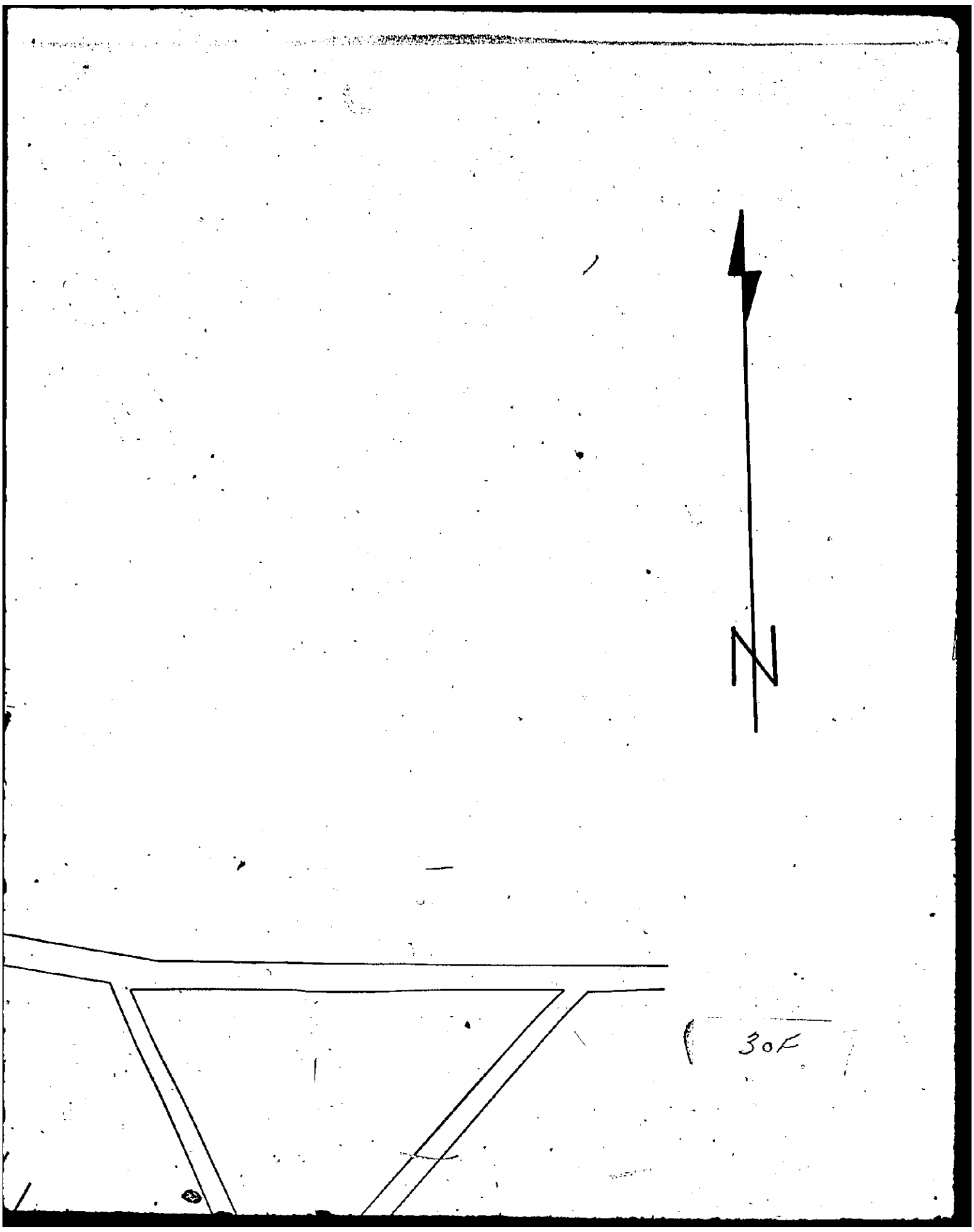
N

Map 7

BUFFALO ANKERITE MINE AREA
DELORO TWP. STUDY AREA

LEGEND

5 Iron Tholeiitic Metavolcanics
- a Unsubdivided
- b Pillowed

4 Magnesium Tholeiitic Metavolcanics
- a Massive
- b Pillowed

3 Volcaniclastic Metasediments
- a Conglomerate
- b Argillite

3A Chemical Metasediments
- a Auriferous cherty dolomite
- b Siliceous limestone
- c Chert

2 Calc Alkalic Metavolcanics
- a Quartz-feldspar-sericite schist

1 Komatiitic Metavolcanics
- a Ultramafic
- b Mafic

4 of

- Pillow attitude
- Bedding
- Foliation
- Lineation
- Flow contact

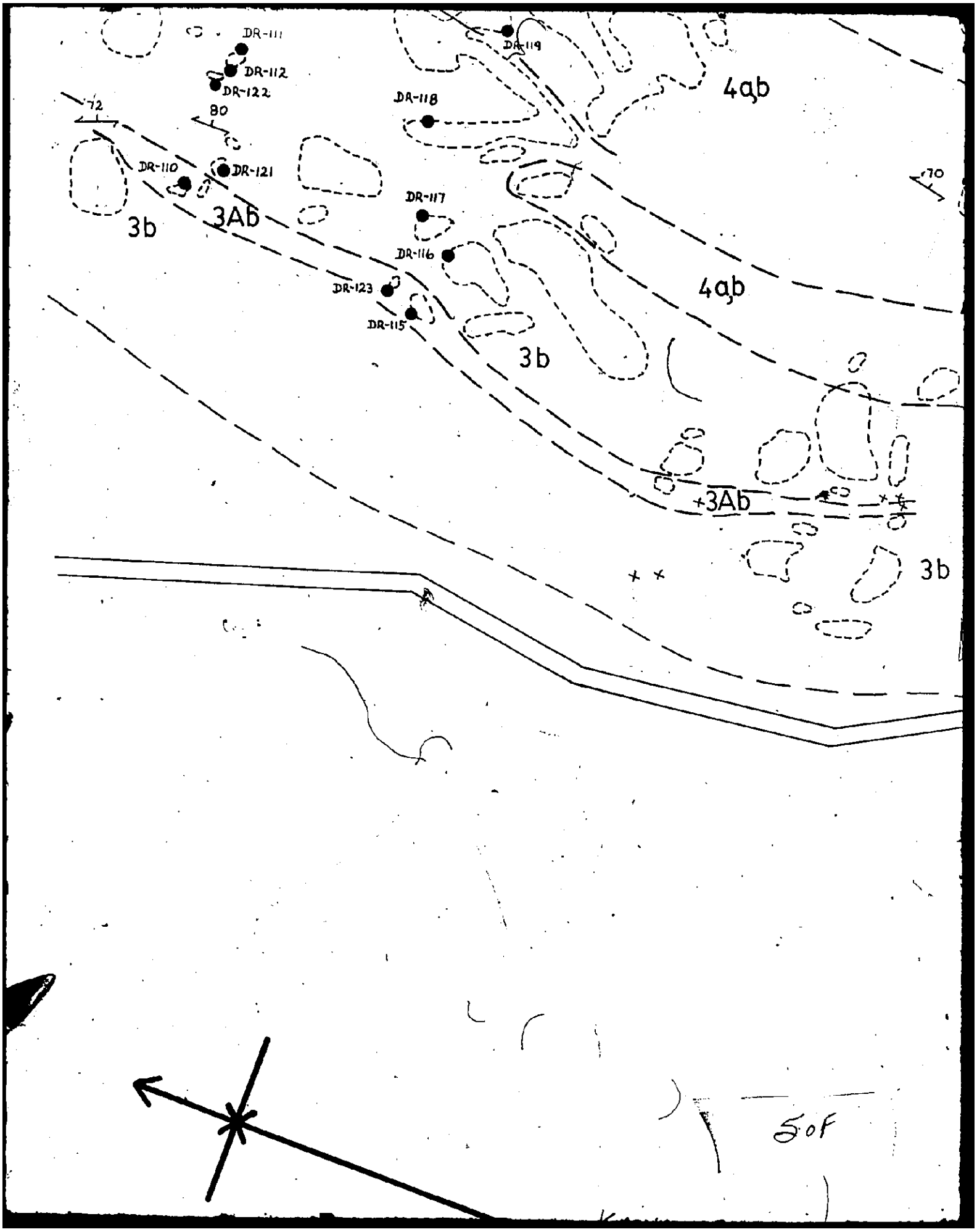
DR-111
DR-112
DR-122
DR-119
DR-118
DR-110
DR-121
DR-117
DR-116
DR-123
DR-115
72
80
70
3b
3Ab
4ab
4ab
3b
+3Ab
3b
5 of

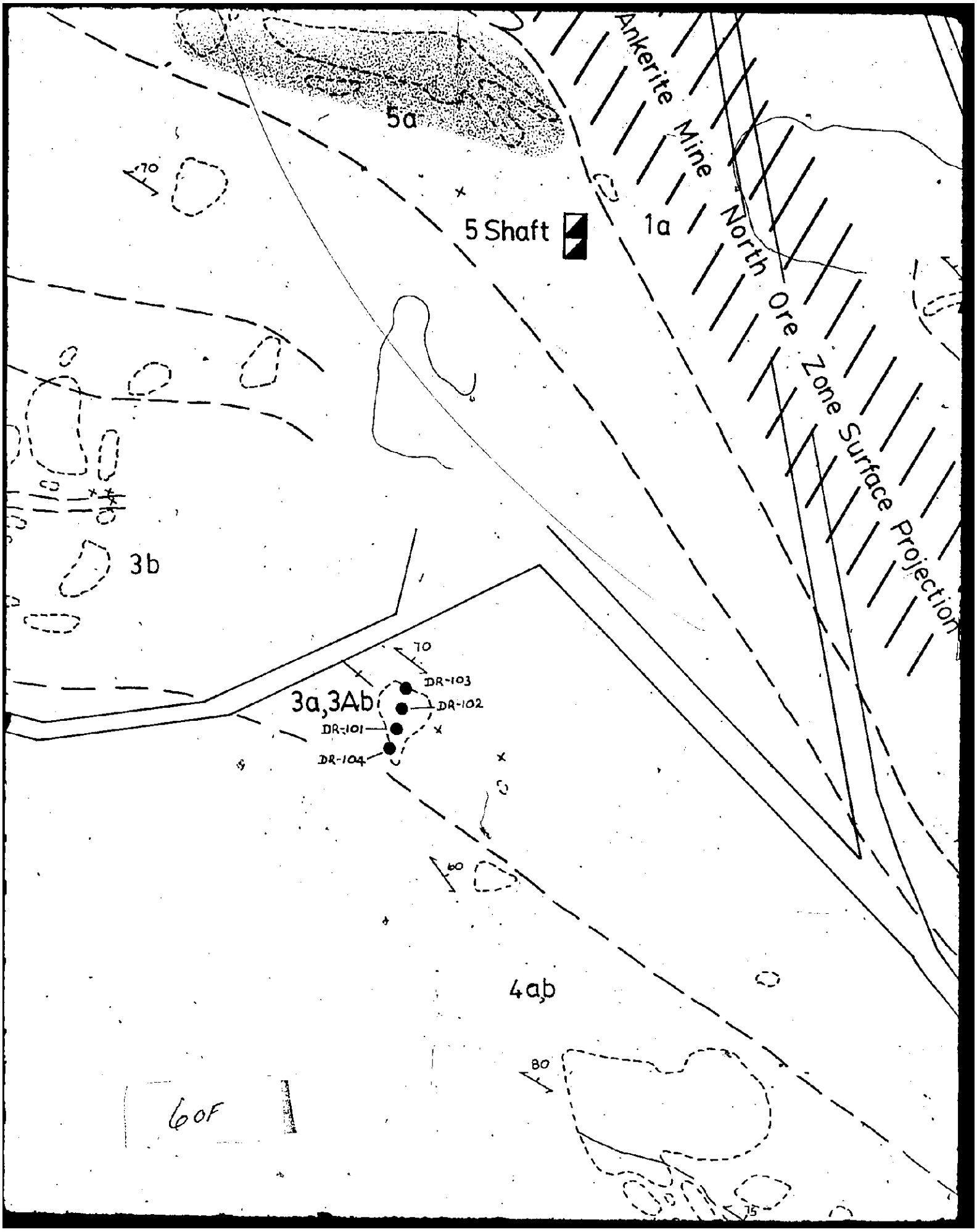
Ankerite Mine
North Ore Zone Surface Projection
5a
5 Shaft
1a
3b
3a,3Ab
DR-103
DR-102
DR-101
DR-104
4a,b
70
60
80
75
6 of

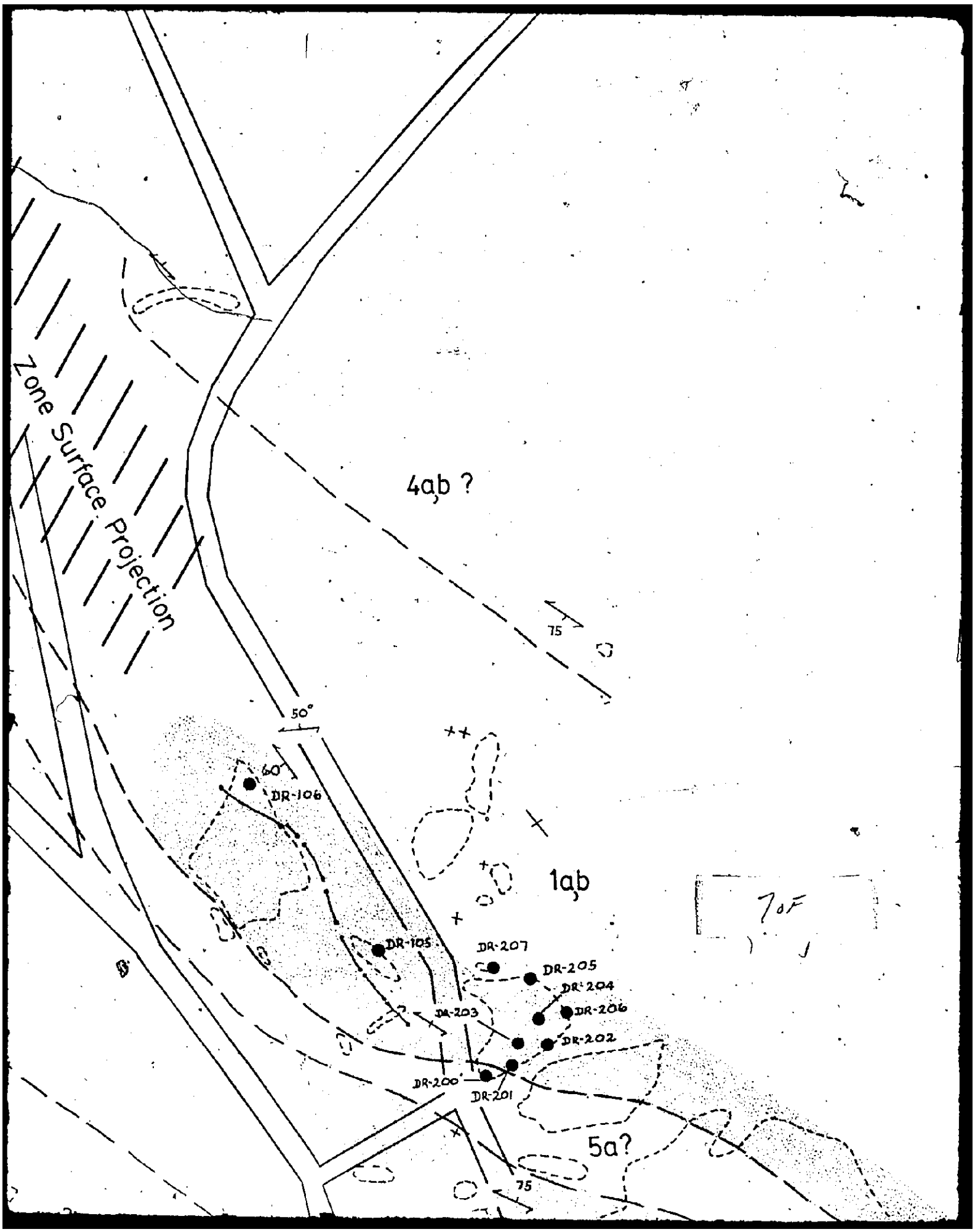
Zone Surface Projection
4a,b ?
75
50°
60
DR-106
1a,b
DR-105
DR-207
DR-205
DR-204
DR-206
DR-203
DR-202
DR-200
DR-201
5a?
75

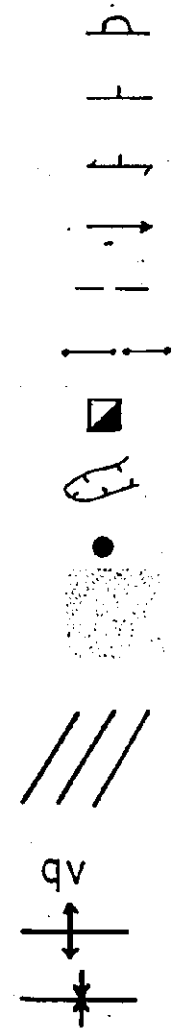

Pillow attitude
Bedding
Foliation
Lineation
Flow contact
Intraflow facies contact
Shaft
Open pit
Sample location
Pervasive carbonatization

Ore zone surface projection using a composite level plan

qv Quartz vein

Anticline

Syncline

0 30 60 90 m.

0 100 200 300 ft.

Geology by J.A. Fyon 1977-78
modified after Ferguson (1958 a,b)

8 of

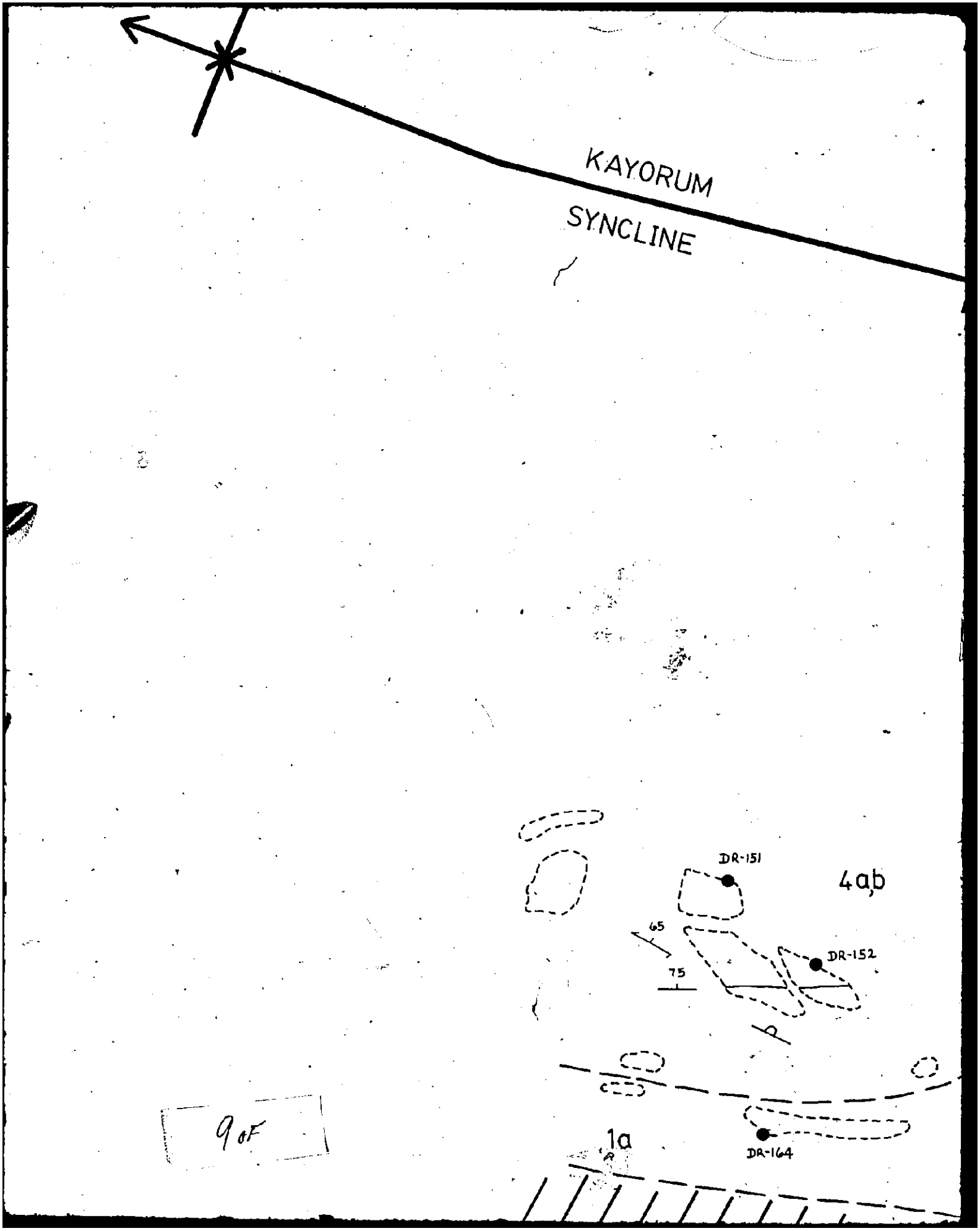

9 OF

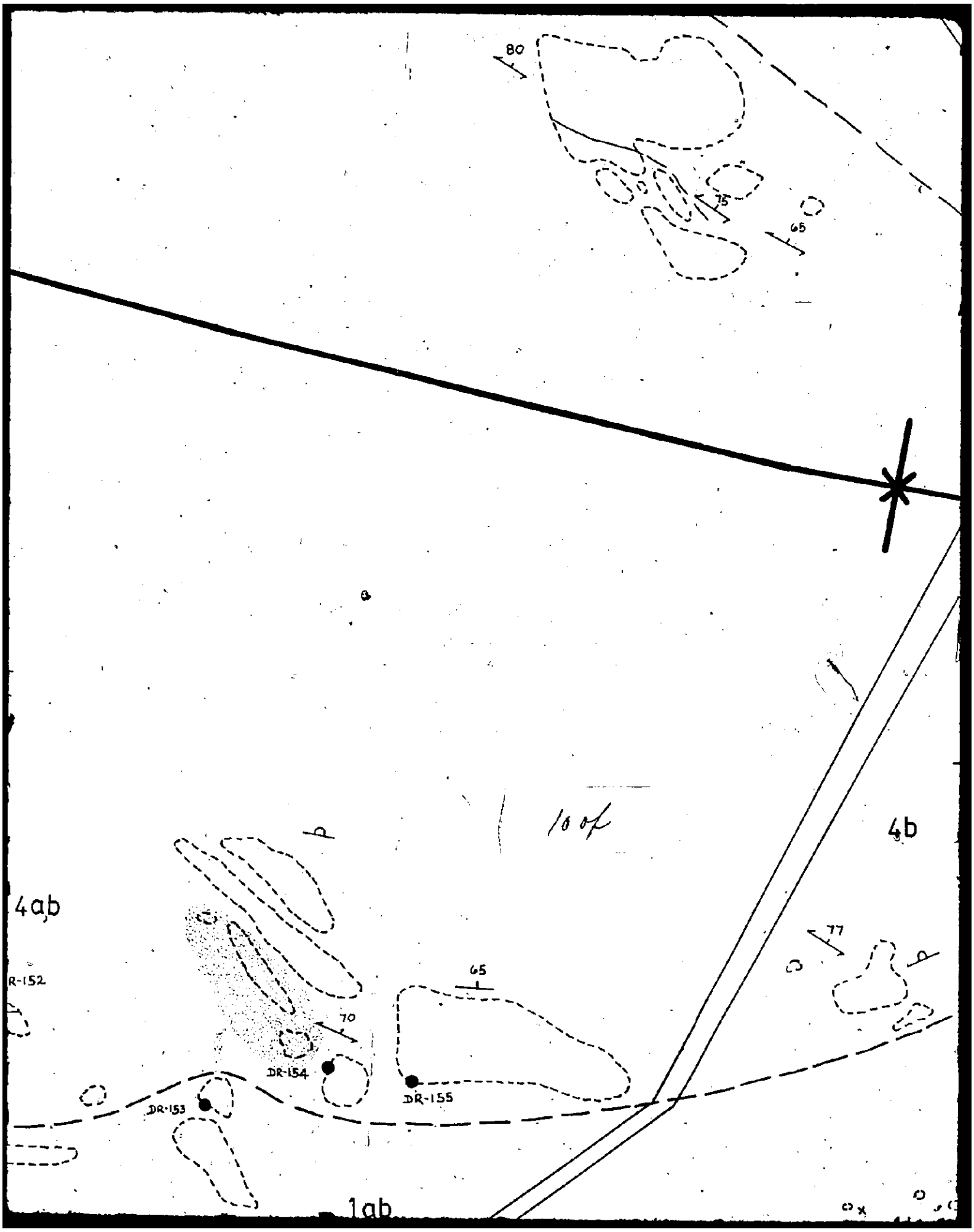
80
75
65
10 of
4b
4a,b
77
65
70
DR-154
DR-155
DR-153
R-152
1ab

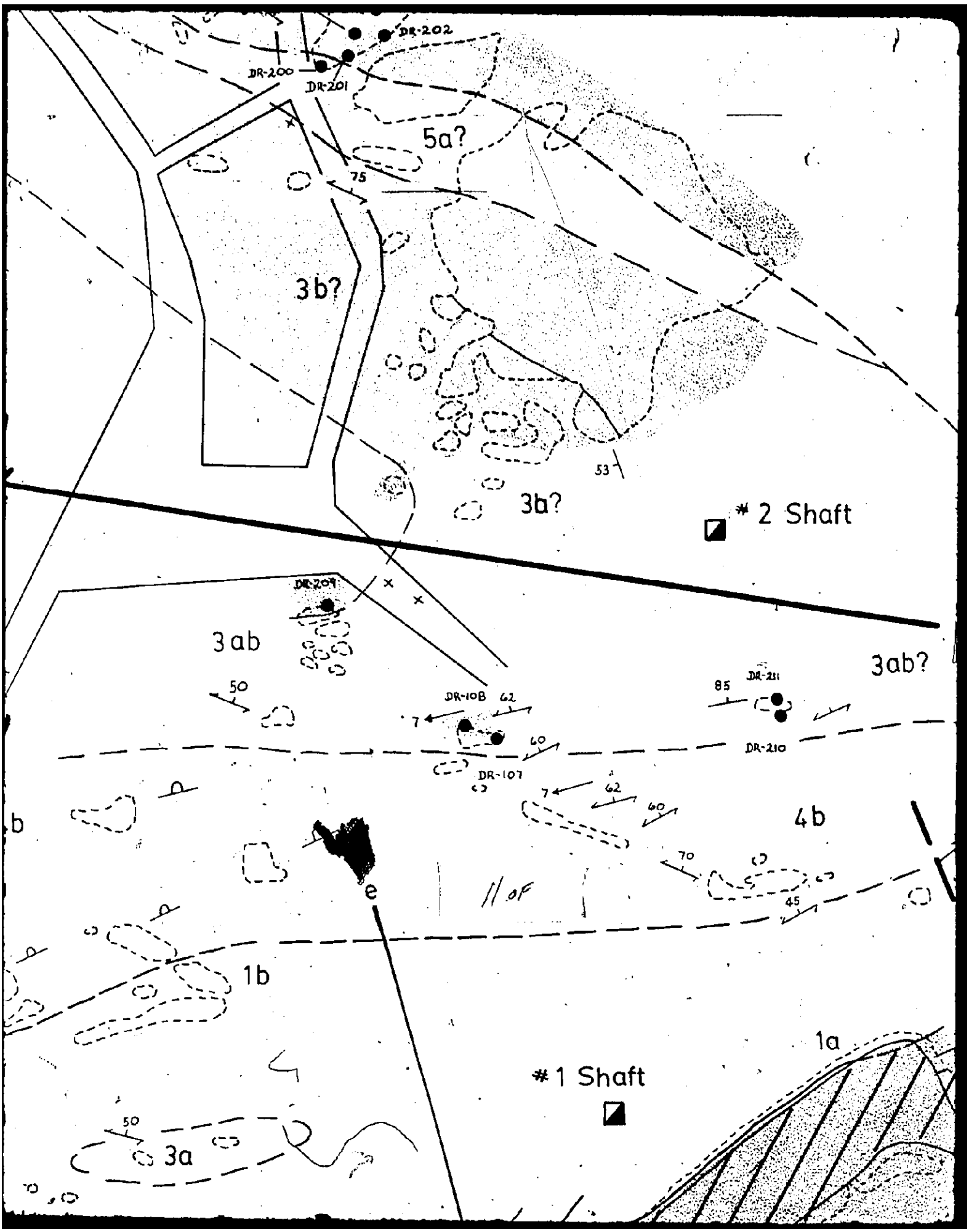
DR-202
DR-200
DR-201
5a?
75
3b?
53
3b?
2 Shaft
DR-209
3ab
50
3ab?
DR-211
85
DR-108
62
7
40
DR-210
DR-107
7
62
60
4b
70
45
b
e
// OF
1b
1a
1 Shaft
50
3a

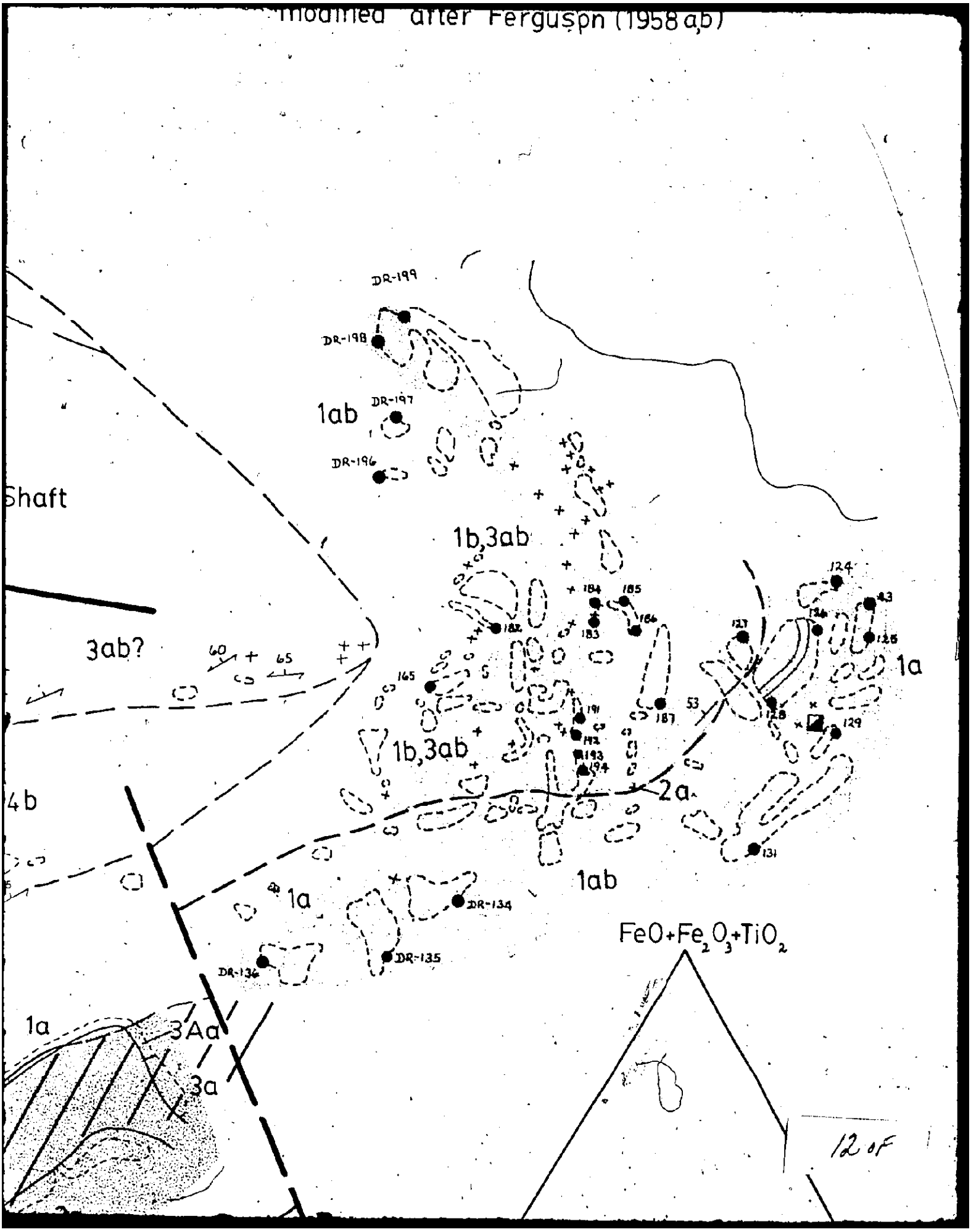
Modified after Ferguson (1958 a,b)
DR-199
DR-198
DR-197
DR-196
1ab
Shaft
1b,3ab
3ab?
60
65
184
185
182
183
164
165
191
187
53
192
193
194
1b,3ab
2a
124
123
134
125
1a
128
129
131
4b
1ab
1a
DR-134
DR-135
DR-136
1a
3Aa
3a
FeO+Fe2O3+TiO2
12 of

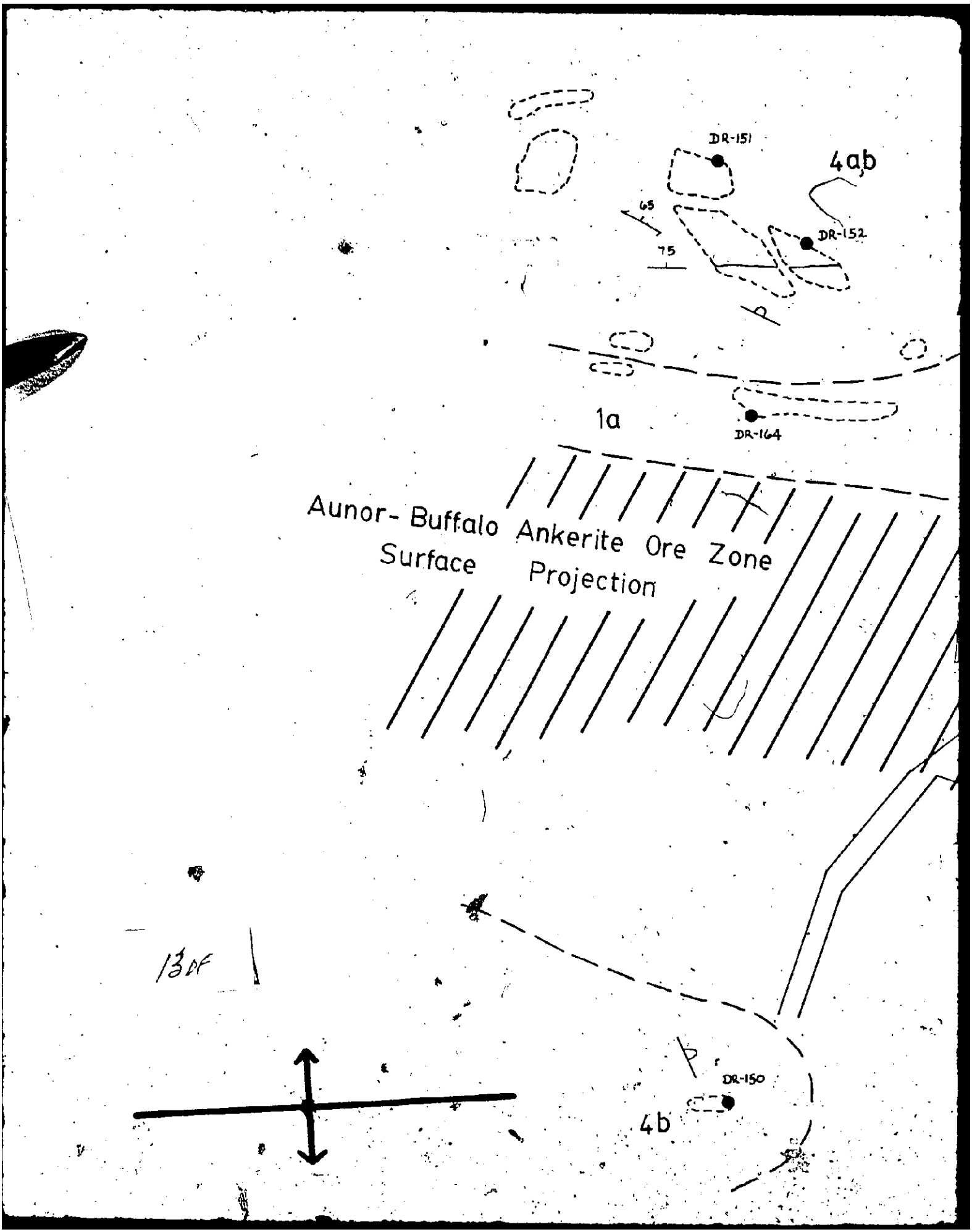
DR-151
4a,b
65
75
DR-152
1a
DR-164
Aunor- Buffalo Ankerite Ore Zone
Surface Projection
13DF
DR-150
4b

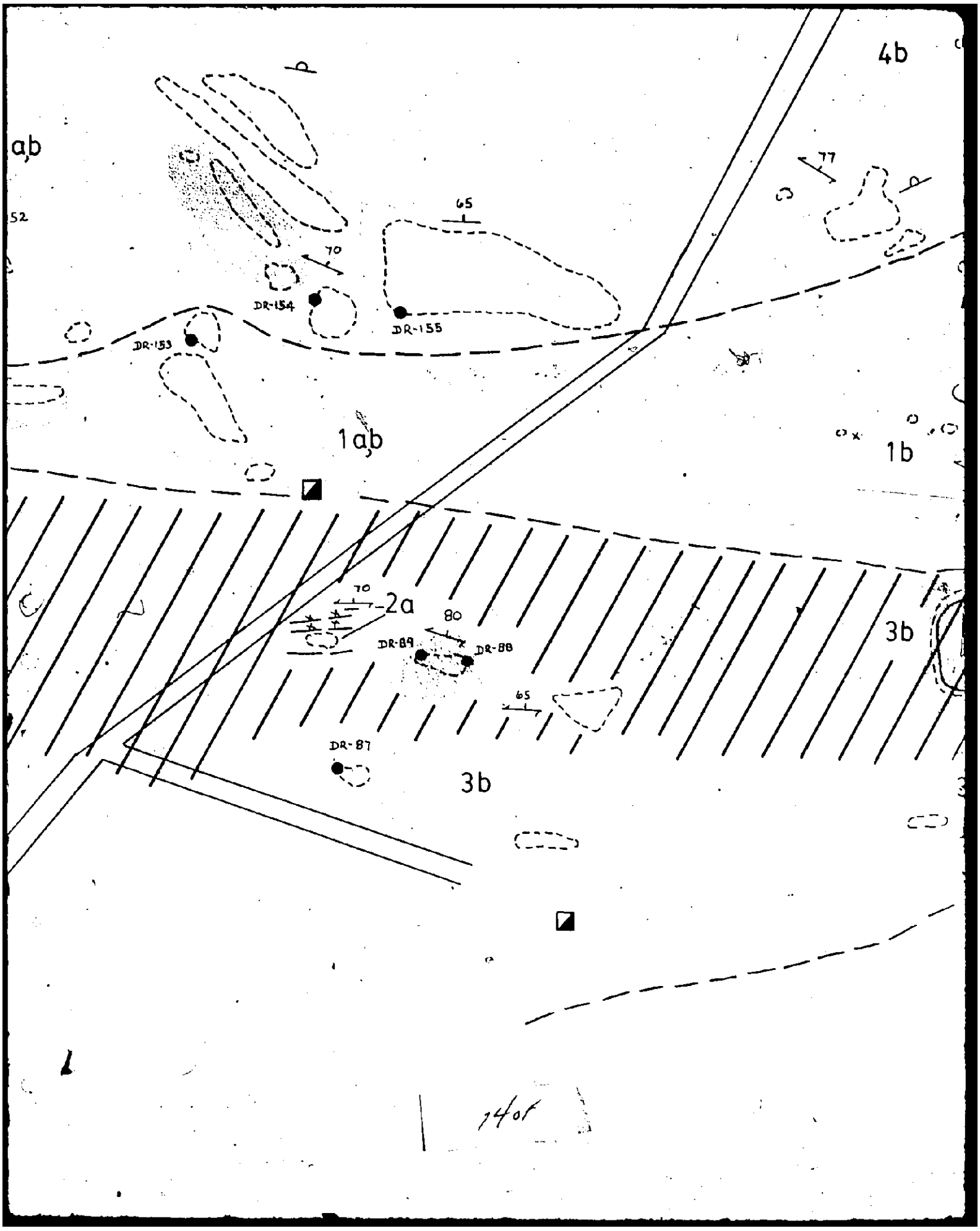
4b
a,b
52
77
65
70
DR-154
DR-155
DR-153
1a,b
1b
70
2a
80
DR-89
DR-88
3b
65
DR-87
3b

14 of

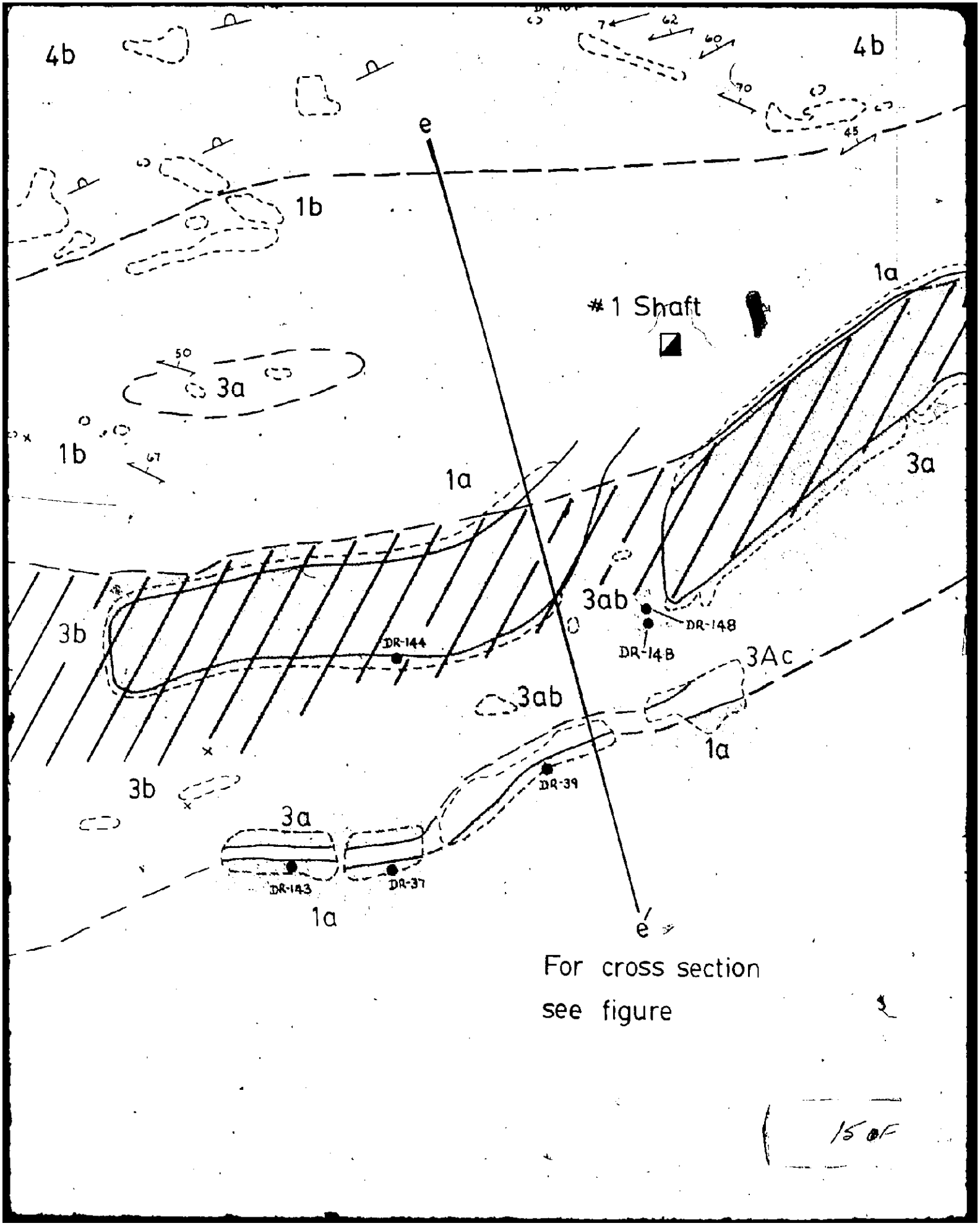
4b
4b
e
1b
1a
1 Shaft
3a
1b
1a
3a
3b
3ab
DR-148
DR-14B
DR-144
3Ac
3ab
1a
3b
DR-39
3a
DR-143
DR-37
1a
e'
For cross section
see figure

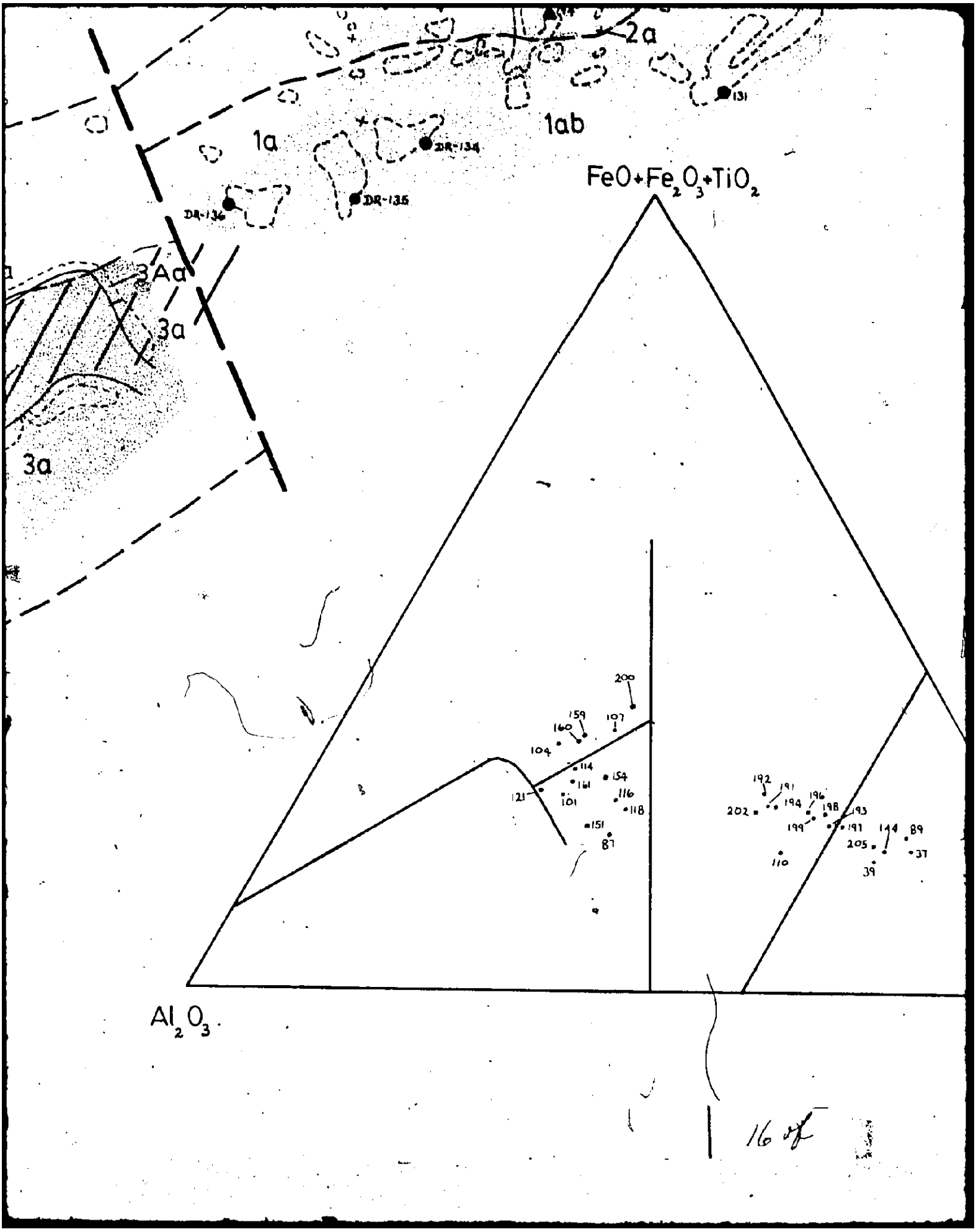
2a
1ab
131
1a
DR-134
DR-135
DR-136
3Aa
3a
3a
FeO+Fe2O3+TiO2
200
159
160
107
104
114
154
161
121
101
116
118
151
87
192
191
194
196
198
202
193
199
191
144
89
205
37
110
39
Al2O3

16 of

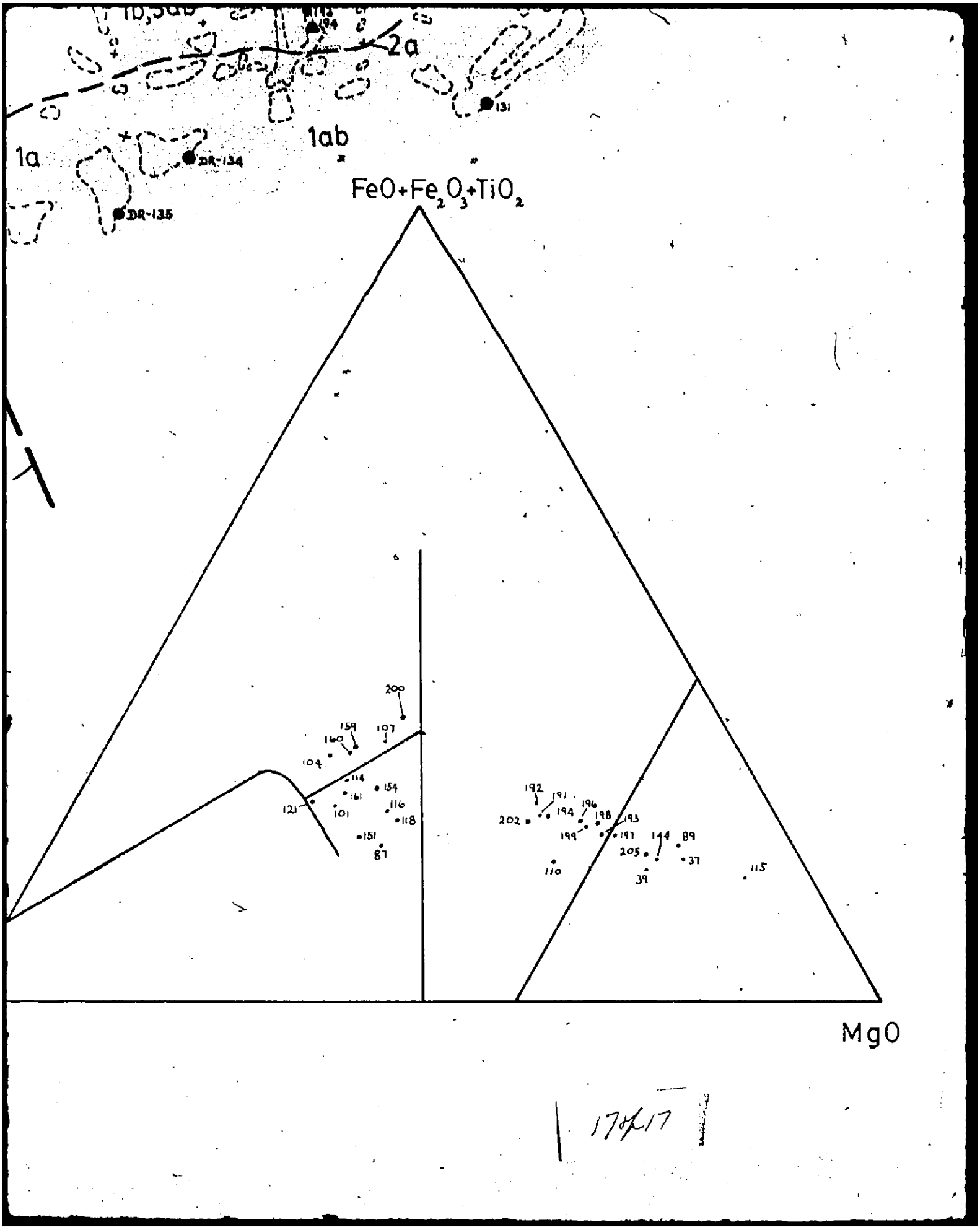
1b,3ab
2a
1ab
1a
DR-134
DR-135
131
$FeO+Fe_2O_3+TiO_2$
200
159
160
107
104
114
161
154
121
101
116
118
151
87
192
191
194
196
198
193
202
199
191
144
89
205
37
110
39
115
MgO

17417

Map 8
DELNITE MINE AREA
DELORO TWP. STUDY AREA

LEGEND

4 Volcaniclastic Metasediments
- a Argillite

3 Magnesium Tholeiitic Metavolcanics
- a Massive
- b Pillowed

2 Calc Alkalic Metavolcanics
- a Quartz-feldspar-sericite schist

1 Komatiitic Metavolcanics
- a Ultramafic
- b Mafic

4a

- Pillow attitude
- Foliation
- Geological contact
- Shaft
- Sample location
- Pervasive carbonatization

1 of

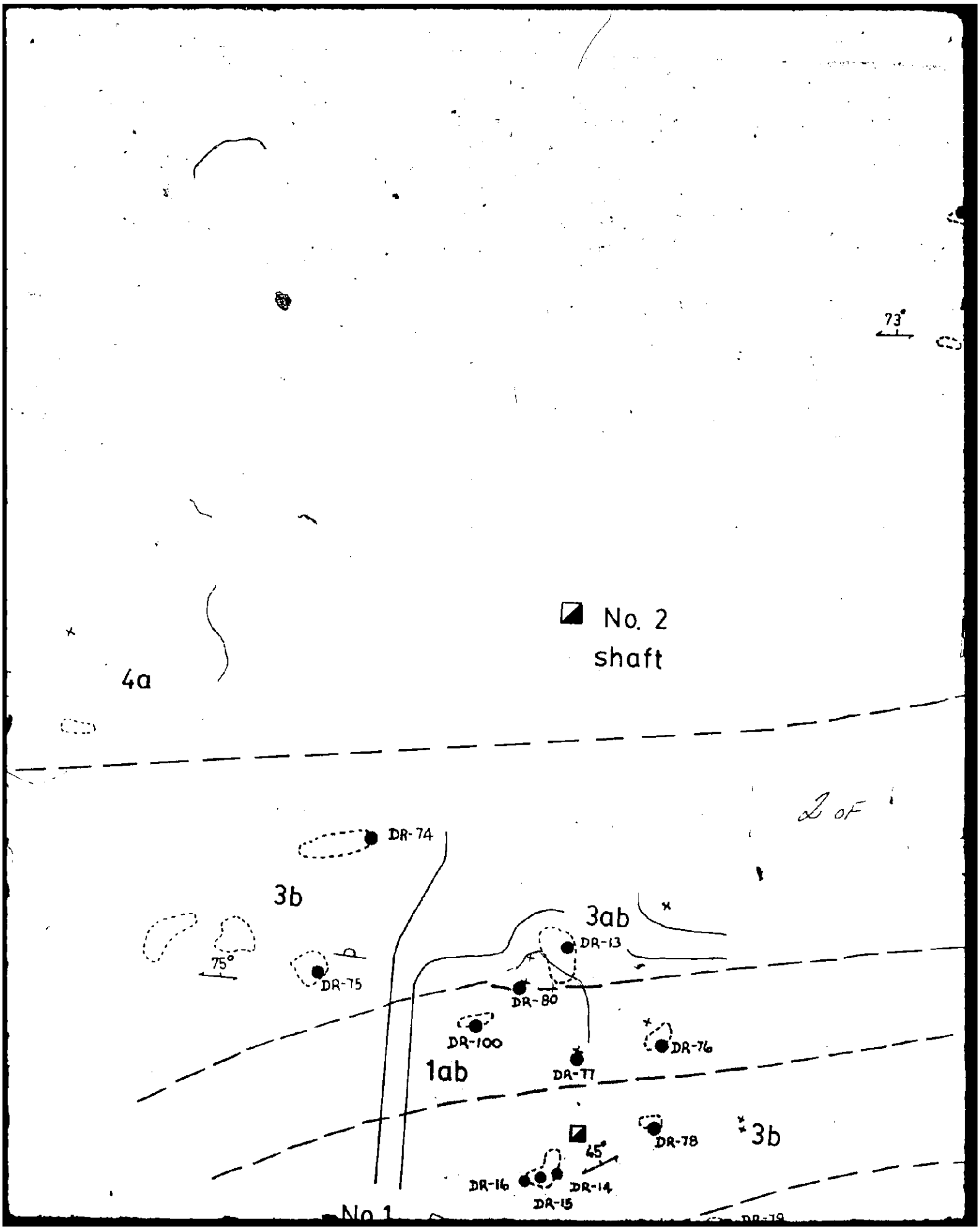
73°
No. 2
shaft
4a
2 OF
DR-74
3b
3ab
75°
DR-75
DR-13
DR-80
DR-100
DR-76
1ab
DR-77
DR-78
3b
45°
DR-16
DR-14
DR-15
No. 1
DR-79

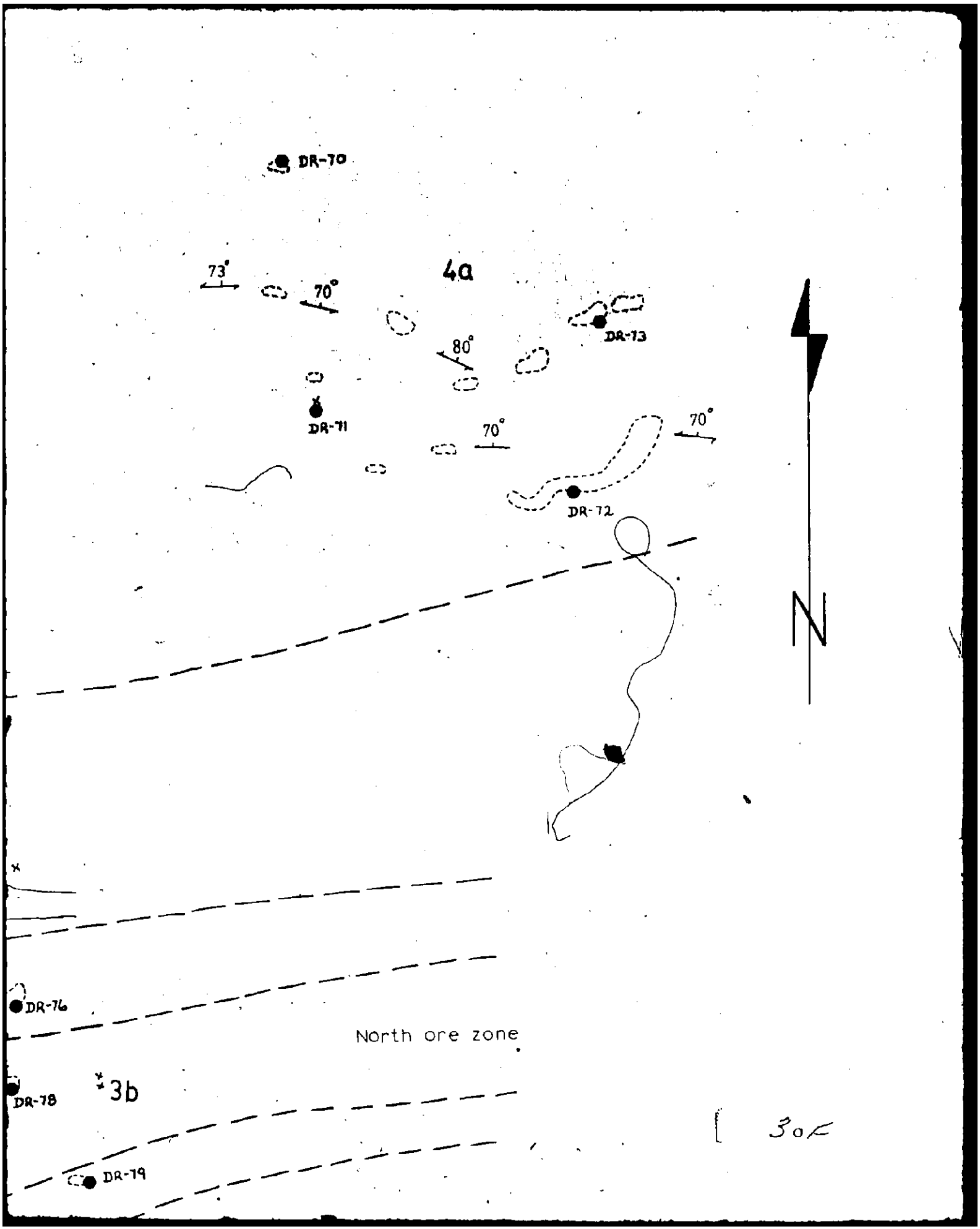
DR-70
73°
70°
4a
80°
DR-73
DR-71
70°
70°
DR-72
N
DR-74
North ore zone
DR-78
3b
DR-79

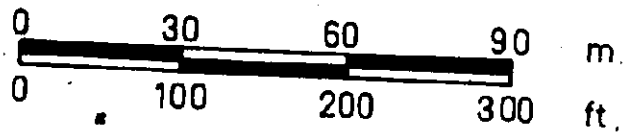

Geology by J A Fyon 1977-78
modified after Ferguson (1958a)

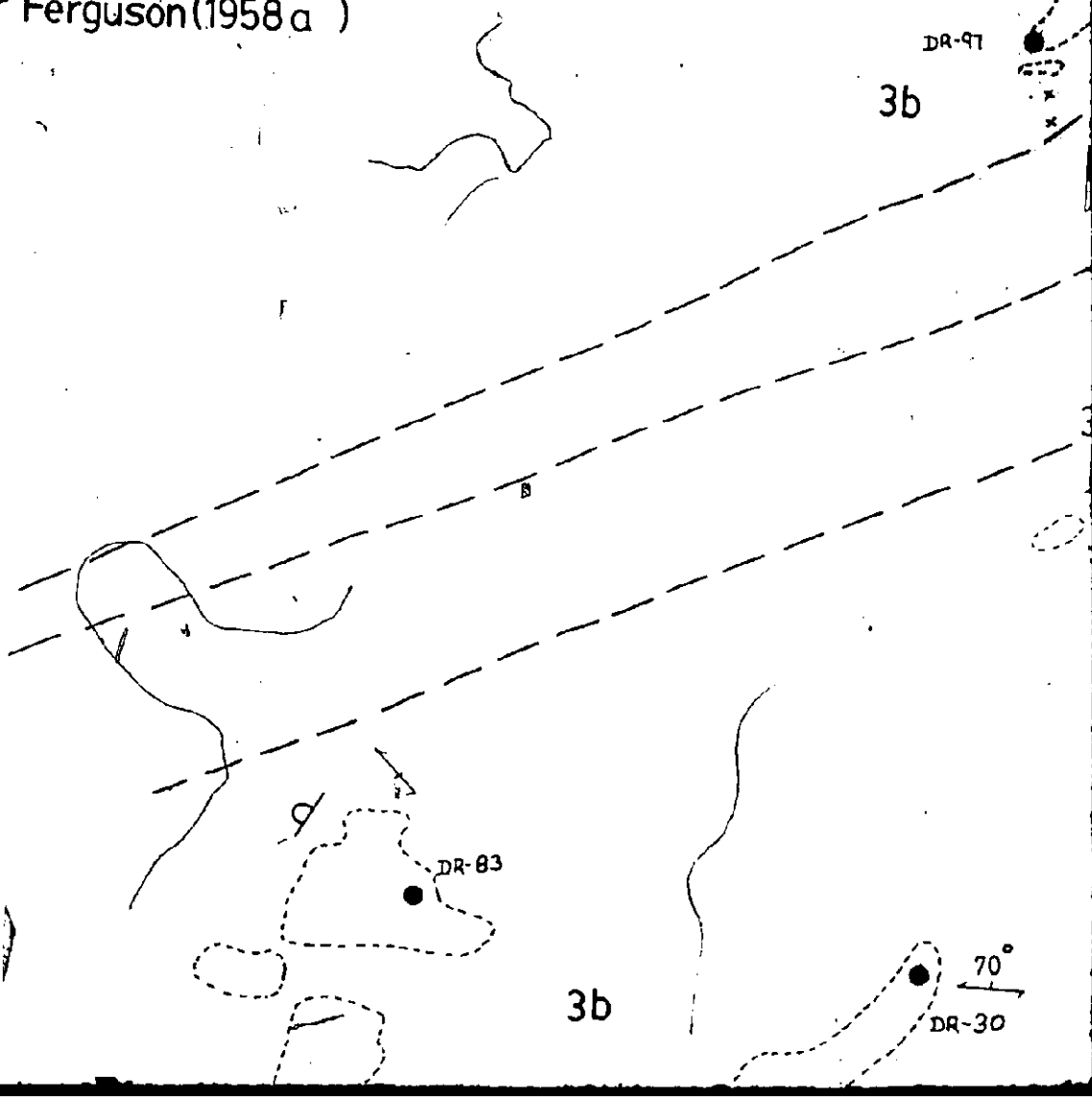

4 of

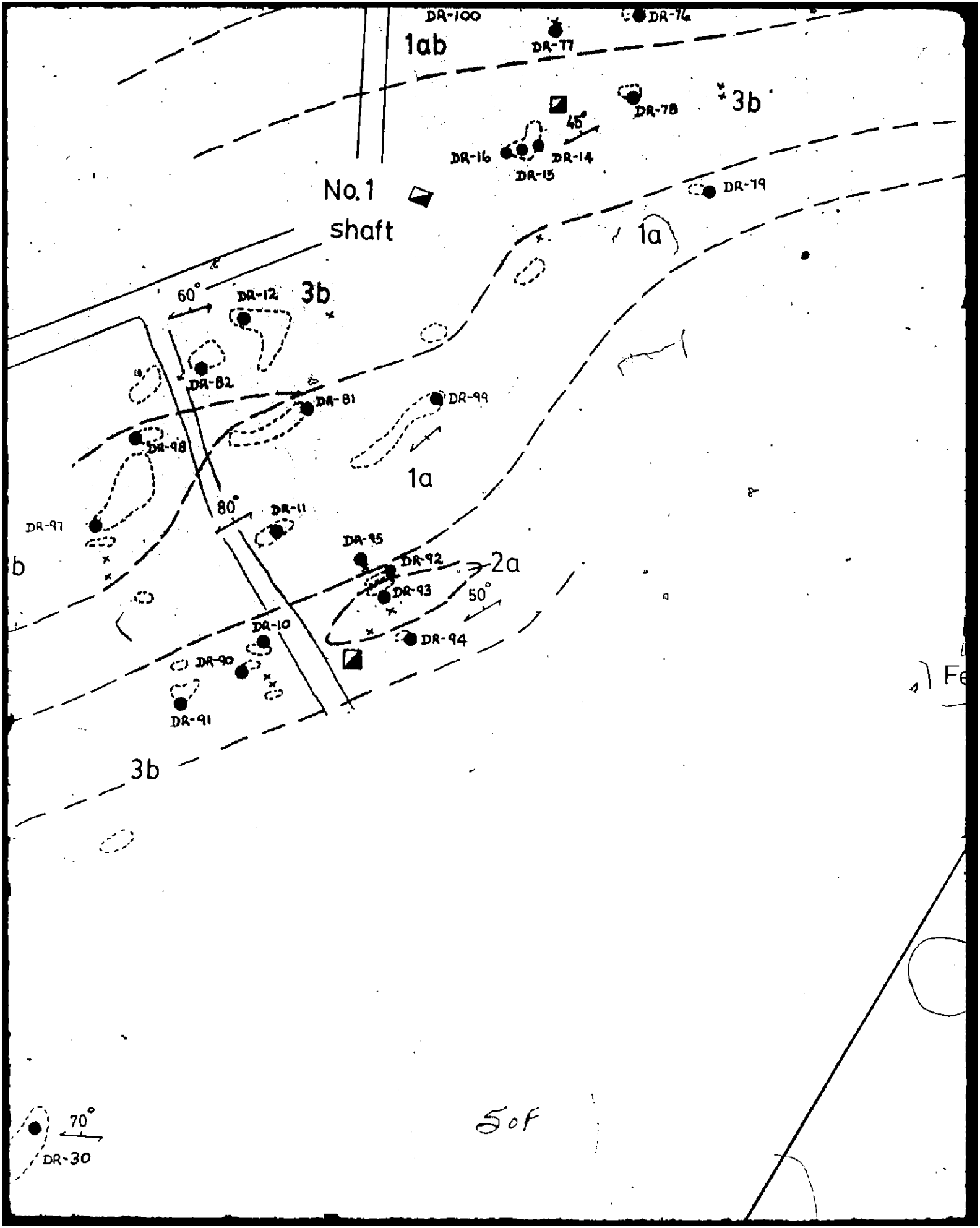
DR-100
DR-76
1ab
DR-77
DR-78
3b
45°
DR-16
DR-14
DR-15
No.1
shaft
DR-79
1a
60°
DR-12
3b
DR-82
DR-81
DR-99
DR-98
1a
80°
DR-11
DR-97
DR-95
DR-92
2a
DR-93
50°
DR-10
DR-94
DR-90
DR-91
3b
70°
DR-30

5 of

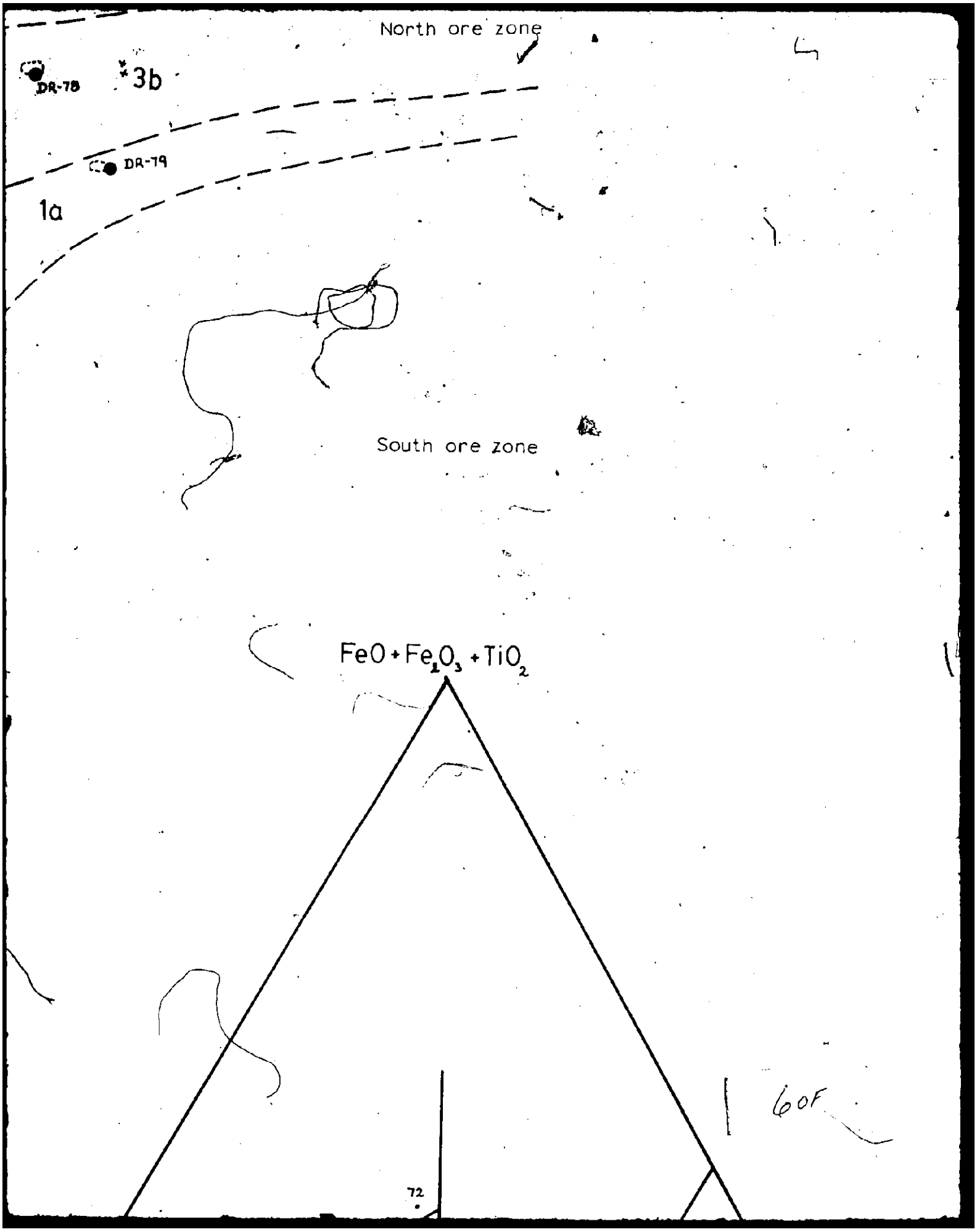
North ore zone
DR-78
3b
DR-79
1a
South ore zone
FeO + Fe2O3 + TiO2
60F
72

Geology by J A Fyon 1977-78
modified after Ferguson (1958a)

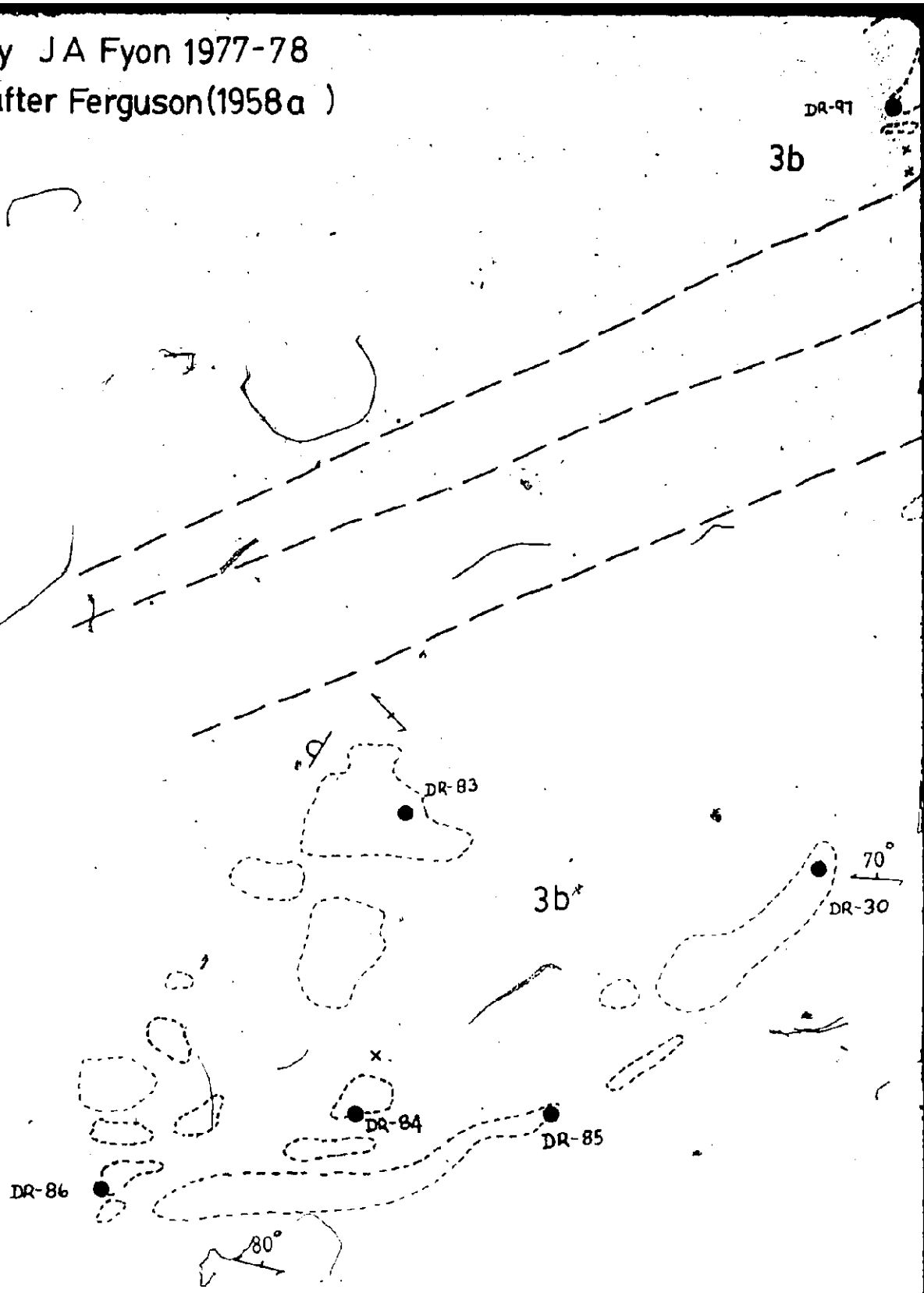

7 of

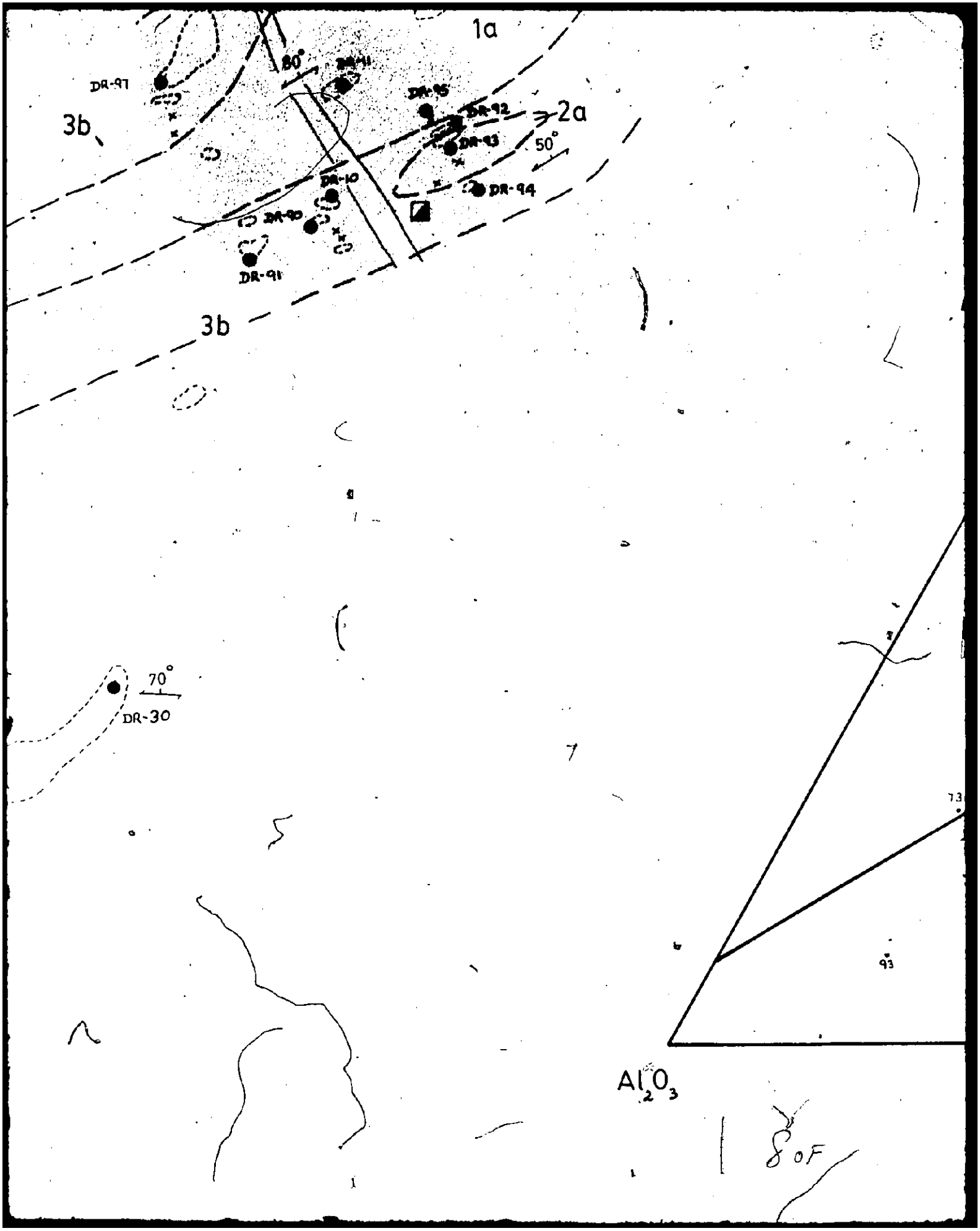
1a
2a
3b
3b
DR-97
80°
DR-11
DR-95
DR-92
DR-93
50°
DR-10
DR-94
DR-90
DR-91
70°
DR-30
7.3
93
Al_2O_3

South ore zone

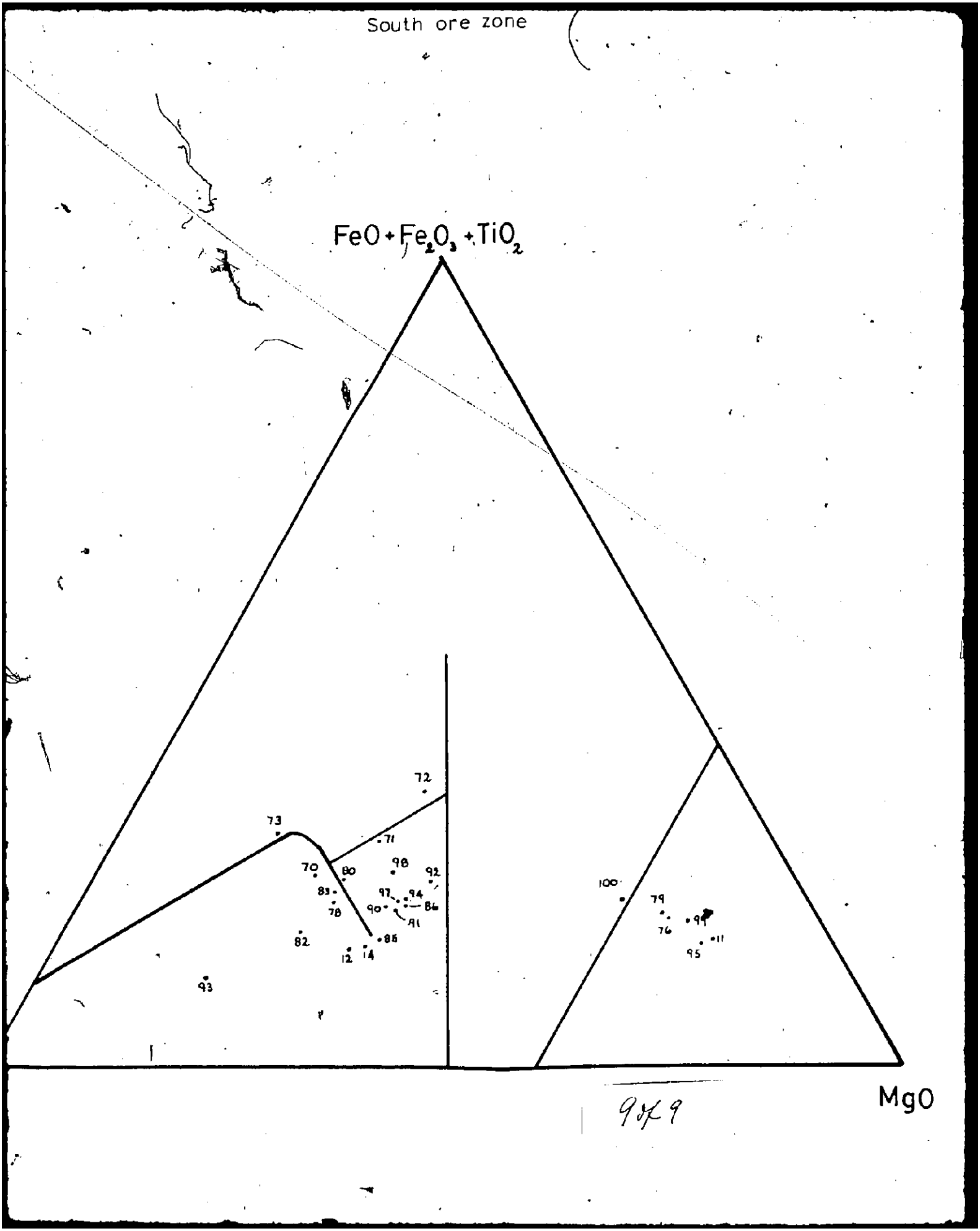

9 of 9